



Provided by the author(s) and University of Galway in accordance with publisher policies. Please cite the published version when available.

| | |
|------------------|---|
| Title | Sparse surface graphs |
| Author(s) | Shakir, Qays Rashid |
| Publication Date | 2019-12-20 |
| Publisher | NUI Galway |
| Item record | http://hdl.handle.net/10379/15659 |

Downloaded 2024-04-26T19:22:33Z

Some rights reserved. For more information, please see the item record link above.





NUI Galway
OÉ Gaillimh

Sparse Surface Graphs

A thesis submitted
by

Qays Rashid Shakir (M.Sc.)

to the

School of Mathematics, Statistics and Applied Mathematics,
National University of Ireland, Galway

in fulfillment of the requirements for the degree of
Doctor of Philosophy

Supervisor: Dr James Cruickshank

September 2019



Contents

| | | |
|----------|--|-----------|
| 1 | Introduction | 1 |
| 1.1 | Overview | 1 |
| 1.2 | The outline of the thesis | 2 |
| 2 | Surface Graphs | 7 |
| 2.1 | Graph theory | 7 |
| 2.2 | Surface graphs | 9 |
| 2.2.1 | Surfaces | 9 |
| 2.2.2 | Rectangular representation of the cylinder and torus | 11 |
| 2.2.3 | Definition of surface graphs | 13 |
| 2.3 | Rotation system | 15 |
| 2.3.1 | Rotation systems of surface graphs | 15 |
| 2.3.2 | Constructing a surface graph from a rotation system | 17 |
| 2.4 | Euler polyhedral formula | 19 |
| 3 | Sparsity of Graphs and Surface Graphs | 21 |
| 3.1 | Sparsity of graphs | 22 |
| 3.1.1 | Definition of sparsity | 22 |
| 3.1.2 | Some basic lemmas | 23 |
| 3.1.3 | Extending the sparsity definition for $l \geq k + 1$ | 24 |
| 3.1.4 | Examples of (k, l) -sparse graphs | 24 |
| 3.1.5 | Examples of (k, l) -tight graphs | 25 |
| 3.1.6 | Applications | 26 |
| 3.2 | The hole filing theorem | 30 |
| 3.2.1 | Faces of surface subgraphs | 30 |

CONTENTS

| | | |
|----------|--|-----------|
| 3.2.2 | The hole filling theorem | 31 |
| 3.3 | Contractions on closed walks | 31 |
| 3.3.1 | Some operations on graphs | 32 |
| 3.3.2 | 2-cycle contractions | 33 |
| 3.3.3 | 3-cycle contractions | 36 |
| 3.3.4 | 4-cycle contractions | 41 |
| 3.4 | Inductive operations on surface graphs | 45 |
| 3.4.1 | Topological contraction and deletion of an edge | 45 |
| 3.4.2 | Digon contraction | 47 |
| 3.4.3 | Triangle contraction | 48 |
| 3.4.4 | Quadrilateral contraction | 49 |
| 3.4.5 | Topological vertex splitting | 52 |
| 3.5 | Rotation systems and topological contraction moves | 53 |
| 3.5.1 | Edge contraction and deletion moves in terms of rotation system | 53 |
| 3.5.2 | Rotation systems of digon, triangle and quadrilateral contractions | 56 |
| 4 | Finiteness Theorems | 59 |
| 4.1 | Irreducibility and inductive constructions: Literature review | 60 |
| 4.1.1 | Inductive constructions of some kinds of tight graphs | 60 |
| 4.1.2 | Inductive constructions of some tight surface graphs | 63 |
| 4.2 | (2,2)-tight sphere graphs | 75 |
| 4.3 | Curves in surfaces | 76 |
| 4.3.1 | Some definitions | 76 |
| 4.3.2 | Cutting and capping surfaces along loops | 79 |
| 4.4 | Structures of irreducible (2,2)-tight torus graphs | 80 |
| 4.5 | The structure of blockers of quadrilateral faces in irreducible torus graphs | 88 |
| 4.6 | (2,2)-tight cylindrical graphs | 91 |
| 4.7 | The finiteness theorem of irreducible (2,2)-tight torus graphs | 93 |
| 4.8 | Examples and a conjecture | 100 |
| 4.8.1 | Examples | 100 |
| 4.8.2 | Finiteness conjecture | 105 |

| | | |
|----------|---|------------|
| 5 | Irreducible (2,2) -Tight Torus Graphs | 107 |
| 5.1 | Embedding lemmas in the torus | 107 |
| 5.1.1 | Cycles of length two and three in (2,2) -tight torus graphs | 108 |
| 5.1.2 | Subgraphs of irreducible graphs | 110 |
| 5.1.3 | Polygonal representation | 112 |
| 5.2 | Searching for all irreducible (2,2)-tight torus graphs | 116 |
| 5.2.1 | Two independent methods for conducting the search | 117 |
| 5.2.2 | Basic technical results for both methods | 118 |
| 5.2.3 | Computations by hand | 120 |
| 5.2.4 | Computer search approach | 122 |
| 5.2.5 | Surface graphs: the <code>OrientedRotationSystem</code> class | 124 |
| 5.2.6 | A sample interactive session | 126 |
| 5.3 | Irreducible (2,2)-tight torus graphs with less than three vertices | 128 |
| 5.4 | Irreducible (2,2)-tight torus graphs with four vertices | 131 |
| 5.4.1 | Embedding Θ_1 | 132 |
| 5.4.2 | Embedding Θ_2 | 133 |
| 5.4.3 | Irreducible (2,2)-tight \mathbb{T} -graphs that are derived from either G_1^3 or G_2^3 | 134 |
| 5.4.4 | The smallest (2,2)-tight graph with no irreducible embedding | 137 |
| 5.5 | Irreducible (2,2)-tight torus graphs with five vertices | 138 |
| 5.5.1 | Embedding Δ_1 | 139 |
| 5.5.2 | Embedding Δ_2 | 141 |
| 5.5.3 | Embedding Δ_3 | 142 |
| 5.5.4 | Embedding Δ_4 | 144 |
| 5.5.5 | Irreducible (2,2)-tight torus graphs in which G_2^4 is a torus sub- graph of each of them | 145 |
| 5.5.6 | Irreducible (2,2)-tight torus graphs which are derived from G_1^3 or G_2^3 | 146 |
| 5.6 | Irreducible (2,2) -tight torus graphs with six and seven vertices | 152 |
| 5.7 | Irreducible (2,2)-tight torus graphs with eight vertices | 154 |
| 6 | Contacts of Circular Arcs Representation | 161 |
| 6.1 | Intersection graphs | 162 |

CONTENTS

| | | |
|----------|--|------------|
| 6.1.1 | Definition of intersection graphs | 162 |
| 6.1.2 | Intersection graphs of some geometric contexts | 163 |
| 6.2 | Contact graphs | 164 |
| 6.2.1 | Circle packing theorem | 164 |
| 6.2.2 | Some types of contact representations | 164 |
| 6.3 | Contact graphs of curves | 165 |
| 6.3.1 | Contacts of curves in surfaces | 165 |
| 6.3.2 | Embedding a contact graph of curves in a surface | 168 |
| 6.4 | Contacts of circular arcs representation | 173 |
| 6.4.1 | CCA representations of digon, triangle and quadrilateral splitting moves | 173 |
| 6.4.2 | CCA representation of (2,2)-tight cylindrical graphs | 176 |
| 6.5 | CCA representations of (2,2)-tight torus graphs | 178 |
| 6.5.1 | Contacts of circular arcs representations of irreducible (2,2)-tight torus graphs | 178 |
| 6.5.2 | The outline of the main theorem | 180 |
| | Bibliography | 191 |
| A | Base irreducible (2,2)-tight torus graphs | 193 |
| B | Polygon representations derived from G_1^3 and G_2^3 | 195 |
| C | Notations for all irreducible (2,2)-tight torus graphs with 6 and 7 vertices. | 203 |
| D | Ancestor trees for all 116 irreducible (2,2)-tight torus graphs. | 207 |
| E | Irreducible (2,2)-tight torus graphs | 211 |
| E.1 | Irreducible (2,2)-tight torus graphs with less than 4 vertices. | 212 |
| E.2 | Irreducible (2,2)-tight torus graphs with 4 vertices. | 213 |
| E.3 | Irreducible (2,2)-tight torus graphs with 5 vertices. | 214 |
| E.4 | Irreducible (2,2)-tight torus graphs with 6 vertices. | 217 |
| E.5 | Irreducible (2,2)-tight torus graphs with 7 vertices. | 222 |
| E.6 | Irreducible (2,2)-tight torus graphs with 8 vertices. | 225 |

CONTENTS

| | | |
|----------|---|------------|
| F | CCA representations of the base irreducible (2,2)-tight torus graphs | 227 |
|----------|---|------------|

CONTENTS

List of Tables

| | | |
|-----|--|-----|
| 4.1 | A summary of minimal triangulations of some surfaces of low genus. | 74 |
| 5.1 | The notations for all nonisomorphic $(2,2)$ -tight graphs with four vertices. Abbreviations: Gr.=Graph, Ref.=Reference(s). | 131 |
| 5.2 | The notations for all nonisomorphic irreducible $(2,2)$ -tight \mathbb{T} -graphs with four vertices. Abbreviations: Gr.= \mathbb{T} -Graph, Ref.=Reference(s). | 132 |
| 5.3 | The notations of all nonisomorphic irreducible $(2,2)$ -tight \mathbb{T} -graphs with five vertices. Abbreviations: Gr.= \mathbb{T} -Graph, Ref.=Reference(s). | 140 |
| 5.4 | Irreducible $(2,2)$ -tight \mathbb{T} -graphs with n vertices. | 159 |

LIST OF TABLES

Symbols

LIST OF TABLES

| Symbol | Meaning | Page |
|------------------------|---|----------|
| Γ | graph | 7 |
| $V(\Gamma)$ | vertex set of Γ | 7 |
| $E(\Gamma)$ | edge set of Γ | 7 |
| $s(e)$ | source of an edge e | 7 |
| $t(e)$ | target of an edge e | 7 |
| Σ | surface | 9 |
| \mathbb{T} | torus | 10 |
| \mathbb{S} | sphere | 10 |
| S^1 | circle | 10 |
| $ \Gamma $ | geometric realisation of Γ | 13 |
| G | surface graph | 13 |
| \mathbb{S} -graph | spherical graph | 13 |
| \mathbb{T} -graph | torus graph | 13 |
| \mathbb{T} -subgraph | torus subgraph | 15 |
| K_4 | complete graph with 4 vertices | 14 |
| σ | permutation | 15 |
| τ | permutation | 15 |
| Γ_R | constructed graph from rotation system R . | 17 |
| R_G | rotation system of surface graph G | 16 |
| G_R | surface graph that is constructed from a rotation system R | 17 |
| γ_k | sparsity function | 19 |
| $\deg(v)$ | degree of a vertex v | 24 |
| $\text{int}_G(F)$ | Σ -subgraph of G | 30 |
| $\text{ext}_G(F)$ | Σ -subgraph of G | 30 |
| ∂F | boundary of a face F | 30 |
| $\Gamma - e$ | deleting edge e from Γ | 32 |
| $\Gamma/u \sim v$ | identifying vertices u and v in Γ | 32 |
| Γ/e | contraction edge e in Γ | 32 |
| $\overline{\Omega}$ | lifting a subgraph Ω | 34,37,42 |
| Θ | projection of a subgraph Θ | 35, 38 |
| G/e | contraction edge e in G | 45 |
| $G - e$ | deleting edge e in G | 46 |
| G_B | contracting a digon B in G | 47 |
| G_{T,e_1} | contracting a triangle T by contracting edge e_1 in G | 48 |
| G_{Q,v_1,v_3} | contracting a quadrilateral Q by identifying v_1 and v_3 in G | 50 |
| G_{H_0} | surface graph obtained by a topological Henneberg type 0 move | 64 |
| G_{H_1} | surface graph obtained by a topological Henneberg type 1 move | 65 |
| G_{H_2} | surface graph obtained by a topological Henneberg type 2 move | 66 |
| G^* | dual surface graph of G | 67 |
| $\text{im}(f)$ | image of a function | 76 |
| $i(\alpha, \beta)$ | geometric intersection number of loops α and β | 77 |

LIST OF TABLES

| Symbol | Meaning | Page |
|-------------------------|---|------|
| H_1^Q | blocker for $G \rightarrow G_{Q,v_1,v_3}$ | 83 |
| H_2^Q | blocker for $G \rightarrow G_{Q,v_2,v_4}$ | 83 |
| α_1^Q | simple loop in the blocker H_1^Q | 84 |
| α_2^Q | simple loop in the blocker H_2^Q | 84 |
| β_i^Q | nonseparating cycle lies in H_i^Q | 87 |
| J_i^Q | face in H_i^Q but not a face in G | 88 |
| \tilde{H}_i^Q | \mathbb{S} -graph results from cutting and capping along α_{3-i} | 88 |
| \tilde{J}_1^Q | face in \tilde{H}_i^Q provided that α_1^Q is nonseparating | 88 |
| \tilde{J}_-^Q | face in \tilde{H}_i^Q but not a face in G | 88 |
| \tilde{J}_+^Q | face in \tilde{H}_i^Q but not a face in G | 88 |
| c_+^Q | boundary walk for ∂J_1^Q | 89 |
| c_-^Q | boundary walk for ∂J_1^Q | 89 |
| F_+^Q | face in J_1^Q but not in G | 90 |
| F_-^Q | face in J_1^Q but not in G | 90 |
| L_1 | component of $H_1^Q \cap H_1^R$ | 97 |
| L_3 | component of $H_1^Q \cap H_1^R$ | 97 |
| $R = (H, \sigma, \tau)$ | rotation system, where H is a set of half edges | 54 |
| G_j^i | irreducible $(2, 2)$ -tight graph with i vertices | 121 |
| $\Gamma_{\mathcal{C}}$ | contact graph of a collection of curves | 168 |
| $G_{\mathcal{C}}$ | embedding of $\Gamma_{\mathcal{C}}$ | 169 |
| C_j^i | CCA representation of G_j^i | 182 |

Declaration

I hereby declare that this thesis entitled "Sparse Surface Graphs" represents my own work and I have not obtained a degree at the National University of Ireland, Galway, or elsewhere, on the basis of the work described in the thesis. The collaborative contributions have been indicated clearly and acknowledged. Due references have been provided on all supporting literatures and resources.

Qays Shakir
September, 2019

Abstract

This thesis is concerned with building certain classes of sparse and tight surface graphs via suitable sets of inductive moves from specified sets of irreducible surface graphs. In particular, we derive topological inductive constructions for $(2,2)$ -tight surface graphs in the case of the sphere, the cylinder and the torus. We present theorems and results that determine the number of the irreducible $(2,2)$ -tight sphere, cylinder and torus graphs. We also found all irreducible $(2,2)$ -tight torus graphs using two independent approaches. One of these approaches is based on calculation by hand. We employed a mixture of brute force methods and theoretical insight into the structure of such graphs. The other approach is a computer assisted search. Consequently, we found that there are exactly 116 irreducible $(2,2)$ -tight torus graphs. We also organise and present all irreducible $(2,2)$ -tight torus graphs. This thesis also includes a geometric application of configurations to circular arcs, in the spirit of the Keobe-Andreev-Thurston circle packing theorem. We used the inductive construction of $(2,2)$ -tight torus graphs to show that every $(2,2)$ -tight torus graph is the contact graph of a collection of circular arcs in the flat torus.

Acknowledgements

I offer my deep, sincere thanks to my supervisor Dr James Curickshank for the continuous support of my PhD study and related research, for his patience, motivation, and immense knowledge. His guidance helped me in all the time of research and writing of this thesis. I will be forever influenced by his incisive wit, tenacity, and clarity of thought and I count myself most fortunate to have been afforded his instruction.

I am profoundly grateful to the Middle Technical University, Iraq for being my financial sponsor during my study abroad. Also, my special gratitude goes out to all down at the Technical College of Management, Baghdad, for nominating me to study abroad.

I would like to thank Derek Kitson, Stephen Power, Bernd Schulze and Anthony Nixon for inviting me many times to their annual workshop on rigidity theory in Lancaster university, where I gained a lot of information related to my work.

I would like to thank the academic and the administrative staff of the School of Mathematics, Statistics and Applied Mathematics in the National University of Ireland, Galway for their support. My sincere thanks go to Dr Aisling McCulskey for her support that I and my family received from her during our stay in Galway.

Last but not least, I would like to thank my family in Iraq, especially, my father Rashid Shakir, for their support and encouragement. I am exceptionally grateful to my family. My wife, Izdihar, has been extremely supportive of me throughout this entire process and has made countless sacrifices to help me get to this point. My children, thank you all for giving me the hope and energy to complete this thesis.

Chapter 1

Introduction

1.1 Overview

This thesis studies inductive constructions for certain kinds of sparse graphs that are embedded in surfaces without edge crossing. In general, to build a class of graphs with particular properties, one needs to start from certain 'small' graphs in that class which they were not built from other graphs in the class. Then there is a need to find specific rules to expand the small graphs to build all other graphs in the class. Such rules are usually called inductive moves. The choice of using inductive moves is subject to some restrictions. One restriction is that such inductive moves have to preserve the properties that the class of graphs possesses. In this thesis, we investigate inductive constructions of sparse surface graphs. In particular, we find inductive constructions of certain sparse graphs that are embedded in surfaces of low genus. The great challenge that we faced in this thesis is to find the small graphs, we call them here irreducible surface graphs of certain kind of sparsity. However, we found in this thesis inductive constructions for sparse surface graphs with low genus. This includes finding all the irreducible graphs in these classes of surface graphs and also choosing suitable inductive moves. The inductive constructions that we initiated are used to investigate a geometric application.

1.2 The outline of the thesis

This thesis is concerned with studying inductive constructions of surface graphs. We in particular, focus on certain kinds of sparse graphs that are embedded in surfaces of low genus. Also, a geometric application of the inductive constructions that we found have been included in this thesis. In the following, we briefly present an outline of the layout of this thesis.

Chapter 2: Surface graphs This chapter includes some fundamental concepts of surface graph theory. Among those concepts, we provide a detailed definition of the embedding of a graph in a surface. We also discuss the rotation system in detail. This chapter consists of the following sections.

Section 1 is devoted to recalling some basic concepts of graph theory.

Section 2 reviews some fundamental concepts of surface graphs. We include a detailed definition of surface graphs and the concept of isomorphic surface graphs.

Section 3 investigates the concept of rotation systems of surface graphs.

Section 4 includes a new form of the Euler's Formula by including counting on the sparsity of surface graphs.

Contribution This chapter provides a modified form of Euler's Formula.

Chapter 3: Sparsity of graphs and surface graphs

The purpose of this chapter is to investigate the sparsity and tightness of graphs and surface graphs. We set a fundamental background for the rest of the thesis by introducing some definitions and lemmas which they are used later on in this thesis. For example, we introduce a significant theorem related to the sparsity of surface subgraphs of sparse surface graphs. Also, we survey various results on sparse and tight graphs. We also survey the most known facts and results related to sparse and tight graphs and their applications in various areas. This chapter consists of five sections.

Section 1 presents a brief survey on the sparsity and also tightness of graphs. We also include some basic results that emerge from the sparsity of

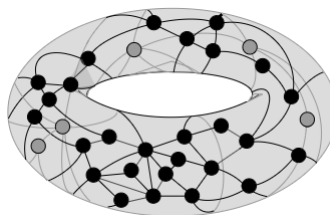


Figure 1.1: A surface graph.

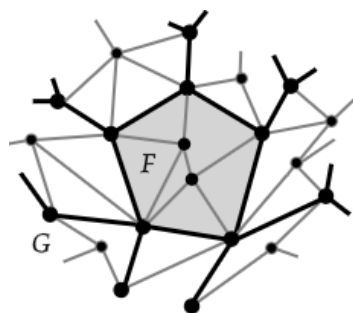


Figure 1.2: The shaded region is the surface subgraph $int_G(F)$.

graphs.

Section 2 states and proves a significant theorem which contributes in finding the crucial results of this thesis. We call this theorem the hole filling theorem.

Section 3 serves as a skeleton to the next section. It sets the definitions of three contraction moves on certain kinds of closed walks in sparse graphs. Naturally, some results related to the three contraction moves have been included in this section.

Section 4 investigates contraction moves which are introduced in the previous section. However, such contraction moves defined on surface graphs not on 'abstract' graphs.

Section 5 studies the three topological inductive contraction moves in the previous section by using rotation systems.

Contribution In this chapter, we state and prove a fundamental theorem, we call it the hole filling lemma. This theorem is used many times in the rest of the thesis to obtain the core results of this thesis. Also, in this chapter, we study and investigate three types of contraction moves on graphs and surface graphs. Following to that, we redefine the topological versions of the three contraction moves using the rotation system.

Chapter 4: Finiteness Theorems This chapter includes the key results of this thesis. These results are showing that the numbers of irreducible $(2,2)$ -tight surface graphs of some low genus are finite. A conjecture has been introduced which concerns the existence of finite number of irreducible $(2,2)$ -tight surface graphs for any surface. We bound the number of vertices of the irreducible $(2,2)$ -tight torus graphs, and we get rich combinatorial information of such irreducible graphs. This chapter consists of the following sections.

Section 1 provides a brief literature review of studies and results on some inductive constructions. In this section, we review some known results on inductive constructions of some types of tight abstract graphs and surface graphs including surface triangulations.

Section 2 gives an inductive construction for the class of $(2,2)$ -tight sphere graphs.

Section 3 This section recalls some types of curves in a surface. More attention has been given to the curves in the torus.

Section 4 is devoted to study the structure of irreducible $(2,2)$ -tight torus graphs. We prove some structural results which will be used in the next two sections.

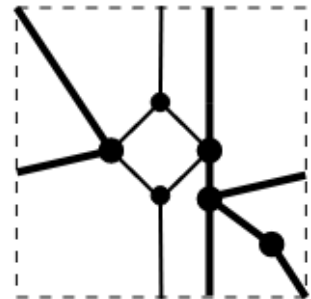


Figure 1.3: An essential blocker that is bold.

Section 5 investigates the structures of the blockers of quadrilateral faces in irreducible $(2,2)$ -tight torus graphs.

Section 6 concerns with finding an inductive construction for the class of $(2,2)$ -tight cylindrical graphs.

Section 7 contains the key results of this thesis. The finiteness theorem of an existing finite number of irreducible $(2,2)$ -tight torus graphs is stated and proved in this section.

Section 8 exhibits a variety of examples which cover most of the concepts that have been introduced and investigated in the previous sections of this chapter.

Contribution We proved for small genus that there are a finite number of irreducible $(2,2)$ -tight surface graphs. This chapter enables us to find all the irreducible $(2,2)$ -tight torus graphs in the next chapter by bounding the number of vertices of such irreducible torus graphs and provides rich combinatorial information about the irreducible $(2,2)$ -tight torus graphs. We include a conjecture for finiteness of irreducible $(2,2)$ -tight surface graphs for surfaces of any genus.

Chapter 5: Irreducible $(2,2)$ -tight torus graphs This chapter presents all irreducible $(2,2)$ -tight \mathbb{T} -graphs. We explain in detail how we found all the irreducible $(2,2)$ -tight torus graphs by using two independent approaches. One approach is computing by hand all the irreducible $(2,2)$ -tight torus graphs. The other approach is a computer assisted search. The number of all irreducible $(2,2)$ -tight torus graphs that we found is 116. This chapter comprises the following sections.

Section 1 This section presents some lemmas which can help in embedding $(2,2)$ -tight graphs in the torus.

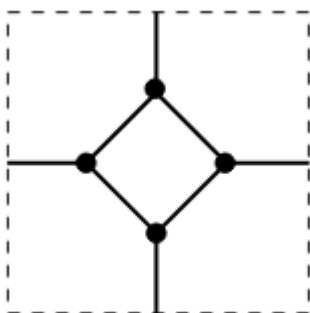


Figure 1.4: An irreducible $(2,2)$ -tight \mathbb{T} -graph.

Section 2 exhibits how we found all irreducible $(2,2)$ -tight torus graphs. Detailed explanations have been given in this section of the two methods that we used to find all irreducible $(2,2)$ -tight torus graphs. Also, we initiated a way to present all the 116 irreducible $(2,2)$ -tight torus graphs.

Section 3 presents all irreducible $(2,2)$ -tight \mathbb{T} -graphs with less than four vertices.

Section 4 declares all irreducible $(2,2)$ -tight torus graphs with four vertices.

Section 5 presents all irreducible $(2,2)$ -tight torus graphs with five vertices.

Section 6 explains how we found all irreducible $(2,2)$ -tight torus graphs with six and

1.2. THE OUTLINE OF THE THESIS

seven vertices using a computer assisted search.

Section 7 presents irreducible $(2,2)$ -tight torus graphs with 8 vertices.

Contribution We found all nonisomorphic irreducible $(2,2)$ -tight torus graphs. The total number of them is 116. We found them using two methods. A hand calculating method we used to find all irreducible $(2,2)$ -tight torus graphs. This has been done using some technique and lemmas that helped us to embed $(2,2)$ -tight graphs in the torus. We found all the irreducible $(2,2)$ -tight torus graphs with six and seven vertices by hand. However, in this chapter we also describe how we used a computer assisted search to find such irreducible $(2,2)$ -tight torus graphs.

Chapter 6: Contacts of circular arcs representation In this chapter, we describe an application to the study of contact graphs. We benefit from the inductive constructions of the classes of $(2,2)$ -tight surface graphs with low genus. In this chapter, we investigate the recognition problem for contact graphs. Specifically, this chapter is designed to find necessary and/or sufficient conditions for a surface graph to be the contact graph of a collection of curves. Consequently, we showed that every $(2,2)$ -tight torus graph admits a contacts of circular arcs representation. This chapter comprises the following sections.

Section 1 surveys the intersection graphs theory and related topics in the literature.

Section 2 surveys the topic of contact graphs in some details.

Section 3 investigates contact graphs of curves in surfaces in more details. We define the embedding of contact graphs of curves in surfaces.

Section 4 is devoted to investigate the contacts of circular arcs representation on the flat surfaces. This includes investigating the contacts of circular arcs representability of the three topological inductive moves that are used to build some classes of $(2,2)$ -tight surface graphs in this thesis.

Section 5 investigates representing $(2,2)$ -tight torus graphs as contacts of circular arcs in the flat torus. We prove that every $(2,2)$ -tight torus graph admits a contact of circular arcs representation on the flat torus.

Contribution In this chapter, we show that $(2,2)$ -tight torus graphs are the contact graphs of a collection of circular arcs in the corresponding flat surfaces.

Appendices: We provide at the end of this thesis a few appendices. These appendices



Figure 1.5: A contacts of circular arcs representation of the torus graph in Figure 1.4.

CHAPTER 1. INTRODUCTION

serve as complementary catalogues of various groups of figures and diagrams to their corresponding relevant sections and chapters throughout this thesis.

Publications and Collaborations: So far there is one publication associated to this thesis [19] which has appeared on arxiv.org and has been submitted to a journal. This paper is based in part on the material from Chapter 4 and is written in collaboration with Stephen Power (Lancaster University), Derek Kitson (Lancaster University) and James Cruickshank as part of a larger project on the sparsity and rigidity properties of surface graphs. Also, we published the SageMath code that we used for the computer assisted search, [20].

Chapter 2

Surface Graphs

Surface graph theory concerns drawing graphs on surfaces without edge crossing. This theory has a long period of developments date back to the work of Leonhard Euler. During its relatively old age, surface graph theory possessed various names such as the theory of maps, [53], [63], maps on surfaces, [53], combinatorial maps [98] and the most common name is the topological graph theory, [6], [43].

In this chapter, we survey some fundamental concepts of the theory of surface graphs. We also present a detailed definition of surface graphs. This chapter also discusses rotation systems of surface graphs. Such rotation systems will be used to encode surface graphs by a sequence of permutations.

2.1 Graph theory

In the following we define a directed multigraph which is also known as a quiver. More background on graph theory can be found in [23] and [11].

Definition 2.1.1. [23] *A (directed) multigraph Γ is a quadruple (V, E, s, t) where V and E are sets and $s : E \rightarrow V$ and $t : E \rightarrow V$ are functions.*

We refer to elements of V ($V(\Gamma)$) as vertices and E ($E(\Gamma)$) as edges. The functions s and t can be thought as specifying the source and the target respectively of each edge. See Figure 2.1 which depicts some small multigraphs.

In the following we give an example of a multigraph by declaring the functions s and t .

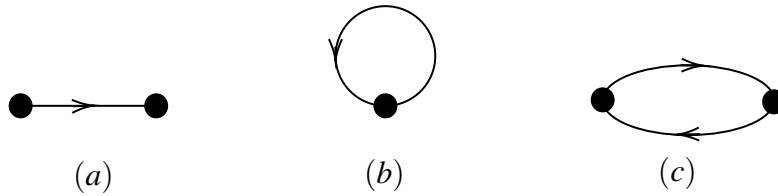


Figure 2.1: (a) A directed edge. (b) A self-loop (or loop). (c) A pair of parallel edges (multiple edges).

Example 2.1.2. Let $\Gamma = (V, E, s, d)$ be a multigraph where $V = \{u, v, w\}$, $E = \{e, f, g, h, i\}$, $s(e) = u, s(f) = u, s(g) = v, s(h) = w, s(i) = v$ and $t(e) = v, t(f) = u, t(g) = u, t(h) = u, t(i) = w$. The graph Γ can be represented as in Figure 2.2.

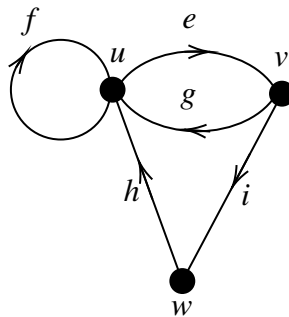


Figure 2.2: An example of a multigraph which is defined by the terms of source and target.

Definition 2.1.3. A walk is a sequence $v_1, e_1, v_2, e_2, \dots, e_k, v_{k+1}$ where $i = 1, 2, \dots, k$ and either $s(e_i) = v_i$ and $t(e_i) = v_{i+1}$ or $s(e_i) = v_{i+1}$ and $t(e_i) = v_i$. The walk is simple if no vertex in that walk is repeated. The walk is closed if $v_{k+1} = v_1$ and is a cycle if $v_{k+1} = v_1$ is the only repeated vertex.

Figure 2.3 provides various kinds of walks in a multigraph, say Γ . We emphasise that the previous definition of a walk means that a walk is not required to respect the orientation of the edge. Notice that throughout this thesis, whenever we deal with a graph, then that graph is a multigraph which is defined as in Definition 2.1.1.

Definition 2.1.4. Let $\Gamma = (V, E, s, t)$ be a graph. A half edge is a pair (e, r) where $e \in E$ and $r \in \{s, t\}$.

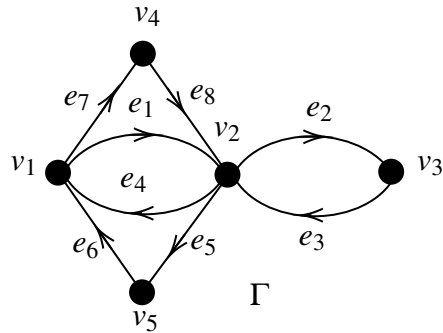


Figure 2.3: In the graph Γ ; v_1, e_1, v_2, e_8, v_4 is a simple walk. $v_1, e_1, v_2, e_2, v_3, e_3, v_2, e_4, v_1$ is a nonsimple closed walk, v_2 is a repeated vertex. $v_1, e_4, v_2, e_5, v_5, e_6, v_1$ is a simple closed walk.

Example 2.1.5. Let Γ be a graph defined as in Figure 2.4. We use numbers to represent each half edge in Γ . Hence $H = \{1, 2, 3, 4, 5, 6, 7, 8\}$ is a set of half edges of Γ and $\{1, 3\}$ respectively $\{2, 4\}$, $\{6, 7\}$ and $\{5, 8\}$ are the half edges of the edge e respectively f , g and h .

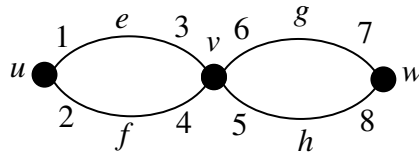


Figure 2.4: A multigraph Γ with a labelling of all of its half edges.

2.2 Surface graphs

In this section we define surface graphs and state some of their properties.

2.2.1 Surfaces

In the following, we briefly review some concepts of surface theory. More background on surface theory can be found in [32], [95], [36] and [37].

Definition 2.2.1. [66] A surface is a connected compact Hausdorff topological space Σ which is locally homeomorphic to an open disc in the plane, i.e. each point of Σ has an open neighbourhood homeomorphic to the open unit disc in \mathbb{R}^2 .

Definition 2.2.2. [56] A surface with a boundary is a surface Σ such that every point of Σ has a neighbourhood homeomorphic either to an open disc or to the set $\{(x, y) \in \mathbb{R}^2 : x^2 + y^2 < 1, x \geq 1\}$.

See Figure 2.5 which provides some examples of surfaces.

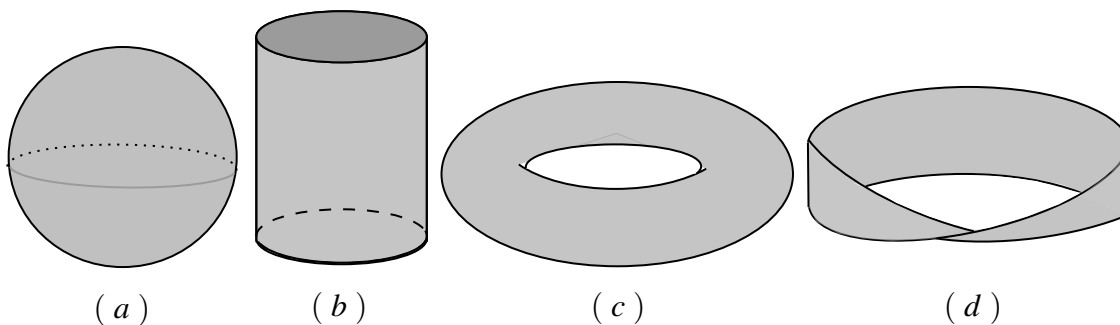


Figure 2.5: Some examples of surfaces: (a) The sphere $\mathbb{S} = \{(x, y, z) \in \mathbb{R}^3 : x^2 + y^2 + z^2 = 1\}$. (b) The cylinder $\{(x, y, z) \in \mathbb{R}^3 : x^2 + y^2 = 1 \text{ and } 0 \leq z \leq 1\}$. (c) The torus $\mathbb{T} = \{(x, y, z, w) \in \mathbb{R}^4 : x^2 + y^2 = 1; z^2 + w^2 = 1\}$. (d) The Möbius strip $\{(x, y) : 0 \leq x, y \leq 1\} / \sim$ where $(0, t) \sim (1, 1 - t)$ and $t \in [0, 1]$. Notice that the surfaces (a) and (c) have no boundary while (b) has two boundaries and (d) has one boundary.

Definition 2.2.3. [40], [58] A surface Σ is nonorientable if some subset of it (with the induced topology) is homeomorphic to the Möbius strip. Otherwise, it is orientable.

Certain loops on surfaces can be used to determine many properties of surfaces. For instance, existing specific loops on a surface can be used to determine the genus of that surface and also can be used to determine whether a surface is orientable or nonorientable. Let us consider the concept of a loop in a surface.

Definition 2.2.4. [35] Let Σ be a surface. A loop in Σ is a map $\alpha : S^1 \rightarrow \Sigma$. A loop α is called simple if it is injective.

An alternative definition to Definition 2.2.3 can be stated as follows.

Definition 2.2.5. [96] A surface Σ is said to be orientable if for every simple loop α in Σ , a clockwise sense of rotation is preserved by travelling once around α . Otherwise, Σ is nonorientable.

2.2. SURFACE GRAPHS

As we mentioned above, the genus of a surface can be determined by using loops. In the following, we define the genus of a surface.

Definition 2.2.6. Let \mathcal{C} be a collection of pairwise disjoint simple loops in a surface Σ . We say that \mathcal{C} is nonseparating in Σ if $\Sigma - \mathcal{C}$ has the same number of components as Σ . The genus g of Σ is the cardinality of a maximal nonseparating collection \mathcal{C} .

See Figure 2.6.

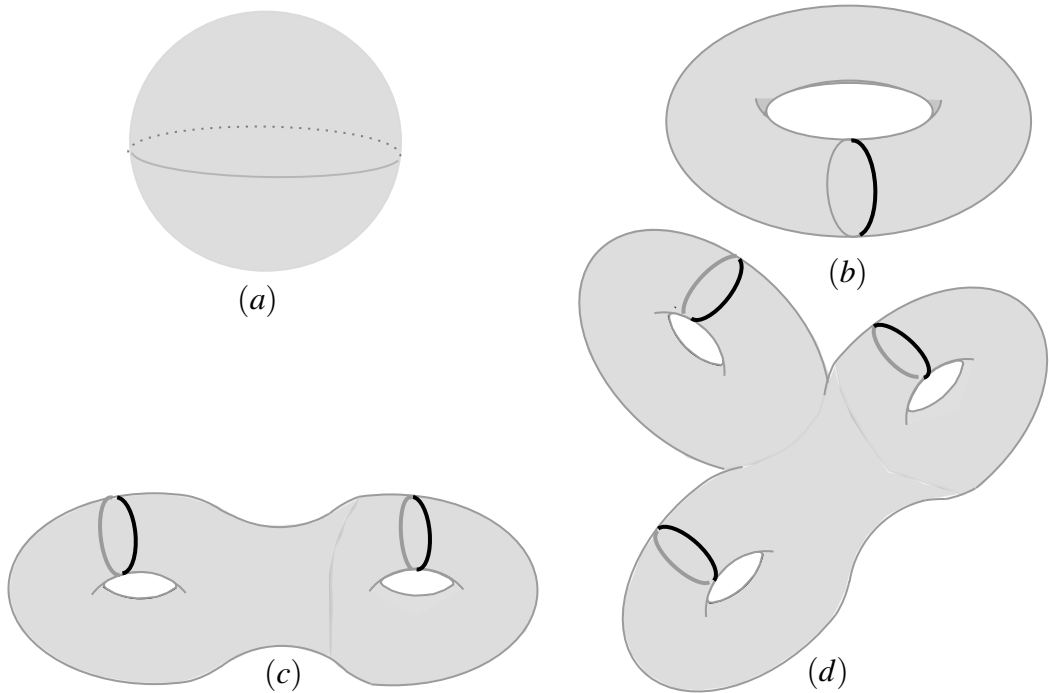


Figure 2.6: Surfaces with various genera. (a) No nonseparating loop exists on the sphere, so its genus equal to 0. While the genus of the surface in (b), (c) and (d) is 1, 2 and 3 respectively. Notice that the nonseparating loops are clearly depicted.

Throughout this thesis, we let Σ to be an oriented, compact and connected surface of genus g with no boundary unless we declare a different hypothesis.

2.2.2 Rectangular representation of the cylinder and torus

Representing surfaces by a specific drawing can help to understand various properties of surfaces. One method of drawing surfaces is the planar model. In such a model, plane

polygons are used to represent surfaces. For example, the torus can be represented by a polygon of degree 4 with indicating that the opposite edges of this polygon are identified together. This representation is also called rectangular representation of the torus. We use this representation to represent torus graphs later.

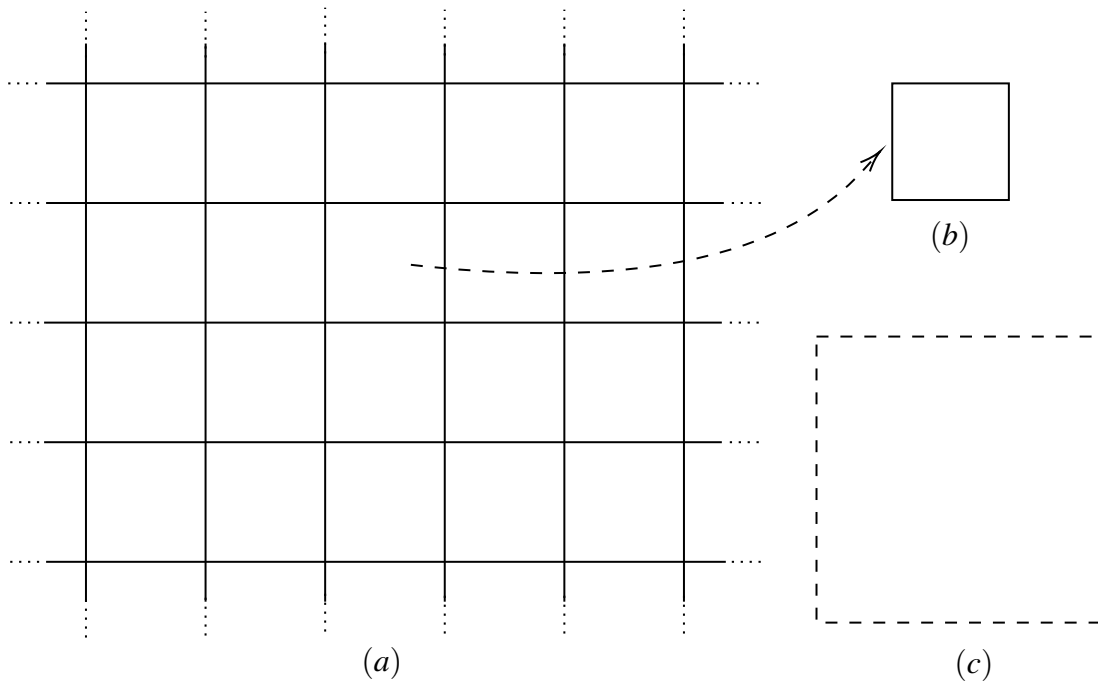


Figure 2.7: (a) The tilling of the plane with the unit square. (b) The fundamental domain of the action of \mathbb{Z}^2 on the space \mathbb{R}^2 . (c) Rectangular representation of the torus.

Notice that the torus is the quotient group $\mathbb{R}^2/\mathbb{Z}^2$, so we consider the fundamental domain of the action of \mathbb{Z}^2 on the space \mathbb{R}^2 by translation. The fundamental domain is the unit square, i.e. the Cartesian product $I \times I$ where I is the closed unit interval $[0, 1]$, Figure 2.7(b). We allow the boundary of the unit square to be dashed, Figure 2.7(c).

Observe that the action of \mathbb{Z}^2 on the space \mathbb{R}^2 by translation gives the classical tessellation of the plane by a square, Figure 2.7(a). More sources on torus can be found in [24] and [10].

The cylinder is a surface with two boundaries. It can be represented using the rectangular representation. We represent the cylinder as in Figure 2.8.

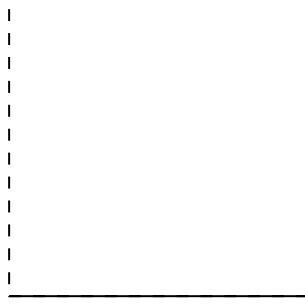


Figure 2.8: Rectangular representation of the cylinder.

2.2.3 Definition of surface graphs

In the following we state the definition of the embedding of a graph in a surface. More background on the theory of surface graphs can be found in [9] and [6].

Definition 2.2.7. *The geometric realisation $|\Gamma|$ of a graph $\Gamma = (V, E, s, t)$ is the topological space*

$$|\Gamma| = \frac{V \sqcup (E \times [0, 1])}{\sim}$$

where V, E are discrete spaces and $s(e) \sim (e, 0)$ and $t(e) \sim (e, 1)$.

Definition 2.2.8. *Let Σ be a compact connected surface without a boundary of genus g . A Σ -graph is a pair $G = (\Gamma, \phi)$ where $\phi : |\Gamma| \rightarrow \Sigma$ is a continuous injective map.*

The map ϕ is called the embedding of Γ in Σ . See Figure 2.9 that illustrates an example of embedding a graph in the sphere respectively torus to get an \mathbb{S} respectively \mathbb{T} -graph.

Definition 2.2.9. *Let $G = (\Gamma, \phi)$ be a Σ -graph. A face of G is a component of $\Sigma - \phi(|\Gamma|)$.*

Definition 2.2.10. *Let $G_i = (\Sigma_i, \phi_i)$ be a Σ_i -graph for $i = 1, 2$. G_1 and G_2 are isomorphic if there is a homeomorphism $h : \Sigma_1 \rightarrow \Sigma_2$ and a graph isomorphism $g : \Gamma_1 \rightarrow \Gamma_2$ such that $h \circ \phi_1 = \phi_2 \circ |g|$ where $|g| : |\Gamma_1| \rightarrow |\Gamma_2|$ is the map induced by the graph isomorphism g .*

We comment on how the map $|g|$ is defined. For $v \in V$, let \bar{v} be the equivalence class of v under the equivalence relation \sim . So \bar{v} is the point of $|\Gamma|$ that corresponds to v .

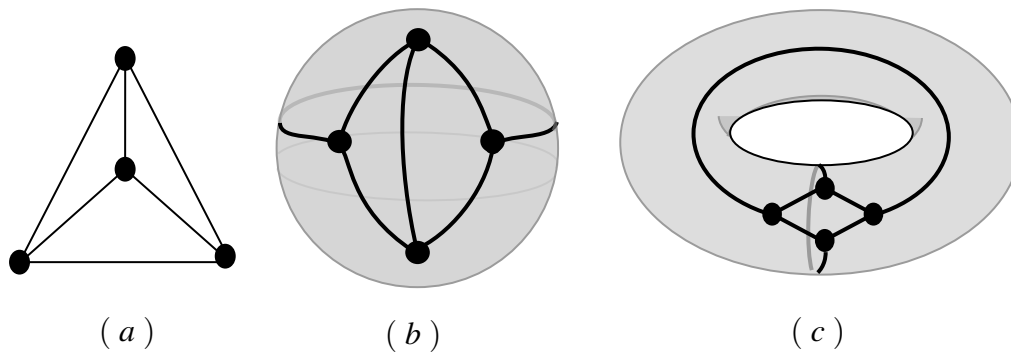


Figure 2.9: (a) An abstract graph, K_4 . (b) An embedding of K_4 in the sphere, an \mathbb{S} -graph. (c) An embedding of K_4 in the torus, a \mathbb{T} -graph.

Similarly, for $e \in E$ and $t \in I$, let $\overline{(e,t)}$ be the point of $|\Gamma|$ corresponding to (e,t) . Define $|g|(\overline{v}) = \overline{g(v)}$ and $|g|(\overline{(e,t)}) = \overline{(g(e),t)}$.

Notice that it can happen that two surface graphs are nonisomorphic to each other but their underlying graphs are isomorphic. See the following example.

Example 2.2.11. *The two torus graphs in Figure 2.10 are nonisomorphic to each other although their underlying graphs are isomorphic.*

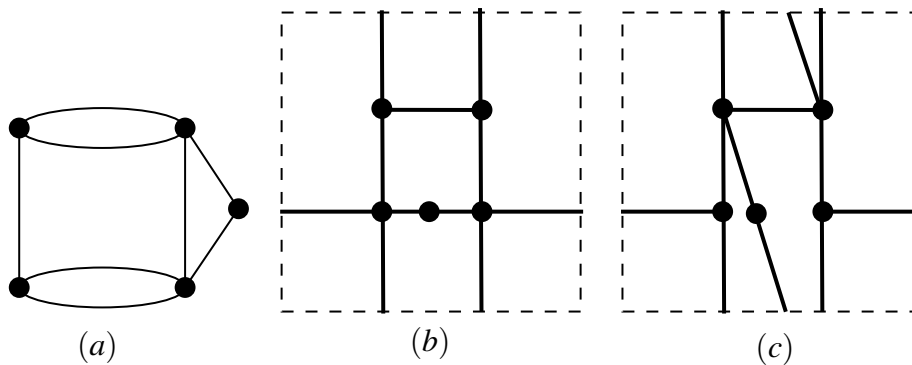


Figure 2.10: The \mathbb{T} -graphs in (b) and (c) are nonisomorphic, one can use the SageMath code in [20] to verify that. However, the graph in (a) is the underlying abstract graph of both of the torus graphs in (b) and (c).

Definition 2.2.12. *Let Ω be a subgraph of Γ where Γ is the underlying graph of a Σ -graph G . The pair $H = (\Omega, \phi_{|\Omega|})$ is called a Σ -subgraph of G .*

Figure 2.11 provides an example of a \mathbb{T} -subgraph of a \mathbb{T} -graph.

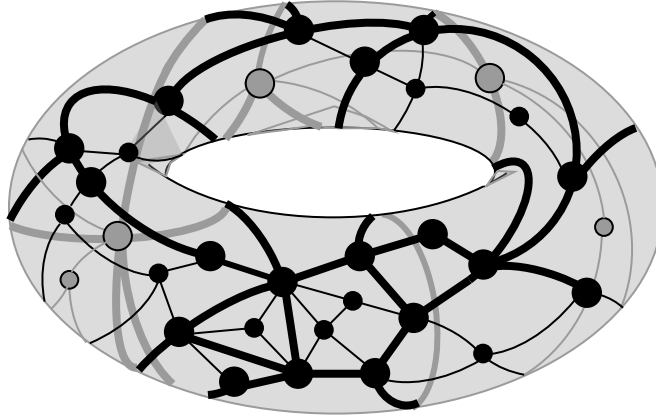


Figure 2.11: A \mathbb{T} -subgraph that is bold of a \mathbb{T} -graph.

Definition 2.2.13. *Let G be a Σ -graph. A face of G is cellular if it is homeomorphic to an open disc. G is cellular if all its faces are cellular.*

Figure 2.12 presents two torus graphs. One of them is a noncellular torus graph, Figure 2.12(a). The other one is a cellular torus graph, Figure 2.12(b). The faces of each of them are highlighted.

2.3 Rotation system

In this section, we state the concept of rotation system. Also we survey the rotation system of surface graphs, and then we show how one can construct a surface graph from a given rotation system. For more survey on this topic, see [89], [72] and [60].

2.3.1 Rotation systems of surface graphs

In the following we state the definition of a rotation system and the rotation system of a surface graph.

Definition 2.3.1. *An oriented rotation system is a triple (X, σ, τ) where X is a nonempty set, $\sigma : X \rightarrow X$ is a permutation and $\tau : X \rightarrow X$ is a fixed point free involution (permutation of order 2).*

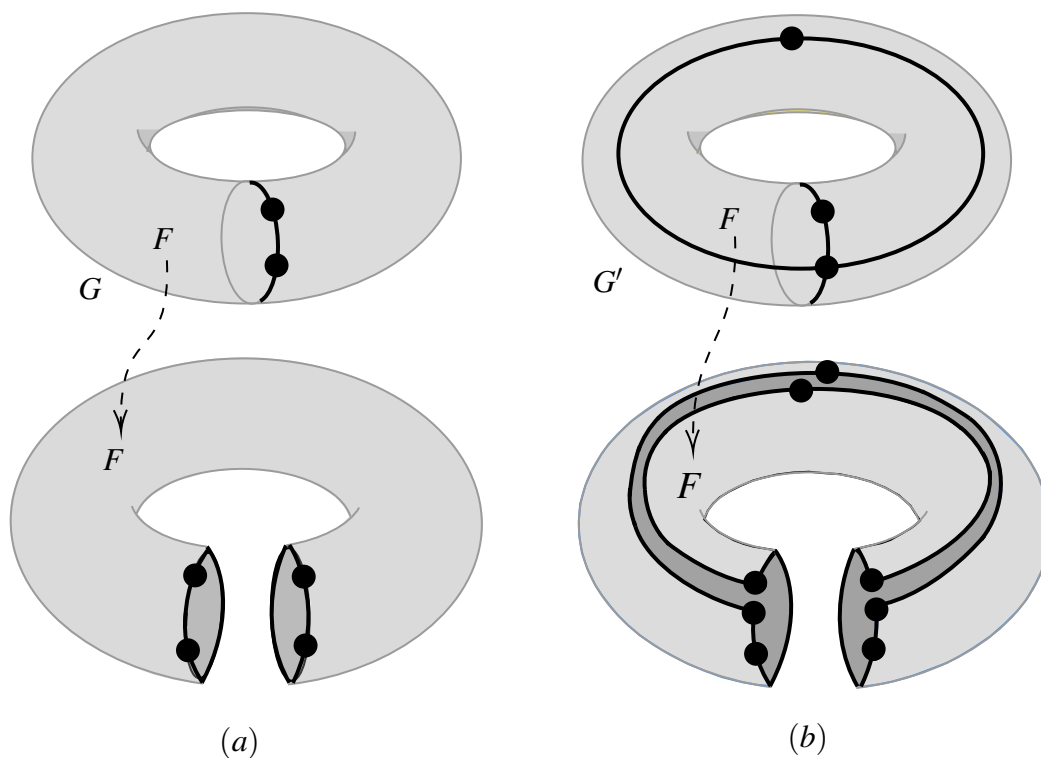


Figure 2.12: (a) G is a \mathbb{T} -graph that has only one face and that face F is noncellular. (b) G' is a \mathbb{T} -graph that has only one face F and that face is cellular.

Let Σ be an oriented surface. Let G be a Σ -graph with vertex set V and edge set E . The rotation system of G is the triple $R_G = (H, \sigma, \tau)$ of G where H is the set of half edges of G . The permutation $\sigma : H \rightarrow H$ is a map defined as $\sigma(h) = m$ where $h, m \in H$ and m is the half edge immediately following h in an anticlockwise direction in G . On the other hand, the permutation $\tau : H \rightarrow H$ is a map defined as $\tau(p) = q$ where $p, q \in H$ such that both of p and q are half edges of an edge in G .

Notice that there is a one-to-one correspondence between orbits of σ and vertices. Also there is a one-to-one correspondence between orbits of τ and edges.

Example 2.3.2. Consider the \mathbb{T} -graph G in Figure 2.13. The permutations σ and τ are specified as follows.

$$\sigma = (1, 2, 3)(4, 5, 6)(7, 8, 9)(10, 11, 12) \text{ and } \tau = (1, 5)(2, 6)(3, 10)(4, 8)(7, 12)(9, 11).$$

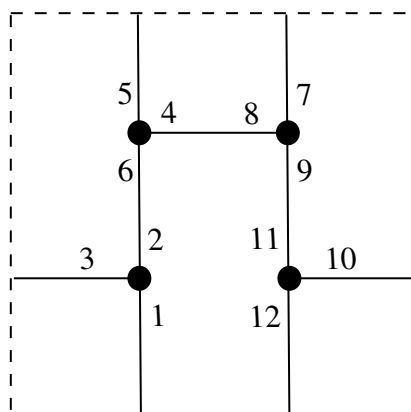


Figure 2.13: A \mathbb{T} -graph with its half edges labelled with numbers.

2.3.2 Constructing a surface graph from a rotation system

Let $R = (X, \sigma, \tau)$ be a rotation system. We define a graph $\Gamma_R = (V_R, E_R, s_R, t_R)$ as follows. $V_R = \{\text{cycles of } \sigma\}$ and $E_R = \{\text{cycles of } \tau\}$. For $(i, j) \in E_R$ define $s_R((i, j))$ to be the σ -orbit (σ -cycle) of i and $t_R((i, j))$ to be the σ -orbit (σ -cycle) of j . Notice that there is an arbitrary choice for specifying the source and the target since $(i, j) = (j, i)$. However, the underlying undirected graph will be independent of this choice.

A boundary walk in Γ_R is a closed walk $v_1, e_1, v_2, e_2, \dots, e_k, v_{k+1} = v_1$ satisfying the following condition. At each vertex v_i (including v_1), let $e_{i-1} = (a, b)$ where $a, b \in X$, $v_i = \sigma$ -orbit of b then $e_i = (\sigma(b), c)$ where $c \in X$.

For each of the boundary walks of length k in Γ_R , we take a polygon in the plane of degree k . Notice that each edge of Γ_R appears exactly twice in the boundary walks of Γ_R and this determines the orientations of the sides of the polygons. Now, by pasting each side of the polygons with its mate we obtain a Σ -graph $G_R = (\Gamma_R, \phi)$. In the following we state a theorem that was established independently by Heffter [48] and Edmonds [25].

Theorem 2.3.3. *If G is a cellular Σ -graph and R be the rotation system of G , then $G \cong G_R$. In particular, every cellular Σ -graph is uniquely determined, up to homeomorphism, by its rotation system. Conversely, if R is a rotation system, then $R \cong R_{G_R}$.*

Definition 2.3.4. *Let R be the rotation system of a cellular Σ -graph G . A boundary walk of G is a boundary walk of G_{R_G} .*

The previous definition of the boundary walks can be extended to noncellular surface

graphs by tracking of the homeomorphism type of each face.

Definition 2.3.5. Let F be a cellular face of a Σ -graph $G = (\Gamma, \phi)$. We say that F has nondegenerate boundary if no vertex occurs more than once among all boundary walks of F .

In Figure 2.14, the \mathbb{S} -graph G has degenerate and nondegenerate faces.

Lemma 2.3.6. A cellular face has nondegenerate boundary if and only if its unique boundary walk is a cycle in the graph.

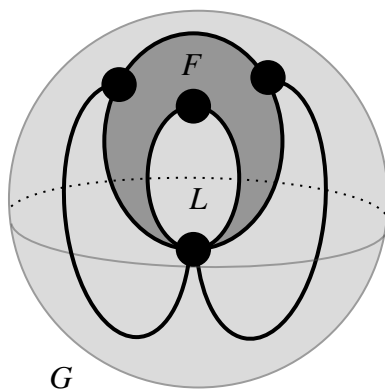


Figure 2.14: The face F of the \mathbb{S} -graph G is degenerate while the face L is nondegenerate.

Definition 2.3.7. Let F be a cellular face of a Σ -graph G . The degree of F is the length of its boundary walk.

Figure 2.15 provides two cellular surface graphs such that the degree of each face in such surface graphs is declared.

Lemma 2.3.8. For $i \geq 0$, let f_i be the number of faces of a cellular Σ -graph G with i edges. Then

$$\sum_{i \geq 0} i f_i = 2e \quad (2.1)$$

Proof. $\sum_{i \geq 0} i f_i$ is the sum of all face degrees. Each edge is counted twice in this sum. \square

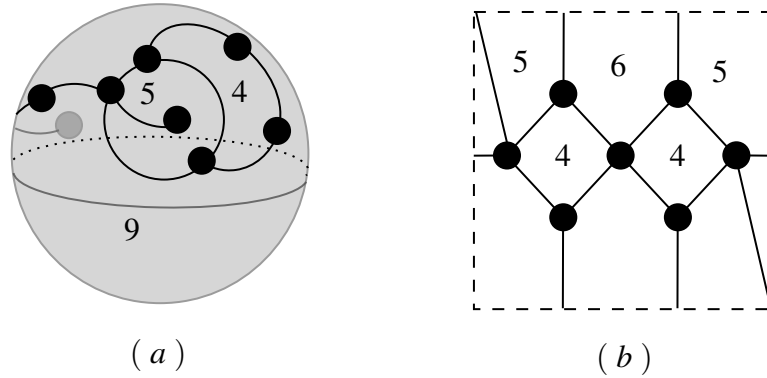


Figure 2.15: The degrees of the faces of the \mathbb{S} -graph in (a) and the \mathbb{T} -graph in (b) are written inside the faces.

2.4 Euler polyhedral formula

In this section we modify Euler polyhedral formula so that sparsity of a surface graph is included in the counting faces of the surface graph.

Definition 2.4.1. (*sparsity function*) Let Γ be a graph with vertex set V and edge set E . Let k be a nonnegative integer. Define $\gamma_k(\Gamma) = k|V| - |E|$.

For $i \geq 0$, let f_i be the number of faces of a cellular Σ -graph G with e edges. Let H be the set of the half edges of G . It is clear that $|H| = 2|E| = \sum_{i \geq 0} i f_i$. In the following we state the Euler's polyhedral formula, [2], [44], [99].

Theorem 2.4.2. Let G be a Σ -graph with vertex set V and edge set E . Let f be the number of the faces of G . If G is cellular, then

$$f - |E| + |V| = 2 - 2g \tag{2.2}$$

where g is the genus of Σ .

Notice that, for a cellular Σ -graph G , we have $f_0 \neq 0$ if and only if $\Sigma = \mathbb{S}$ and G has one vertex and no edges. The following theory is a modification of Theorem 2.4.2.

Theorem 2.4.3. Let $G = (\Gamma, \phi)$ be a cellular Σ -graph where $\Gamma = (V, E, s, t)$. Let k be a

nonnegative integer. Then

$$\sum_{i \geq 0} (i(k-1) - 2k)f_i = 2\gamma_k(G) + 4k(g-1) \quad (2.3)$$

Proof. Let v respectively e and f be the number of the vertices respectively edges and faces of G . By Euler's formula we get the following.

$$kf - (k-1)e = -(kv - e) + 2k - 2kg$$

The previous equation can be rewritten as follows.

$$2k \sum_{i \geq 0} f_i - 2e(k-1) = -2\gamma_k(G) - 4k(g-1)$$

By Lemma 2.3.8, the previous equation can be rewritten as follows.

$$2k \sum_{i \geq 0} f_i - \sum_{i \geq 0} i f_i (k-1) = -2\gamma_k(G) - 4k(g-1)$$

The required equation can be simply derived from the last equation. \square

Lemma 2.4.4. *Suppose that G is a cellular Σ -graph with genus g . Then*

$$4f_0 + 3f_1 + 2f_2 + f_3 = 8(1-g) - 2\gamma_2(G) + f_5 + 2f_6 + \dots$$

Proof. Substituting $k = 2$ in Equation 2.3 results the following.

$$\sum_{i \geq 0} (i-4)f_i = 2\gamma_2(G) + 8(g-1) \quad (2.4)$$

Expanding the summation in Equation 2.4 gives the following equation.

$$-4f_0 - 3f_1 - 2f_2 - f_3 + f_5 + 2f_6 + \dots = 2\gamma_2(G) - 8(1-g) \quad (2.5)$$

Reordering the terms in Equation (2.5) gives the required equation. \square

Chapter 3

Sparsity of Graphs and Surface Graphs

Sparse and tight graphs have been subject of much research and investigations. They have been used in many topics for their counting properties. In graph decomposition, for instance, Nash-William and Tutte stated and proved the well-known tree packing theorem, see Subsection 3.1.6.

Sparse and tight graphs have been inspired by the mathematical theory of rigidity theory (also known as geometric rigidity theory). The famous result in determining the rigidity status of a framework in two dimensions dates back to the work of Hilda Pollaczek-Geiringer, [78], [79] and Gerard Laman, [59]. They independently found a combinatorial characterisation for bar-joint frameworks in two dimensions, see Subsection 3.1.6. Their result is known as Laman's theorem. The combinatorial aspect of rigidity theory has been extended to involve different types of sparse and tight graphs. For example, Tay used a certain type of tight graphs to determine the rigidity status of body-bar frameworks in any dimension, see Subsection 3.1.6.

Sparsity and tightness of graphs have been also employed in geometric graph theory. Different geometric representations have been used to represent special kinds of sparse and tight graphs, [1].

In this chapter, we discuss the sparsity and tightness of graphs and surface graphs. We also state an important theorem, we call it hole filling theorem, which will be used frequently through this thesis.

3.1 Sparsity of graphs

In this section, we state the definitions of sparsity and tightness of graphs and provide some examples of such graphs. More background on the sparsity of graphs can be found in [29] and [75].

3.1.1 Definition of sparsity

We recall the following definition of the sparsity function.

Definition 3.1.1. *Let Γ be a graph with vertex set V and edge set E . Let k be a nonnegative integer. Define $\gamma_k(\Gamma) = k|V| - |E|$.*

Intuitively, we think of γ_k as a function that measures the k -dimensional 'degree of freedom' of the graph under consideration. An immediate property of the function γ_k is stated in the following lemma.

Lemma 3.1.2. *Let Γ_1 and Γ_2 be subgraphs of a graph $\Gamma = (V, E, s, t)$. Then*

$$\gamma_k(\Gamma_1 \cup \Gamma_2) = \gamma_k(\Gamma_1) + \gamma_k(\Gamma_2) - \gamma_k(\Gamma_1 \cap \Gamma_2)$$

Proof.

$$\begin{aligned} \gamma_k(\Gamma_1 \cup \Gamma_2) &= k|V(\Gamma_1 \cup \Gamma_2)| - |E(\Gamma_1 \cup \Gamma_2)| \\ &= k(|V(\Gamma_1)| + |V(\Gamma_2)| - |V(\Gamma_1 \cap \Gamma_2)|) - (|E(\Gamma_1)| + |E(\Gamma_2)| - |E(\Gamma_1 \cap \Gamma_2)|) \\ &= k|V(\Gamma_1)| - |E(\Gamma_1)| + k|V(\Gamma_2)| - |E(\Gamma_2)| - (k|V(\Gamma_1 \cap \Gamma_2)| - |E(\Gamma_1 \cap \Gamma_2)|) \\ &= \gamma_k(\Gamma_1) + \gamma_k(\Gamma_2) - \gamma_k(\Gamma_1 \cap \Gamma_2) \end{aligned}$$

□

Definition 3.1.3. *Let l, k be nonnegative integers with $l \leq k$. A graph Γ is called (k, l) -sparse if, for every nonempty subgraph Ω of Γ ,*

$$\gamma_k(\Omega) \geq l \tag{3.1}$$

If Γ is (k, l) -sparse and, in addition, $\gamma_k(\Gamma) = l$ then Γ is called (k, l) -tight.

3.1.2 Some basic lemmas

In the following we present some lemmas which survey some of the properties of (k, l) -sparse graphs. It is easy to prove the following lemma.

Lemma 3.1.4. *Let $\Gamma = (V, E, s, t)$ be a (k, l) -sparse graph. If $l = k$ then Γ has no loop edges.*

Lemma 3.1.5. *Let Ω be a subgraph of a graph Γ . If Γ is (k, l) -sparse then so is Ω .*

Proof. By sparsity definition. □

Lemma 3.1.6. *Let Ω be a subgraph of a (k, l) -sparse graph Γ . Then Ω is (k, l) -tight if and only if $\gamma_k(\Omega) = l$.*

Proof. By Lemma 3.1.5. □

Lemma 3.1.7. *Suppose that Γ_1 and Γ_2 are (k, l) -tight subgraphs of a (k, l) -tight Γ such that $\Gamma_1 \cap \Gamma_2$ is nonempty. Then $\Gamma_1 \cap \Gamma_2$ and $\Gamma_1 \cup \Gamma_2$ are (k, l) -tight.*

Proof. By Lemma 3.1.2, we get.

$$\gamma_k(\Gamma_1 \cup \Gamma_2) + \gamma_k(\Gamma_1 \cap \Gamma_2) = 2l \tag{3.2}$$

Since $\Gamma_1 \cap \Gamma_2$ and $\Gamma_1 \cup \Gamma_2$ are nonempty subgraphs of Γ . Thus, $\gamma_k(\Gamma_1 \cap \Gamma_2), \gamma_k(\Gamma_1 \cup \Gamma_2) \geq l$. However, (3.2) leads to $\gamma_k(\Gamma_1 \cap \Gamma_2) = \gamma_k(\Gamma_1 \cup \Gamma_2) = l$. Therefore, the require conclusion follows from Lemma 3.1.6. □

Lemma 3.1.8. *Let Γ be a (k, l) -sparse graph. If $\gamma_k(\Gamma) \leq 2l - 1$, then Γ is connected.*

Proof. Assume that Γ has two components Γ_1 and Γ_2 . By Lemma 3.1.2,

$$\begin{aligned} 2l - 1 &\geq \gamma_k(\Gamma) = \gamma_k(\Gamma_1 \cup \Gamma_2) \\ &= \gamma_k(\Gamma_1) + \gamma_k(\Gamma_2) - \gamma_k(\Gamma_1 \cap \Gamma_2) \\ &= \gamma_k(\Gamma_1) + \gamma_k(\Gamma_2) - 0 \\ &\geq 2l \end{aligned}$$

This is a contradiction. □

Lemma 3.1.9. *Let $\Gamma = (E, V, s, t)$ be a $(2, 2)$ -tight graph. Then the minimum degree of Γ is greater than 1.*

Proof. For contradiction, suppose that $v \in V$ with $\deg(v) = 1$. Let $e \in E$ such that $s(e) = v$ and $t(e) = u$ for some $u \in V$. Consider the subgraph $\Omega = (V', E', s', t')$ with $V' = V - \{v\}$ and $E' = E - \{e\}$, $s|_{E'} = s'$ and $t|_{E'} = t'$. Then

$$\begin{aligned} \gamma_2(\Omega) &= 2|V'| - |E'| \\ &= 2(|V| - 1) - (|E| - 1) \\ &= 2|V| - 2 - |E| + 1 \\ &= 2|V| - |E| - 1 \\ &= \gamma_2(\Gamma) - 1 \\ &= 1 < 2 \end{aligned}$$

□

3.1.3 Extending the sparsity definition for $l \geq k + 1$

The definition of sparsity can be extended to include the cases where $l \geq k + 1$ by the requirement that the inequality (3.1) is only satisfied for sufficiently large graphs. The sufficiently large depends on the particular k and l . For example, in the range $k + 1 \leq l \leq 2k - 1$, we generally require the inequality (3.1) only for subgraphs with at least one edge. More investigations on sparseness can be found in [45] and [84].

Lemma 3.1.10. *Suppose that $k + 1 \leq l \leq 2k - 1$ and Γ_1 and Γ_2 are (k, l) -tight subgraphs of a (k, l) -tight Γ such that $\Gamma_1 \cap \Gamma_2$ has at least two vertices. Then $\Gamma_1 \cap \Gamma_2$ and $\Gamma_1 \cup \Gamma_2$ are (k, l) -tight.*

3.1.4 Examples of (k, l) -sparse graphs

In the following we list a few examples of well-known graphs where they are also sparse graphs.

1. Planar graphs are $(3, 6)$ -sparse, Figure 3.1(a).

3.1. SPARSITY OF GRAPHS

2. An outerplanar graph is a planar graph which can be embedded in the plane so that all its vertices lie on the boundary of one face. Notice that outerplanar graphs are $(2,3)$ -sparse, Figure 3.1(b).

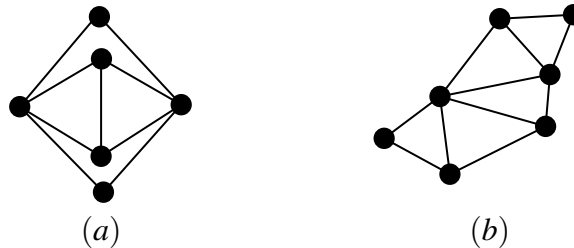


Figure 3.1: (a) A planar $(3,6)$ -sparse graph. (b) An outerplanar graph.

3.1.5 Examples of (k,l) -tight graphs

We provide some examples of various kinds of (k,l) -tight graphs.

Examples in figures

In Figure 3.2, we consider two types of tightness; $(2,0)$ -tight graph and $(2,2)$ -tight graphs.

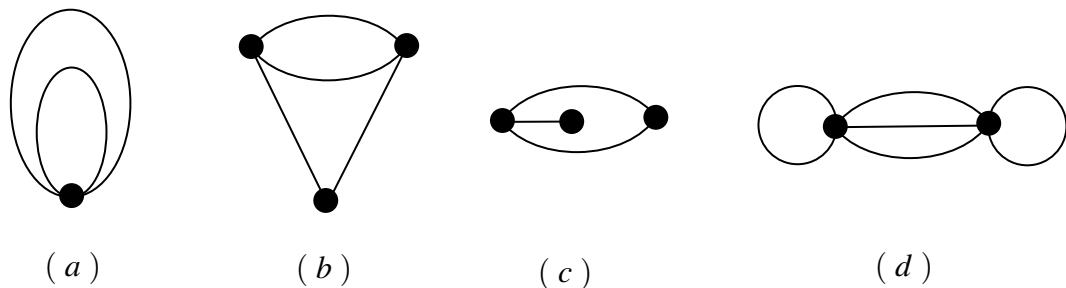


Figure 3.2: (a) A $(2,0)$ -tight graph. (b) A $(2,2)$ -tight graph. (c) A graph that is not $(2,2)$ -tight. However, this graph is $(2,2)$ -sparse. (d) A graph that is not $(2,0)$ -tight.

Well-known graphs

We include two examples where tightness is another characteristic of the corresponding graphs.

1. $(1, 1)$ -tight graphs are trees, see Figure 3.3(a).
2. $(1, 0)$ -tight graphs are graphs that are connected and have exactly one cycle, see Figure 3.3(b).

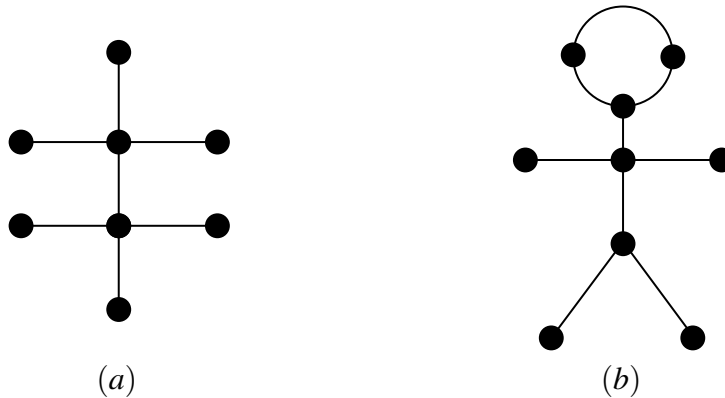


Figure 3.3: (a) A tree graph which is also $(1, 1)$ -tight. (b) A $(1, 0)$ -tight graph.

3.1.6 Applications

The robust counting of sparse and tight graphs has been employed in many areas whenever such graphs arise. Such counting applied in some topics in graph theory, like graph decomposition as we will see later. In the rigidity theory, counting on sparse and tight graphs found its way to contribute in solving many problems that arise in the combinatorial aspect of such theory. In geometric graph theory, tight graphs also have their contributions, see for example [3] and [1]. We will discuss representing certain tight torus graphs in the flat torus in Chapter 6. However, here we summarise two topics where sparse and tight graphs play significant roles in such topics.

Graph decomposition

The topic of graph decomposition concerns with finding a partition of the edge set of a graph into edge-disjoint subgraphs, although there is another kind of graph decomposition known as vertex-disjoint decomposition. Graph decomposition has been involved in many different areas such as network theory, coding theory, geometry, design theory and not ending with graphic theory. As an example, graph decomposition has been used in solving

3.1. SPARSITY OF GRAPHS

some geometric problems. In this area, a geometric problem is translated into a graph such that the vertex set of such a graph is the set of the geometric elements of the geometric problem and its edge set consists of the constraints, see [82] and [52]. The well-known result in graph decomposition is due to Tutte, [93], and Nash-Williams, [70]. They proved the following classical theorem.

Theorem 3.1.11. *A graph Γ is the union of k edge-disjoint trees if and only if Γ is (k, k) -tight.*

In Figure 3.4, there is a simple example of decomposing a $(2, 2)$ -tight graph.

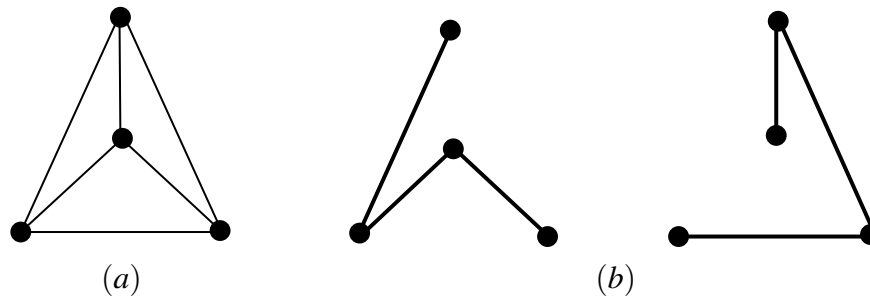


Figure 3.4: (a) A $(2, 2)$ -tight graph. (b) The decomposition of the graph in (a) into 2 edge-disjoint trees.

Nash-Williams also showed that every $(2, 2)$ -tight graph has a decomposition into two spanning trees, [71].

Rigidity theory

Rigidity theory studies the following question: Given a geometric embedding (typically a bar-joint framework) of a graph in a specific dimension, when is there a continuous motion or deformation of the vertices into a non-congruent embedding without changing the distances between pairs of vertices that are connected by edges? The process of investigating rigidity depends on combinatorial and geometric tools.

Historically, Cauchy, [2], and Maxwell, [34], introduced the mathematical theory of structural rigidity in the mid 19th century, which is, later on, was known as rigidity theory. In 1927, Pollaczek-Geiringer proved Theorem 3.1.14, [78], [79]. Then in 1970, Laman rediscovered and proved Theorem 3.1.14, [59]. Since then, rigidity theory is receiving

a lot of attention. In the following, we briefly survey some fundamental concepts of the rigidity theory, [41], [42], [54], [76].

A bar-joint framework is an ordered pair (G, p) where $G = (V, E)$ is a graph and $p : V \rightarrow \mathbb{R}^d$ is an embedding of the vertices into \mathbb{R}^d . A framework is generic if the coordinates of the framework points form an algebraically independent set (over \mathbb{Q}). Two frameworks on the same graph (G, p) and (G, q) are equivalent if the edge lengths in (G, p) are the same as those in (G, q) and are congruent if the distance between any pairs of points in (G, p) are the same as those in (G, q) .

Definition 3.1.12. A framework (G, p) is flexible in \mathbb{R}^d if there is a continuous motion $x(t)$ of the framework points such that $(G, x(t))$ is equivalent to (G, p) for all t but it is not congruent to (G, p) for some t (where $x(t) \neq p$). A framework (G, p) is rigid if it is not flexible.

Definition 3.1.13. A graph $G = (V, E)$ is called rigid if the framework (G, p) is rigid. G is called minimally rigid if removing any edge from G results flexibility.

Notice that every minimally rigid graph is rigid but the converse is not true in general, see Figure 3.5.

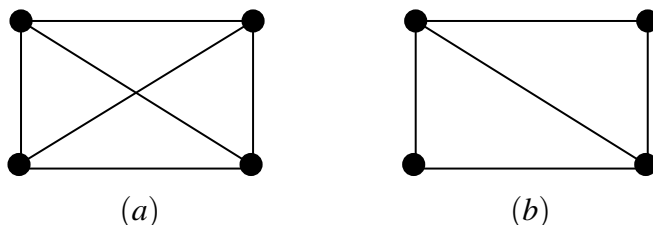


Figure 3.5: (a) A rigid graph in \mathbb{R}^2 . (b) A minimally rigid graph in \mathbb{R}^2 . Notice that the graph in (a) is not minimally rigid.

Theorem 3.1.14. A graph G is (generically) minimally rigid in the plane \mathbb{R}^2 if and only if G is $(2,3)$ -tight.

A graph that is $(2,3)$ -tight is known as Laman graph. Notice that Theorem 3.1.14, cannot be extended into three-dimension. The graph in Figure 3.6(e) (which is called the double banana graph) is a counterexample of such an extension.

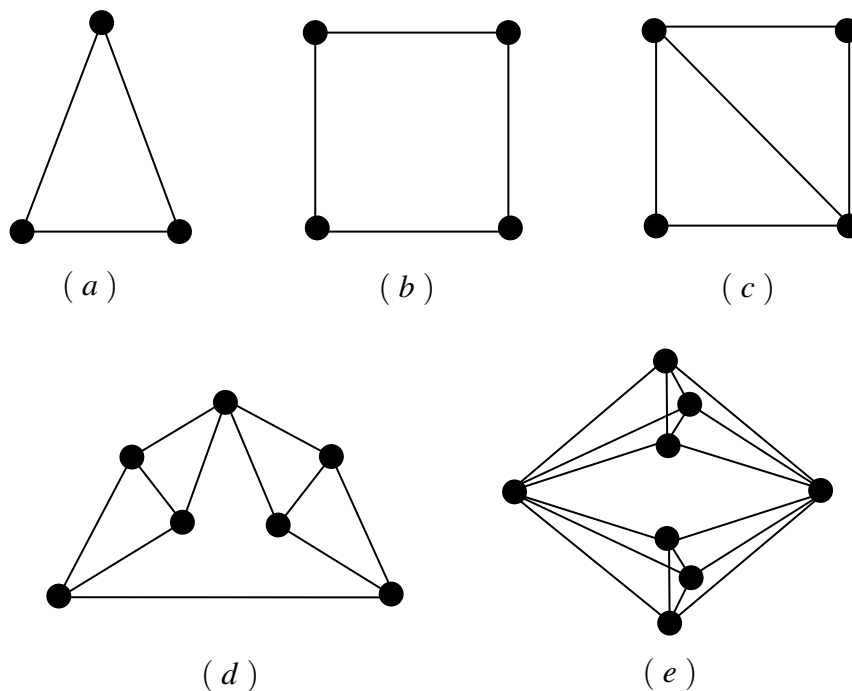


Figure 3.6: The graphs in (a), (c) and (d) are $(2,3)$ -tight and so they are rigid in the plane. The graph in (b) is not a $(2,3)$ -tight and the graph in (e), known as the double banana graph, is $(3,6)$ -tight.

In attempting to find a partial solution for the problem of deciding the rigidity in three dimensions, some works have been achieved on the rigidity of surface graphs. Gluck, [38], presented and proved the following theorem.

Theorem 3.1.15. [38] *Let $G = (\Gamma, \phi)$ be an \mathbb{S} -graph such that Γ is a triangulation. Then G is rigid if and only if G is $(3,6)$ -tight.*

This work has been followed by some other nice results. We recall some of them in Chapter 4 Section 4.1.

We end this brief survey on rigidity theory by stating a nice result which was established by Tay, [88]. Tay proved that $((\binom{d}{2}, \binom{d}{2}))$ -tight graphs are precisely those that admit a realisation as a generic rigid body-bar framework in \mathbb{R}^d . Where A d -dimensional body-and-bar framework is a bar-and-joint framework $G(p)$ in which the vertex set of G is partitioned into pairwise disjoint complete graphs (the bodies) and the remaining edges (bars), connecting these bodies, are pairwise disjoint, see [16].

3.2 The hole filing theorem

In this section, we state and prove a theorem, informally we call it the hole filling theorem which will be often used through the rest of this thesis.

3.2.1 Faces of surface subgraphs

In this subsection, we discuss the structure of the faces of surface subgraphs.

Definition 3.2.1. *Assume that $l \leq k$ and $G = (\Gamma, \phi)$ be a (k, l) -tight Σ -graph. Let F be a face of a Σ -subgraph H of G . We define $int_G(F)$ to be the Σ -subgraph of G corresponding to the vertices and the edges of Γ whose images lie in the topological closure of F . Similarly, we define $ext_G(F)$ to be the Σ -subgraph of G corresponding to those vertices and edges of Γ whose images lie in $\Sigma - F$.*

It is clear that $\partial F = int_G(F) \cap ext_G(F) = H \cap int_G(F)$ where ∂F is the Σ -subgraph $int_G(F) \cap ext_G(F)$ of G , see Figure 3.7.

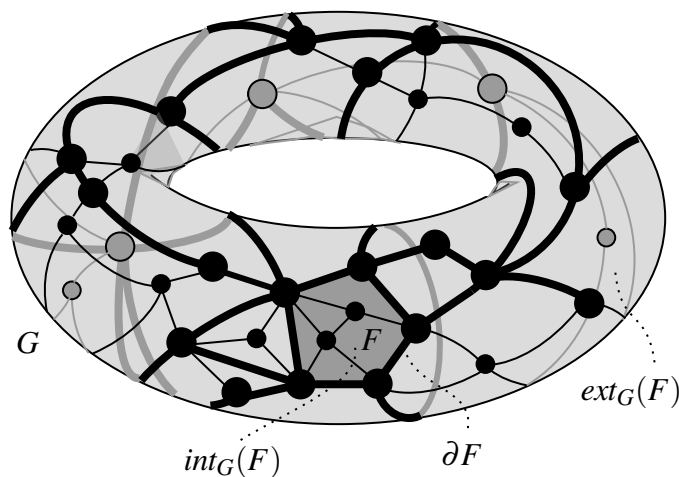


Figure 3.7: Consider the \mathbb{T} -graph G . The \mathbb{T} -subgraph that is bold has a pentagon face F where $int_G(F)$ is the \mathbb{T} -subgraph in the dark gray shaded area together with its boundary (i.e. ∂F). On the other hand, the \mathbb{T} -subgraph in the light gray shaded area together with ∂F is $ext_G(F)$.

3.2.2 The hole filling theorem

Theorem 3.2.2. *Let G be a (k, l) -tight Σ -graph with $l \leq k$ and H be a Σ -subgraph of G . Let F be a face in H . Then*

$$\gamma_k(H \cup \text{int}_G(F)) \leq \gamma_k(H) \quad (3.3)$$

Proof. By Lemma 3.1.2, we have

$$\begin{aligned} \gamma_k(H \cup \text{int}_G(F)) &= \gamma_k(H) + \gamma_k(\text{int}_G(F)) - \gamma_k(H \cap \text{int}_G(F)) \\ &= \gamma_k(H) + \gamma_k(\text{int}_G(F)) - \gamma_k(\partial F) \end{aligned} \quad (3.4)$$

Using Lemma 3.1.2 again, we obtain

$$\begin{aligned} l &= \gamma_k(G) \\ &= \gamma_k(\text{int}_G(F) \cup \text{ext}_G(F)) \\ &= \gamma_k(\text{int}_G(F)) + \gamma_k(\text{ext}_G(F)) - \gamma_k(\text{int}_G(F) \cap \text{ext}_G(F)) \\ &= \gamma_k(\text{int}_G(F)) + \gamma_k(\text{ext}_G(F)) - \gamma_k(\partial F) \end{aligned}$$

Therefore,

$$\gamma_k(\text{int}_G(F)) - \gamma_k(\partial F) = l - \gamma_k(\text{ext}_G(F)) \leq 0 \quad (3.5)$$

The previous inequality is derived from the sparsity of G . Now, by combining (3.4) and (3.5) the result follows. \square

Notice that $(2, 2)$ -tightness is necessary for Theorem 3.2.2. See the two examples in Figure 3.8.

Lemma 3.2.3. *Let G be a (k, l) -tight Σ -graph with $l \leq k$ and H be a Σ -subgraph of G and F be a face in H . Suppose that H is (k, l) -tight. Then $H \cup \text{int}_G(F)$ is also (k, l) -tight.*

Proof. Since G is (k, l) -tight then $\gamma_k(H \cup \text{int}_G(F)) \geq l$. Now, from Theorem 3.2.2,

we get $\gamma_k(H \cup \text{int}_G(F)) \leq \gamma_k(H) = l$. Thus, $\gamma_k(H \cup \text{int}_G(F)) = l$. \square

3.3 Contractions on closed walks

In this section, we consider three kinds of closed walk contractions in sparse graphs. We include some results related to these three contraction moves.

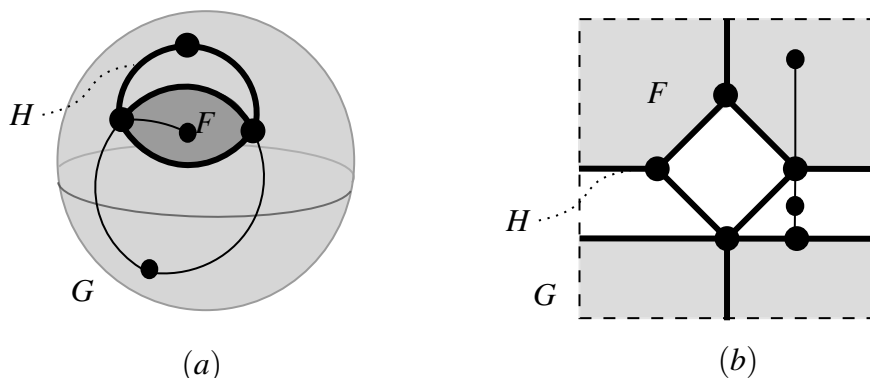


Figure 3.8: (a) The \mathbb{S} -graph G is not $(2,2)$ -tight. Its clear that $\gamma_2(H) = 2$. However, $\gamma_2(H \cup \text{int}_G(F)) = 3$. Thus, the conclusion of Theorem 3.2.2 does not hold. (b) The \mathbb{T} -graph G is not $(2,2)$ -tight. Its clear that $\gamma_2(H) = 2$. However, $\gamma_2(H \cup \text{int}_G(F)) = 3$. Thus, the inequality of Theorem 3.2.2 does not hold. Notice that in Figure (a) respectively (b), H in bold is a $(2,2)$ -tight \mathbb{S} respectively \mathbb{T} -subgraph of G and the face F is the shaded area together with its boundary.

3.3.1 Some operations on graphs

Two of the typical operations on graphs are edge contraction and edge deletion. In the following, we state such operations. For more background on graph operations, one can consult for example [23], [11] and [94].

Definition 3.3.1. Let $\Gamma = (V, E)$ be a graph and e be an edge in Γ . Let $\Gamma - e = (V', E')$ be a graph where $V' = V$ and $E' = E \setminus \{e\}$. We say that $\Gamma - e$ is the graph that is obtained from Γ by edge deletion.

Edge deletion operation is illustrated in Figure 3.9(a).

Definition 3.3.2. Let $\Gamma = (V, E)$ be a graph and $u, v \in V$. Let $\Gamma/u \sim v = (V', E')$ be a graph where $V' = (V \cup \{z\}) \setminus \{u, v\}$ and $E' = E$ such that z is incident to all edges in E which were incident to u and v . We say that $\Gamma/u \sim v$ is the graph that is obtained from Γ by identifying two vertices.

Figure 3.9(b) illustrates the operation of identifying two vertices.

Definition 3.3.3. Let $\Gamma = (V, E)$ be a graph and e be an edge in Γ that is incident to v and u where $u, v \in V$. Define Γ/e to be $(\Gamma - e)/u \sim v$. We say that Γ/e is the graph that is obtained from Γ by contracting the edge e .

Figure 3.9(c) illustrates the edge contraction operation.

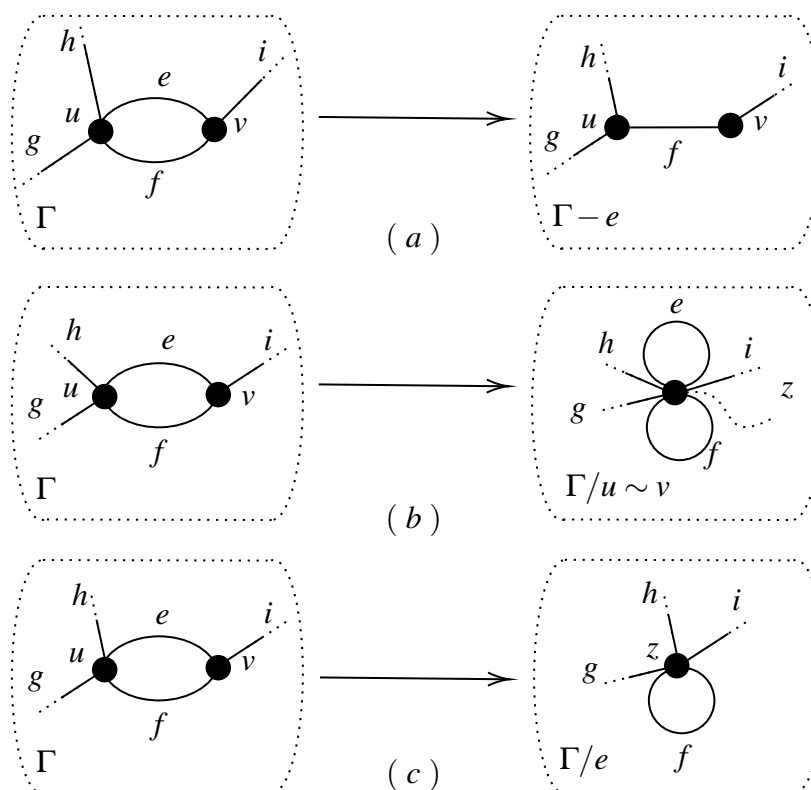


Figure 3.9: (a) The graph $\Gamma - e$ is obtained from Γ by deleting the edge e from the graph Γ . (b) The graph $\Gamma / u \sim v$ is obtained from Γ by identifying the vertices u and v together. (c) The graph Γ / e is obtained from Γ by contracting the edge e .

Now, we are ready to discuss in details contractions on three kinds of cycles. Namely 2-cycle, 3-cycle and 4-cycle contractions.

3.3.2 2-cycle contractions

Definition 3.3.4. A nondegenerate 2-cycle is a closed walk v_1, e_1, v_2, e_2, v_1 such that $e_1 \neq e_2$ and $v_1 \neq v_2$.

Definition 3.3.5. Let Γ be a $(2, l)$ -tight graph and v_1, e_1, v_2, e_2, v_1 be a nondegenerate 2-cycle in Γ . Define the 2-cycle contraction to be $(\Gamma / e_1) - e_2$.

The 2-cycle contraction move is illustrated in Figure 3.10. In the following we exhibit some fundamental properties of the 2-cycle contraction move.

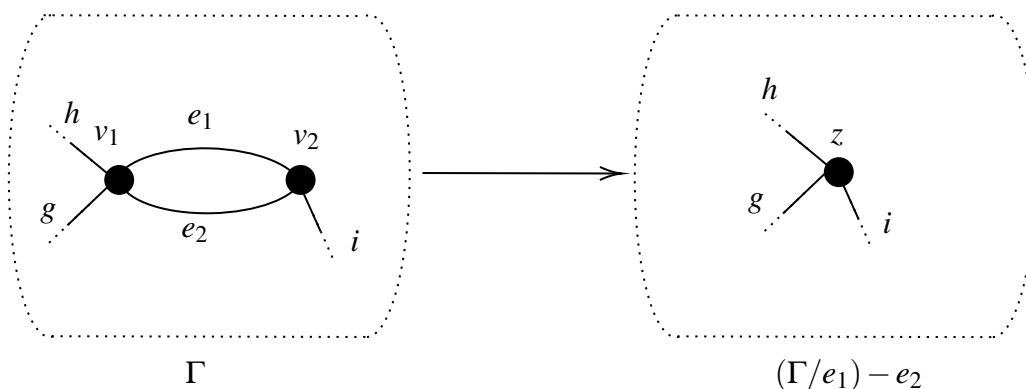


Figure 3.10: A 2-cycle contraction move.

Lemma 3.3.6. *Let $\Gamma = (V, E)$ be a graph and v_1, e_1, v_2, e_2, v_1 be a nondegenerate 2-cycle. Then $\gamma_2((\Gamma/e_1) - e_2) = \gamma_2(\Gamma)$.*

Proof. Consider the graph $(\Gamma/e_1) - e_2 = (V', E')$. Then $|V'| = |V| - 1$ and $|E'| = |E| - 2$. Hence

$$\begin{aligned}
 \gamma_2((\Gamma/e_1) - e_2) &= 2|V'| - |E'| \\
 &= 2(|V| - 1) - (|E| - 2) \\
 &= 2|V| - |E| \\
 &= \gamma_2(\Gamma)
 \end{aligned}$$

□

Lifting of a subgraph with respect to 2-cycle contraction

Let $\Gamma = (V, E, s, t)$ be a graph. Let Ω be a subgraph of $(\Gamma/e_1) - e_2$, we construct a lift $\bar{\Omega}$ as follows. $V(\bar{\Omega})$ is the preimage of $V(\Omega)$ under the quotient map $V(\Gamma) \rightarrow V((\Gamma/e_1) - e_2)$.

Given $e \in E(\Gamma)$, then $e \in \bar{\Omega}$ if and only if either e corresponds to an edge of Ω or $e = e_i$ for $i = 1$ or 2 , and $v_i, v_{i+1} \in V(\bar{\Omega})$, see Figure 3.11. Hence the proof of the following lemma follows easily from the previous setting.

Lemma 3.3.7. *Let $\Gamma = (V, E, s, t)$ be a graph and v_1, e_1, v_2, e_2, v_1 be a nondegenerate 2-cycle in Γ . Consider the graph $(\Gamma/e_1) - e_2$. Let Ω be a subgraph of $(\Gamma/e_1) - e_2$ and z*

3.3. CONTRACTIONS ON CLOSED WALKS

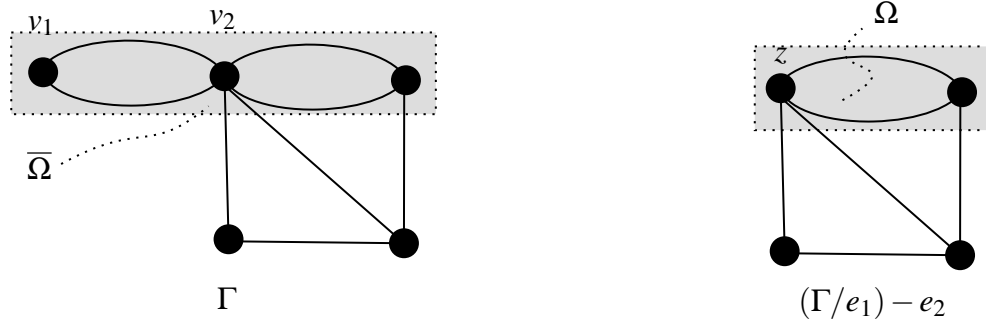


Figure 3.11: The subgraph $\bar{\Omega}$ of the graph Γ is the lift of the subgraph Ω of the 2-cycle contraction graph $(\Gamma/e_1) - e_2$.

be a vertex in $(\Gamma/e_1) - e_2$ such that z is resulted from $v_1 \sim v_2$. Then $\bar{\Omega} \cong \Omega$ if and only if $z \notin \Omega$.

Projection of a subgraph with respect to 2-cycle contraction

Let v_1, e_1, v_2, e_2, v_1 be a nondegenerate 2-cycle of a graph Γ . Given a subgraph, Θ , of Γ , we define the projection $\underline{\Theta}$ as follows. If $v_2 \notin \Theta$ then $\underline{\Theta} = \Theta$. If $v_2 \in \Theta$, then $\underline{\Theta} = (\Theta \cup e_1)/e_1 - e_2$.

Remark 3.3.8. Let v_1, e_1, v_2, e_2, v_1 be a nondegenerate 2-cycle of a graph Γ . Let Θ be a subgraph of Γ . Consider the graph $(\Gamma/e_1) - e_2$. Then $\underline{\Theta} \cong \Theta$ if and only if at least one vertex of e_1 does not belong to Θ and e_2 does not belong to Θ , see Figure 3.12.

Lemma 3.3.9. Let v_1, e_1, v_2, e_2, v_1 be a nondegenerate 2-cycle of a graph Γ . Then Γ is $(2, l)$ -sparse if and only if the 2-cycle contraction $(\Gamma/e_1) - e_2$ of Γ is $(2, l)$ -sparse.

Proof. Suppose that $(\Gamma/e_1) - e_2$ is not $(2, l)$ -sparse. So let $\Omega \subset (\Gamma/e_1) - e_2$ with $\gamma_2(\Omega) < l$. If $z \notin \Omega$, then by Lemma 3.3.7, $\bar{\Omega} \cong \Omega$ and so $\gamma_2(\bar{\Omega}) = \gamma_2(\Omega)$. If $z \in \Omega$ then by the construction of $\bar{\Omega}$ we have also $\gamma_2(\bar{\Omega}) = \gamma_2(\Omega)$. Both of the previous cases lead to a contradiction to the sparsity of Γ .

Now, suppose that Γ is not $(2, l)$ -sparse. Let $\Theta \subset \Gamma$ with $\gamma_2(\Theta) < l$. If $\{v_1, v_2\} \not\subset \Theta$, then $\underline{\Theta} \cong \Theta$. So $\gamma_2(\underline{\Theta}) = \gamma_2(\Theta) < l$. On the other hand, if $\{v_1, v_2\} \subset \Theta$, then $\gamma_2(\underline{\Theta}) = \gamma_2(\Theta \cup \{e_1, e_2\}) \leq \gamma_2(\Theta) < l$. This contradicts the sparsity of $(\Gamma/e_1) - e_2$. \square

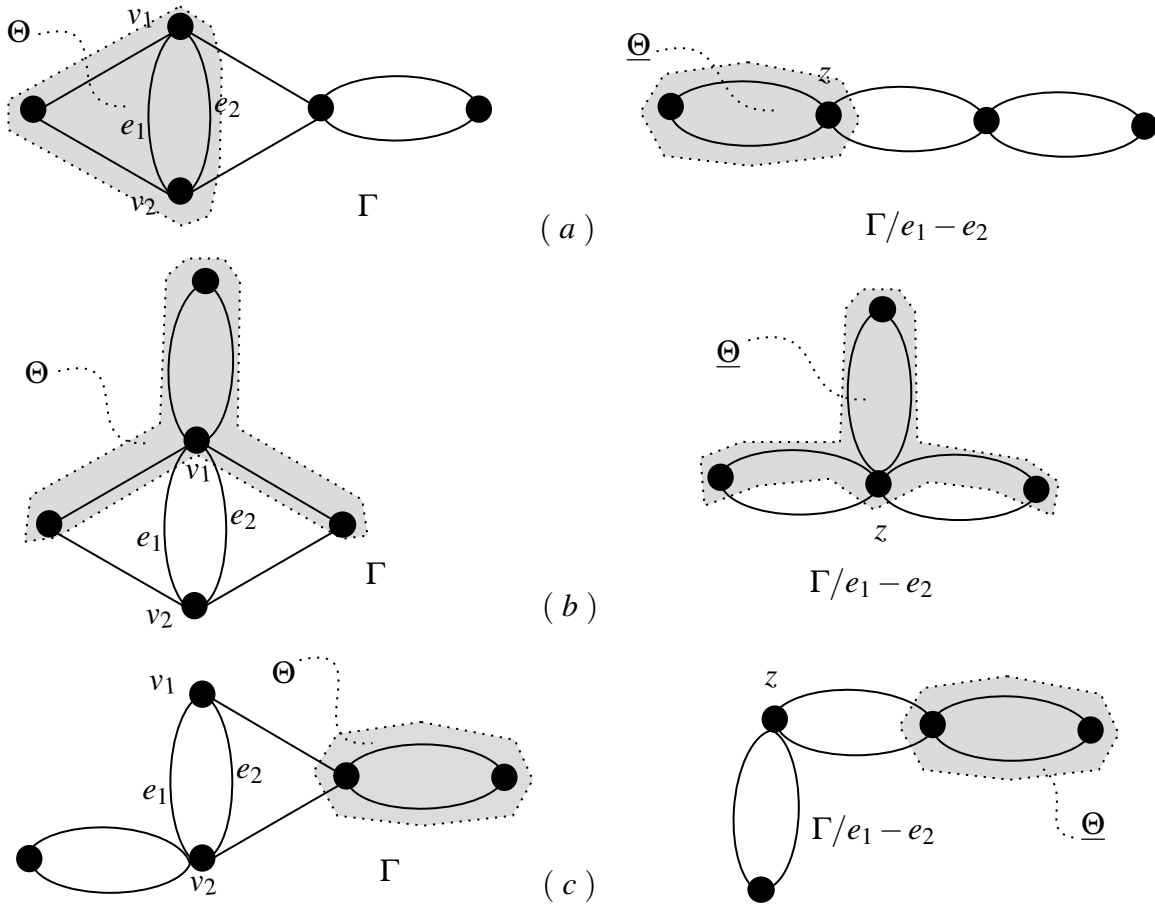


Figure 3.12: The subgraph $\underline{\Theta}$ of the 2-cycle contraction graph $(\Gamma/e_1) - e_2$ of Γ in (a) respectively (b) and (c) is the projection of the subgraph Θ of the graph Γ in (a) respectively (b) and (c).

3.3.3 3-cycle contractions

In $(2,2)$ -sparse graph, any closed walk of length 3 is necessary a cycle. More generally, we may consider closed walk $v_1, e_1, v_2, e_2, v_3, e_3, v_1$ such that $v_1 \neq v_2$.

Definition 3.3.10. Let Γ be a $(2,l)$ -tight graph and $v_1, e_1, v_2, e_2, v_3, e_3, v_1$ be a closed walk as described above. Let $(\Gamma/e_1) - e_i$ be the graph that is obtained from Γ by contracting the edge e_1 and then deleting e_i where $i = 2$ or 3 and e_i is different from e_1 . Let z be the vertex of $(\Gamma/e_1) - e_i$ corresponding to the identification $v_1 \sim v_2$.

We denote the move which obtains $(\Gamma/e_1) - e_i$ from Γ by $\Gamma \rightarrow (\Gamma/e_1) - e_i$, see Figure

3.13.

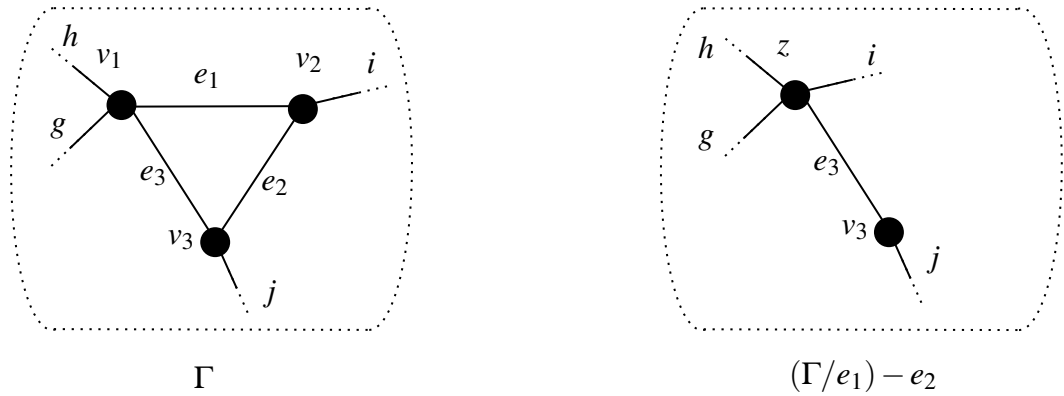


Figure 3.13: A 3-contraction move.

We observe in the case that both e_2 and e_3 are different from e_1 , then, in Γ/e_1 , the edges e_2 and e_3 are parallel. Thus, the choice of which one is deleted does not affect the isomorphism class of the resulting graph, Figure 3.14. Note that in our later work

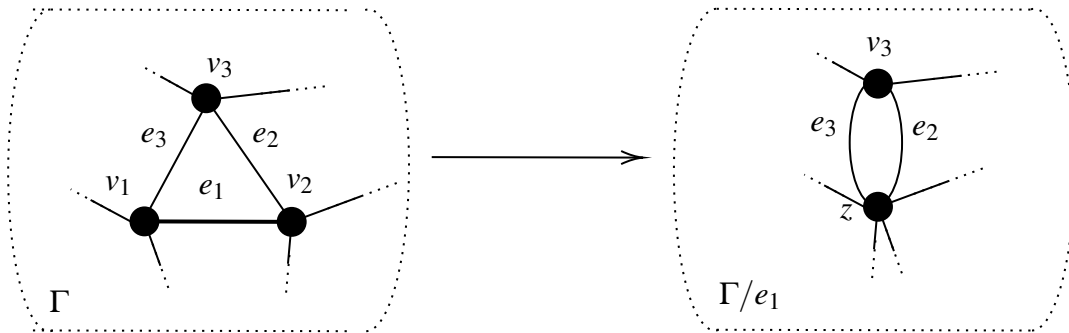


Figure 3.14: Contracting e_1 in Γ results a pair of parallel edges e_2 and e_3 in Γ/e_1 . Thus, deleting the edge e_2 or e_3 yields no affect.

we will mainly be focused on the $(2, 2)$ -sparse graphs. In that case, as noted above, all closed walks of length 3 are necessarily cycles, so we do not have to worry about any degeneracies in that case. However, we have tried to state the following lemmas in a more general setting to allow for possible future applications to $(2, 1)$ and $(2, 0)$ -sparse graphs.

Lifting of a subgraph with respect to 3-cycle contraction

Let Γ be a $(2, l)$ -tight graph and $v_1, e_1, v_2, e_2, v_3, e_3, v_1$ be a closed walk of length 3 in Γ with $v_1 \neq v_2$.

Given a subgraph Ω of $(\Gamma/e_1) - e_i$ we define $\bar{\Omega}$ as follows. $V(\bar{\Omega})$ is the preimage of $V(\Omega)$ under the quotient map $V(\Gamma) \rightarrow V((\Gamma/e_1) - e_i)$ and $E(\bar{\Omega})$ consists of $E(\Omega)$ together with any e_1, e_2, e_3 spanned by $V(\bar{\Omega})$. Figure 3.15 presents an example of lifting a subgraph with respect to 3-cycle contraction.

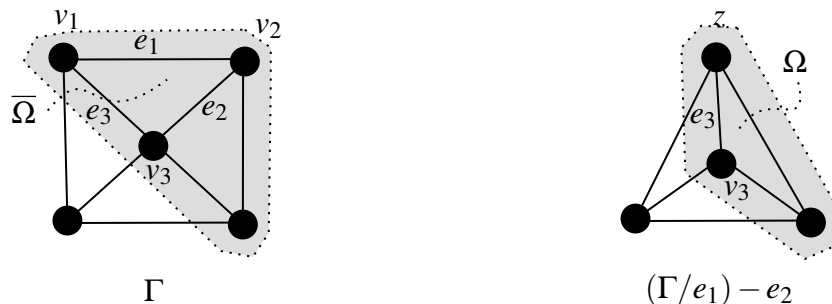


Figure 3.15: The subgraph $\bar{\Omega}$ of the graph Γ is the lift of the subgraph Ω of the 3-cycle contraction graph $\Gamma/e_1 - e_2$ (of Γ).

Projection of a subgraph with respect to 3-cycle contraction

Let Γ be a $(2, l)$ -tight graph and $v_1, e_1, v_2, e_2, v_3, e_3, v_1$ be a closed walk of length 3 in Γ with $v_1 \neq v_2$.

Given a subgraph Θ of Γ , we define $\underline{\Theta}$ to be the subgraph of $(\Gamma/e_1) - e_i$ which is obtained by identifying v_1 and v_2 and then deleting any of the edges e_1, e_2, e_3 from the resulting graph which they are not in $(\Gamma/e_1) - e_i$. See the example in Figure 3.16.

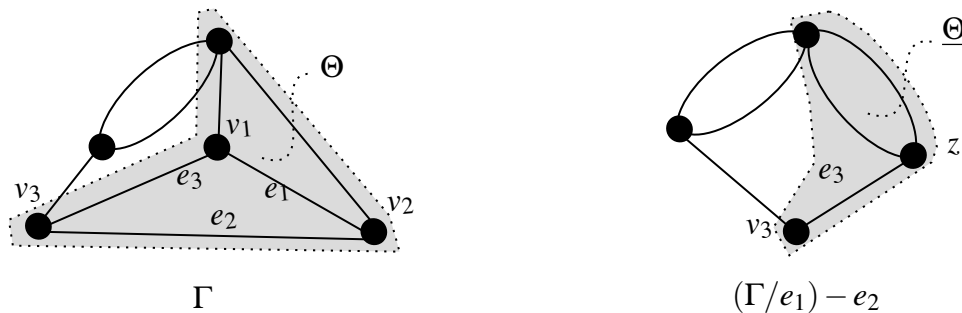


Figure 3.16: The subgraph $\underline{\Theta}$ of the 3-cycle contraction graph $(\Gamma/e_1) - e_2$ (of Γ) is the projection of the subgraph Θ of the graph Γ .

3.3. CONTRACTIONS ON CLOSED WALKS

Lemma 3.3.11. *Suppose that e_1, e_2 and e_3 are the edges of a 3-cycle in a graph Γ such that $e_1 \neq e_2, e_3$. For $i = 2$ or 3 , if $(\Gamma/e_1) - e_i$ is $(2, l)$ -sparse then so is Γ .*

Proof. From the hypothesis and a previous assumption that $v_1 \neq v_2$, we can see that the three edges e_1, e_2 and e_3 are distinct. Now let Θ be an induced subgraph of Γ . Then it is clear that $\gamma_2(\underline{\Theta}) \leq \gamma_2(\Theta)$. From the sparsity of $(\Gamma/e_1) - e_i$ we get that $\gamma_2(\Theta) \geq l$. \square

We comment that Lemma 3.3.11 holds even in degenerate cases where one of e_2 or e_3 is a loop edge. On the other hand, the hypothesis $e_1 \neq e_2, e_3$ is necessary. For example if $l = 2$, $e_1 = e_3$ and e_2 is a loop edge, then the conclusion is false, see the example in Figure 3.17.

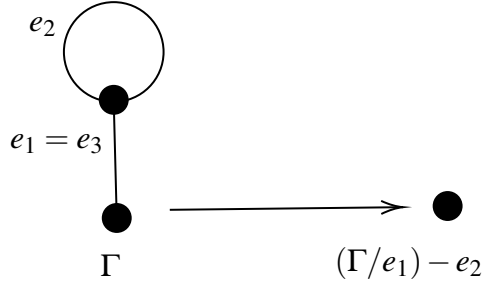


Figure 3.17: The graph $(\Gamma/e_1) - e_2$ is $(2, 2)$ -tight while the graph Γ is not $(2, 2)$ -tight.

Lemma 3.3.12. *Suppose that Γ is a $(2, l)$ -sparse and let $v_1, e_1, v_2, e_2, v_3, e_3, v_1$ be a 3-cycle in Γ with $v_1 \neq v_2$. Then for $i = 2$ or 3 , $(\Gamma/e_1) - e_i$ is not $(2, l)$ -sparse if and only if there is some subgraph Π of Γ such that Π is $(2, l)$ -tight and $e_1 \in \Pi$ but $v_3 \notin \Pi$.*

Proof. Suppose Π exists as in the statement. It is clear that $\gamma_2(\underline{\Pi}) = \gamma_2(\Pi) - 1 = l - 1$. Hence $\gamma_2(\underline{\Pi}) < l$.

On the other hand, suppose that $\Gamma/e_1 - e_i$ is not $(2, l)$ -sparse. Let $\gamma_2(\Omega) < l$ for some subgraph Ω of $\Gamma/e_1 - e_i$. Without loss of generality, assume that Ω is an induced subgraph of $\Gamma/e_1 - e_i$. Let $\Pi = \overline{\Omega}$. Let z be the vertex in $(\Gamma/e_1) - e_i$ that is corresponding to the identification $v_1 \sim v_2$. Clearly $z \in \Omega$ since if not then $\Pi \cong \Omega$ which contradicts the sparsity of Γ . Notice that $\gamma_2(\Pi) \leq \gamma_2(\Omega) + 1$. Therefore, $\gamma_2(\Omega) = l - 1$ and $\gamma_2(\Pi) = l$ and so Π is $(2, l)$ -tight. Therefore, $e_1 \in \Pi$ and $e_2, e_3 \notin \Pi$. Finally, since Ω is induced by its vertex set, then it is clear that $v_3 \notin \Pi$. \square

Definition 3.3.13. The subgraph Π in Lemma 3.3.12 is called a blocker for the 3-cycle contraction move of $\Gamma \rightarrow (\Gamma/e_1) - e_i$ where $i = 2$ or 3.

In general such a blocker looks like the one in Figure 3.18.

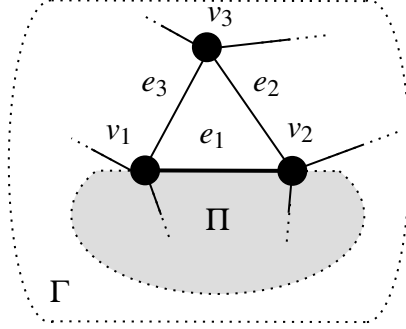


Figure 3.18: Π is a blocker for a 3-contraction move.

In Figure 3.19, we provide some examples of graphs where blockers of conducting certain 3-contraction moves are highlighted.

Lemma 3.3.14. Suppose that Γ is $(2,2)$ -sparse graph. Let $v_1, e_1, v_2, e_2, v_3, e_3, v_1$ be a closed walk in Γ . Then at least two of the graphs $\Gamma/e_1 - e_2$, $\Gamma/e_2 - e_3$ or $\Gamma/e_3 - e_1$ are $(2,2)$ -sparse.

Proof. Since Γ is $(2,2)$ -sparse then v_1, v_2, v_3 are distinct. So the closed walk $v_1, e_1, v_2, e_2, v_3, e_3, v_1$ is simple. In particular, this means that the three graphs $\Gamma/e_1 - e_2$, $\Gamma/e_2 - e_3$ or $\Gamma/e_3 - e_1$ are 3-cycle contractions of Γ . Now, suppose that Π_1 , respectively Π_2 is a blocker for the move $\Gamma \rightarrow \Gamma/e_1 - e_2$, respectively $\Gamma \rightarrow \Gamma/e_2 - e_3$. It follows that $v_1, v_2, v_3 \in \Pi_1 \cup \Pi_2$ and $e_3 \notin \Pi_1 \cup \Pi_2$. Notice that by Lemma 3.1.7, $\Pi_1 \cup \Pi_2$ is $(2,2)$ -tight. Therefore,

$$\begin{aligned} \gamma_2(\Pi_1 \cup \Pi_2 \cup \{e_3\}) &= \gamma_2(\Pi_1 \cup \Pi_2) + \gamma_2(\{e_3\}) - \gamma_2(\Pi_1 \cap \Pi_2 \cap \{e_3\}) \\ &= \gamma_2(\Pi_1 \cup \Pi_2) + \gamma_2(\{e_3\}) - \gamma_2(\{v_2, v_3\}) \\ &= 2 + 3 - 4 \end{aligned}$$

This contradicts the sparsity of Γ . □

We observe that Lemma 3.3.14 also works for $(2, l)$ -sparseness for $l \leq 1$ if we add the additional hypothesis that v_1, v_2 and v_3 are pairwise distinct.

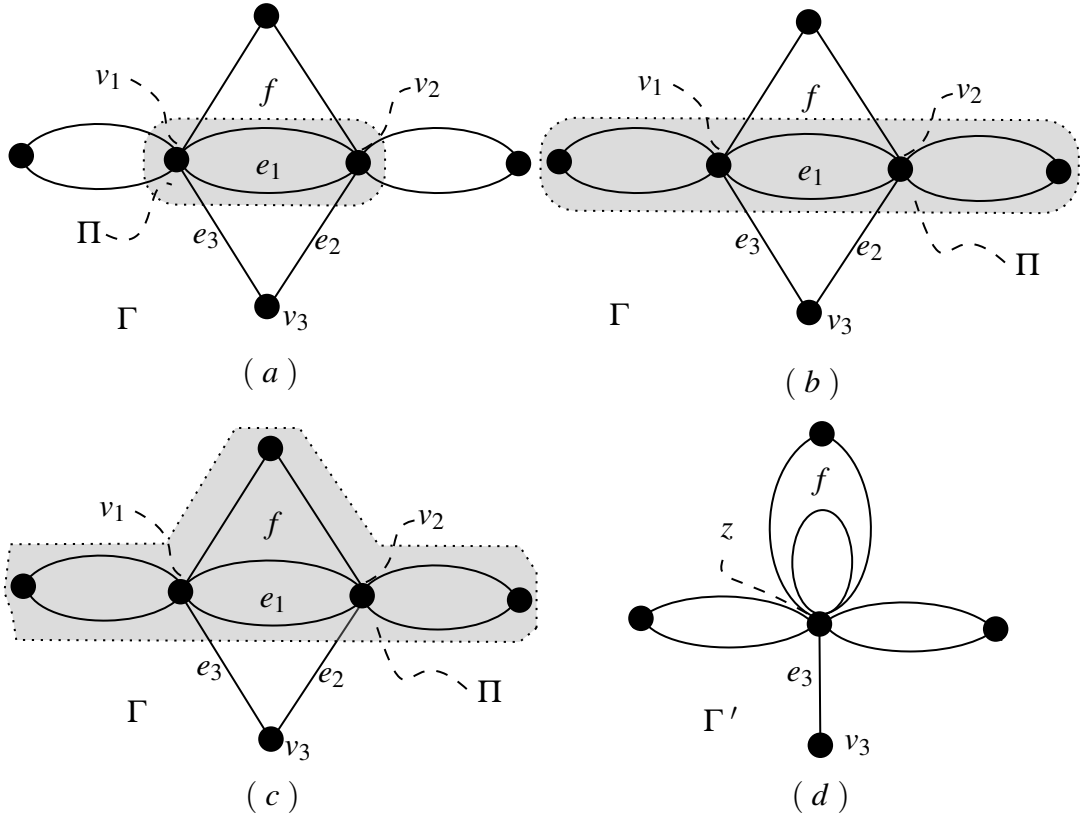


Figure 3.19: In each of (a), (b) and (c), the $(2,2)$ -tight subgraph Π of the $(2,2)$ -tight graph Γ is a blocker for the 3-cycle contraction $\Gamma/e_1 - e_2$. The blocker Π in (c) is the maximal blocker for $\Gamma \rightarrow \Gamma/e_1 - e_2$. The graph Γ' in (d) is obtained by performing $\Gamma \rightarrow \Gamma/e_1 - e_2$. However, It is clear that Γ' is not a $(2,2)$ -sparse graph as there is a loop in it.

3.3.4 4-cycle contractions

Definition 3.3.15. A nondegenerate 4-cycle is a closed walk $v_1, e_1, v_2, e_2, v_3, e_3, v_4, e_4, v_1$ such that $v_i \neq v_{i+1}$ for $i = 1, \dots, 4$, $e_i \neq e_{i+1}$ for $i = 1, 2, 3$, $e_1 \neq e_3$ and $e_2 \neq e_4$.

Lemma 3.3.16. let $v_1, e_1, v_2, e_2, v_3, e_3, v_4, e_4, v_1$ be a closed walk in a graph Γ . If $v_1 \neq v_3$ and $e_1 = e_3$ then $e_2 \neq e_4$.

Proof. The hypothesis indicates that $v_2 = v_3$ and $v_1 = v_4$. Therefore, $e_2 \neq e_4$. See Figure 3.20. \square

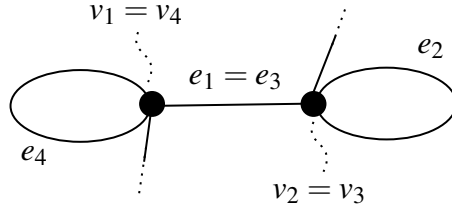


Figure 3.20: The conclusion of Lemma 3.3.16.

Definition 3.3.17. Let Γ be a $(2, l)$ -tight graph and let $v_1, e_1, v_2, e_2, v_3, e_3, v_4, e_4, v_1$ be a closed walk in Γ . Assume that $v_1 \neq v_3$ and define the 4-cycle contraction $(\Gamma/v_1 \sim v_3) - \{e_1, e_3\}$ to be the graph that is obtained from Γ by identifying v_1 and v_3 together and deleting the edges e_1 and e_3 . In case $e_1 = e_3$, we notice from the previous lemma that $e_2 \neq e_4$, hence we can define the 4-cycle contraction $(\Gamma/v_1 \sim v_3) - \{e_2, e_4\}$.

Figure 3.21 shows how 4-contraction move can be performed. Notice that for the previous definition, in case $e_1 = e_3$, defining the 4-cycle contraction $(\Gamma/v_1 \sim v_3) - \{e_2, e_4\}$ has no effect on any of the rest of the arguments in this thesis. Moreover, such a case cannot even arise in the case of $(2, 2)$ -tight graphs since loop edges are prohibited in that case.

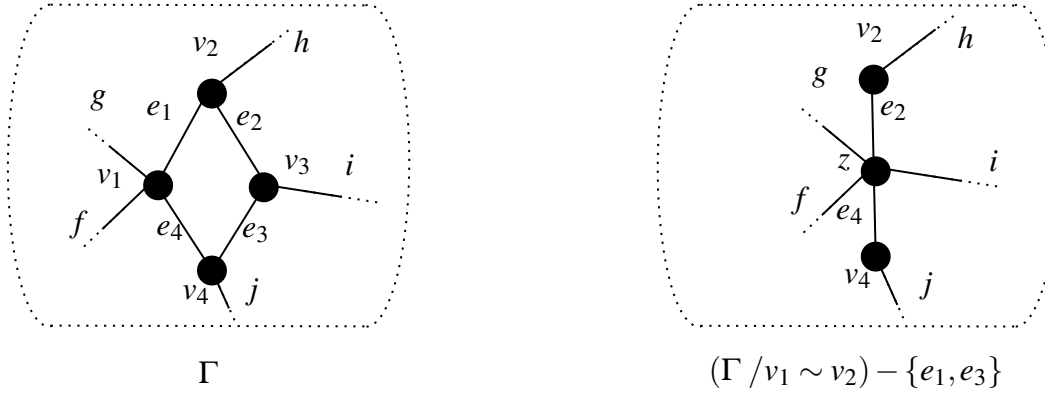


Figure 3.21: A 4-cycle contraction on the graph Γ .

Lifting a subgraph with respect to 4-cycle contraction

Let Γ be a $(2, l)$ -tight graph and let $v_1, e_1, v_2, e_2, v_3, e_3, v_4, e_4, v_1$ be a closed walk in Γ with $v_1 \neq v_3$. Let Ω be a subgraph of $(\Gamma/v_1 \sim v_3) - \{e_1, e_3\}$. We can define a lift $\bar{\Omega}$

3.3. CONTRACTIONS ON CLOSED WALKS

as follows. $V(\overline{\Omega})$ is the preimage of $V(\Omega)$ under the quotient map $V(\Gamma) \longrightarrow V((\Gamma/v_1 \sim v_3) - \{e_1, e_3\})$.

Given $e \in E(\Gamma)$, then $e \in \overline{\Omega}$ if and only if either e corresponds to an edge of Ω or $e = e_i$ for $i = 1$ or 3 , and $v_i, v_{i+1} \in V(\overline{\Omega})$. See the example in Figure 3.22.

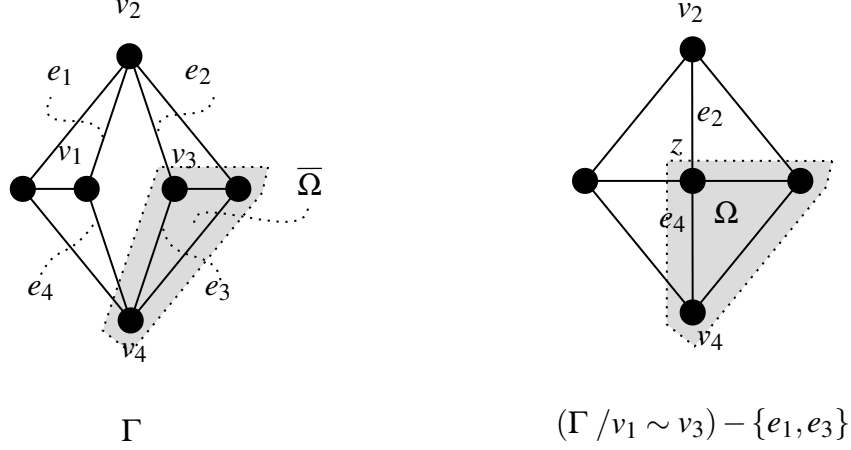


Figure 3.22: The subgraph $\overline{\Omega}$ of the graph Γ in (a) is the lift of the subgraph Ω of the 4-cycle contraction graph $(\Gamma/v_1 \sim v_3) - \{e_1, e_3\}$ (of Γ) in (b).

Theorem 3.3.18. *Let $v_1, e_1, v_2, e_2, v_3, e_3, v_4, e_4, v_1$ be a closed walk in a graph Γ . Suppose that $e_i \neq e_{i+1}$ for $i = 1, 2, 3$ and $e_4 \neq e_1$. If Γ is $(2, l)$ -sparse and $(\Gamma/v_1 \sim v_3) - \{e_1, e_3\}$ is not $(2, l)$ -sparse. Then at least one of the following statements is true.*

1. *There is a subgraph Π of Γ such that $\gamma_2(\Pi) = l, \{v_1, v_3\} \subset \Pi$ and exactly one of v_2 or v_4 belong to Π .*
2. *There is a subgraph Π of Γ such that $\gamma_2(\Pi) = l + 1, \{v_1, v_3\} \subset \Pi$ and $v_2, v_4 \notin \Pi$.*

Proof. Suppose that Ω be a subgraph of $(\Gamma/v_1 \sim v_3) - \{e_1, e_3\}$ such that $\gamma_2(\Omega) < l$. Without loss of generality, we assume that Ω is induced by its vertex set. Let $\Pi = \overline{\Omega}$ and let z be the vertex in $(\Gamma/v_1 \sim v_3) - \{e_1, e_3\}$ that corresponds to v_1 and v_2 . It is clear that $z \in \Omega$ since if not then $\Pi \cong \Omega$. Also, it is clear that $\{v_2, v_4\} \not\subset \Pi$, otherwise $\gamma_2(\Pi) = \gamma_2(\Omega)$, since Ω is an induced subgraph of $(\Gamma/v_1 \sim v_3) - \{e_1, e_3\}$.

Now, suppose that $v_2 \in \Pi$. Then $v_4 \notin \Pi$ and $e_1, e_2 \in \Pi$ and $\gamma_2(\Pi) = \gamma_2(\Omega) + 1 \leq l$. Since Γ is $(2, l)$ -sparse then $\gamma_2(\Pi) = l$ and clearly (1) holds in this case. Similar arguments apply if $v_4 \in \Pi$. Now if $v_2, v_4 \notin \Pi$ then $\gamma_2(\Pi) = \gamma_2(\Omega) + 2 \leq l + 1$. If $v_2 = v_4$ then

$\gamma_2(\Pi \cup \{v_2\} \cup \{e_1, e_2, e_3, e_4\}) \leq l - 1$ contradicting the sparsity of Γ . Hence $v_2 \neq v_4$ in this case.

Now, if $\gamma_2(\Pi) = l + 1$, then (2) holds. Thus, we suppose that $\gamma_2(\Pi) = l$. If $v_2 \notin \{v_1, v_3\}$, then replace Π by $\Pi \cup \{v_2, e_1, e_2\}$ and (1) holds. Similarly if $v_4 \notin \{v_1, v_3\}$. There is only one possibility that remains in this case is that $v_2 \in \{v_1, v_3\}$ and that $v_4 \in \{v_1, v_3\}$. One readily checks that in this case that $\Gamma \longrightarrow (\Gamma/v_1 \sim v_3) - \{e_1, e_3\}$ is in fact equivalent to a contraction on a pair of parallel edges.

By Lemma 3.3.9, this preserves the sparseness contradicting the assumption that $(\Gamma/v_1 \sim v_3) - \{e_1, e_3\}$ is not $(2, l)$ -sparse. \square

Definition 3.3.19. We call the subgraph Π in Lemma 3.3.18(1) respectively Lemma 3.3.18(2) a blocker of type 1 respectively of type 2 for the 4-cycle contraction move $\Gamma \longrightarrow (\Gamma/v_1 \sim v_3) - \{e_1, e_3\}$.

In general, the blocker of type 1 respectively type 2 looks like as in Figure 3.23(a) respectively 3.23(b).

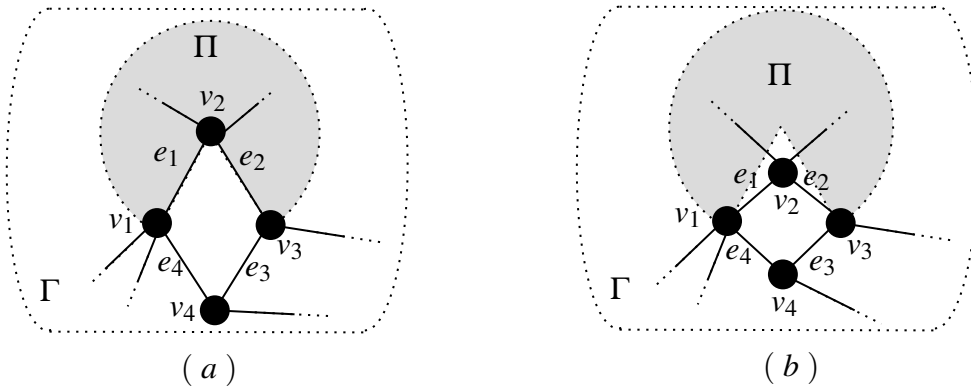


Figure 3.23: (a) Π is a blocker of type 1. (b) Π is a blocker of type 2.

In Figure 3.24, we include more examples of blockers for certain 4-contraction moves.

We observe that it is possible that a 4-cycle contraction move can have more than one blockers of type 1 or type 2. See Figure 3.24(b).

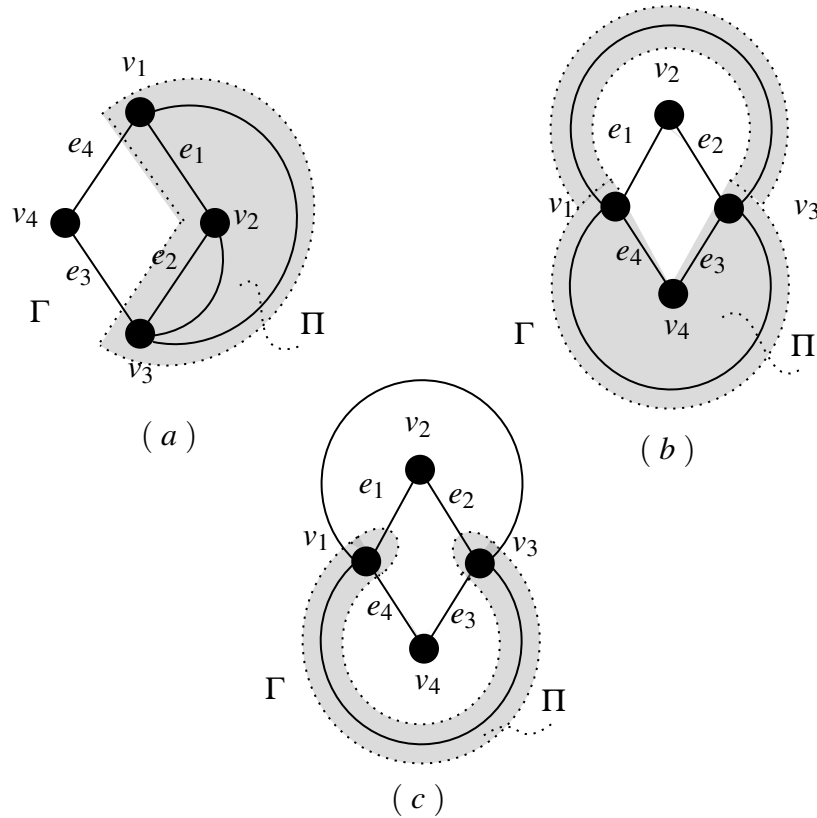


Figure 3.24: The $(2, 2)$ -tight subgraph Π of the $(2, 2)$ -tight graph Γ in (a) respectively (b) is a blocker of type 1 for $\Gamma \rightarrow (\Gamma/v_1 \sim v_3) - \{e_1, e_3\}$. This blocker is also maximal. The subgraph Π of the $(2, 2)$ -tight graph Γ in (c) is a blocker of type 2 for $\Gamma \rightarrow (\Gamma/v_1 \sim v_3) - \{e_1, e_3\}$. This blocker is also maximal.

3.4 Inductive operations on surface graphs

In this section, we discuss three inductive operations on surface graphs. Each of these three topological inductive moves is indeed the topological version of one of the three contractions that we discussed in the previous section.

3.4.1 Topological contraction and deletion of an edge

We define the topological version of contracting and deleting an edge of a surface graph. We state first the definition of an edge contraction of a Σ -graph.

Definition 3.4.1. Let $G = (\Gamma, \phi)$ be a Σ -graph. Let e be an edge in $\Gamma = (V, E, s, t)$ such that $s(e) = u, t(e) = v, \phi(u) \neq \phi(v)$. Let $|e| = \phi(e \times I)$ be the realisation of the edge e . There is a quotient map $q : \Sigma \rightarrow \Sigma/|e|$. As a consequence of the Jordan-Schoenflies theorem ([13]), we can fix a homeomorphism $h : \Sigma \rightarrow \Sigma/|e|$ such that $h^{-1} \circ q$ is the identity outside a regular neighbourhood of $|e|$. Now, let Γ/e be the graph that is obtained from Γ by contracting the edge e . It is clear that $q \circ \phi$ induces an embedding $\bar{\phi} : |\Gamma/e| \rightarrow \Sigma/|e|$. Hence we define a Σ -graph G/e to be the pair $(\Gamma/e, h^{-1} \circ q)$ and we say that G/e is obtained from G by a topological edge contraction.

Figure 3.25 clarifies Definition 3.4.1.

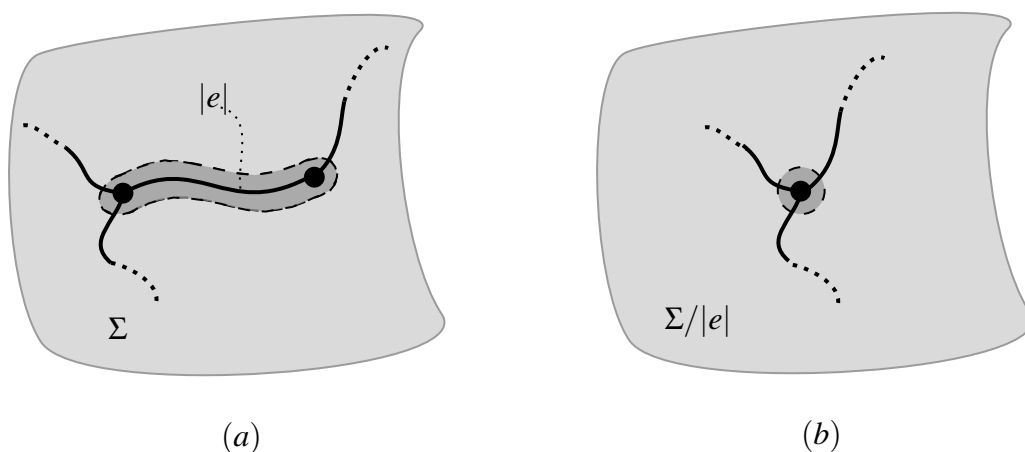


Figure 3.25: (a) The realisation of the edge e in Σ . A regular neighbourhood of $|e|$ is in the shaded dark gray area. (b) Contracting $|e|$ in Σ .

Topological edge deletion on the other hand is more straightforward to be defined than edge contraction as we can see in the following.

Definition 3.4.2. Let $G = (\Gamma, \phi)$ be a Σ -graph. Let e be an edge in Γ . Let $\Gamma - e$ is the graph that is obtained from Γ by deleting the edge e . We define the Σ -graph $G - e$ to be the pair $(\Gamma - e, \phi|_{|\Gamma - e|})$ and we say that $G - e$ is obtained from G by a topological edge deletion.

We note that topological edge deletion may change a cellular surface graph into a noncellular surface graph, see Figure 3.26 (a). On the other hand, topological edge contraction preserves the homeomorphism type of all faces. However, it is not necessary that topological edge contraction preserves the boundary of all the faces, see Figure 3.26(b).

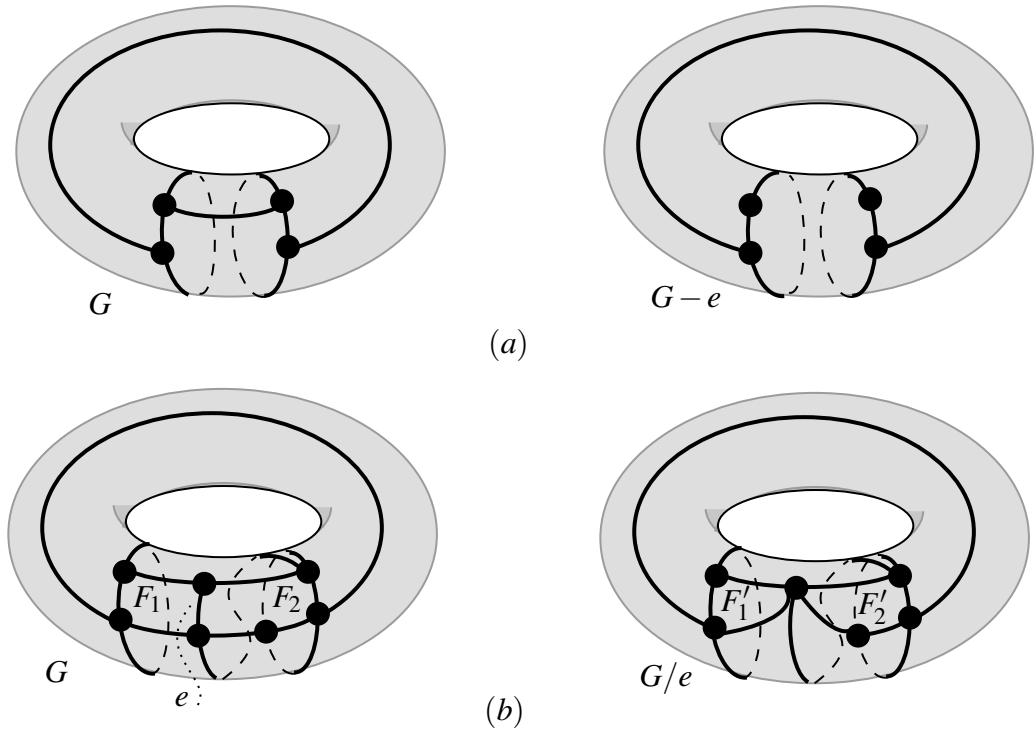


Figure 3.26: (a) The \mathbb{T} -graph G is cellular while $G - e$ is noncellular. (b) The degree of the face F_1 respectively F_2 of the \mathbb{T} -graph G is 4 respectively 5 while its corresponding face F'_1 respectively F'_2 of G/e has degree 3 respectively 4.

3.4.2 Digon contraction

In this subsection we consider the topological version of the 2-cycle contraction operation which is discussed in Subsection 3.3.2.

Definition 3.4.3. Let G be a Σ -graph. A digon B of G is a face of G such that its boundary walk has length 2. A nondegenerate digon is a digon such that its boundary walk is a nondegenerate 2-cycle.

Definition 3.4.4. Let G be a Σ -graph and B be a nondegenerate digon of G with boundary walk v_1, e_1, v_2, e_2, v_1 . Let $G_B = G/e_1 - e_2$ be the Σ -graph that is obtained from G by contracting the edge e_1 and deleting the edge e_2 . We say that G_B is the Σ -graph that is obtained from G by a digon contraction. We call the move $G \rightarrow G_B$ a digon contraction.

Figure 3.27 clarifies the digon contraction.

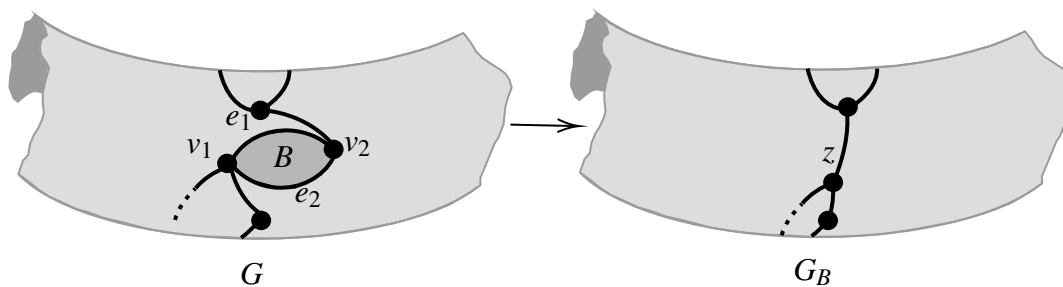


Figure 3.27: A digon contraction move. Notice that the digon B in G is nondegenerate. In G_B , the vertex z corresponds to the vertices v_1 and v_2 in G .

We observe that since B is a cellular face, then $G/e_1 - e_2$ is canonically isomorphic to $G/e_2 - e_1$. Therefore, there is no need to declare which edge is contracted and which is deleted in the notation.

Lemma 3.4.5. G_B is $(2, l)$ -sparse if and only if G is $(2, l)$ -sparse.

Proof. This follows from Lemma 3.3.9. □

3.4.3 Triangle contraction

In this subsection we consider the topological version of the 3-cycle contraction operation which is discussed in Subsection 3.3.3.

Definition 3.4.6. Let G be a Σ -graph. A triangle T of G is a face of G such that its boundary walk has length 3. A nondegenerate triangle is a triangle such that its boundary walk is a cycle.

Definition 3.4.7. Let G be a Σ -graph and let T be a nondegenerate triangle of G with boundary walk $v_1, e_1, v_2, e_2, v_3, e_3, v_4 = v_1$. Let $G_{T, e_1} = G/e_1 - e_2$ be the Σ -graph that is obtained from G by contracting the edge e_1 and deleting the edge e_2 . We say that G_{T, e_1} is the Σ -graph that is obtained from G by a triangle contraction. We call the move $G \rightarrow G_{T, e_1}$ a triangle contraction.

Figure 3.28 clarifies the triangle contraction move. Notice that since T is cellular, then $G/e_1 - e_2$ is canonically isomorphic as a Σ -graph to $G/e_1 - e_3$. So it is unambiguous to only declare the contracted edge in the notation.

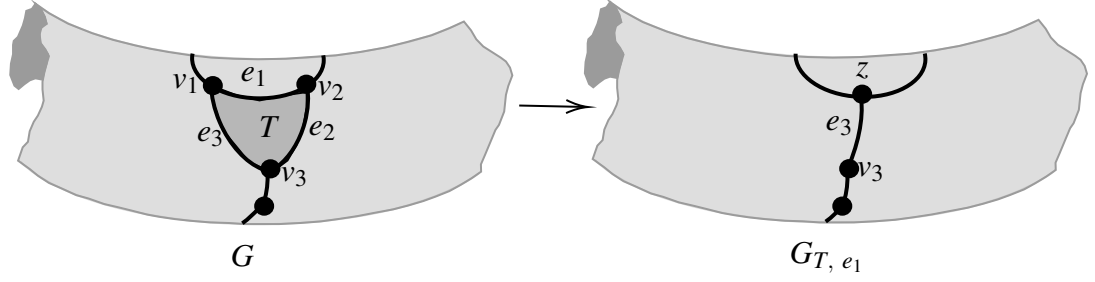


Figure 3.28: A triangle contraction move. Notice that the triangle T in G is nondegenerate. The Σ -graph G_{T,e_1} is obtained from G by contracting e_1 and deleting e_2 . The vertex z corresponds to the vertices v_1 and v_2 in G .

Lemma 3.4.8. *Suppose that G is $(2,2)$ -sparse and let T be a triangular face in G with boundary walk $v_1, e_1, v_2, e_2, v_3, e_3, v_1$. Then at least two of G_{T,e_1} , G_{T,e_2} , G_{T,e_3} are $(2,2)$ -sparse.*

Proof. This follows from Lemma 3.3.14. □

Suppose that G_{T,e_1} is not $(2,2)$ -sparse. By Lemma 3.3.12, there is some blocker in G for the contraction $G \rightarrow G_{T,e_1}$. Let H be such a blocker that is maximal with respect to inclusion.

The following lemma is analogous to Lemma 9 in Fekete *et al.* [28].

Lemma 3.4.9. *Let G be a $(2,2)$ -tight Σ -graph and T be a triangular face of G with a boundary walk $v_1, e_1, v_2, e_2, v_3, e_3, v_1$. Let H be a maximal blocker for the contraction $G \rightarrow G_{T,e_1}$. Let F be a face in H that does not contain v_3 . Then F is also a face of G .*

Proof. Since G is $(2,2)$ -tight, by Theorem 3.2.2, $\gamma_2(H \cup \text{int}_G(F)) \leq \gamma_2(H) = 2$. By the sparsity of G , $\gamma_2(H \cup \text{int}_G(F)) = 2$. It is clear that $v_3 \notin H \cup \text{int}_G(F)$. So $H \cup \text{int}_G(F)$ is a blocker for $G \rightarrow G_{T,e_1}$. By the maximality of H , $H \cup \text{int}_G(F) \subseteq H$ and so $\text{int}_G(F) \subset H$. Therefore, there are no vertices or edges of G in F . □

3.4.4 Quadrilateral contraction

In this subsection we consider the topological version of the 4-cycle contraction operation which is discussed in Subsection 3.3.4.

Definition 3.4.10. Let G be a Σ -graph. A quadrilateral Q of G is a face of G such that its boundary walk has length 4. A nondegenerate quadrilateral is a quadrilateral such that its boundary walk is nondegenerate 4-cycle.

Definition 3.4.11. Let $v_1, e_1, v_2, e_2, v_3, e_3, v_4, e_4, v_5 = v_1$ be the boundary walk of a cellular quadrilateral face, Q , of a $(2, l)$ -sparse Σ -graph G . Suppose that $v_1 \neq v_3$ and $e_1 \neq e_3$. The 4-cycle contraction operation is a composition of an edge contraction and two deletions. The edge contraction operation can be performed by adding an edge, d , joining v_1 and v_3 . We embed d as a diagonal of the quadrilateral face Q . Since Q is homeomorphic to an open disc this uniquely defines the isotopy class of $|d|$. Thus, we define $G_{Q, v_1, v_3} = (G \cup d) / d - \{e_1, e_3\}$ where d is embedded as described above. We say that G_{Q, v_1, v_3} is the Σ -graph that is obtained from G by a quadrilateral contraction. We call the move $G \rightarrow G_{Q, v_1, v_3}$ a quadrilateral contraction.

Figure 3.29 illustrates the quadrilateral contraction move.

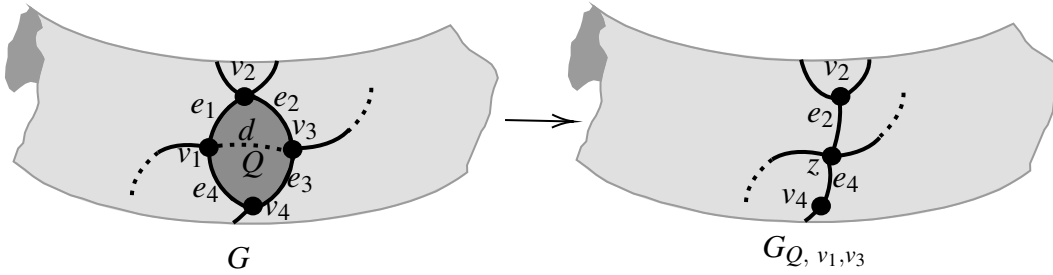


Figure 3.29: A quadrilateral contraction move. Notice that the quadrilateral Q in G is nondegenerate. The Σ -graph G_{Q, v_1, v_3} is obtained from G by contracting the (temporary) edge d and deleting e_1 and e_3 . The vertex z corresponds to the vertices v_1 and v_3 in G .

Suppose that G is $(2, 2)$ -tight surface graph and G_{Q, v_1, v_3} is not $(2, 2)$ -tight. Since G is $(2, 2)$ -tight, by Lemma 3.3.18 there is some (type 1 or type 2) blocker H .

Lemma 3.4.12. Let G be a $(2, 2)$ -tight Σ -graph and Q be a quadrilateral face with boundary walk $v_1, e_1, v_2, e_2, v_3, e_3, v_4, e_4, v_5 = v_1$. Let H be a type 1 blocker for $G \rightarrow G_{Q, v_1, v_3}$ and that H is maximal with respect to inclusion among all such blockers. Then there is exactly one face of H that is not a face of G .

Proof. Suppose that $v_2 \notin H$ and let F be a face in H such that $v_2 \notin F$. Then by Theorem 3.2.2, $\gamma_2(H \cup \text{int}_G(F)) \leq \gamma_2(H) = 2$. By the sparsity of G , $\gamma_2(H \cup \text{int}_G(F)) = 2$. Hence

3.4. INDUCTIVE OPERATIONS ON SURFACE GRAPHS

$H \cup \text{int}_G(F)$ is a blocker of type 1 for $G \rightarrow G_{Q,v_1,v_3}$. By the maximality of H , $H \cup \text{int}_G(H) \subseteq H$ which means $\text{int}_G(H) \subset H$. Therefore, F is also a face of G .

□

See Figure 3.30.

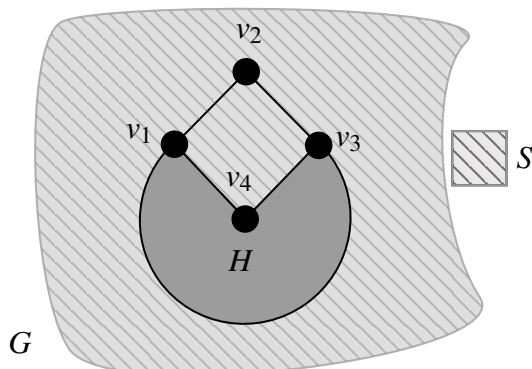


Figure 3.30: The face S of the Σ -subgraph H is not a face of the Σ -graph G .

Lemma 3.4.13. *Suppose that there is no type 1 blocker of $G \rightarrow G_{Q,v_1,v_3}$ and that H is a type 2 blocker for $G \rightarrow G_{Q,v_1,v_3}$ that is maximal with respect to inclusion among all such blockers. Then there is exactly one face of H that is not also a face of G .*

Proof. It is clear that v_2 and v_4 both belong to the same face say I of H . Suppose that $F \neq I$ is another face of H . By Theorem 3.2.2 we see that $\gamma_2(H \cup \text{int}_G(F)) \leq \gamma_2(H) = 3$. By the sparsity of G , $\gamma_2(H \cup \text{int}_G(F)) \in \{2, 3\}$. If $\gamma_2(H \cup \text{int}_G(F)) = 2$ then $\gamma_2((H \cup \text{int}_G(F)) \cup \{v_2\} \cup \{e_1, e_2\}) = 2$. Hence $H \cup \text{int}_G(F)$ is a blocker of type 1 for $G \rightarrow G_{Q,v_1,v_3}$ which contradicts the hypothesis. Therefore, $\gamma_2(H \cup \text{int}_G(F)) = 3$ and so $H \cup \text{int}_G(F)$ is a blocker of type 2 for $G \rightarrow G_{Q,v_1,v_3}$. By the maximality of H , $H \cup \text{int}_G(F) \subseteq H$ and so $\text{int}_G(F) \subset H$ as required. □

See Figure 3.31.

Figure 3.32 provides an example of a $(2,2)$ -tight \mathbb{T} -graph with a quadrilateral face. The two blockers for the contraction move $G \rightarrow G_{Q,v_1,v_3}$ are also illustrated.

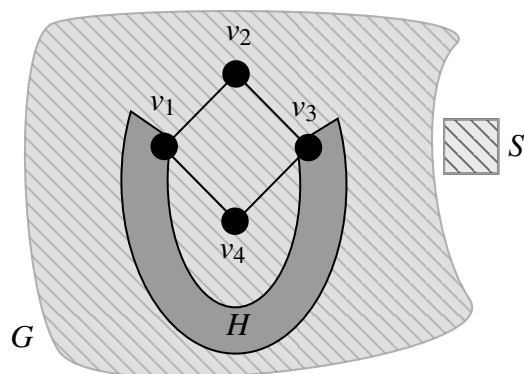


Figure 3.31: The face S of the Σ -subgraph H is not a face of the Σ -graph G .

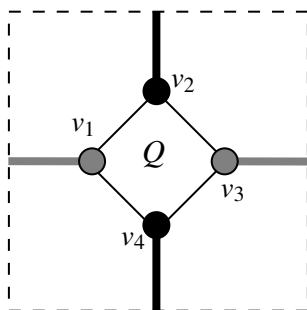


Figure 3.32: The black respectively gray bold edge is a blocker of type 2 for the contraction move $G \rightarrow G_{Q,v_2,v_4}$ respectively $G \rightarrow G_{Q,v_1,v_3}$.

3.4.5 Topological vertex splitting

Let G' be the contraction G/e of a surface graph G . We say that G is obtained by a topological vertex split on G' . Thus, we distinguish three types of topological vertex splits that are of particular interest. Those are digon splits, triangle splits and quadrilateral splits that are the inverse to the digon contractions, triangle contractions and quadrilateral contractions respectively. In Figure 3.33, we provide examples of the three splitting moves.

Definition 3.4.14. A $(2,2)$ -tight Σ -graph G is irreducible if there is no digon, triangle or quadrilateral contraction of G that is also $(2,2)$ -tight.

It is clear that every $(2,2)$ -tight Σ -graph can be obtained from some irreducible Σ -graph by applying a sequence of digon/triangle/quadrilateral splitting moves.

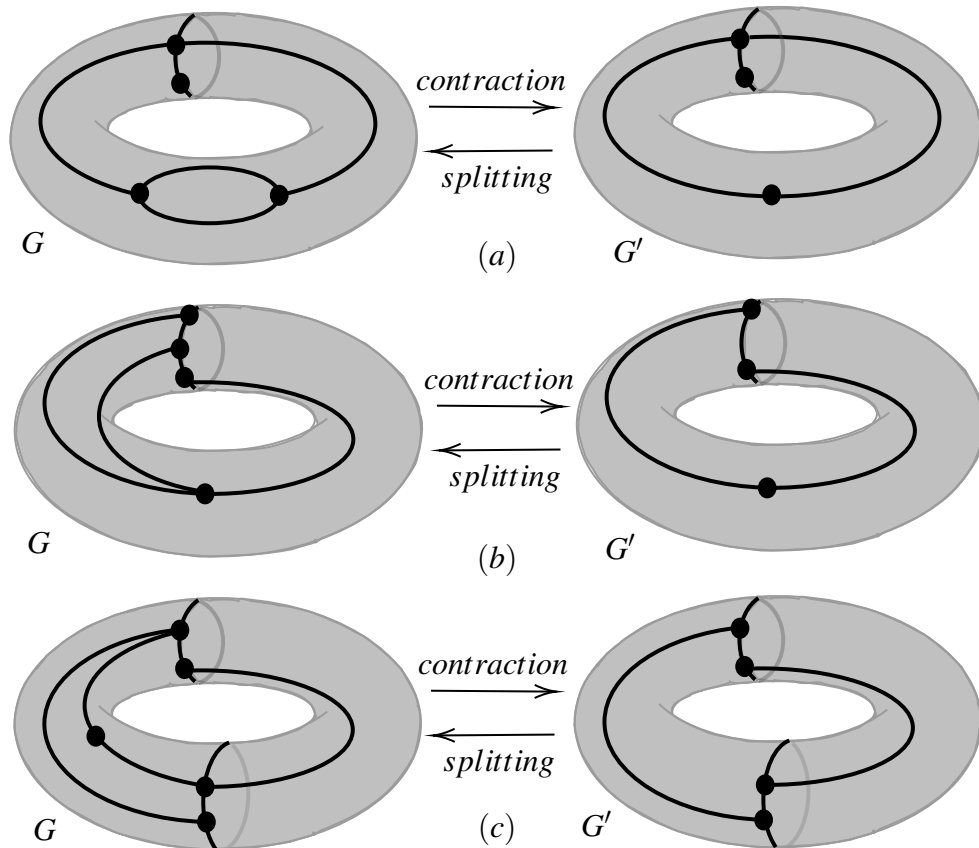


Figure 3.33: (a) The inverse of a digon contraction move. (b) The inverse of a triangle contraction move. (c) The inverse of a quadrilateral contraction move.

3.5 Rotation systems and topological contraction moves

In this section, we explain how the topological contraction moves that we defined in the previous section can be recalled using rotation system.

3.5.1 Edge contraction and deletion moves in terms of rotation system

In the following, we describe how the rotation systems of Σ -graphs which are obtained by edge contraction or deletion can be derived from the (original) rotation systems.

Topological edge deletion move

Definition 3.5.1. Let $R = (H, \sigma, \tau)$ be the rotation system of a Σ -graph G . Let e be an edge in G and let (a, b) be the corresponding transposition in τ . Let $G - e$ be the Σ -graph which is obtained from G by deleting e . We define the rotation system R' of $G - e$ to be (H', σ', τ') where $H' = H - \{a, b\}$, $\sigma' = (b, \sigma(b))(a, \sigma(a))\sigma$ and $\tau' = (a, b)\tau$.

See Figure 3.34.

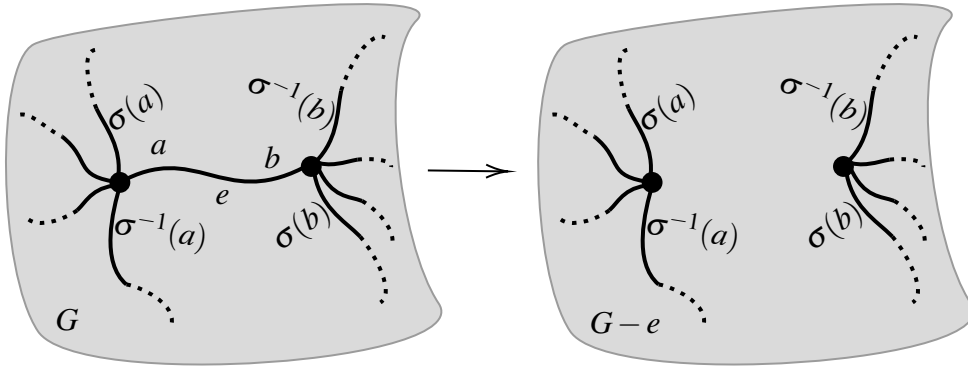


Figure 3.34: Deleting an edge e and its corresponding half edges a and b .

Example 3.5.2. Consider the \mathbb{T} -graph G in Figure 3.35. The rotation system of this graph is $R = (H, \sigma, \tau)$ where $H = \{1, 2, \dots, 8\}$, $\sigma = (1, 2, 3, 4, 5)(6, 7, 8)$ and $\tau = (1, 3)(2, 7)(4, 6)(5, 8)$. On the other hand, the rotation system of the \mathbb{T} -graph $G - e$ in Figure 3.35 is (H', σ', τ') where $H' = \{1, 2, 3, 5, 7, 8\}$, $\tau' = (1, 2, 3, 5)(7, 8)$. It is clear that $H' = H - \{4, 6\}$ where $(4, 6)$ is the corresponding transposition of the edge e in τ , $\sigma' = (6, \sigma(6))(4, \sigma(4))\sigma = (6, 7)(4, 5)\sigma$ and $\tau' = (4, 6)\tau$.

Topological edge contraction move

Definition 3.5.3. Let $R = (H, \sigma, \tau)$ be the rotation system of a Σ -graph G . Let e be an edge in G and let (a, b) be the corresponding transposition in τ . Let G/e be the Σ -graph which is obtained from G by contracting e . We define the rotation system R' of G/e to be (H', σ', τ') where $H' = H - \{a, b\}$, $\sigma' = (b, \sigma(a))(a, \sigma(b))\sigma$ and $\tau' = (a, b)\tau$.

See Figure 3.36.

3.5. ROTATION SYSTEMS AND TOPOLOGICAL CONTRACTION MOVES

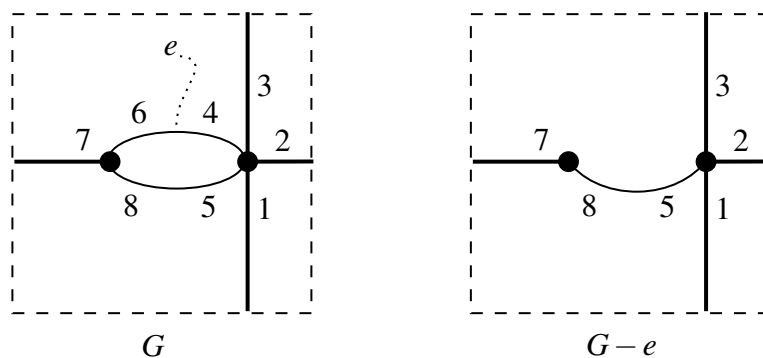


Figure 3.35: A labelling of the half edges of the \mathbb{T} -graphs G and $G - e$.

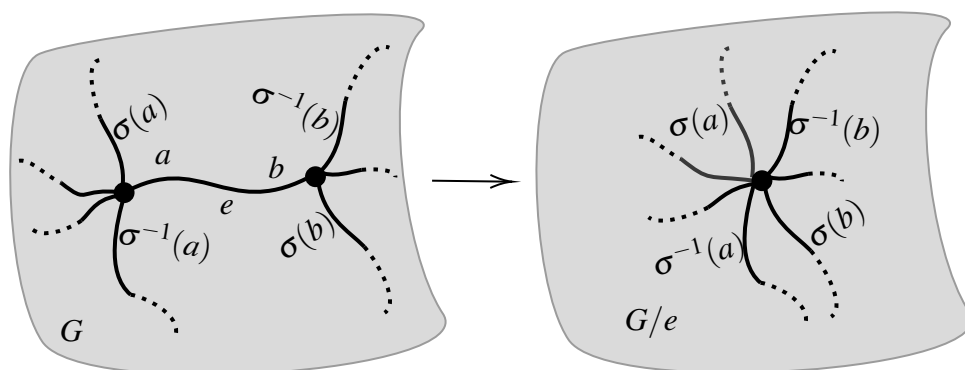


Figure 3.36: Contracting an edge e with the half edges a and b .

Example 3.5.4. Consider the \mathbb{S} -graph G in Figure 3.37. The rotation system of this graph is $R = (H, \sigma, \tau)$ where $H = \{1, 2, \dots, 12\}$, $\sigma = (1, 2, 3)(4, 5, 6)(7, 8, 9)(10, 11, 12)$ and $\tau = (1, 7)(6, 8)(9, 10)(2, 12)(3, 4)(5, 11)$. On the other hand, the rotation system of the \mathbb{S} -graph G/e in Figure 3.37 is (H', σ', τ') where $H' = \{2, 3, \dots, 6, 8, \dots, 12\}$, $\tau' = (2, 3, 8, 9)(4, 5, 6)(10, 11, 12)$. It is clear that $H' = H - \{1, 7\}$ where $(1, 7)$ is the corresponding transposition of the edge e in τ , $\sigma' = (7, \sigma(1))(1, \sigma(7))\sigma = (7, 2)(1, 8)\sigma$ and $\tau' = (1, 7)\tau$.

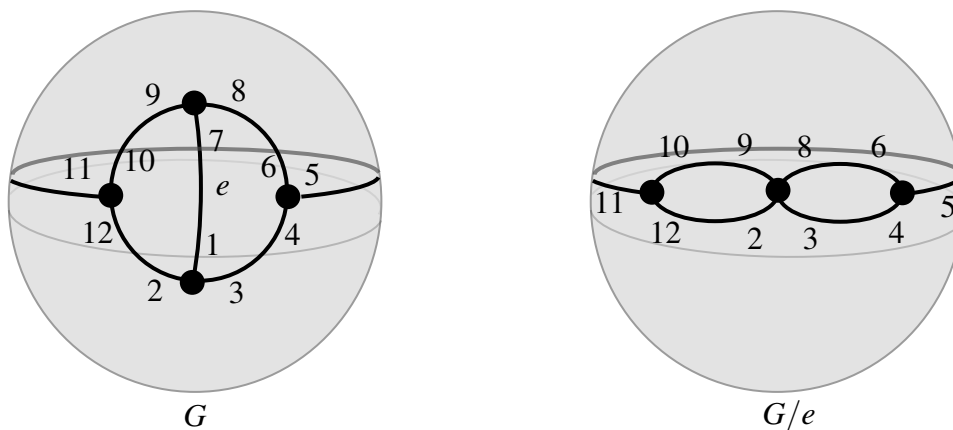


Figure 3.37: A Labelling of the half edges of the \mathbb{S} -graphs G and G/e .

3.5.2 Rotation systems of digon, triangle and quadrilateral contractions

In the following we describe the three topological contraction moves in terms of rotation systems.

Rotation system of a digon contraction

Given G be a Σ -graph with a rotation system R . Let B be a digon of G with boundary walk v_1, e_1, v_2, e_2, v_1 . The rotation system of G_B can be easily obtained from R by specifying the rotation system R' of $G/e_1 - e_2$.

Rotation system of a triangle contraction

Given G be a Σ -graph with a rotation system R . Let T be a triangle of G with boundary walk $v_1, e_1, v_2, e_2, v_3, e_3, v_1$. The rotation system of G_{T, e_1} can be obtained from R by specifying the rotation system R' of $G/e_1 - e_2$.

Rotation system of a quadrilateral contraction

Let $R = (H, \sigma, \tau)$ be the rotation system of a Σ -graph G . Let Q be a quadrilateral in G with boundary walk $v_1, e_1, v_2, e_2, v_3, e_3, v_4, e_4, v_1$. The rotation system of G_{Q, v_1, v_3} can

3.5. ROTATION SYSTEMS AND TOPOLOGICAL CONTRACTION MOVES

be obtained from R by specifying the rotation system R' of $(G \cup d)/d - \{e_1, e_3\}$. See Definition 3.4.11 for the embedding of d .

Chapter 4

Finiteness Theorems

Constructing a class of graphs that have specific properties can be achieved by finding small graphs that have the desired properties and a set of inductive moves. The term 'small' is subject to missing the desired properties once the inverse of one of the inductive moves performs on such graphs. Inductive moves, on the other hand, have to maintain the desired properties of the class. Thus, by performing a sequence of the inductive moves that we choose on the small graphs, we can generate the class of interest. In the literature, the term 'small' possesses other names such as minimal or irreducible.

The typical examples of inductive constructions have been done on triangulations of surfaces. The natural inductive move in that sequel is the vertex splitting and its inverse (edge contraction). In the study of triangulations of surfaces, vertex splitting has an important role. In Subsection 4.1, we survey some of the results in the area of triangulations of surfaces and finding irreducible triangulations. Quadrangulations of surfaces also have been investigated in a similar vein to the triangulations of surfaces. More background on quadrangulations of surfaces can be found in [68] and [67].

Various inductive constructions of various subclass of sparse graphs have been initiated in [29], [33] and [86].

For some classes of $(2,2)$ -tight Σ -graphs with small genus, we show through this chapter that there are finite number of irreducible graphs for such classes of graphs. In 4.8, we provide various examples for all the concepts that we will introduce in this chapter.

4.1 Irreducibility and inductive constructions: Literature review

In this section we recall and restate some well-known results of inductive constructions of some classes of graphs. Note that the material that we present in Section 4.1 is not strictly required for our own work. We present these results to provide some context and motivation for our results.

4.1.1 Inductive constructions of some kinds of tight graphs

Inductive constructions of Laman graphs

Before stating the inductive constructions of some classes of graphs, we state some moves which they extend the graphs under consideration. These moves are also known as Henneberg extension moves. The following three definitions can be also found in [75] and [82].

Definition 4.1.1. *Let $\Gamma = (V, E, s, t)$ be a graph and let $u, v \in V$. Note that we do not assume that u and v are necessarily distinct. Define $V' = V \cup \{z\}$ (where z is a 'new' vertex) and $E' = E \cup \{e, f\}$. Extend s, t to E' as follows: $s(e) = u, s(f) = v, t(e) = t(f) = z$. We say that the graph (V', E', s, t) is a Henneberg type 0 extension of Γ . If u and v are distinct, then we call the graph (V', E', s, t) a simple Henneberg type 0 extension of Γ .*

Definition 4.1.2. *Let $\Gamma = (V, E, s, t)$ be a graph. Let $u, v, w \in V$ and $e \in E$ such that $s(e) = u$ and $t(e) = v$. Define $V' = V \cup \{z\}$ (where z is a 'new' vertex) and $E' = (E - \{e\}) \cup \{f, g, h\}$. Extend s, t to E' as follows: $s(f) = u, s(g) = v, s(h) = w, t(f) = t(g) = t(h) = z$. We say that the graph (V', E', s, t) is a Henneberg type 1 extension of Γ . If u and v are distinct, then we call the graph (V', E', s, t) a simple Henneberg type 1 extension of Γ .*

Definition 4.1.3. *Let $\Gamma = (V, E, s, t)$ be a graph. Let $u, v, w, x \in V$ and $e, f \in E$ such that $s(e) = u, s(f) = w, t(e) = v$ and $t(f) = x$. Define $V' = V \cup \{z\}$ (where z is a 'new' vertex) and $E' = (E - \{e, f\}) \cup \{g, h, i, j\}$. Extend s, t to E' as follows: $s(g) = u, s(h) = v, s(i) = w, s(j) = x, t(g) = t(h) = t(i) = t(j) = z$. We say that the graph (V', E', s, t) is a Henneberg type 2 extension of Γ . If u and v are distinct, then we call the graph (V', E', s, t) a simple Henneberg type 2 extension of Γ .*

4.1. IRREDUCIBILITY AND INDUCTIVE CONSTRUCTIONS:
LITERATURE REVIEW

Figure 4.1 clarifies the above three Henneberg moves.

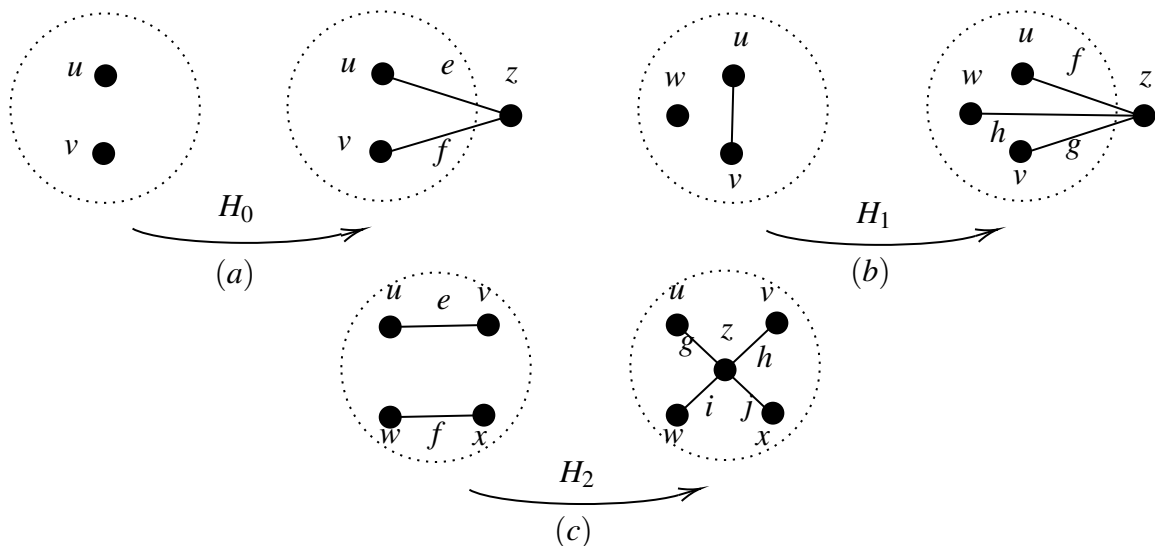


Figure 4.1: (a) Henneberg type 0 move, H_0 . (b) Henneberg type 1 move, H_1 . (c) Henneberg type 2 move, H_2 .

Definition 4.1.4. A graph Γ with vertex set V and edge set E is called a Laman graph if it is $(2,3)$ -tight.

Laman [59] and Henneberg [49] proved independently the following inductive construction.

Theorem 4.1.5. A graph Γ is a Laman graph if and only if it can be constructed from a single edge by a sequence of simple Henneberg type 0 or simple Henneberg type 1 moves.

See Figure 4.2 which provides an inductive construction of a $(2,3)$ -tight graph with 7 vertices.

Inductive constructions for various classes of $(2,1)$ -tight graphs

Here we briefly survey some inductive constructions from the existing literature. There are various different types of "moves" were used. Rather than give a complete description we have illustrated some examples of each type of the moves in Figure 4.3. For detailed descriptions the reader should refer to the cited sources.

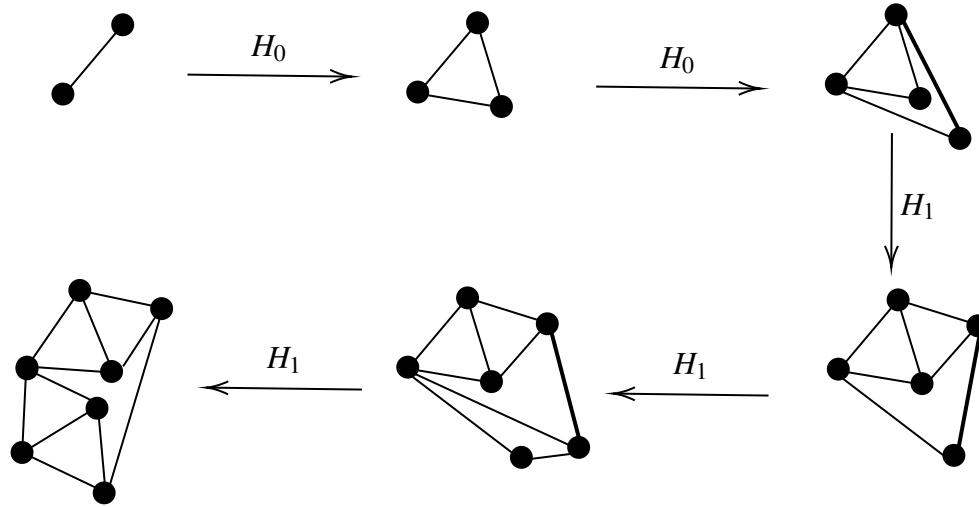


Figure 4.2: Constructing a $(2, 3)$ -tight graph from a single edge by Henneberg type 0 (H_0) and Henneberg type 1 (H_1) moves.

Theorem 4.1.6. [74] *A simple graph Γ is $(2, 2)$ -tight if and only if Γ can be derived from K_4 by a sequence of simple Henneberg type 0, simple Henneberg type 1 and graph extension.*

The following is an alternative construction for the previous construction of $(2, 2)$ -tight graphs.

Theorem 4.1.7. [73] *A simple graph Γ is $(2, 2)$ -tight if and only if Γ can be constructed from K_4 by the simple Henneberg 0, simple Henneberg 1, vertex-to- K_4 and edge-to- K_3 moves.*

We emphasise here that the two previous constructions of $(2, 2)$ -tight graphs are non topological inductive constructions. Indeed, this thesis will provide a topological inductive construction of $(2, 2)$ -tight graphs which are embedded in the torus.

Theorem 4.1.8. [73] *A simple graph Γ is $(2, 1)$ -tight if and only if Γ can be constructed from $K_5 - e$ or $K_4 \sqcup K_4$ by a sequence of simple Henneberg type 0, simple Henneberg type 1, vertex-to- K_4 , edge joining or edge-to- K_4 moves.*

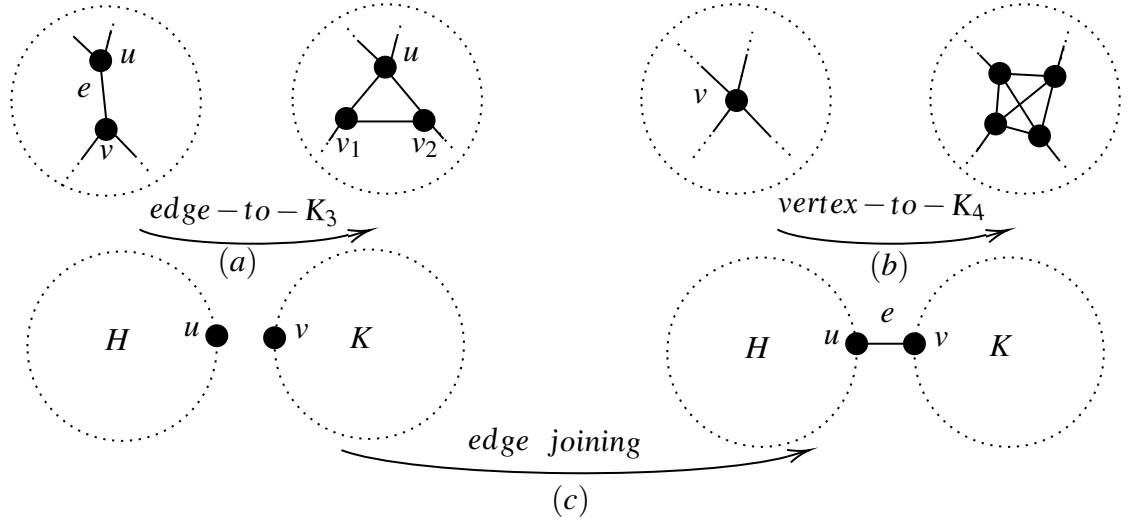


Figure 4.3: (a) This move replaces the edge e by K_3 . This move is the inverse of a triangle contraction move. (b) This move replaces a vertex by K_4 . Following [74], this is an example of graph extension. (c) This move forms the graph Γ by joining two $(2, 1)$ -tight graphs H respectively K with an edge e of endpoints u and v where u respectively v is a vertex in H respectively K .

4.1.2 Inductive constructions of some tight surface graphs

In this subsection, We first define the topological version of the Henneberg moves that we stated in the previous subsection, i.e. topological Henneberg moves. Also, we state the relationship between these three topological moves and the digon, triangle and quadrilateral contraction moves. Moreover, we restate some known results of constructing some class of surface graphs using some topological inductive moves.

Topological Henneberg moves

In the following, we redefine Henneberg moves but this time on surface graphs. We also highlight the relationship between these topological Henneberg moves with the three contraction moves that we dealt with in the previous chapter, i.e. digon, triangle and quadrilateral contractions.

Definition 4.1.9. Let $G = (\Gamma, \phi)$ be a cellular Σ -graph with $\Gamma = (V, E, s, t)$. Let F be a face in G and $u, v \in V$ such that $\phi(u)$ and $\phi(v)$ be two vertices on the boundary of F . Let $\Gamma' = (V', E', s, t)$ be a graph where $V' = V \cup \{z\}$ (where z is a 'new' vertex) and

$E' = E \cup \{e, f\}$. s, t are extended to E' as follows. $s(e) = u, s(f) = v, t(e) = t(f) = z$. Let $G_{H_0} = (\Gamma', \phi')$ where $\phi'|_{|\Gamma|} = \phi$, $\phi'(z)$ is any element of F , $\phi'(e)$ respectively $\phi'(f)$ is a path joins $\phi'(z)$ and $\phi'(u)$ respectively $\phi'(v)$ in F . We say that G_{H_0} is the Σ -graph that is obtained from G by a topological Henneberg type 0 move.

If u and v are distinct, then we say that G_{H_0} is the Σ -graph that is obtained from G by a simple topological Henneberg type 0 move.

It is clear that the topological Henneberg operation preserves $(2, l)$ -sparseness for $l \leq 2$. This is because topological Henneberg type 0 is the inverse move to divalent vertex move which preserves $(2, l)$ -sparseness for all l . See Figure 4.4.

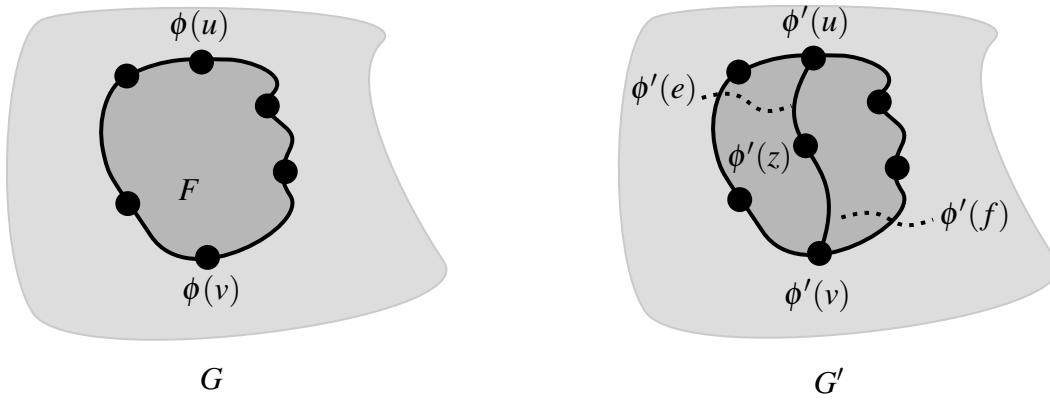


Figure 4.4: The Σ -graph G has a face F . The Σ -graph G_{H_0} is obtained from G by a topological Henneberg type 0 move.

Definition 4.1.10. Let $G = (\Gamma, \phi)$ be a cellular Σ -graph with $\Gamma = (V, E, s, t)$. Let F and R be two faces in G . Let $u, v, w \in V$ such that $\phi(u), \phi(v)$ and $\phi(w)$ be three vertices on the boundary of F . Let $e \in E$ such that $\phi(e)$ be an edge on the boundary of F such that $s(e) = u$ and $t(e) = v$. Let $\Gamma' = (V', E', s, t)$ be a graph where $V' = V \cup \{z\}$ (where z is a 'new' vertex) and $E' = (E - e) \cup \{f, g, h\}$. s, t are extended to E' as follows. $s(f) = u, s(g) = v, s(h) = w, t(f) = t(g) = t(h) = z$. Let $G_{H_1} = (\Gamma', \phi')$ where $\phi'|_{|\Gamma|} = \phi$, $\phi'(z)$ is any element of $F \cup R$, $\phi'(f)$ respectively $\phi'(g)$ and $\phi'(h)$ is a path joins $\phi'(z)$ and $\phi'(u)$ respectively $\phi'(v)$ and $\phi'(w)$. We say that G_{H_1} is a topological Henneberg type 1 extension of G . We also say that G_{H_1} is the Σ -graph that is obtained from G by a topological Henneberg type 1 move.

4.1. IRREDUCIBILITY AND INDUCTIVE CONSTRUCTIONS:
LITERATURE REVIEW

If u, v and w are distinct, then we say that G_{H_1} is the Σ -graph that is obtained from G by a simple topological Henneberg type 1 move. See Figure 4.5.

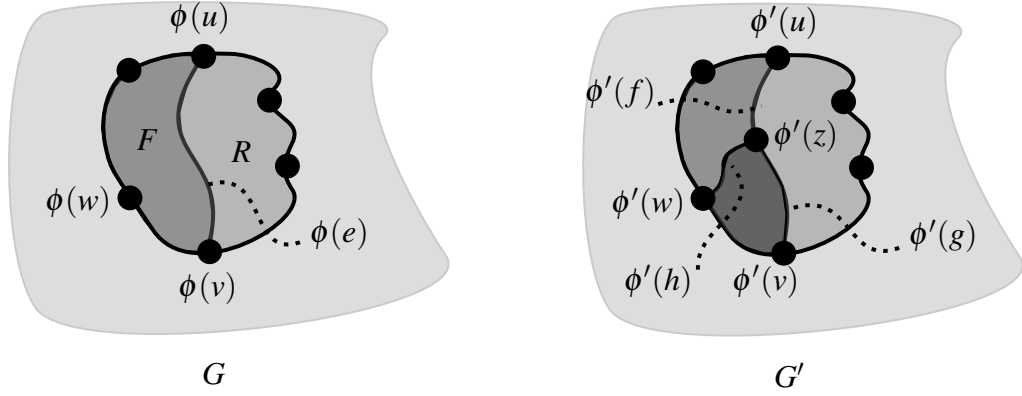


Figure 4.5: The Σ -graph G has the faces F and R . The Σ -graph G_{H_1} is obtained from G by a topological Henneberg type 1 move.

Definition 4.1.11. Let $G = (\Gamma, \phi)$ be a cellular Σ -graph with $\Gamma = (V, E, s, t)$. Let F, R and S be three faces in G . Let $u, v, w, x \in V$ such that $\phi(u), \phi(v), \phi(w)$ and $\phi(x)$ be four vertices on the boundary of F . Let $e, f \in E$ such that $\phi(e)$ and $\phi(f)$ be two edges on the boundary of F such that $s(e) = u, s(f) = w, t(e) = v$ and $t(f) = x$. Let $\Gamma' = (V', E', s, t)$ be

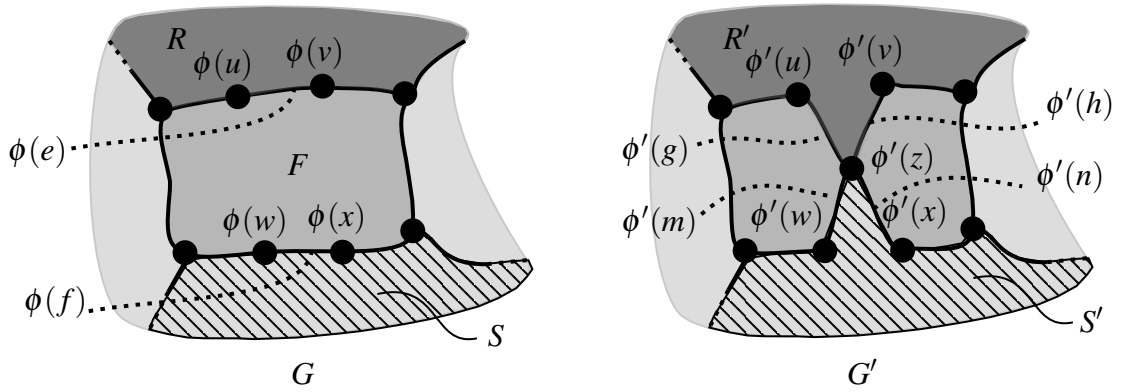


Figure 4.6: The Σ -graph G has the faces F, R and S . The Σ -graph G_{H_2} is obtained from G by a topological Henneberg type 2 move.

a graph where $V' = V \cup \{z\}$ (where z is a 'new' vertex) and $E' = (E - \{e, f\}) \cup \{g, h, m, n\}$. s, t are extended to E' as follows. $s(g) = u, s(h) = v, s(m) = w, s(n) = x, t(g) = t(h) =$

$t(m) = t(n) = z$. Let $G_{H_2} = (\Gamma', \phi')$ where $\phi'|_{|\Gamma|} = \phi$, $\phi'(z)$ is any element of $F \cup R \cup S$, $\phi'(g)$ respectively $\phi'(h), \phi'(m)$ and $\phi'(n)$ is a path joins $\phi'(z)$ and $\phi'(u)$ respectively $\phi'(v), \phi'(w)$ and $\phi'(x)$. We say that G_{H_2} is a topological Henneberg type 2 extension of G . We also say that G_{H_2} is the Σ -graph that is obtained from G by a topological Henneberg type 2 move.

If u, v, w and x are distinct, then we say that G_{H_2} is the Σ -graph that is obtained from G by a simple topological Henneberg type 2 move. See Figure 4.6.

Note that the constructions described in the previous three definitions depend essentially on the choice of paths between the new vertex and the existing vertices. In fact, different choices can yield different Σ -graphs. In the Figure 4.7 and Figure 4.8, we give two examples to point out this issue. On the other hand, we emphasise that even though this depends on the choice of the path is unavoidable, it does not affect any of the results of this thesis.

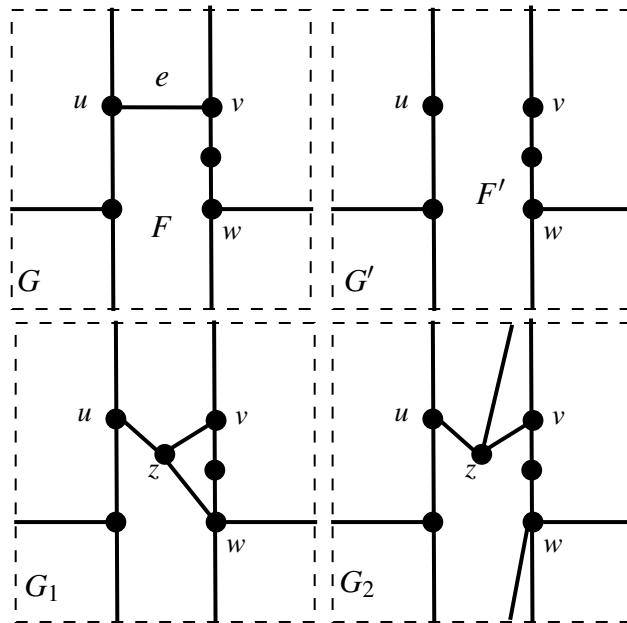


Figure 4.7: Deleting the edge e in the \mathbb{T} -graph G results noncellular face F' in G' . On the other hand, the two \mathbb{T} -graphs G_1 and G_2 which they are the Henneberg type 1 extensions of G are not isomorphic to each other.

Example 4.1.12. Consider the degenerate face F of the \mathbb{S} -graph G in Figure 4.8. There are two possible topological Henneberg type 0 extensions such that the new vertex z can

4.1. IRREDUCIBILITY AND INDUCTIVE CONSTRUCTIONS:
LITERATURE REVIEW

be embedded in the face F such that it is adjacent to the repeated vertex u and the vertex v . Specifically, there are two nonhomotopic paths can be chosen, the dashed and the dotted ones, such that their endpoints are u and z . However, the two ways of embedding the mentioned paths result two nonisomorphic \mathbb{S} -graphs.

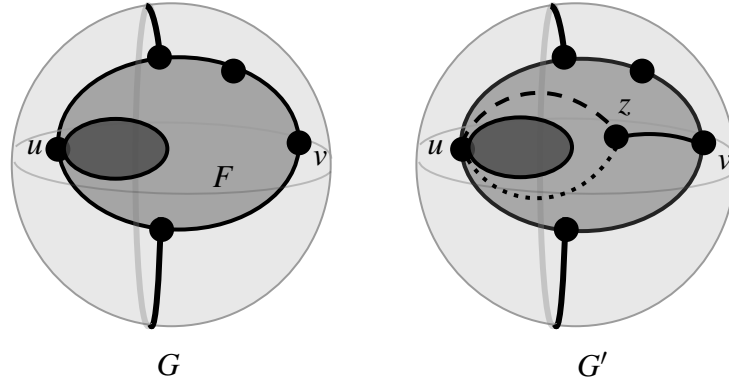


Figure 4.8: Topological Henneberg type 0 move with two possible embeddings.

Figure 4.9 clarifies performing the three topological Henneberg moves on a spherical graph.

Digon, triangle and quadrilateral contractions vs topological Henneberg moves

We state the relationships between our three topological contraction moves, i.e digon, triangle and quadrilateral contractions, and the topological Henneberg moves that we stated in the previous subsection. Here we are presuming that no degenerate or noncellular faces are created during conducting the three topological Henneberg moves that we described in the previous discussion.

1- Digon contraction vs the topological Henneberg type 0 move: Let $G = (\Gamma, \phi)$ be a Σ -graph and B, R and S are faces in G . Let B be a digon and u, e, v, f, u be the boundary walk of B such that $e \in \partial B \cap \partial R$ and $f \in \partial B \cap \partial S$. Let G^* be the dual graph of G . Let e^* and f^* be the dual edge of e respectively f .

Let G_B be the Σ -graph which is obtained from G by contracting the digon B . Let z be the vertex which replaces the vertices u and v in G_B .

Now, it is clear that if we delete the edges e^* and f^* and also delete the dual vertex corresponding to the face B , then (the resulting) graph is $(G_B)^*$. Consequently, we realise

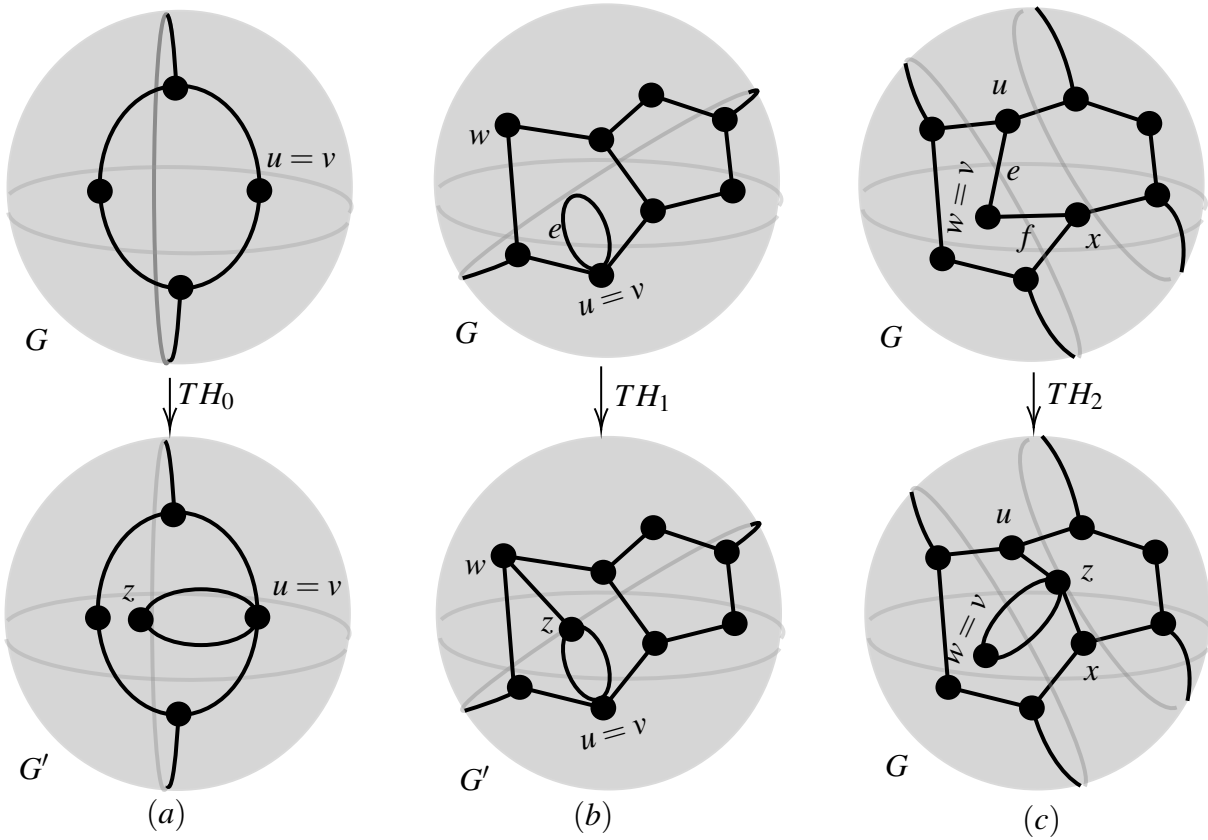


Figure 4.9: (a) A topological Henneberg type 0 move. (b) A topological Henneberg type 1 move. (c) A topological Henneberg type 2 move.

that G^* is obtained from $(G_B)^*$ by a topological Henneberg type 0 move. Therefore, the digon contraction is the dual move of the inverse of the topological Henneberg type 0 move.

Figure 4.10 clarifies the above discussion.

2- Triangle contraction vs the topological Henneberg type 1 move: Let $G = (\Gamma, \phi)$ be a Σ -graph and R, S, T and Y are faces in G . Let T be a triangle and u, e, v, f, w, g, u be the boundary walk of T such that $e \in \partial T \cap \partial R$, $f \in \partial T \cap \partial S$ and $g \in \partial T \cap \partial Y$. Let e^* respectively f^* and g^* be the dual of the edge e respectively f and g .

Let $G_{T,e}$ be the triangle contraction of G . Let z be the vertex which replaces the vertices u and v in $G_{T,e}$. It is clear that $(G_{T,e})^*$ is obtained from G^* by deleting the edges e^* , f^* and g^* and also deleting the vertex T^* . Then adding an edge h^* (such that its endpoints are the dual of the faces Y and S).

4.1. IRREDUCIBILITY AND INDUCTIVE CONSTRUCTIONS:
LITERATURE REVIEW

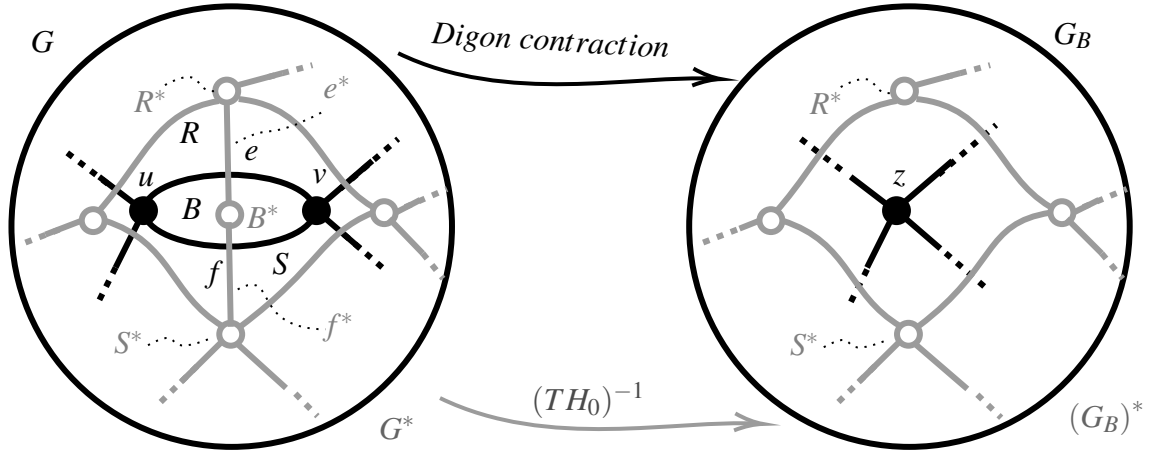


Figure 4.10: The Σ -graphs G and G_B are in black color. On the other hand, the dual Σ -graphs G^* and $(G_B)^*$ are in gray color.

Consequently, we realise that G^* is obtained from $(G_{T,e})^*$ by a topological Henneberg type 1 move. Therefore, the triangle contraction is the dual move of the inverse of the topological Henneberg type 1 move. Figure 4.11 clarifies the above discussion.

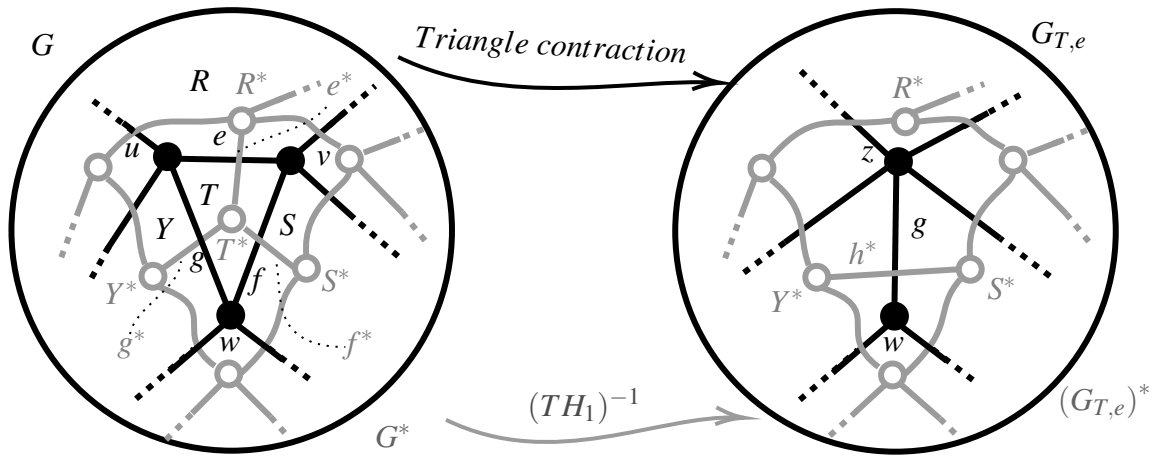


Figure 4.11: The Σ -graphs G and $G_{T,e}$ are in black color. On the other hand, the dual Σ -graphs G^* and $(G_{T,e})^*$ are in gray color.

3- Quadrilateral contraction vs the topological Henneberg type 2 move: Let $G = (\Gamma, \phi)$ be a Σ -graph and Q, R, S, T and Y are faces in G . Let Q be a quadrilateral and $u, e, v, f, w, g, x, h, u$ be the boundary walk of Q such that $e \in \partial Q \cap \partial R$, $f \in \partial Q \cap \partial S$, $g \in \partial Q \cap \partial T$ and $h \in \partial Q \cap \partial Y$. Let e^* respectively f^* , g^* and h^* be the dual edge of e

respectively f , g and h .

Let $G_{Q,u,w}$ be the quadrilateral contraction of G . Let z be the vertex which replaces the vertices u and w in $G_{Q,u,w}$. It is clear that $(G_{Q,u,w})^*$ is obtained from G^* by deleting the edges e^* , f^* , g^* and h^* and also deleting the vertex Q^* . Then adding the edges m^* and n^* where the endpoints of m^* respectively n^* are the dual of the faces R, S respectively Y, T .

Consequently, we realise that G^* is obtained from $(G_{Q,u,w})^*$ by a topological Henneberg type 2 move. Therefore, the quadrilateral contraction is the dual move of the inverse of the topological Henneberg type 2 move. Figure 4.12 clarifies the above discussion.

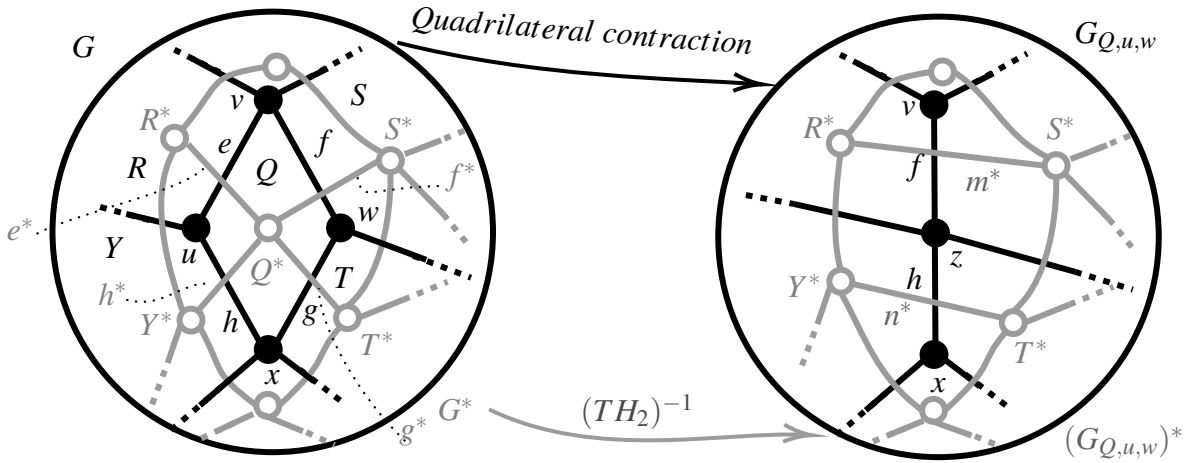


Figure 4.12: The Σ -graphs G and $G_{Q,u,w}$ are in black color. On the other hand, the dual Σ -graphs G^* and $(G_{Q,u,w})^*$ are in gray color.

Inductive construction of plane Laman graphs

In [28], Fekete, Jordán and Whitely found a topological construction for plane Laman graphs using the inverse of triangle contraction move. Their result is a major motivation for us to find a topological inductive construction of $(2, 2)$ -tight torus graphs.

Theorem 4.1.13. [28] *If G is a plane Laman graph with at least 3 vertices, then there is some triangular face T and edge e of T such that $G_{T,e}$ is a plane Laman graph.*

Corollary 4.1.14. [28] *Every plane Laman graph can be constructed from a single edge by a sequence of triangle splitting moves.*

4.1. IRREDUCIBILITY AND INDUCTIVE CONSTRUCTIONS: LITERATURE REVIEW

From the previous theorem, up to homeomorphism, a single edge is the irreducible graph of plane Laman graphs.

An alternative topological inductive construction for plane Laman graphs was presented in [46]. The following theorem states such construction.

Theorem 4.1.15. *Every plane Laman graph can be constructed from a single edge by a sequence of simple topological Henneberg type 0 or type 1 moves.*

Block and hole graphs

In rigidity theory, the general problem is to characterise the rigidity or minimal rigidity of generic three-dimensional bar-joint frameworks. Many approaches have been used to attack such an open problem. One combinatorial approach to solve special cases of this problem is considering an interesting class of graphs which are derived from convex polyhedra. The graphs of this class are called block and hole graphs. This class of graphs was introduced in [97], [30] and [31]. Such graphs arise from a surgery on a triangulated sphere by removing edges from some triangles and inserting minimal rigid blocks into some of the resulting holes. Specifically, removing some edges from a triangulated sphere results in some holes. In [17], such a graph is called a facegraph after labelling all non triangular faces with B or H .

In [17], a special class of graphs of block and hole graphs, called discus and hole graphs, was investigated. Each graph in this class is constructed from a facegraph by substituting a $(3,6)$ -tight graph called simplicial discus in each block, see Figure 4.13. An inductive construction has been given for minimally rigid discus and hole graphs with at most one block.

Theorem 4.1.16. *A discus and hole graph with at most one block is minimally rigid if and only if it can be reduced into K_4 by a sequence of triangle contractions such that in each such contraction no multigraph is constructed.*

Back to the facegraphs, the authors in [17] characterised $(3,6)$ -tightness of facegraphs with at most one block by the following theorem.

Theorem 4.1.17. *A facegraph with at most one block is $(3,6)$ -tight if and only if its corresponding discus and hole graph is minimally rigid.*

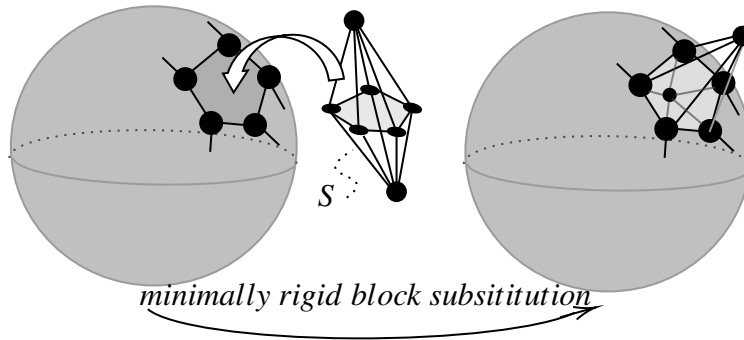


Figure 4.13: A minimally rigid block substitution move performs by inserting the $(3,6)$ -tight graph (which is called simplicial disc in [17]) S in the block B .

Notice that the class of facegraphs has many irreducible graphs. The irreducibility here is subject to the triangle contraction move. For example, there are many irreducible graphs in which contracting an edge which lies in two adjacent triangles, called TT edge, can not be performed. Specifically, contracting TT edges for such irreducible graphs result a facegraph such that its corresponding disc and hole graph is not $(3,6)$ -tight, Figure 4.14.

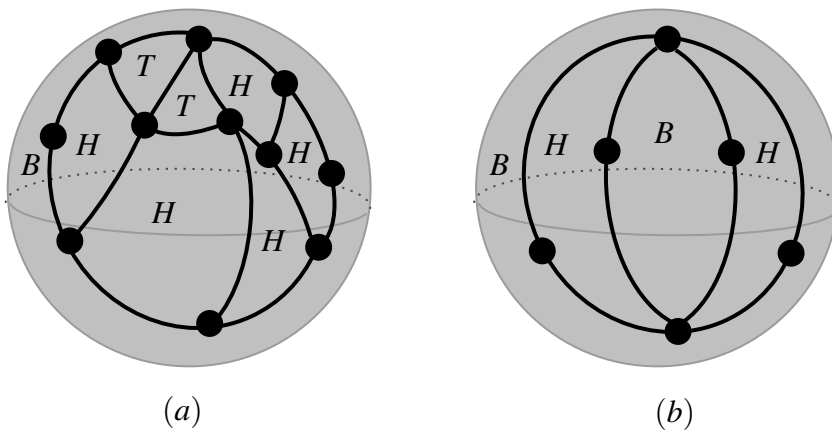


Figure 4.14: Two irreducible spherical facegraphs.

Cruikshank, Kitson and Power in [18] investigated triangulated torus graphs with a single hole. They presented the following construction.

Theorem 4.1.18. [18] *Let $G = (\Gamma, \phi)$ be a \mathbb{T} -graph such that Γ is a triangulation. Suppose a single disc removed from G . Then G is minimally rigid if and only if G is $(3,6)$ -tight.*

The authors found that there are 17 irreducible graphs for such class of torus graphs. Figure 4.15 provides two of such irreducible graphs.

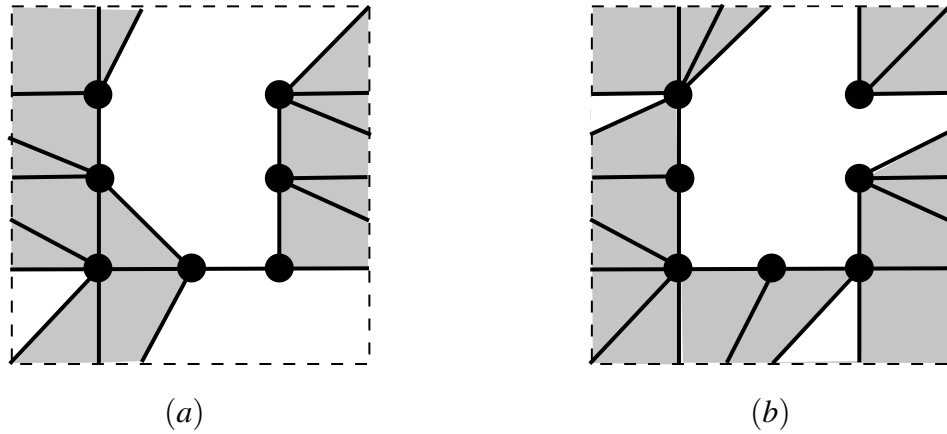


Figure 4.15: Two irreducible facegraphs among the 17 irreducible \mathbb{T} -graphs that are provided in [18].

Topological triangulations

In the following we briefly survey minimal triangulations of surfaces and summarise some well-known results of this topic.

Definition 4.1.19. *A surface triangulation is a Σ -graph $G = (\Gamma, \phi)$ such that Γ is a simple graph. Each face of G is a nondegenerate triangle and each two triangles in G intersect either on a single edge, a single vertex or they are disjoint.*

Definition 4.1.20. *A surface triangulation G is called minimal if for every edge e in G there is a blocker for the triangle contraction move $G \rightarrow G_{T,e}$.*

In the following, we briefly summarise some results related to the number of minimal surface triangulations in the literature. Barnette and Allan [8] proved the following theorem.

Theorem 4.1.21. *If Σ is a surface of genus g , then there are finitely many minimal surface triangulations of Σ .*

CHAPTER 4. FINITENESS THEOREMS

In a similar vein, Nakamoto and Ota, [69], have given a bound for the size of an irreducible quadrangulation of a compact boundaryless surface. In [12], minimal triangulations of surfaces with boundary have been investigated. It has been shown that the number of vertices of such a minimal triangulation admits an upper bound that is linear in the genus and the number of boundaries of the surface.

The previous results were partly motivated us to set a conjecture at the end of this chapter for existing a finite number of irreducible $(2, l)$ -tight Σ -graphs for any surface with finite topological property for $0 \leq l \leq 3$. In Table 4.1, we end this survey section by providing a summary of some known results of the number of minimal surface triangulations of some low genus surfaces.

| Surface | no. of minimal surface triangulations | Author | Reference |
|------------------|---------------------------------------|------------|-----------|
| Sphere | 1 | Steintz | [83] |
| Projective plane | 2 | Barnette | [7] |
| Torus | 21 | Lawercenko | [61] |
| Klein bottle | 29 | Sulanke | [85] |

Table 4.1: A summary of minimal triangulations of some surfaces of low genus.

Figure 4.16 illustrates the minimal triangulation of the sphere and one of the 21 minimal triangulations of the torus.

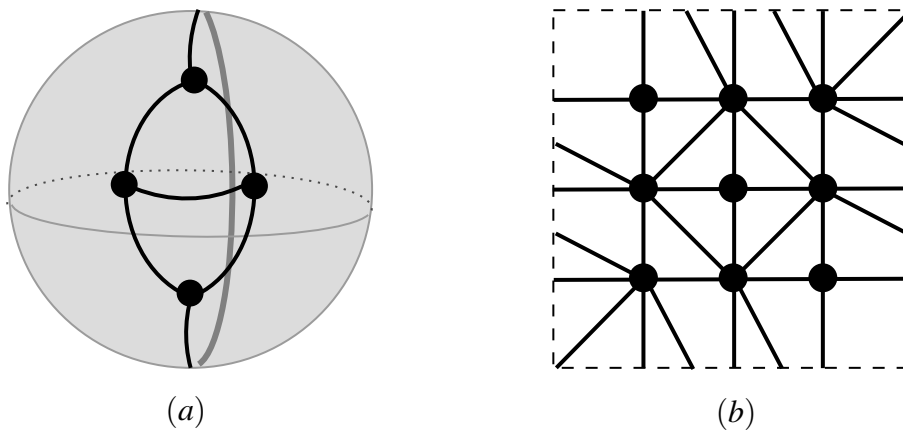


Figure 4.16: (a) The minimal triangulation of the sphere, [83]. (b) One of the 21 minimal triangulations of the torus, [61].

4.2 (2, 2)-tight sphere graphs

In this section we give an inductive construction for the class of (2, 2)-tight sphere graphs. We start by presenting some simple results and facts of such class of spherical graphs.

Lemma 4.2.1. *Suppose that G is a (2, 2)-sparse \mathbb{S} -graph with at least two vertices. If $\gamma_2(G) \leq 3$, then G is cellular.*

Proof. By Lemma 3.1.8, G is connected. But \mathbb{S} has genus 0. It follows that G is cellular. \square

Lemma 4.2.2. *Suppose that G is a (2, 2)-sparse \mathbb{S} -graph with at least two vertices. If $\gamma_2(G) = 2$, then*

$$2f_2 + f_3 = 4 + f_5 + 2f_6 + \dots$$

Proof. By Lemma 4.2.1, G is cellular. Since G is (2, 2)-sparse, then by Lemma 3.1.4, $f_1 = 0$. Now apply Lemma 2.4.4. \square

Lemma 4.2.3. *Suppose that G is a (2, 2)-sparse \mathbb{S} -graph with at least two vertices. If $\gamma_2(G) = 3$, then*

$$2f_2 + f_3 = 2 + f_5 + 2f_6 + \dots$$

Proof. By Lemma 4.2.1, G is cellular. By Lemma 3.1.4, $f_1 = 0$. Now apply Lemma 2.4.4. \square

Corollary 4.2.4. *If G is a (2, 2)-tight \mathbb{S} -graph with at least two vertices, then*

$$2f_2 + f_3 \geq 4$$

Proof. Since G is (2, 2)-tight, then by Lemma 3.1.4, $f_1 = 0$. By Lemma 4.2.1, G is cellular. Now the required inequality can be derived from Lemma 4.2.2. \square

Corollary 4.2.5. *If G is a simple (2, 2)-tight \mathbb{S} -graph, then it has at least four triangular faces.*

Proof. Since G is simple, then $f_2 = 0$. So by Lemma 4.2.2 we have $f_3 = 4 + f_5 + 2f_6 + \dots$. Thus, $f_3 \geq 4$. \square

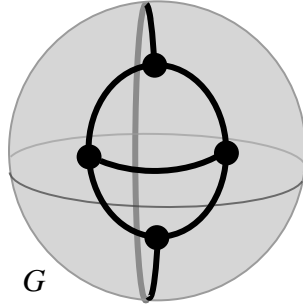


Figure 4.17: The \mathbb{S} -graph G is the smallest simple $(2, 2)$ -tight spherical graph.

It is clear that the \mathbb{S} -graph in Figure 4.17 is the smallest simple $(2, 2)$ -tight \mathbb{S} -graph.

Theorem 4.2.6. *Every $(2, 2)$ -tight \mathbb{S} -graph can be reduced into a single vertex by a sequence of digon or triangle contractions.*

Proof. Suppose that G has at least two vertices. By Lemma 3.1.8, G is connected and $f_1 = 0$. By Lemma 4.2.2, $2f_2 + f_3 \geq 4$ which means in particular G either has a digon or a triangle and G is not irreducible. \square

In Figure 4.18, we include a construction of a $(2, 2)$ -tight \mathbb{S} -graph.

4.3 Curves in surfaces

In this section, we recall some types of curves in a surface. We focus in particular on curves in the torus. We start first by reviewing some basic terminology associated to curves in surfaces. More background on this section can be found in [64], [92], [95], [55] and [15].

4.3.1 Some definitions

In the following we recall some definitions that concern loops in surfaces, see Definition 2.2.4.

Definition 4.3.1. *A simple loop α is nonseparating if $\Sigma - im(\alpha)$ has the same number of connected components as Σ .*

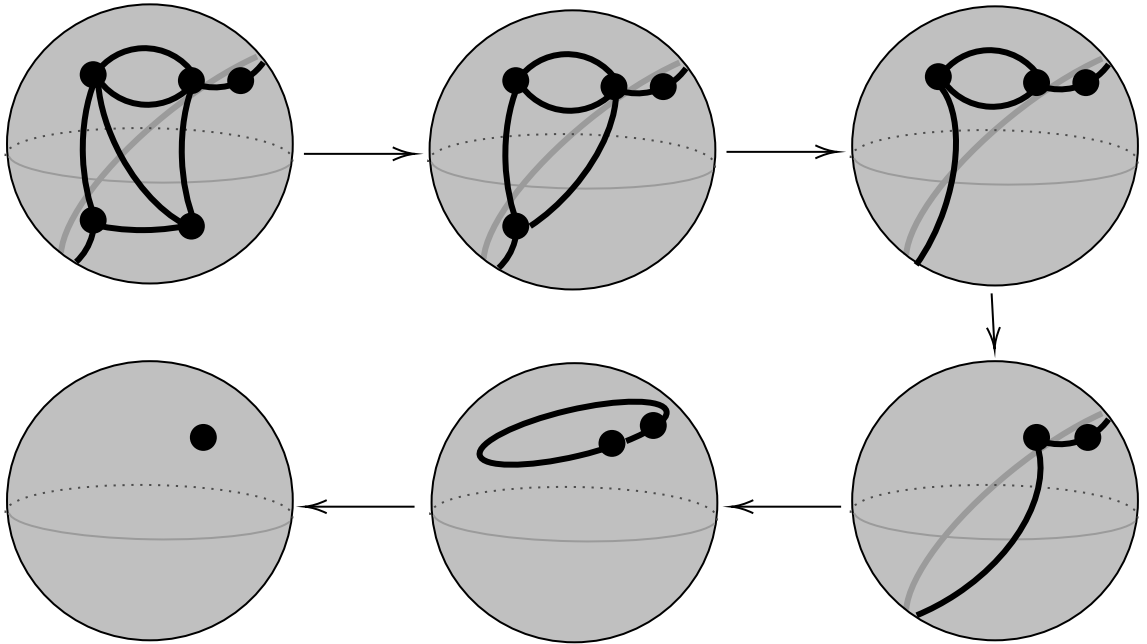


Figure 4.18: A sequence of digon and triangle contractions performed on a $(2,2)$ -tight \mathbb{S} -graph. The contraction sequence ends with the irreducible $(2,2)$ -tight \mathbb{S} -graph.

In the torus, a simple loop is nonseparating if and only if it does not bound an embedded disc. Figure 4.19 provides various kinds of loops.

In the following we state the definition of homotopy, [64], [92].

Definition 4.3.2. *Let α and β be loops in Σ . We say that α and β are homotopic if there is a continuous function $F : [0, 1] \times S^1 \rightarrow \Sigma$ such that $F(0, t) = \alpha(t)$ and $F(1, t) = \beta(t)$ for all $t \in S^1$.*

Definition 4.3.3. *Let α be a loop in Σ . We say that α is null homotopic if α is homotopic to a constant map.*

Definition 4.3.4. [35] *A loop α in Σ is called essential if it is not null homotopic. Otherwise α is called inessential.*

The loop β in Figure 4.19 is essential while the two loops α and γ are inessential.

Definition 4.3.5. [27] *Let α and β be two simple loops in Σ . The geometric intersection number $i(\alpha, \beta)$ is defined as follow.*

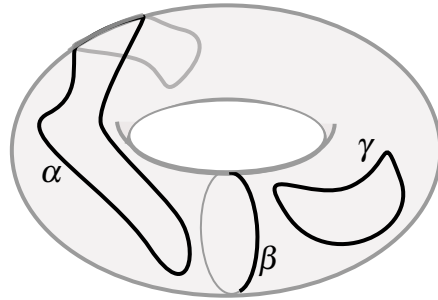


Figure 4.19: The loop β is nonseparating while the loops α and γ are separating loops in \mathbb{T} .

$$i(\alpha, \beta) = \min\{|\alpha' \cap \beta'|\}$$

where α' , respectively β' varies over the set of simple loops homotopic to α , respectively β .

In Figure 4.20, we provide some examples that illustrate the geometric intersection number of loops in the sphere and the torus.

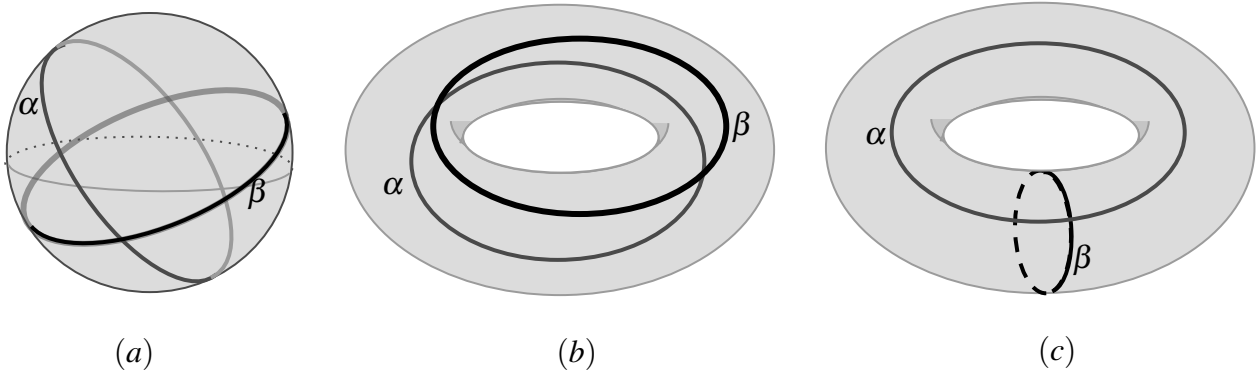


Figure 4.20: The geometric intersection of α and β , i.e. $i(\alpha, \beta)$, in (a) respectively (b), (c) is 0 respectively 0, 1.

Lemma 4.3.6. *Suppose that α and β are smooth simple curves in an orientable surface Σ and that α and β intersect transversely at exactly one point. Then $i(\alpha, \beta) = 1$ and consequently both α and β are essential loops in the surface.*

Proof. [27]

□

4.3.2 Cutting and capping surfaces along loops

Let α be a nonseparating loop in an oriented surface Σ without boundary. If we cut Σ along α , then a new surface Σ' will be created with two boundary components, see Figure 4.21.

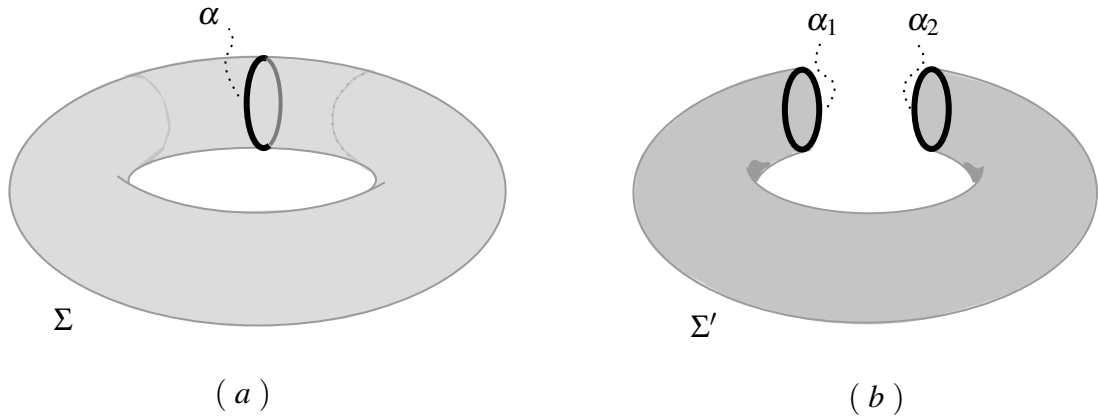


Figure 4.21: (a) The surface Σ (the torus) contains a nonseparating loop α . (b) The surface Σ' (the cylinder) is obtained by cutting Σ along α . The boundary loops of Σ' are α_1 and α_2 .

Now, suppose that L is a Σ -graph where Σ has genus g . Suppose that ζ is a nonseparating loop in Σ that is contained within some face F of L . By cutting Σ along ζ and filling in the two resulting boundary curves with open discs, we obtain a $\tilde{\Sigma}$ -graph, denoted by \tilde{L} , where $\tilde{\Sigma}$ is a surface of genus $g - 1$. We call this surgical procedure cutting and capping along ζ . Notice that if ζ is a separating loop in Σ , then the cutting and capping along ζ results in two surfaces such that the sum of the genera of the resulting surfaces is equal to the genus of the original surface in the case of a separating loop .

Lemma 4.3.7. *If ζ is nonseparating in F , then \tilde{L} has exactly one face, denoted by \tilde{F} , that is not also a face of L . On the other hand, if ζ is separating in F , then \tilde{L} has exactly two faces, denoted by \tilde{F}_+ and \tilde{F}_- that are not also faces of L .*

See Figure 4.22 and Figure 4.23 which describe the previous lemma.

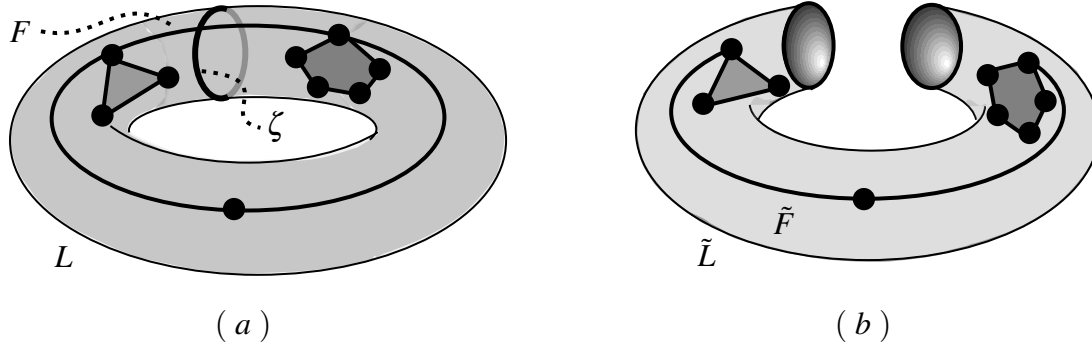


Figure 4.22: (a) The loop ζ in the face F of the \mathbb{T} -graph L is nonseparating in \mathbb{T} . Moreover, ζ is not separating in F . (b) The face \tilde{F} of the \mathbb{S} -graph \tilde{L} is generated by cutting \mathbb{T} along ζ and then filling the two boundaries with open discs.

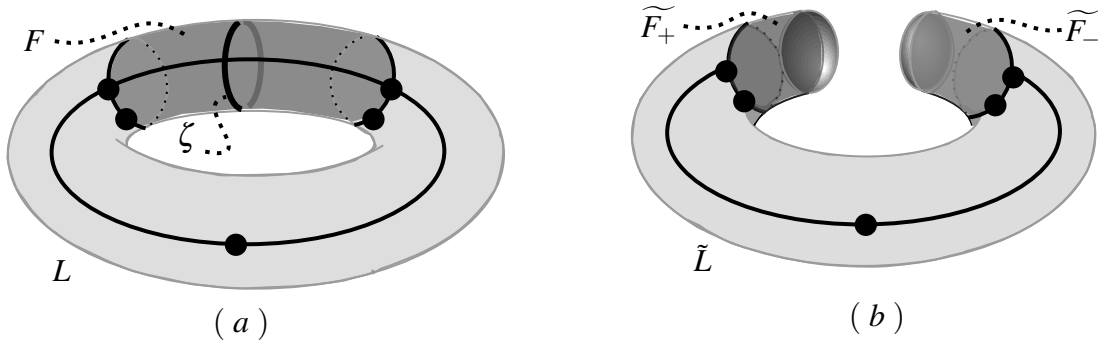


Figure 4.23: (a) The loop ζ in the face F of the \mathbb{T} -graph L is nonseparating in \mathbb{T} and it is also separating in F . (b) The two faces \tilde{F}_+ and \tilde{F}_- of the \mathbb{S} -graph \tilde{L} are generated by cutting \mathbb{T} along ζ and then filling the two boundaries with open discs.

4.4 Structures of irreducible (2,2)-tight torus graphs

In this section we study the structure of an irreducible (2,2)-tight torus graph. We prove some structural results that will later help us to prove our main finiteness theorem about irreducible (2,2)-tight \mathbb{T} -graphs.

We recall that a (2,2)-tight \mathbb{T} -graph G is irreducible if there is no digon, triangle or quadrilateral contraction of G that is also (2,2)-tight.

Definition 4.4.1. *Let c be a cycle in a Σ -graph $G = (\Gamma, \phi)$. The geometric realisation of c is a subspace in Σ which is homeomorphic to S^1 . Notice that c has two possible*

4.4. STRUCTURES OF IRREDUCIBLE (2,2)-TIGHT TORUS GRAPHS

orientations. We can find a loop α homotopy to S^1 with an orientation that coincides with the orientation of the cycle c . The loop α is called the associated loop of c .

Definition 4.4.2. A separating, respectively nonseparating cycle c in a Σ -graph G is a simple closed walk whose associated simple loop is separating, respectively nonseparating in Σ .

We emphasise here that a cycle in a Σ -graph is distinct from a cycle of a graph. Consequently, a separating cycle in a Σ -graph is distinct from the normal usage in the graph theory literature. See Figure 4.24.

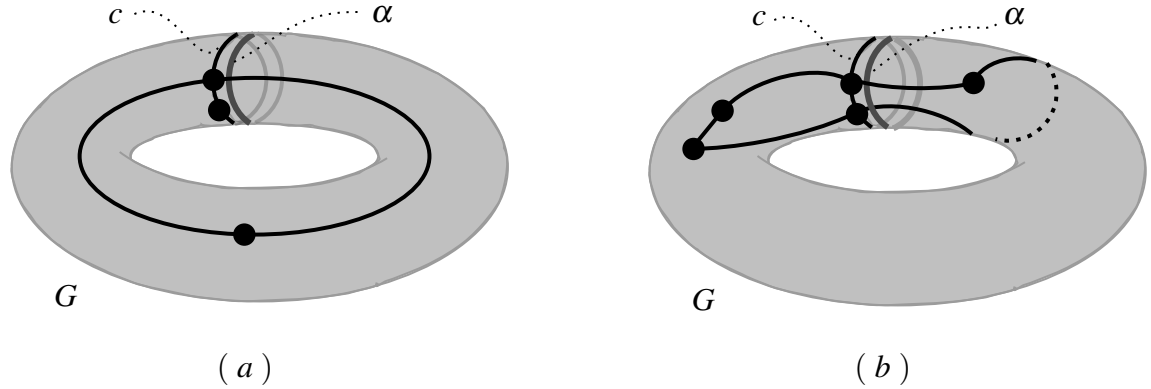


Figure 4.24: (a) The nonseparating cycle c is nonseparating in the \mathbb{T} -graph G . (b) The nonseparating cycle c is separating in the \mathbb{T} -graph G . The nonseparating loop α is the associated loop for the cycle c in (a) and (b).

Lemma 4.4.3. Suppose that H is a \mathbb{T} -subgraph of a (2,2)-tight \mathbb{T} -graph G and that there is some closed walk in H that is not null homotopic. Then there is a nonseparating cycle in H .

Proof. Consider all the closed walks in H that are not null homotopic. Choose one of such closed walks with minimal edge length. Notice that as this closed walk is minimal then there is no repeated vertex in this walk. Therefore, this closed walk is a nonseparating cycle in H . \square

Notation 4.4.4. (Q) Let G be an irreducible (2,2)-tight \mathbb{T} -graph. We consider a quadrilateral face Q of G with boundary walk

$$v_1^Q, e_1^Q, v_2^Q, e_2^Q, \dots, e_4^Q, v_5^Q = v_1^Q$$

See Figure 4.25.

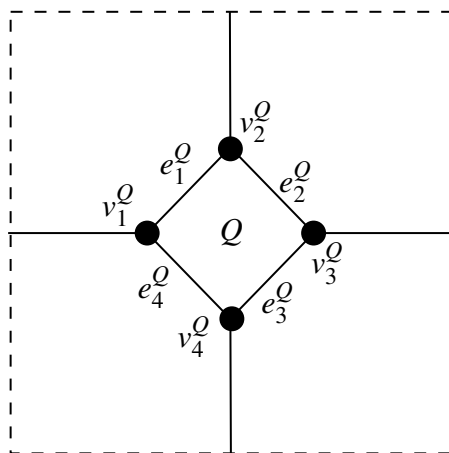


Figure 4.25: A labelling of a nondegenerate quadrilateral face of an irreducible $(2, 2)$ -tight \mathbb{T} -graph.

For the rest of this section, we deal with only one quadrilateral face. Thus, apart from setting new notations, we remove the superscript Q from all notations that include such superscript. This applies to only for the rest of this section.

Lemma 4.4.5. *Let G be an irreducible $(2, 2)$ -tight \mathbb{T} -graph. Then Q has a nondegenerate boundary.*

Proof. Since G is $(2, 2)$ -tight, then by Lemma 3.1.4, G has no loop. So $v_1 \neq v_{i+1}$ for $i = 1, \dots, 4$. Since G is $(2, 2)$ -tight, by Lemma 3.1.9, G has no vertex of degree 1, so $e_i \neq e_{i+1}$ for $i = 1, 2, 3$ and $e_4 \neq e_1$. Suppose that $v_1 = v_3$. If $v_2 = v_4$, then by the sparsity of G , the boundary of Q has at most two edges. In this case we see that Q is not adjacent to any other face, so Q must be the unique face of G . This contradicts Lemma 4.2.2.

Therefore, supposing $v_1 = v_3$ indicates that $v_2 \neq v_4$. Since G is irreducible there is a blocker, H , for $G \rightarrow G_{Q, v_2, v_4}$. Notice that since $v_1 = v_3$, then H cannot be a type 1 blocker and so H is a blocker of type 2. Therefore, $v_1, v_3 \notin H$. It follows that $\gamma_2(H \cup \partial Q) = \gamma_2(H) + \gamma(\partial Q) - \gamma_2(H \cap \partial Q) = 3 + 2 - 4 = 1$ which contradicts the sparsity of G . Hence $v_1 \neq v_3$. A similar argument can be used to show that $v_2 \neq v_4$. \square

We comment that the irreducibility assumption is necessary in Lemma 4.4.5. To see why, let us consider the example in Figure 4.26.

4.4. STRUCTURES OF IRREDUCIBLE (2,2)-TIGHT TORUS GRAPHS

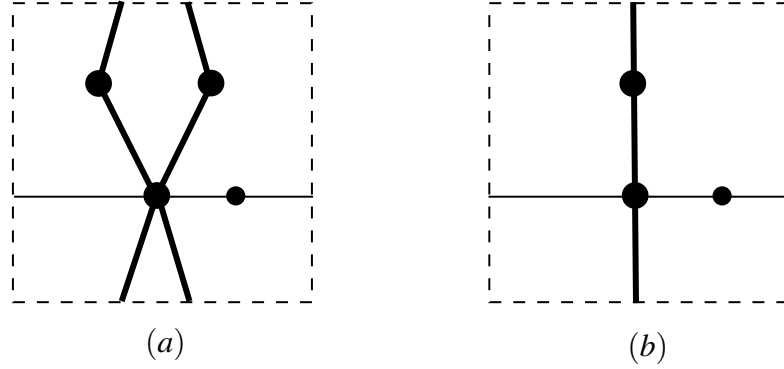


Figure 4.26: (a) The (2,2)-tight \mathbb{T} -graph is not irreducible. This \mathbb{T} -graph contains a degenerate quadrilateral face that is bold. Notice that this \mathbb{T} -graph can be reduced into the \mathbb{T} -graph in (b).

Notation 4.4.6. (H_1^Q and H_2^Q) Let G be an irreducible (2,2)-tight \mathbb{T} -graph. Since G is irreducible, by Theorem 3.3.18, there are maximal blockers H_1^Q , respectively H_2^Q , for the contractions $G \rightarrow G_{Q,v_1,v_3}$, respectively $G \rightarrow G_{Q,v_2,v_4}$.

Lemma 4.4.7. Let G be an irreducible (2,2)-tight \mathbb{T} -graph. Then both H_1 and H_2 are type 2 blockers for their respective contractions.

Proof. Suppose that H_1 is a blocker of type 1. Then $H_1 \cap H_2 \neq \emptyset$. Now, if H_2 is a blocker of type 1, then by Lemma 3.1.7 the \mathbb{T} -subgraph $H_1 \cup H_2$ is (2,2)-tight. Also, notice that $H_1 \cup H_2$ misses exactly one edge of ∂Q . Now, by Lemma 3.1.2:

$$\begin{aligned} \gamma_2(H_1 \cup H_2 \cup \partial Q) &= \gamma_2(H_1 \cup H_2) + \gamma_2(\partial Q) - \gamma_2((H_1 \cup H_2) \cap \partial Q) \\ &= 2 + 4 - 5 \\ &= 1 \end{aligned}$$

This contradicts the sparsity of G . On the other hand, if H_2 is a blocker of type 2, then $H_1 \cup H_2$ is missing exactly two edges of ∂Q . So

$$\begin{aligned} \gamma_2(H_1 \cup H_2) &= \gamma_2(H_1) + \gamma_2(H_2) - \gamma_2(H_1 \cap H_2) \\ &\leq 2 + 3 - 2 = 3 \end{aligned}$$

Therefore,

$$\begin{aligned}
 \gamma_2(H_1 \cup H_2 \cup \partial Q) &= \gamma_2(H_1 \cup H_2) + \gamma_2(\partial Q) - \gamma_2((H_1 \cup H_2) \cap \partial Q) \\
 &\leq 3 + 4 - 6 \\
 &= 1
 \end{aligned}$$

Which again contradicts the sparsity of G . Therefore, the conclusion is true. \square

Lemma 4.4.8. *Let G be an irreducible $(2, 2)$ -tight \mathbb{T} -graph and H_1 and H_2 are the blockers of a quadrilateral face Q of G . Then $H_1 \cap H_2 = \emptyset$.*

Proof. From Lemma 4.4.7, we notice that each of $H_1 \cap \partial Q$ and $H_2 \cap \partial Q$ has exactly one vertex of each of the edges e_1, e_2, e_3, e_4 . Thus,

$$\begin{aligned}
 2 \leq \gamma_2(H_1 \cup H_2 \cup \partial Q) &= \gamma_2(H_1) + \gamma_2(H_2) + \gamma_2(\partial Q) - \gamma_2(H_1 \cap H_2) \\
 &\quad - \gamma_2(H_1 \cap \partial Q) - \gamma_2(H_2 \cap \partial Q) + \gamma_2(H_1 \cap H_2 \cap \partial Q) \\
 &= 3 + 3 + 4 - \gamma_2(H_1 \cap H_2) - 4 - 4 + 0 \\
 &= 2 - \gamma_2(H_1 \cap H_2)
 \end{aligned}$$

So $\gamma_2(H_1 \cap H_2) \leq 0$. Therefore, $H_1 \cap H_2 = \emptyset$. \square

Lemma 4.4.9. *Let G be an irreducible $(2, 2)$ -tight \mathbb{T} -graph. Let H_1 and H_2 be the blockers of a quadrilateral face Q of G . Then both H_1 and H_2 are connected.*

Proof. Since G is $(2, 2)$ -tight, then H_1 and H_2 are $(2, 2)$ -sparse. But $\gamma_2(H_1) = \gamma_2(H_2) = 3$. Therefore, by Lemma 3.1.8, H_1 and H_2 are connected. \square

Lemma 4.4.10. *Let G be an irreducible $(2, 2)$ -tight \mathbb{T} -graph. Then every face of H_1 or H_2 is homeomorphic to either an open disc, an open cylinder or a once punctured torus.*

Proof. By Lemma 4.4.9, both H_1 and H_2 are connected. Since \mathbb{T} has genus one, then the required conclusion follows. \square

Notation 4.4.11. (α_1^Q and α_2^Q) *Consider the maximal blocker H_1 . Since H_1 is connected we can create a simple loop α_1^Q in \mathbb{T} by concatenating a minimal walk in H_1 joining v_1 and v_3 with the diagonal of Q that joins v_1^Q and v_3^Q . Define α_2^Q in the obviously analogous way, see Figures 4.30 and 4.32.*

4.4. STRUCTURES OF IRREDUCIBLE (2,2)-TIGHT TORUS GRAPHS

Notice that α_i is not necessarily uniquely defined even up to homotopy class, see Figure 4.27.

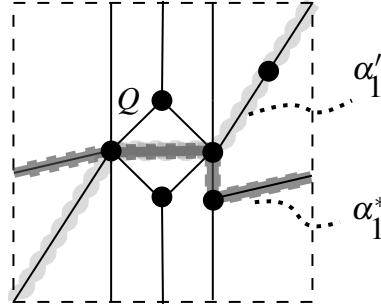


Figure 4.27: α'_1 and α_1^* are non homotopic to each other.

Lemma 4.4.12. *Consider the simple loops α_i , $i = 1, 2$ of a (2,2)-tight \mathbb{T} -graph G with a quadrilateral face Q . Then the geometric intersection number of α_1 and α_2 is 1. i.e.*

$$i(\alpha_1, \alpha_2) = 1 \quad (4.1)$$

Proof. Since $H_1 \cap H_2 = \emptyset$, by construction α_1 and α_2 intersect transversely at exactly one point (where the diagonals of Q meet). Thus, Lemma 4.3.6 gives the desired conclusion. \square

Lemma 4.4.13. *Consider the simple loops α_i , $i = 1, 2$ of a (2,2)-tight \mathbb{T} -graph G with a quadrilateral face Q . Then α_i is a nonseparating simple loop for $i = 1, 2$.*

Proof. In any orientable surface, $i(\alpha, \beta) = 1$ implies that both α and β are nonseparating loops. Thus, Lemma 4.4.12 gives the required conclusion. \square

Theorem 4.4.14. *Let G be a noncellular irreducible (2,2)-tight \mathbb{T} -graph. Then G comprises either a single vertex or a pair of parallel edges embedded as a nonseparating cycle in \mathbb{T} .*

Proof. Since \mathbb{T} has genus one and G is connected (Lemma 3.1.8), then G has exactly one face that is not an open disc. So G might have only one vertex. Now, suppose that G has more than one vertex. If the noncellular face is a punctured torus, then Lemma 4.2.2 implies that G has a cellular face that is either a triangle or a digon, contradicting the

irreducibility of G . Thus, the noncellular face of G must be an open cylinder. Let ζ be a loop in this face that is nonseparating in \mathbb{T} . By cutting and capping along ζ , we obtain \tilde{G} which is a $(2,2)$ -tight \mathbb{S} -graph with two faces that are not faces of G . By Lemma 4.2.2, the two exceptional faces of G must be digons. By using Lemma 4.2.2 again, we see that any other faces must be quadrilaterals. Now, consider one of these quadrilateral faces, say Q . Then $i(\alpha_1, \zeta) = i(\alpha_2, \zeta) = 0$. But \mathbb{T} has genus one. It follows that $i(\alpha_1, \alpha_2) = 0$ contradicting Lemma 4.4.12. So G has no quadrilateral faces. Therefore, G comprises exactly two edges, embedded as a nonseparating cycle. \square

Figure 4.28 presents the conclusion of the previous theorem.

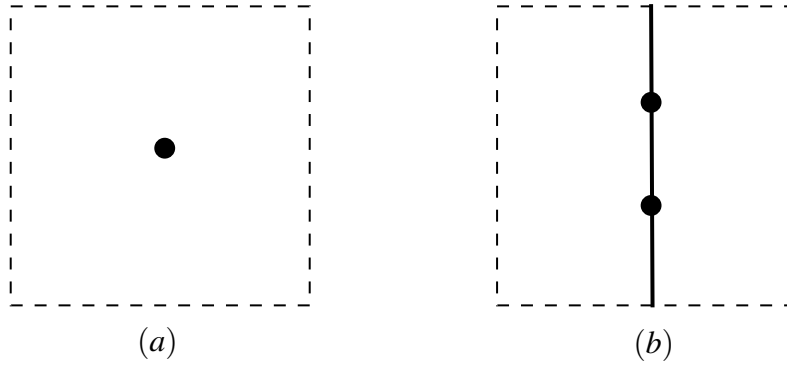


Figure 4.28: The conclusion of Theorem 4.4.14: (a) The irreducible $(2,2)$ -tight \mathbb{T} -graph with one vertex. (b) The irreducible $(2,2)$ -tight \mathbb{T} -graph with two vertices.

Definition 4.4.15. Let L be a \mathbb{T} -subgraph of a $(2,2)$ -tight \mathbb{T} -graph G . The \mathbb{T} -subgraph L is called *inessential* if it is contained in some embedded open disc in \mathbb{T} . Otherwise L is called *essential*.

In Figure 4.29, we provide examples of essential and inessential torus subgraphs.

Lemma 4.4.16. For a connected \mathbb{T} -subgraph L of a $(2,2)$ -tight \mathbb{T} -graph G , the following are equivalent.

1. L is essential.
2. L contains a nonseparating cycle.
3. L does not have any face homeomorphic to a once punctured torus.

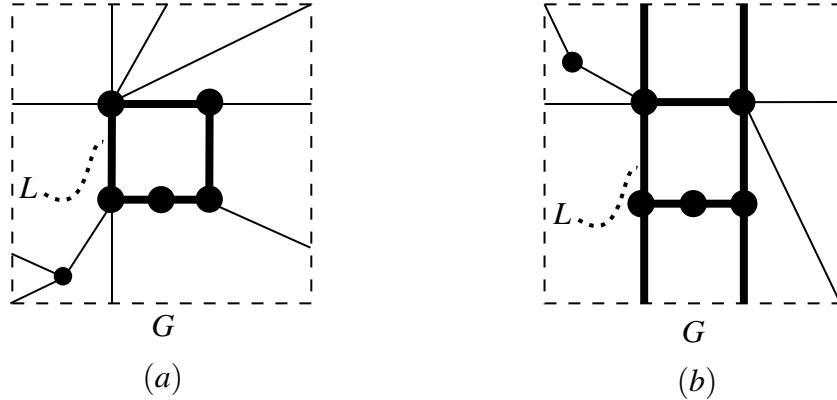


Figure 4.29: (a) The \mathbb{T} -subgraph L of the \mathbb{T} -graph G is inessential. (b) The \mathbb{T} -subgraph L of the \mathbb{T} -graph G is essential.

Proof. (1) \Rightarrow (3) Since L is essential so it is not contained in an open disc. So there is no face of L homeomorphic to a once punctured torus.

(2) \Rightarrow (1) Since L contains a nonseparating cycle so L cannot be contained in an open disc.

(3) \Rightarrow (2) Suppose that (3) is true. Notice that \mathbb{T} has genus one and L is connected. So L is either cellular or has exactly one face that is not a disc and that face is a cylinder. In either case we can see that there is a closed walk in L that is not null homotopic. By Lemma 4.4.3 there is a nonseparating cycle in L and so the statement 2 is true. \square

Notice that if H_i is an essential blocker of a quadrilateral face of an irreducible (2,2)-tight \mathbb{T} -graph, then we may choose a nonseparating cycle (notation β_i^Q) β_i that lies in H_i . Since $H_1 \cap H_2 = \emptyset$,

$$i(\beta_i, \alpha_{3-i}) = 0 \text{ for } i = 1, 2. \tag{4.2}$$

Given that \mathbb{T} has genus one, it follows that β_i is unique up to homotopy.

Lemma 4.4.17. *Let G be an irreducible (2,2)-tight \mathbb{T} -graph with a quadrilateral face Q . Then at most one of H_1 or H_2 is essential.*

Proof. Suppose that both of H_1 and H_2 are essential. Observe that $i(\beta_1, \beta_2) = i(\beta_1, \alpha_2) = i(\alpha_1, \beta_2) = 0$. Since \mathbb{T} has genus one, so $i(\alpha_1, \alpha_2) = 0$ contradicting Lemma 4.4.12. \square

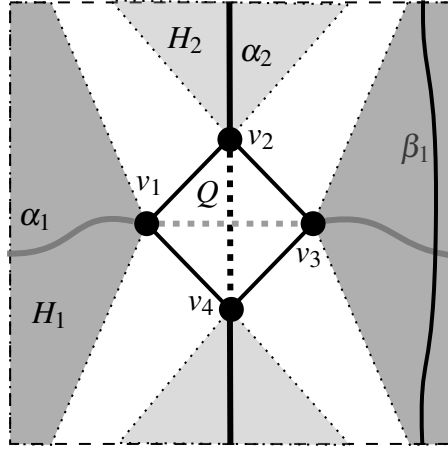


Figure 4.30: A summary for the previous notations and concepts in this section. Following Lemma 4.4.17 the blocker H_1 is essential and the blocker H_2 is inessential.

4.5 The structure of blockers of quadrilateral faces in irreducible torus graphs

In this section we explore the structure of the blockers of quadrilateral face(s) in an irreducible $(2, 2)$ -tight \mathbb{T} -graph. Here again, as we deal with only one quadrilateral face, then we remove the superscript Q from all notations that include such superscript. This applies to only for the rest of this section. However, We put such superscripts only for setting new notations.

Notation 4.5.1. (J_i^Q , \tilde{H}_i^Q , \tilde{J}_+^Q and \tilde{J}_-^Q) Since H_i^Q is a maximal blocker, by Lemma 3.4.13, there is exactly one face, denoted by J_i^Q , of H_i^Q that is not also a face of G . Observe that, by construction, J_i^Q is a noncellular face of H_i^Q since it contains α_{3-i}^Q which is nonseparating in \mathbb{T} . Therefore, we can form an \mathbb{S} -graph \tilde{H}_1^Q , respectively \tilde{H}_2^Q , by cutting and capping along α_2^Q , respectively α_1^Q . We note that if α_2^Q is nonseparating in J_1^Q , as opposed to just in \mathbb{T} , then \tilde{H}_1^Q has exactly one face, denoted by \tilde{J}_1^Q , that is not a face of G . On the other hand, if α_2^Q separates J_1^Q , then \tilde{H}_1^Q has exactly two faces, denoted by \tilde{J}_+^Q and \tilde{J}_-^Q , that are not faces of G .

Lemma 4.5.2. Let G be an irreducible $(2, 2)$ -tight \mathbb{T} -graph. Let Q be a quadrilateral face of G . Let H_1 and H_2 be the blockers of Q . If H_i , $i = 1, 2$ is inessential, then it is a single edge.

4.5. THE STRUCTURE OF BLOCKERS OF QUADRILATERAL FACES IN IRREDUCIBLE TORUS GRAPHS

Proof. Assume without loss of generality that H_1 is inessential. By Lemma 4.4.16, J_1 is isomorphic to a once punctured torus. So α_2 is nonseparating in J_1 . Now, consider the \mathbb{S} -graph \tilde{H}_1 and the unique face, \tilde{J}_1 , of \tilde{H}_1 that is not also a face of G . It is clear that $\gamma_2(\tilde{H}_1) = 3$. Now, by Lemma 4.2.3, \tilde{H}_1 satisfies $2f_2 + f_3 \geq 2$. On the other hand, G is irreducible, so it has no digonal or triangular faces. In particular, the only face of \tilde{H}_1 that could be a digon or a triangle is \tilde{J}_1 . Thus, the only possibility is that \tilde{J}_1 is in fact a digon. Now, if the boundary of \tilde{J}_1 is nondegenerate, then $\gamma_2(\partial J_1) = \gamma_2(\partial \tilde{J}_1) = 2$. Hence by Theorem 3.2.2, we get $\gamma_2(H_1) = 2$ contradicting $\gamma_2(H_1) = 3$. Therefore, the boundary of \tilde{J}_1 must be degenerate. Therefore, \tilde{H}_1 and H_1 also must consist of just a single edge. \square

Lemma 4.5.3. *Let G be an irreducible $(2, 2)$ -tight \mathbb{T} -graph and Q be a quadrilateral face of G . Then the graph spanned by the vertices of Q is isomorphic either to K_4 or K_4 with one edge deleted.*

Proof. By Lemma 4.4.17, at least one of the blockers is inessential. By Lemma 4.5.2, an inessential blocker is a single edge. \square

Notation 4.5.4. (c_+^Q and c_-^Q) *Let G be an irreducible $(2, 2)$ -tight \mathbb{T} -graph with a quadrilateral face Q . Consider the structure of an essential blocker. Suppose that H_1 is essential. Then J_1^Q is homeomorphic to an open cylinder. Let c_+^Q and c_-^Q denote the two boundary walks for ∂J_1^Q .*

Lemma 4.5.5. *Consider the boundary walks c_+ and c_- . If c_+ and c_- are simple then they are nonseparating.*

Proof. This follows from the fact that H_1 is essential. \square

Lemma 4.5.6. *Consider the boundary walks c_+ and c_- . Then both of these boundary walks are homotopic to α_2 .*

Proof. This follows from $i(c_+, \alpha_2) = i(c_-, \alpha_2) = 0$. \square

Lemma 4.5.7. *The closed walks c_+ and c_- satisfy the following inequalities:*

$$2 \leq |c_+|, |c_-| \leq 4 \text{ and } |c_+| + |c_-| \leq 6.$$

Proof. Consider the \mathbb{S} -graph \tilde{H}_1 with faces \tilde{J}_+ and \tilde{J}_- . It is clear that c_+ respectively c_- is the boundary walk of \tilde{J}_+ respectively \tilde{J}_- and $\gamma_2(\tilde{H}_1) = 3$. All other faces of \tilde{H}_1 are

also faces of G . But G is irreducible so such faces are not digons or triangles. But \tilde{H}_1 is an \mathbb{S} -graph so by Lemma 4.2.3, \tilde{H}_1 satisfies $2f_2 + f_3 \geq 2 + \sum_{i \geq 5} (i-4)f_i$. Therefore, the required conclusion follows easily. \square

Lemma 4.5.8. *If H_1 is essential, then either H_1 is isomorphic to the \mathbb{T} -graph in Figure 4.31, or c_+ and c_- are cycles.*

Proof. If c_+ has a repeated vertex, then since G has no loop edges it follows that $|c_+| \geq 4$. But by Lemma 4.5.7, $|c_-| = 2$ and in that case, let w be the repeated vertex of c_+ . This must be a cut vertex of H_1 . Thus, $H_1 = X \cup Y$ where $X \cap Y = \{w\}$. Then $\gamma_2(X) + \gamma_2(Y) - 2 = \gamma_2(H_1) = 3$. Thus, $\gamma_2(X) + \gamma_2(Y) = 5$. Without loss of generality, suppose that $\gamma_2(X) = 2$ and $\gamma_2(Y) = 3$. So X is a $(2, 2)$ -tight \mathbb{T} -subgraph of G . By Theorem 5.1.1, X is irreducible. So X is either isomorphic to the \mathbb{T} -graph in Figure 4.28(a) or Figure 4.28(b). But X has more than one vertex. Therefore, X is isomorphic to the \mathbb{T} -graph in Figure 4.28(b). By a similar argument as in the proof of Lemma 4.5.2, Y is a single edge. \square

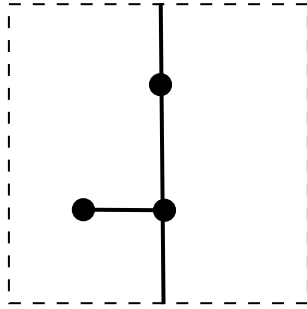


Figure 4.31: The \mathbb{T} -graph is isomorphic to the blocker H_1 provided that c_- and c_+ are not cycles.

Notation 4.5.9. (F_+^Q and F_-^Q) *Consider the $(2, 2)$ -tight subgraph $\partial Q \cup H_1 \cup H_2$. This \mathbb{T} -graph has two faces, denoted by $F_+^Q \subset J_1^Q$ and $F_-^Q \subset J_1^Q$ that may not be faces of G . We choose our labels so that $v_1^Q \in F_-^Q$ and $v_3^Q \in F_+^Q$. As a consequence of Lemma 4.5.8, we see that the boundary walk of F_+^Q is the walk $v_3^Q, e_3^Q, v_4^Q, H_2^Q, v_2^Q, e_2^Q, v_3^Q$ followed by a traverse of c_+^Q back to v_3^Q . In particular, v_3^Q is the only repeated vertex in that boundary walk. Similar comments apply to the boundary walk of F_-^Q . In Figure 4.32 we summarise the various structural elements associated with a quadrilateral face that has an essential blocker.*

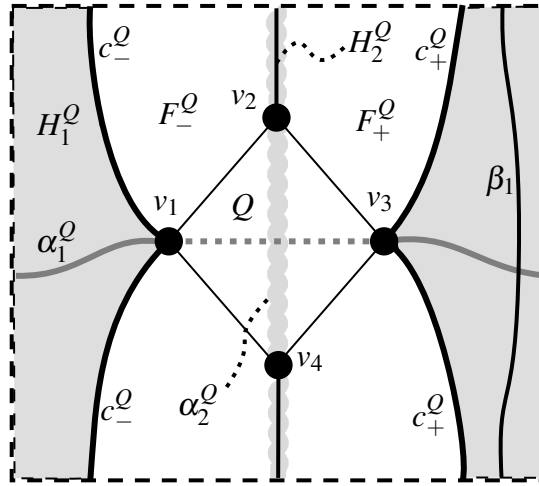


Figure 4.32: A summary for various concepts and notations for the blocker structure.

4.6 (2, 2)-tight cylindrical graphs

Here we provide an inductive construction for the class of (2, 2)-tight cylindrical graphs.

In this section we prove the following theorem.

Theorem 4.6.1. *If G is an irreducible (2, 2)-tight cylindrical graph, then G is isomorphic to one of the cylindrical graphs shown in Figure 4.33.*

Proof. Since G is a cylindrical graph, then either G separates the cylinder or does not. So suppose first that G does not separate the cylinder. Then there is a unique noncellular face of G , see Figure 4.34(a). By capping this face (i.e. filling the two boundaries of the cylinder with two open discs) we create a cellular (2, 2)-tight \mathbb{S} -graph \tilde{G} . By Corollary 4.2.4, we see that either \tilde{G} has a single vertex or it has at least two faces that are digons or triangles. In both cases, one of these faces must be also a face in G . Thus, if G has at least two vertices, then G is not irreducible.

Now, suppose that G separates the cylinder. It is clear that G has exactly two noncellular faces, see Figure 4.34(b). By capping the two boundaries of the cylinder, we create a (2, 2)-tight \mathbb{S} -graph \tilde{G} . By Lemma 4.2.2, \tilde{G} satisfies $2f_2 + f_3 = 4 + f_5 + 2f_6 + \dots$. Now, since all but two of the faces of \tilde{G} are also faces of the irreducible G , it follows that the two exceptional faces of \tilde{G} are digons and all other faces are quadrilateral faces of G . Thus, it suffices to show that there cannot be any quadrilateral faces in G .

For a contradiction, suppose that Q is a quadrilateral. Since G is irreducible, both possible contractions of Q are blocked and we infer the existence of simple loops α_1 and α_2 as described in Notation 4.4.11. Recall that these loops intersect transversely at exactly one point and thus α_1 is nonseparating in the cylinder. However, the Jordan Curve Theorem tells that any simple loop in the cylinder must be separating. \square

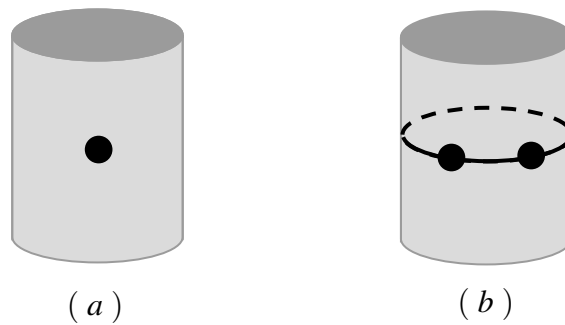


Figure 4.33: The two irreducible $(2,2)$ -tight cylindrical graphs.

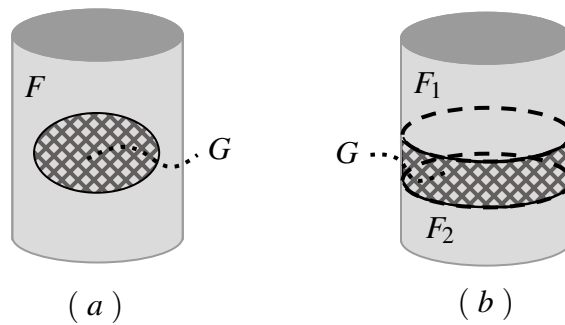


Figure 4.34: (a) G does not separate the cylinder. F is the noncellular face of G . (b) G separates the cylinder. F_1 and F_2 are the noncellular faces of G .

We note that, for any positive integer n , it is straightforward to construct a $(2,2)$ -tight cylindrical graph that has no digons or triangles, but has n quadrilateral faces, see Figure 4.35. So, in contrast to the case of the sphere, we do require the quadrilateral contraction move in order to have finitely many irreducible $(2,2)$ -tight cylindrical graphs.

4.7. THE FINITENESS THEOREM OF IRREDUCIBLE (2,2)-TIGHT TORUS GRAPHS

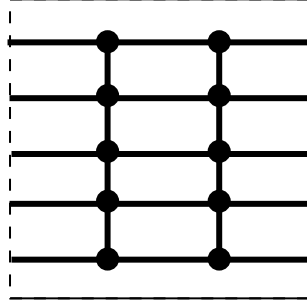


Figure 4.35: An example of a $(2,2)$ -tight cylindrical graph with no digon faces, triangle faces or divalent vertices. It is clear that there are infinitely many such pairwise nonisomorphic examples.

4.7 The finiteness theorem of irreducible $(2,2)$ -tight torus graphs

In this section, we state and prove the finiteness theorem for the class of $(2,2)$ -tight torus graphs. Notice that in this section, we consider irreducible $(2,2)$ -tight torus graphs with more than one quadrilateral faces. Thus, the results on the closed walks c_- and c_+ are applied for any quadrilateral face that we consider in this section.

Lemma 4.7.1. *Suppose that H is a $(2,2)$ -tight \mathbb{T} -subgraph of an irreducible $(2,2)$ -tight \mathbb{T} -graph and that F is a cellular face of H with $|F| \geq 5$. Suppose that R is a nondegenerate quadrilateral face of G that is contained in F and for every vertex $v \in \partial R$ such that $v \in F$ there is an edge $e \in E(G)$ such that e is incident to v and to ∂F but $e \notin \partial F$, $u \in \partial F$, $uv \notin \partial R$. Then $v \in F$ for all vertices $v \in \partial R$.*

Proof. Since both G and H are $(2,2)$ -tight, then it is clear that H is an induced subgraph of G . Now, since $|R| < |F|$, then there is at least one vertex in ∂R does not belong to ∂F . So there is at least one vertex of ∂R in F . On the other hand, if there is at least one vertex of ∂R in ∂F , and I is the subgraph of G spanned by $H \cup \partial R$, then it is easy to see that $\gamma_2(I) \leq 1$ contradicting the sparsity of G . Therefore, all the vertices of ∂R lie in F . \square

Lemma 4.7.2. *Suppose that H is a \mathbb{T} -subgraph of an irreducible $(2,2)$ -tight \mathbb{T} -graph G and that F is a cellular face of H . Let v be a vertex of G with $v \in F$ and suppose that c is a nonseparating cycle in G that contains v and such that $|c| \leq 4$. Then either*

1. c contains an edge that is incident to both v and some vertex of ∂F , or
2. there is some vertex $u \in \partial F$ that is repeated in the boundary walk of F , and such that c consists of the concatenation of two paths of edge length two in $G \cap F$ joining v to u .

Proof. Since c is nonseparating in \mathbb{T} , it cannot be contained within F . Hence the required conclusion follows easily. \square

Notation 4.7.3. (R and K^Q) Let R be a quadrilateral face of the irreducible $(2,2)$ -tight \mathbb{T} -graph G that is distinct from Q . Following Lemma 4.4.17, we will assume that H_2^R is inessential and therefore, by Lemma 4.5.2 H_2^Q consists of a single edge joining v_2^R and v_4^R . Let K^Q denote the \mathbb{T} -subgraph of G that is spanned by the vertices of Q . By Lemma 4.5.3, the underlying graph of K^Q is either K_4 or K_4 with one edge deleted.

Lemma 4.7.4. Let G be an irreducible $(2,2)$ -tight \mathbb{T} -graph. Consider the \mathbb{T} -subgraph K^Q of G . If $K^Q = K_4$, then G has no other quadrilateral face.

Proof. It is clear that K^Q is a $(2,2)$ -tight \mathbb{T} -subgraph of G . Notice that K^Q has an octagonal face O such that $\partial O = K^Q$. Suppose, for a contradiction, that R is a quadrilateral face of G and that $R \subset O$. First we deal with the case where both H_1^R and H_2^R are inessential blockers. By Lemma 4.5.2, each blocker comprises a single edge. Now, α_1^R is a simple nonseparating loop comprising the edge H_1^R and a diagonal of R . Since α_1^R is nonseparating, then it cannot be contained within the open disc O . It follows that at least one of the vertices v_1^R or v_3^R lies in ∂O . We also can observe that if $v_j^R \in O$ for $j = 1$ or 3 , then H_1^R is an edge, that is not in ∂R , joining v_j^R and a vertex of ∂O . Similar comments apply to the vertices v_2^R and v_4^R . Thus, we have a quadrilateral face R contained in an octagonal face O such that at least two vertices of ∂R lie in ∂O , and such that every vertex of ∂R that lies in O is joined by an edge, that is not an edge of ∂R , to a vertex of ∂O . This contradicts Lemma 4.7.1.

Now, suppose the case that one of the two blockers is essential, say H_1^R and the blocker H_2^R is inessential. As in the previous paragraph at least one of v_2^R, v_4^R lies in ∂O and if $v_j^R \in O$ for $j = 2$ or 4 , then H_2^R is an edge joining v_j^R to ∂O . We will suppose that $v_2^R = v_2^Q$ and that $v_4^R \in O$. Similar arguments apply to all other possibilities. Observe that any simple nonseparating loop that does not intersect α_2^R must contain the vertex v_4^Q , see Figure 4.36(a).

4.7. THE FINITENESS THEOREM OF IRREDUCIBLE (2,2)-TIGHT TORUS GRAPHS

Since H_1^R is essential, it contains a simple nonseparating loop that is disjoint from α_2^R . Thus, $v_4^Q \in H_1^R$. However, v_4^Q is adjacent to $v_2^Q = v_2^R$ and since v_1^R and v_3^R are the only vertices of H_1^R that are adjacent to v_2^R it follows that either $v_1^R = v_4^Q$ or $v_3^R = v_4^Q$. Without loss of generality assume that $v_3^R = v_4^Q$. So we have the situation depicted in Figure 4.36(b). Note that $v_1^R \in O$ otherwise v_4^R would be triply adjacent to the (2,2)-tight graph $\partial O = K^Q$, which contradicts the sparsity of G . Now, by applying Lemma 4.7.2 to the simple nonseparating loop c_-^R , we see that there must be an edge incident to v_1^R and ∂O , contradicting Lemma 4.7.1. \square

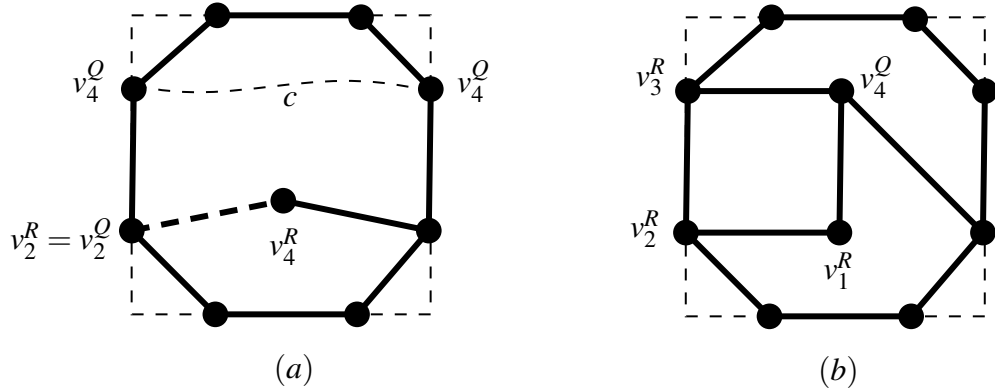


Figure 4.36: In these diagrams the boundary of the octagon is $K^Q \cong K_4$. If c is a nonseparating loop in G disjoint from α_2^R , then it must contain the vertex v_4^Q .

Remark 4.7.5. *If any quadrilateral face of G spans a copy of K_4 , then that is the only quadrilateral face. Thus, we may assume from now on that no quadrilateral face spans a copy of K_4 . In particular, every quadrilateral face has one inessential blocker and one essential blocker. Without loss of generality we assume that H_1^R is essential for any quadrilateral face R of G . So we have faces F_+^Q, F_-^Q of $\partial Q \cup H_1^Q \cup H_2^Q$ as described in the previous section.*

Lemma 4.7.6. *If c_- and c_+ are cycles, then there is no quadrilateral face of an irreducible (2,2)-tight \mathbb{T} -graph G contained in F_+^Q or F_-^Q .*

Proof. Suppose that $R \subset F_+^Q$ is a quadrilateral face of G . We will show that the existence of such a quadrilateral contradicts Lemma 4.7.1. Since H_2^R is inessential, then we can see

that α_2^R is a nonseparating loop of edge length two. So at least one of v_2^R or v_4^R lies in ∂F_+^Q . We can assume without loss of generality that $v_2^R \in \partial F_+^Q$.

Now, suppose that $v_4^R \in F_+^Q$. Since α_2^R is a nonseparating simple cycle of length two, it must be that H_2^R is an edge incident to v_4^R and ∂F_+^Q . Note also that H_2^R is not an edge of ∂R . Moreover, as noted in Notation 4.5.9 that v_3^Q is the only repeated vertex in ∂F_+^Q . So, if $v_4^R \in F_+^Q$, then $v_3^Q \in H_2^R$.

Now, suppose that $v_1^R \in F_+^Q$. Since c_-^R is a simple nonseparating loop that contains v_1^R and has edge length at most 4 (by Lemma 4.5.7). Recall that v_3^Q is the only vertex that is repeated on the boundary walk F_+^Q . If $v_3^Q \in \alpha_2^R$, then since c_-^R is disjoint from α_2^R , it follows from Lemma 4.7.2. that there is an edge of c_-^R that is incident to v_1^R and ∂F_+^Q .

So now we assume that $v_3^Q \notin \alpha_2^R$. As observed above it follows that both v_2^R and v_4^R belong to ∂F_+^Q . Recall that the repeated vertex v_3^Q separates the boundary walk of ∂F_+^Q into two simple walks. The first walk is c_+^R (thought of as a simple walk starting and ending at v_3^Q) and the walk is $w = v_3^Q, e_3^Q, v_4^Q, H_2^Q, v_2^Q, e_2^Q, v_3^Q$. Suppose that both $v_2^R, v_4^R \in w$. Since neither of them is equal to v_3^Q , it follows that $\{v_2^R, v_4^R\} = \{v_2^Q, v_4^Q\}$. Thus, it must be that H_2^Q is also H_2^R . But it is clear that in this case α_2^R is not a nonseparating loop which contradicts Lemma 4.4.12. On the other hand, suppose that $v_2^R, v_4^R \in c_+^Q$. Then at least one of v_1^R, v_3^R lies in F_+^Q and is doubly adjacent to H_1^Q which contradicts the maximality of the blocker H_1^Q . Thus, we see that one of v_2^R, v_4^R lies in $\{v_2^Q, v_4^Q\}$ and the other lies in c_+^Q . In other words the diagonal, d , of R joining v_2^R and v_4^R separates the two occurrences of v_3^Q in the boundary walk of F_+^Q .

Now, suppose that $v_1^R \in F_+^Q$. We know that c_-^R is a nonseparating simple cycle containing v_1^R and disjoint from d . But since d separates the two occurrences of the only repeated vertex on the boundary walk of F_+^Q , it follows from Lemma 4.7.2 that some edge of c_-^R is incident to v_1^R and ∂F_+^Q . Such an edge cannot belong to ∂R . Similarly if $v_3^R \in F_+^Q$, then there is an edge, not in ∂R , that is incident to v_3^R and to ∂F_+^Q .

Thus, we have shown that at least one vertex of ∂R lies in ∂F_+^Q and that any vertex of ∂R in F_+^Q is adjacent to ∂F_+^Q via an edge that is not in ∂R . This contradicts Lemma 4.7.1. \square

Lemma 4.7.7. *Let G be an irreducible $(2,2)$ -tight \mathbb{T} -graph. If G contains a $(2,2)$ -tight \mathbb{T} -subgraph isomorphic to the \mathbb{T} -graph shown in Figure 4.37, then there is no quadrilateral face of G contained in F_-^Q and F_-^Q .*

4.7. THE FINITENESS THEOREM OF IRREDUCIBLE (2,2)-TIGHT TORUS GRAPHS

Proof. The proof is similar to the proof of Lemma 4.7.6. □

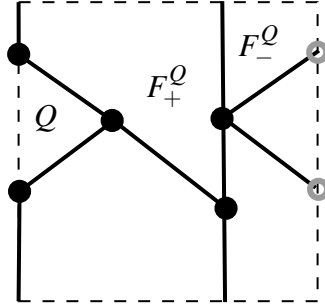


Figure 4.37: A \mathbb{T} -graph isomorphic to a \mathbb{T} -subgraph of an irreducible (2,2)-tight \mathbb{T} -graph, see Lemma 4.7.7.

Notation 4.7.8. (L_1 and L_3) We can assume from now on that the quadrilateral face R is also a face of H_1^Q . So $v_1^R, v_3^R \in H_1^Q \cap H_1^R$. Moreover, these vertices lie in distinct components of $H_1^Q \cap H_1^R$ since they are separated in H_1^Q by H_2^R which is disjoint from H_1^R . Let L_i be the component of $H_1^Q \cap H_1^R$ in which v_i^R lies for $i = 1, 3$. See Figure 4.38.

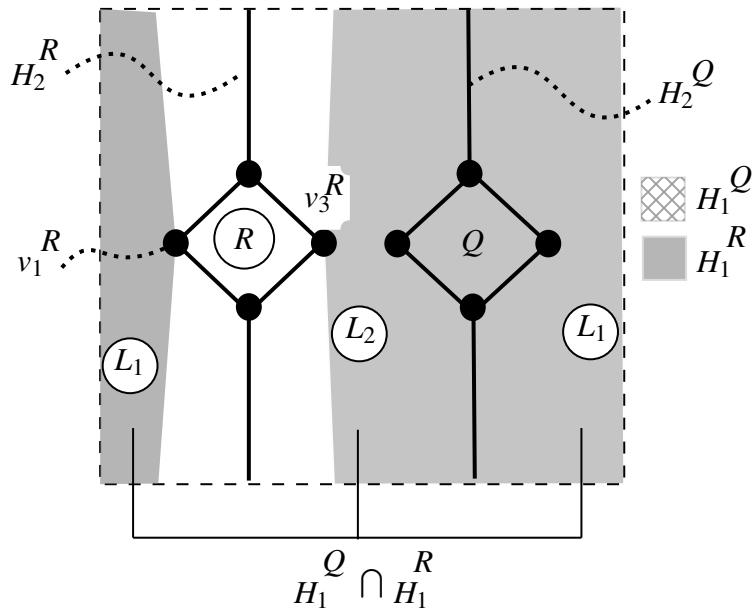


Figure 4.38: A diagram which illustrates L_1 and L_3 .

Lemma 4.7.9. $H_1^Q \cap H_1^R = L_1 \cup L_3$ and $\gamma_2(L_1) = \gamma_2(L_3) = 2$.

Proof. By the sparsity of G , we get

$$\gamma(H_1^Q \cap H_1^R) \geq \gamma(L_1) + \gamma(L_3) \geq 4 \quad (4.3)$$

On the other hand, $\gamma_2(H_1^Q \cap H_1^R) = \gamma_2(H_1^Q) + \gamma_2(H_1^R) - \gamma_2(H_1^Q \cup H_1^R) \leq 3 + 3 - 2 = 4$. Thus, we have equality in (4.3) and hence the required conclusion follows. \square

Lemma 4.7.10. Consider L_i for $i = 1, 3$. Then L_i is either a single vertex or a nonseparating cycle of length two.

Proof. Suppose that L_1 is inessential. Then it is a $(2, 2)$ -tight \mathbb{S} -graph such that all but one of its faces are also faces in G . Since G has no digonal or triangular faces, the only possibility is that L_1 is a single vertex.

Now, suppose that L_1 is essential. It has one face that is not also a face of G . By cutting and capping this face along a nonseparating loop we construct a $(2, 2)$ -tight \mathbb{S} -graph \tilde{L}_1 . By Lemma 4.2.4, \tilde{L}_1 has two digonal faces whose boundary walks must be c_+^Q and c_-^R and all the other faces of \tilde{L}_1 must be quadrilateral faces.

Suppose that S is a quadrilateral face of L_1 . Then it is clear that the inessential blocker H_2^S must lie inside L_1 , since L_1 is $(2, 2)$ -tight. Thus, cutting L_1 along α_2^S yields two nonempty subgraphs, M_1 and M_2 of L_1 . Notice that the union of M_1 and M_2 is L_1 and their intersection is a single edge. But

$$\begin{aligned} 2 = \gamma_2(L_1) &= \gamma_2(M_1 \cup M_2) = \gamma_2(M_1) + \gamma_2(M_2) - \gamma_2(M_1 \cap M_2) \\ &= \gamma_2(M_1) + \gamma_2(M_2) - (2(2) - 1) \\ &= \gamma_2(M_1) + \gamma_2(M_2) - 3 \end{aligned}$$

So $\gamma_2(M_1) + \gamma_2(M_2) = 5$. Now, suppose without loss of generality that $\gamma_2(M_1) = 2$. Clearly M_1 has one face that is not also a face of G . Thus, by cutting and capping along a nonseparating loop in this face we obtain \tilde{M}_1 . Notice that \tilde{M}_1 is a $(2, 2)$ -tight \mathbb{S} -graph that has one digonal face and one triangular face and such that all other faces are also faces in G . But then Lemma 4.2.4 implies that \tilde{M}_1 has another triangular face which is also a face of G . This contradicts the irreducibility of G . \square

See Figure 4.39 which presents examples of all possible cases of L_1 and L_3 .

4.7. THE FINITENESS THEOREM OF IRREDUCIBLE (2,2)-TIGHT TORUS GRAPHS

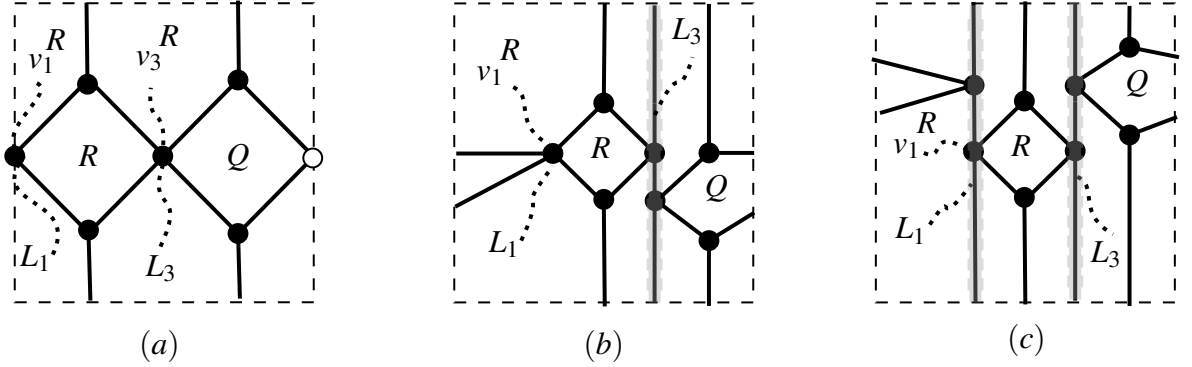


Figure 4.39: Examples of the three possible cases of L_1 and L_3 .

Theorem 4.7.11. *If G is an irreducible (2,2)-tight \mathbb{T} -graph, then G has at most two quadrilateral faces.*

Proof. Suppose that G has three pairwise distinct quadrilateral faces Q, R, S . By Lemma 4.7.4, S is a face of both H_1^Q and H_1^R . Thus, S must be a face of L_1 or L_3 . Clearly either case contradicts Lemma 4.7.10. \square

In the following we state and prove the finiteness theorem.

Theorem 4.7.12. *If G is an irreducible (2,2)-tight \mathbb{T} -graph, then G has at most 8 vertices. In particular, there are finitely many isomorphism classes of such graphs.*

Proof. If G is noncellular, then the required conclusion follows from Theorem 4.4.14. So we assume that G is cellular. Since G is (2,2)-tight, $f_1 = 0$. Since G is irreducible, by Lemma 3.4.5, $f_2 = 0$, and by Lemma 3.4.8, $f_3 = 0$. Therefore, by Lemma 2.4.4, $f_5 + 2f_6 + 3f_7 + 4f_8 = 4$ and $f_i = 0$ for $i \geq 9$. Moreover, by Theorem 4.7.11, $f_4 \leq 2$. Now,

$$\begin{aligned} 2e &= 4f_4 + 5f_5 + 6f_6 + 7f_7 + 8f_8 \\ &\leq 4f_4 + 5(f_5 + 2f_6 + 3f_7 + 4f_8) \\ &\leq 4(2) + 5(4) = 28 \end{aligned}$$

Thus, $e \leq 14$. By (2,2)-tightness of G , $2v - 2 = e$. Hence, $v = \frac{e+2}{2} \leq 8$. \square

4.8 Examples and a conjecture

Through this section we exhibit examples of various concepts that we reviewed and introduced in this chapter. Eventually, we end this chapter with a conjecture.

4.8.1 Examples

Reducible and irreducible $(2,2)$ -tight torus graphs

In Figure 4.40, we include two $(2,2)$ -tight \mathbb{T} -graphs. One of them is reducible and the other is irreducible.

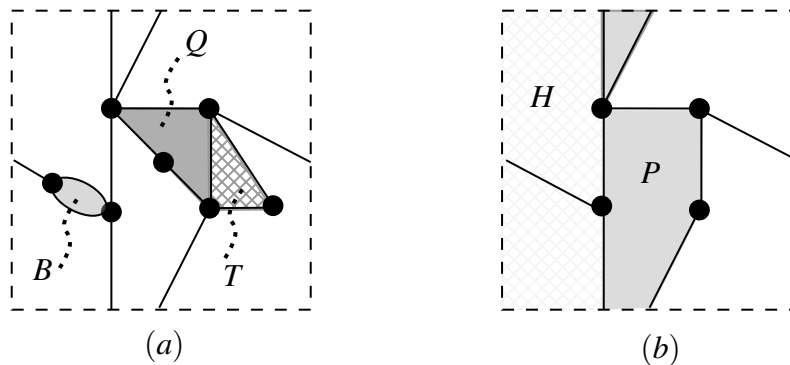


Figure 4.40: The \mathbb{T} -graph in (a) is reducible. It has the digon B , the triangle T and the contractible quadrilateral Q . The \mathbb{T} -graph in (b) is irreducible with two faces, the pentagon P and the heptagon H . Notice that the \mathbb{T} -graph in (a) can be reduced into the \mathbb{T} -graph in (b).

Blockers for a quadrilateral contraction

In Figure 4.41, we provide an example of a blocker of an irreducible $(2,2)$ -tight \mathbb{T} -graph.

Maximal blocker

In Figure 4.42 we depict two blockers of the given irreducible $(2,2)$ -tight torus graph. One of these blockers is maximal and the other is not.

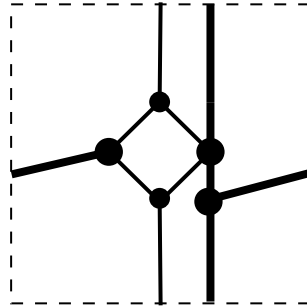


Figure 4.41: The \mathbb{T} -subgraph in bold of the \mathbb{T} -graph is an essential blocker for the quadrilateral face.

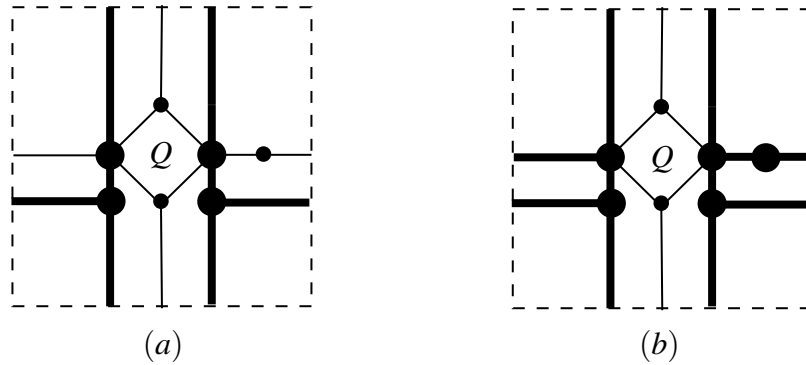


Figure 4.42: (a) The blocker in bold for the quadrilateral face Q is not maximal. (b) The blocker in bold for the quadrilateral face Q is maximal.

An example showing the faces F_-^Q and F_+^Q

Figure 4.43 illustrates the faces F_-^Q and F_+^Q . See also Notation 4.5.9.

An example clarifies the cutting and capping procedure along a nonseparating loop

Figure 4.44 illustrates how the procedure of cutting and capping along a nonseparating loop can be performed on a torus graph.

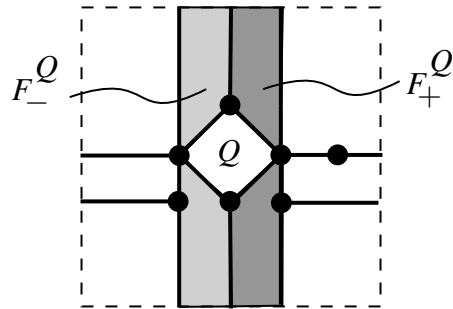


Figure 4.43: The faces F_-^Q and F_+^Q are in the two shaded areas.

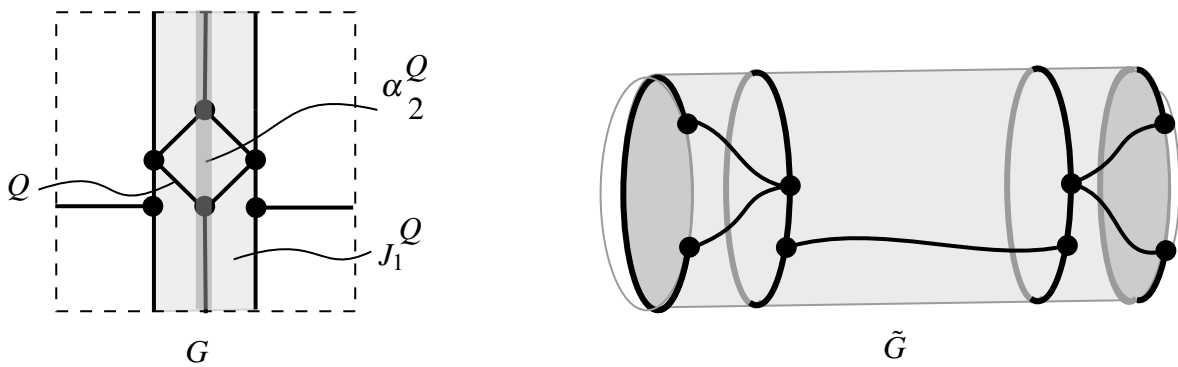


Figure 4.44: We cut along the nonseparating loop α_2^Q in the \mathbb{T} -graph G . Then we fill the resulting two boundary curves with open discs to get the \mathbb{S} -graph \tilde{G} .

An example illustrates α_1^Q and α_2^Q

In Figure 4.45 we provide an example showing the curves α_1^Q and α_2^Q .

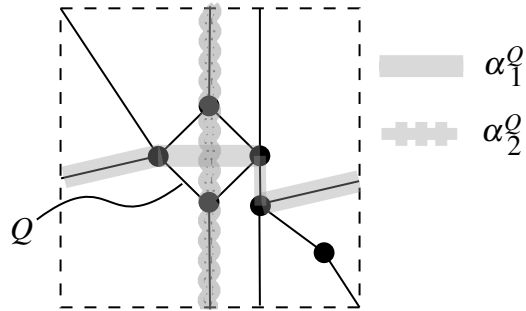


Figure 4.45: The nonseparating loops are illustrated by two different strips.

An example of β_1^Q

In Figure 4.46, we provide an example of the cycle β_1^Q .

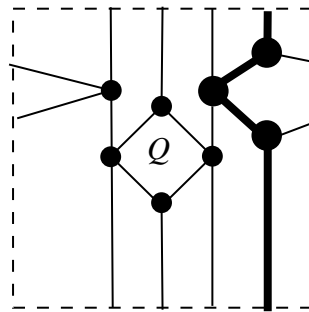


Figure 4.46: The cycle that is bold in the \mathbb{T} -graph is an example of β_1^Q .

c_-^Q and c_+^Q

In Figure 4.47, we give an example for the the closed walks c_-^Q and c_+^Q in case they are cycles.

Two essential blockers of a quadrilateral face

It is possible for an irreducible $(2, 2)$ -tight Σ -graph, where Σ of higher genus, to have two essential blockers of a quadrilateral face. In Figure 4.48, we provide an example of an irreducible $(2, 2)$ -tight double-torus graph such that the two blockers of a quadrilateral face are essential.

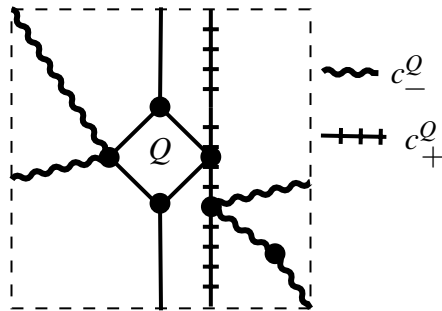


Figure 4.47: c_-^Q and c_+^Q

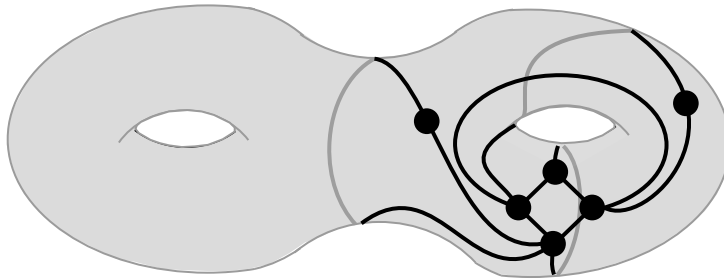


Figure 4.48: An irreducible $(2, 2)$ -tight double torus graph with two essential blockers of the quadrilateral face.

Quadrilateral contractions are necessary

In this section, we include a justification for the necessity of the quadrilateral contractions in the inductive construction of the class of $(2, 2)$ -tight \mathbb{T} -graphs. We observe that there are infinitely many pairwise nonisomorphic $(2, 2)$ -tight torus graphs such that each of these graphs has no digon and no triangle. Moreover, we can construct such a family of graphs so that none of the graphs have vertices of degree 2, Figure 4.49. Therefore, it is clear that it is not possible to prove an inductive contraction result for $(2, 2)$ -tight \mathbb{T} -graphs using just digon constructions, triangle constructions and divalent vertex deletions (the inverse of the topological Henneberg type 0 move), at least if we demand a finite set of irreducible $(2, 2)$ -tight torus graphs.

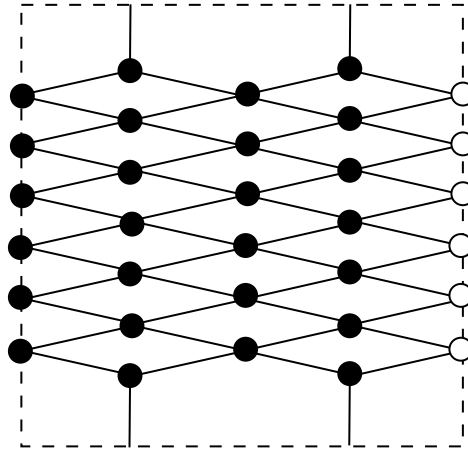


Figure 4.49: An example of $(2, 2)$ -tight torus graph with no digonal faces, triangular faces or divalent vertices. It is clear that there are infinitely many of such pairwise nonisomorphic examples.

4.8.2 Finiteness conjecture

In this section, we post a conjecture concerns with the existing of finite irreducible $(2, l)$ -tight graphs of any surface with finite topological type. Recall that a surface has finite topological type if it has finitely many handles, punctures and boundary components, see Figure 4.50.

Conjecture 4.8.1. *For any surface Σ of finite topological type, and for $0 \leq l \leq 3$, there are finitely many isomorphism classes of irreducible $(2, l)$ -tight Σ -graphs.*

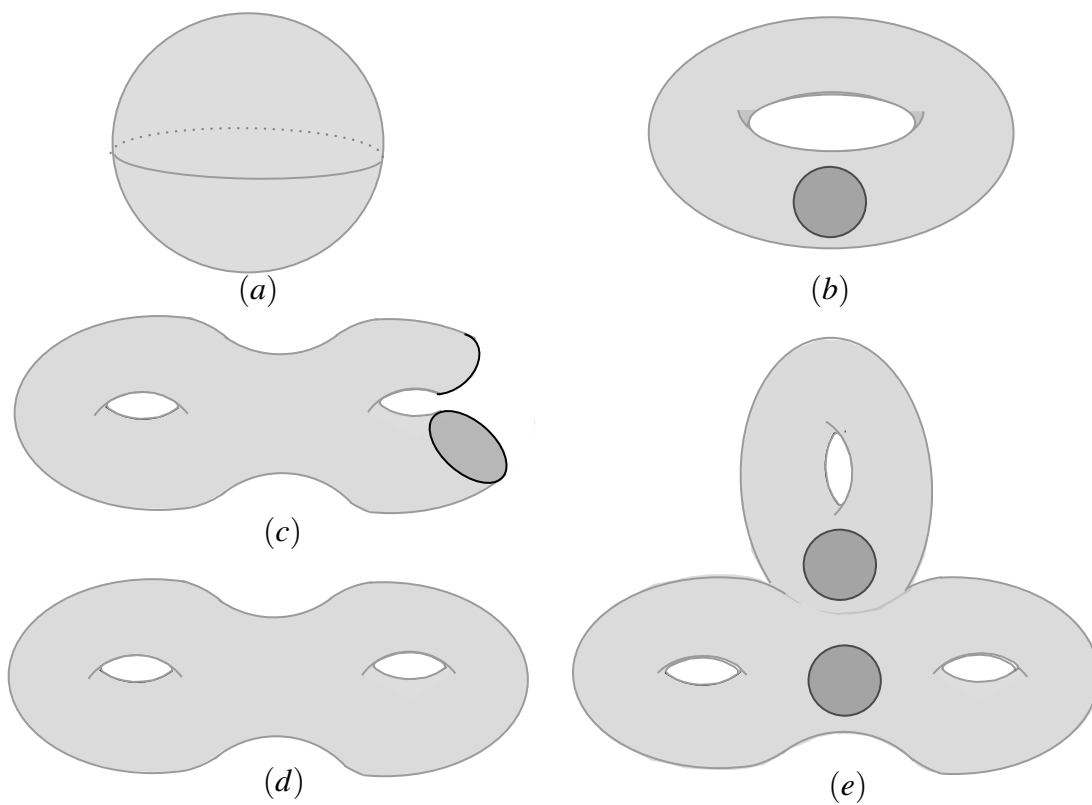


Figure 4.50: Some surfaces with finite topological type.

Chapter 5

Irreducible (2,2) -Tight Torus Graphs

As we have proven in the previous chapter that there are a finite number of irreducible (2,2)-tight torus graphs, this chapter is devoted to present all such torus graphs and explain in detail how we found them. Besides, we prove that the list of all nonisomorphic irreducible (2,2)-tight \mathbb{T} -graphs is exhaustive. Specifically, we prove the following theorem.

Theorem 5.0.1. *There are exactly 116 nonisomorphic irreducible (2,2)-tight \mathbb{T} -graphs.*

As in this chapter we specialise to (2,2)-tight graphs. We use γ instead of γ_2 from now on.

5.1 Embedding lemmas in the torus

Finding all embeddings of a given graph in the torus can be a labour intensive task. However, we can reduce the computations of such embeddings by establishing some rules of embedding certain subgraphs of the (2,2)-tight graphs. Also, we present and prove the following theorem.

Theorem 5.1.1. *Let H be a \mathbb{T} -subgraph of an irreducible (2,2)-tight \mathbb{T} -graph G . If H is (2,2)-tight, then H is irreducible.*

We start by introducing some key lemmas that will be used to prove Theorem 5.1.1 and also be used in later sections. We introduce notations for some small graphs in Figure 5.1.

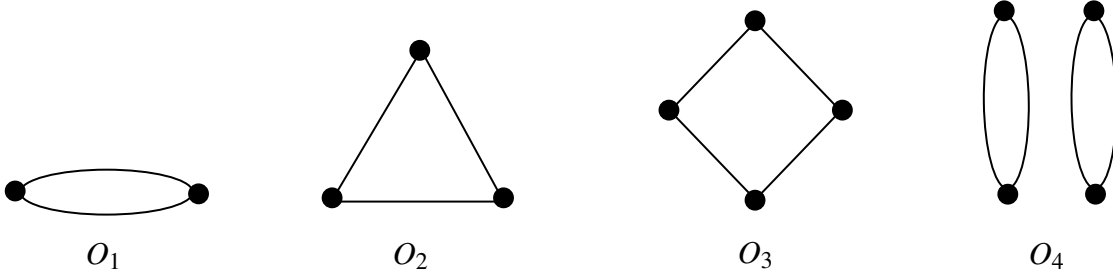


Figure 5.1: Some cycle graphs.

5.1.1 Cycles of length two and three in (2,2) -tight torus graphs

Here we investigate the possible embeddings of \mathbb{T} -subgraphs of an irreducible \mathbb{T} -graph such that their underlying graphs are cycles. To do so, we first recall the construction of the cutting and capping along nonseparating loops, which was introduced in Subsection 4.3.2.

Let H be a \mathbb{T} -subgraph of a (2,2)-tight \mathbb{T} -graph G . Suppose that the underlying graph of H is a cycle and H is separating in the torus. So one face of H , say F , is homomorphic to a punctured torus. Let K be $\widetilde{ext_G(F)}$, that is the \mathbb{S} -graph formed by cutting and capping along a nonseparating loop in F , see Figure 5.2. Let k_i be the number of cellular faces of K that have degree i .

Lemma 5.1.2. *Let H be a \mathbb{T} -subgraph of a (2,2)-tight \mathbb{T} -graph G . If H is a separating cycle of length 2 in the torus, then K is (2,2)-tight.*

Proof. Notice that $\gamma(ext_G(F)) = \gamma(\widetilde{ext_G(F)})$

$$\begin{aligned} 2 &= \gamma(G) = \gamma(int_G(F) \cup ext_G(F)) \\ &= \gamma(int_G(F)) + \gamma(ext_G(F)) - \gamma(\partial F) \\ &= \gamma(int_G(F)) + \gamma(ext_G(F)) - 2 \end{aligned}$$

Hence, $\gamma(int_G(F)) + \gamma(ext_G(F)) = 4$. By Theorem 3.2.2, we get

$$\begin{aligned} \gamma(H \cup int_G(F)) &= \gamma(H) + \gamma(int_G(F)) - 2 \\ &\leq \gamma(H) \end{aligned}$$

Hence, $\gamma(int_G(F)) \leq 2$. From the sparsity of G we have $\gamma(int_G(F)) = 2$.

5.1. EMBEDDING LEMMAS IN THE TORUS

Therefore, $\gamma(\text{ext}_G(F)) = \gamma(\widetilde{\text{ext}_G(F)}) = 2$. Consequently, $\gamma(K) = 2$. \square

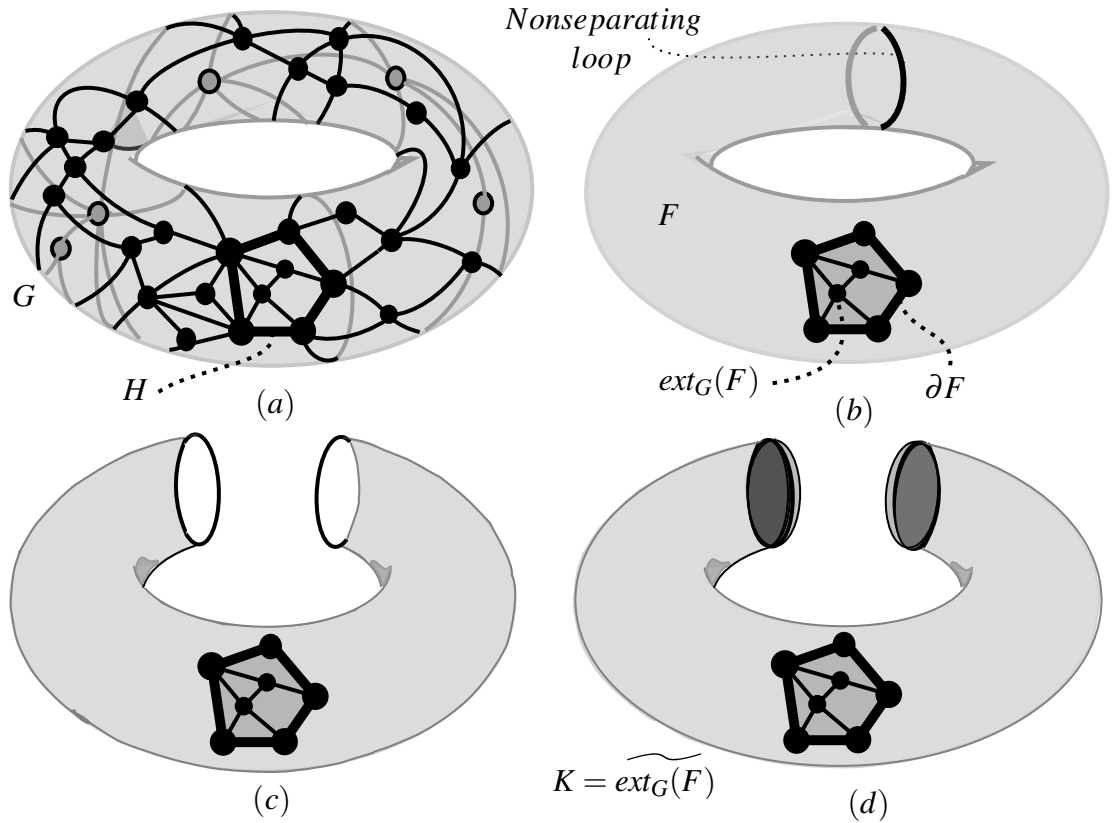


Figure 5.2: (a) A \mathbb{T} -graph G and a separating cycle H in \mathbb{T} . (b) The \mathbb{T} -subgraph H has a face, F , homeomorphic to a punctured torus. This face contains a nonseparating loop in \mathbb{T} . (c) Cutting the \mathbb{T} -graph along the nonseparating loop. (d) An \mathbb{S} -graph which is obtained from capping the two boundaries of the graph in (c) with open discs.

Lemma 5.1.3. *Let H be a \mathbb{T} -subgraph of a $(2,2)$ -tight \mathbb{T} -graph G . If H is a separating cycle of length 3 in the torus, then $\gamma(K) \in \{2, 3\}$.*

Proof. Notice that $\gamma(\text{ext}_G(F)) = \gamma(\widetilde{\text{ext}_G(F)})$

$$\begin{aligned}
 2 &= \gamma(G) = \gamma(\text{int}_G(F) \cup \text{ext}_G(F)) \\
 &= \gamma(\text{int}_G(F)) + \gamma(\text{ext}_G(F)) - \gamma(\partial F) \\
 &= \gamma(\text{int}_G(F)) + \gamma(\text{ext}_G(F)) - 3
 \end{aligned}$$

Hence, $\gamma(\text{int}_G(F)) + \gamma(\text{ext}_G(F)) = 5$. By Theorem 3.2.2, we get

$$\begin{aligned}\gamma(H \cup \text{int}_G(F)) &= \gamma(H) + \gamma(\text{int}_G(F)) - 3 \\ &\leq \gamma(H)\end{aligned}$$

Hence, $\gamma(\text{int}_G(F)) \leq 3$. From the sparsity of G we have $\gamma(\text{int}_G(F)) \in \{2, 3\}$. Therefore, $\gamma(\text{ext}_G(F)) = \gamma(\widetilde{\text{ext}_G(F)}) \in \{2, 3\}$. Consequently, $\gamma(K) \in \{2, 3\}$. \square

5.1.2 Subgraphs of irreducible graphs

The scope of the current section is to show that any (2,2)-tight \mathbb{T} -subgraph of an irreducible (2,2)-tight \mathbb{T} -graph is also irreducible. We start first by presenting some key lemmas.

Lemma 5.1.4. *Let $G = (\Gamma, \phi)$ be an irreducible (2,2)-tight \mathbb{T} -graph. Let d be a non-degenerate 4-cycle in Γ . If d forms a separating loop in \mathbb{T} , then d is the boundary of a quadrilateral face of G .*

Proof. Assume that d forms a separating cycle in \mathbb{T} . By Theorem 3.2.2, we have

$$\begin{aligned}2 &= \gamma(G) = \gamma(K) + \gamma(\text{int}_G(F)) - \gamma(\partial F) \\ &= \gamma(K) + \gamma(\text{int}_G(F)) - 4 \\ &\leq \gamma(K)\end{aligned}$$

Therefore, $\gamma(K) \leq 4$. Now, by Lemma 2.4.4, we get $2k_2 + k_3 - k_5 - 2k_6 - \dots = 8 - 2\gamma(K)$. But $k_2 = k_3 = 0$. Hence, $k_5 + 2k_6 + \dots \leq 0$. This means that all the faces of K are quadrilateral. Pick one of these quadrilateral faces, say Q . Then Q has an inessential blocker by Lemma 4.4.17. It is clear that this blocker must be an edge of G that joins two opposite vertices of the 4-cycle d . Since this is true for all faces of K it follows easily that one of the quadrilaterals has a vertex of degree 2 in G . This clearly contradicts the irreducibility of G . \square

Lemma 5.1.5. *Let $G = (\Gamma, \phi)$ be an irreducible (2,2)-tight \mathbb{T} -graph. Then any 2-cycle in Γ forms a nonseparating cycle in \mathbb{T} .*

Proof. Suppose that Ω is a 2-cycle in Γ which forms a separating cycle H in \mathbb{T} where $H = \phi(\Omega)$. Now, consider the \mathbb{S} -graph $K = \widetilde{\text{ext}_G(F)}$. By Lemma 5.1.2, $\gamma(K) = 2$. Thus,

5.1. EMBEDDING LEMMAS IN THE TORUS

K is $(2,2)$ -tight. Now, by Lemma 4.2.2 we have $2k_2 + k_3 = 4 + k_5 + 2k_6 + \dots \geq 4$. This means that either $k_2 \geq 2$ or $k_3 \geq 2$. If $k_2 \geq 2$, then at least one digon in K is also a face in G which contradicts the irreducibility of G . If $k_3 \geq 2$, then again we get a contradiction. \square

Lemma 5.1.6. *Let $G = (\Gamma, \phi)$ be an irreducible $(2,2)$ -tight \mathbb{T} -graph. Then any 3-cycle in Γ forms a nonseparating cycle in \mathbb{T} .*

Proof. Suppose, for a contradiction, that Ω is a 3-cycle in Γ forms a separating cycle H in \mathbb{T} where $H = \phi(\Omega)$. Now, consider the \mathbb{S} -graph $K = \widetilde{\text{ext}_G(F)}$. By Lemma 5.1.3, $\gamma(K) \in \{2, 3\}$. If $\gamma(K) = 2$, then as in the proof of Lemma 5.1.5, we get a contradiction. Hence, suppose that $\gamma(K) = 3$. By Lemma 4.2.3, we get $2k_2 + k_3 = 2 + k_5 + 2k_6 + \dots \geq 2$. This means that either $k_2 \geq 1$ or $k_3 \geq 2$ and in both cases we get a contradiction to the irreducibility of G . \square

The following lemma is concerned with embedding two disjoint 2-cycles (O_4 in Figure 5.1) in the torus. We assume that both of such cycles are subgraphs of the underlying graph of an irreducible $(2,2)$ -tight \mathbb{T} -graph.

Lemma 5.1.7. *Let $G = (\Gamma, \phi)$ be an irreducible $(2,2)$ -tight \mathbb{T} -graph. Suppose that O_4 is a subgraph of Γ . Then the embedding of O_4 in the torus is isomorphic to the noncellular \mathbb{T} -graph in Figure 5.3.*

Proof. By Lemma 5.1.5, each of the two 2-cycles of O_4 forms a nonseparating cycle in \mathbb{T} . Now, since these two 2-cycles are disjoint from each other, they are homotopic to each other. \square

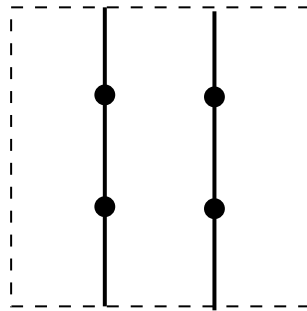


Figure 5.3: Embedding of the graph O_4 such that both of the 2-cycles are embedded as nonseparating cycles in \mathbb{T} .

Now we are ready to present the proof of Theorem 5.1.1.

Proof. (of Theorem 5.1.1) By Lemma 5.1.5 and 5.1.6, H has no digon or triangle. We consider the case that H has a quadrilateral face Q . Suppose that Q has a nondegenerate boundary. Then by Lemma 5.1.4, Q is also a face of G . Now, suppose that H_1 and H_2 are blockers for the contractions of Q in G . One readily checks that $H_1 \cap H$ and $H_2 \cap H$ are blockers for the contraction of Q in H .

In the case that Q has a degenerate boundary, observe first that since H is (2,2)-tight the other possible degeneracy is that a pair of opposite vertices in the boundary of Q coincide. In particular, no edges are repeated and ∂Q is a (2,2)-tight graph with 3 vertices and 4 edges, see Figure 5.4. Now, as in the proof of Lemma 5.1.4, we see that all faces of G that are contained in Q are quadrilaterals. Since all quadrilateral faces of G are nondegenerate it follows that Q must also contain the inessential blocker of any such quadrilateral. It would then follow that there is a cycle in G of odd length contained in Q which contradicts the fact that all faces of G contained in Q are of degree 4. Thus, in fact Q is a face of G which contradicts the fact from Lemma 4.4.5 that all quadrilateral faces of G have nondegenerate boundaries. Therefore, H has no digon, triangle or contractible quadrilateral face. \square

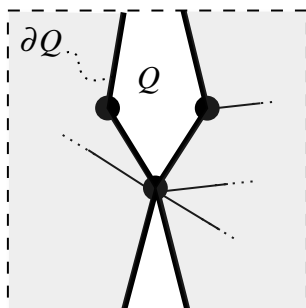


Figure 5.4: A degenerate quadrilateral face, Q .

Figure 5.5 presents two examples of (2,2)-tight \mathbb{T} -subgraphs of irreducible (2,2)-tight \mathbb{T} -graphs. Notice that both of the \mathbb{T} -graphs in Figure 5.5 are irreducible.

5.1.3 Polygonal representation

In the following we describe a useful way of drawing cellular surface graphs. We use this kind of drawing to find many irreducible (2,2)-tight \mathbb{T} -graphs in the next sections.

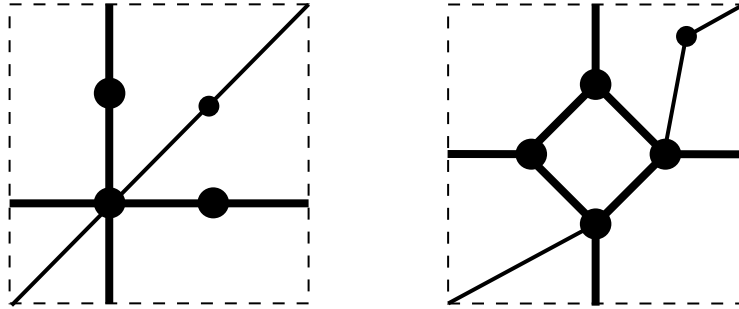


Figure 5.5: Consider the bold $(2,2)$ -tight \mathbb{T} -subgraphs in both the given irreducible $(2,2)$ -tight \mathbb{T} -graphs. Each of these \mathbb{T} -subgraphs is also irreducible.

Definition 5.1.8. Let G be a cellular surface graph with faces F_1, F_2, \dots, F_n . Each face F_i is a plane polygon with boundary vertices and edges are labelled by vertices and edges of G . Thus, we can represent G by drawing a labelled collection of polygons. We call such a drawing a *polygon representation*.

We call an irreducible $(2,2)$ -tight \mathbb{T} -graph G a *base* if it has no vertex of degree two. We label the embedding graphs and trace the labelling on the corresponding polygon representation, see Figure 5.6. We will not include in polygon representations any plane

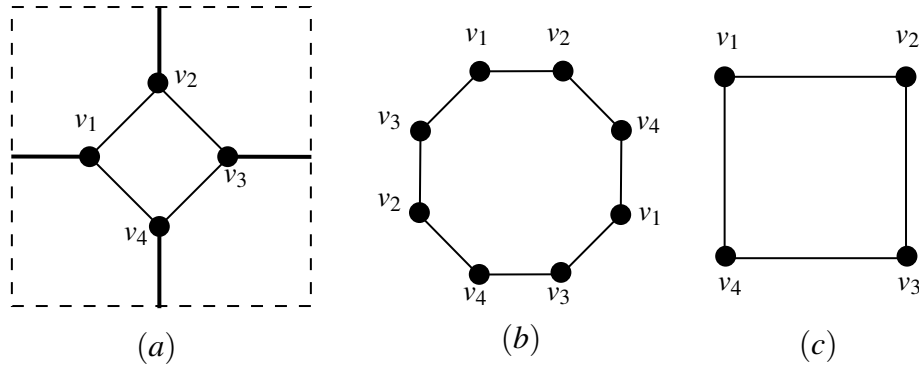


Figure 5.6: (a) A \mathbb{T} -graph. (b) respectively (c) A labelled plane polygon corresponding to the face of degree eight respectively four in the \mathbb{T} -graph in (a). Together (b) and (c) are called the *polygon representation* of the \mathbb{T} -graph in (a).

polygon corresponding to a quadrilateral face. This is because there is no way to add more vertices inside such a face, see Figure 5.7. Moreover, if G is a base \mathbb{T} -graph and has faces of degree five, then we will not depict the plane polygons corresponding to such faces in the polygon representation, see Figure 5.8.

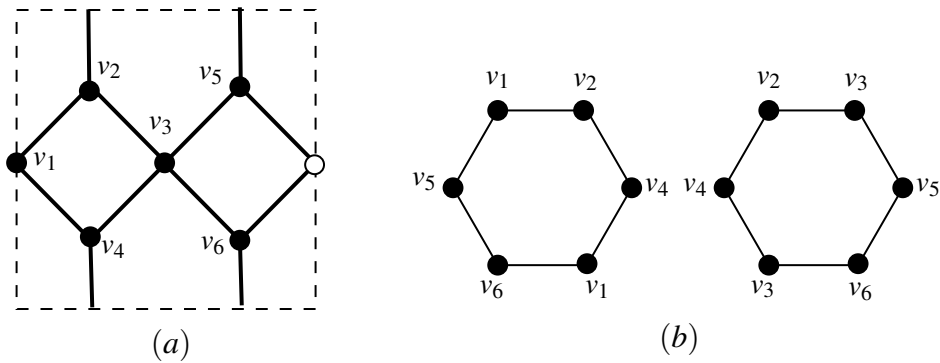


Figure 5.7: (a) A base irreducible (2,2)-tight \mathbb{T} -graph. (b) The polygon representation of the \mathbb{T} -graph in (a). Notice that the plane polygons corresponding to the two quadrilateral faces are deleted.

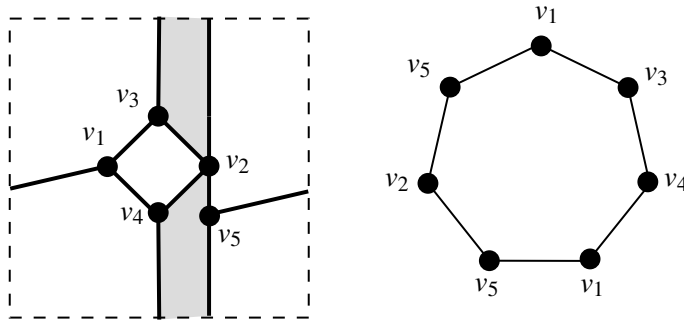


Figure 5.8: On the left, a base irreducible (2,2)-tight \mathbb{T} -graph. On the right, the corresponding polygon representation to the \mathbb{T} -graph on the left. The corresponding plane polygon to the shaded pentagon is not included in the polygon representation.

Generating polygon representations

In the following, we describe a method that we used to find many nonisomorphic irreducible (2,2)-tight \mathbb{T} -graphs. We use the plane polygon in Figure 5.9(a) to explain this method. This plane polygon is a polygon representation of an irreducible (2,2)-tight \mathbb{T} -graph. We would like to add a vertex of degree two that is adjacent to two distinct vertices such that both of the resulting two faces are of degree greater than four. So we can choose a vertex on the boundary of the plane polygon to be adjacent to the new vertex, and then we join the new vertex with another vertex on the boundary of the plane polygon in Figure 5.9(b) to create a face of degree five. Then we look for any other possibility of adjoining the new vertex with another vertex on the boundary so that the new vertex is still adjacent

to the vertex that we choose first, see Figure 5.9(b) .

Then we move in a clockwise direction to fix another vertex on the boundary. By repeating the procedure that we described in the previous paragraph, we can find all possible polygon representations. See Figure 5.9 (c). We continue this procedure until we end with isomorphic polygon representations to those we found in the first round.

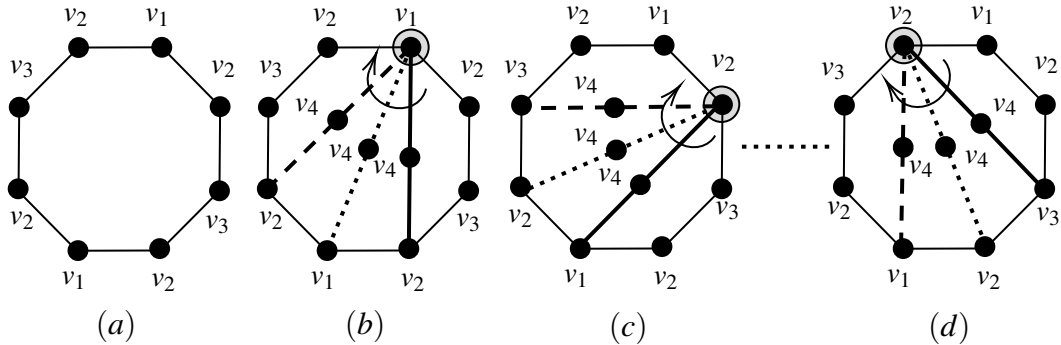


Figure 5.9: (a) A polygon representation of an irreducible $(2,2)$ -tight \mathbb{T} -graph with three vertices. (b) We fix v_1 (inside the shaded circle) and then we add the vertex v_4 in the interior of the plane polygon in (a). Then we adjoin v_4 to v_2 . Notice that the new polygon representation contains a pentagon and a face of degree 7. Thus, the current polygon representation in (b) is corresponding to an irreducible $(2,2)$ -tight \mathbb{T} -graph with four vertices. Now, we keep fixing v_1 (inside the shaded circle) and adjoin v_4 to v_1 (this case is represented by the dotted path of length 2). Again, we keep fixing v_1 (inside the shaded circle) then we join v_4 to v_2 by an edge (to form the dashed path of length 2). Now, we fix the vertex v_2 (inside the shaded circle), then we adjoin v_4 to v_2 and v_1 as in (c). We continue this process as we did in (b). We also continue fixing vertices on the boundary and repeat the processes as in (b) and (c) until we fix the last vertex, v_2 , on the boundary, see (d). See also Appendix B (Figures B.1, B.2 and B.3) which presents all such possible cases.

We notice in Figure 5.9 that there are a lot of polygon representations that are congruent to each other and there are 1-1 correspondings between the vertices of such polygon representations. Any two of such polygon representations are called equivalent to each other, see Figure 5.10.

Later on, we find non-base irreducible $(2,2)$ -tight \mathbb{T} -graphs by declaring their ancestors in paths, see Appendix D. We describe such paths according to the polygon representations of the irreducible $(2,2)$ -tight \mathbb{T} -graphs that contain each other. For example, the irreducible $(2,2)$ -tight \mathbb{T} -graph in Figure 5.11 (a) is contained in the irreducible $(2,2)$ -tight \mathbb{T} -graph in Figure 5.11 (b). The \mathbb{T} -graph in Figure 5.11(b) is contained in the irreducible

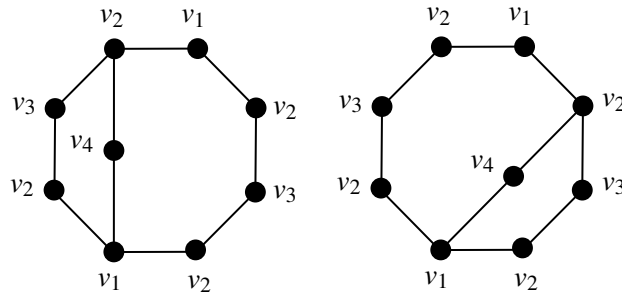


Figure 5.10: Two polygon representations which are equivalent to each other.

(2,2)-tight \mathbb{T} -graph in Figure 5.11(c). The same applies for the corresponding polygon representations Figure 5.11(d), (e) and (f).

Notice that the \mathbb{T} -graph in Figure 5.11(c) is obtained from the \mathbb{T} -graph in Figure 5.11(b) by a topological Henneberg type 0 move. Also the \mathbb{T} -graph in Figure 5.11(b) is obtained from the \mathbb{T} -graph in Figure 5.11(a) by a topological Henneberg type 0 move. We also comment that the irreducible (2,2)-tight \mathbb{T} -graph in Figure 5.11(a) can be derived from the noncellular \mathbb{T} -graph with a single nonseparating cycle of length 2 by a topological Henneberg type 0 move. The noncellular \mathbb{T} -graph also can be constructed from the noncellular \mathbb{T} -graph with one vertex by a topological Henneberg type 0 move.

So we mean by (a) – (b) – (c) that the \mathbb{T} -graph in Figure 5.11(c) is obtained from the \mathbb{T} -graph in Figure 5.11(b) by a topological Henneberg type 0 move. Also, the \mathbb{T} -graph in Figure 5.11(b) is obtained from the \mathbb{T} -graph in Figure 5.11(a) by a topological Henneberg type 0 move.

5.2 Searching for all irreducible (2,2)-tight torus graphs

We recall that the main goal of this chapter is to explain how we found all the nonisomorphic irreducible (2,2)-tight \mathbb{T} -graphs. Specifically, we employed two independent approaches to find such irreducible (2,2)-tight \mathbb{T} -graphs. One approach is by hand. In this approach, we employed a mixture of brute force methods and theoretical insight into the structure of such graphs. The second approach is a computer assisted search. We have used a computer assisted approach to find all irreducible (2,2)-tight torus graphs with at most 7 vertices. If we use a powerful computer, we could also find all eight vertex examples. However, as we shall see the 'by hand' approach suffices for the eight vertex

5.2. SEARCHING FOR ALL IRREDUCIBLE (2,2)-TIGHT TORUS GRAPHS

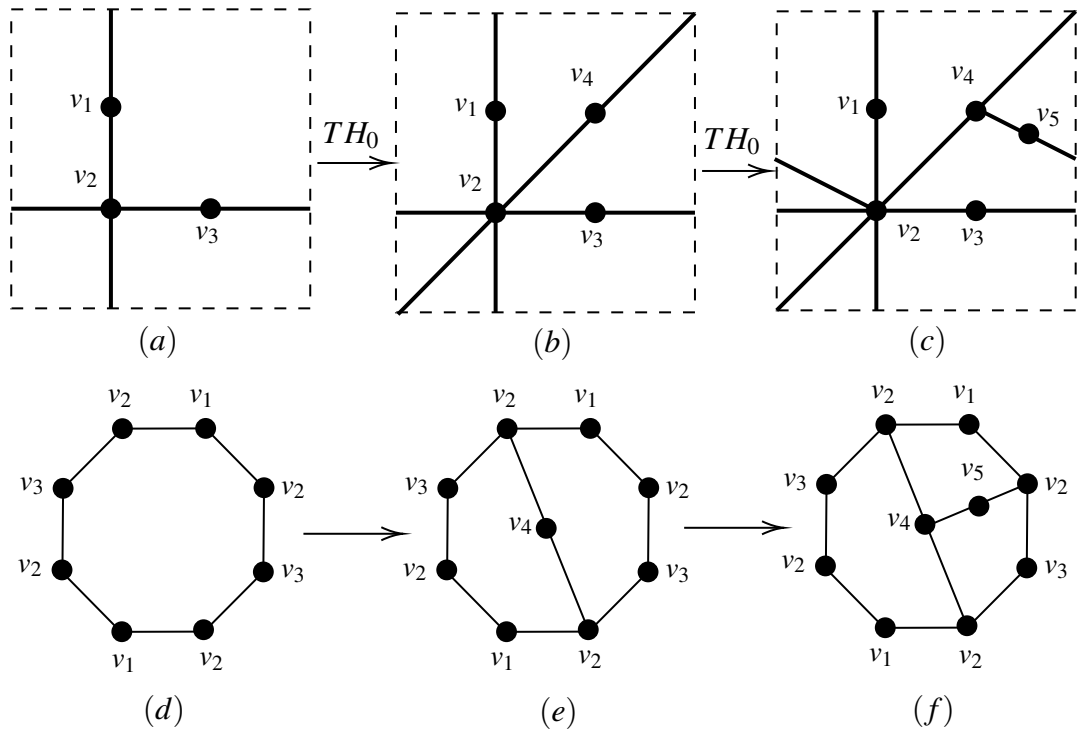


Figure 5.11: An example of an ancestor path.

case.

5.2.1 Two independent methods for conducting the search

For finding irreducible (2,2)-tight \mathbb{T} -graphs, we used the rich combinatorial information of such torus graphs. Therefore, the computing by hand is fitted to find such torus graphs.

We recall that a surface graph is a pair of a graph and an embedding of such a graph in the surface. So it is natural to use the underlying graphs to find irreducible (2,2)-tight \mathbb{T} -graphs. To do so, we tried to embed the (2,2)-tight graphs in the torus so that no digon, triangle or quadrilateral contraction can be made. This goal seems a very computational one and the search domain of such graphs looks massive. However, this goal was achieved by reducing the size of the search domain. We used topological techniques to control the embedding of (2,2)-tight graphs in the torus. In the previous section, we included some of the embedding lemmas. Beside that, some other techniques have been recruited to contribute in reducing the search domain as we discuss that here.

In summary, our justification for using the two approaches that we mentioned above backs to the following reasons.

1. The computer assisted approach was necessary for the 6 and 7 vertex graphs since there are so many possibilities that the 'by hand' approach becomes extremely laborious and also very repetitive to describe.
2. Both methods were carried out for graphs of up to seven vertices, even though we only describe the 'by hand' computations up to five vertices. Thus, the two approaches provide validation of our 'by hand' calculation and also of the implementation of our algorithm.
3. In the case of graphs with 8 vertices, the computer assisted approach was not possible on the hardware available. However, in that case our theoretical results were sufficient to narrow the search space in order to make the 'by hand' approach relatively easy. Thus, we were fortunate that the two methods complemented each other perfectly in this case to complete the entire search for irreducible (2,2)-tight torus graphs.

5.2.2 Basic technical results for both methods

In the following, we list some basic facts related to the number of faces and the vertices of all irreducible (2,2)-tight \mathbb{T} -graphs. The following theorem determines the number of faces of specific degrees of irreducible (2,2)-tight \mathbb{T} -graphs with no quadrilateral face. See also Figure 5.12.

Theorem 5.2.1. *Let G be a cellular irreducible (2,2)-tight \mathbb{T} -graph with $f_4 = 0$. Then G satisfies:*

$$(f_5, f_6, f_7, f_8) \in \{(0, 0, 0, 1), (0, 2, 0, 0), (2, 1, 0, 0), (1, 0, 1, 0), (4, 0, 0, 0)\}$$

Proof. Since G is (2,2)-tight, $f_1 = 0$. Since G is irreducible, by Lemma 3.4.5, $f_2 = 0$ and by Lemma 3.4.8, $f_3 = 0$. Therefore, by Lemma 2.4.4, $f_5 + 2f_6 + 3f_7 + 4f_8 = 4$ and $f_i = 0$ for all $i \geq 9$. Now, because of $f_4 = 0$, the conclusion follows. \square

Figure 5.12 presents some irreducible (2,2)-tight \mathbb{T} -graphs which satisfy the counting of faces given in Lemma 5.2.1.

5.2. SEARCHING FOR ALL IRREDUCIBLE (2,2)-TIGHT TORUS GRAPHS

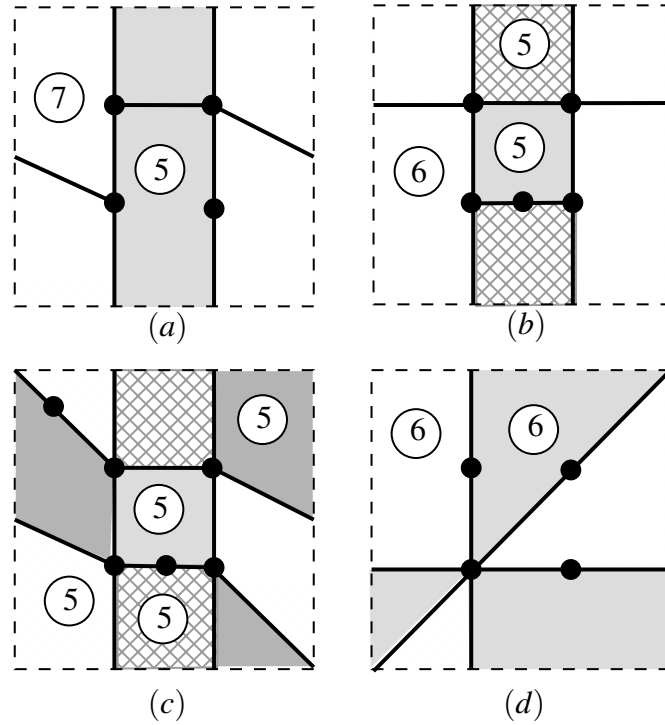


Figure 5.12: The graph in (a) satisfies $(1, 0, 1, 0)$. The graph in (b) satisfies $(2, 1, 0, 0)$. The graph in (c) satisfies $(4, 0, 0, 0)$. The graph in (d) satisfies $(0, 2, 0, 0)$.

Lemma 5.2.2. *Let G be an irreducible $(2, 2)$ -tight \mathbb{T} -graph with $f_4 = 0$. Then G has at most 6 vertices.*

Proof. If G is not cellular, then by Theorem 4.4.14, G has either one vertex or two vertices. Now, suppose that G is cellular. By a similar argument to that one in the proof of Theorem 5.2.1, we have that $f_5 + 2f_6 + 3f_7 + 4f_8 = 4$ and $f_i = 0$ for all $i \in \{1, 2, 3, 4, 9, 10, \dots\}$. So

$$\begin{aligned} 2e &= 5f_5 + 6f_6 + 7f_7 + 8f_8 \\ &\leq 5(f_5 + 2f_6 + 3f_7 + 4f_8) \\ &\leq 5(4) = 20 \end{aligned}$$

Hence, $e \leq 10$ and $v = \frac{e+2}{2} \leq 6$. □

Lemma 5.2.3. *Let G be an irreducible $(2, 2)$ -tight \mathbb{T} -graph with $f_4 = 1$. Then G has at least 4 vertices and at most 7 vertices.*

Proof. It is clear that G is cellular. By a similar argument to that one in the proof of Theorem 5.2.1, we have that $f_5 + 2f_6 + 3f_7 + 4f_8 = 4$ and $f_i = 0$ for all $i \in \{1, 2, 3, 9, 10, \dots\}$. So

$$\begin{aligned} 2e &= 4f_4 + 5f_5 + 6f_6 + 7f_7 + 8f_8 \\ &\leq 4f_4 + 5(f_5 + 2f_6 + 3f_7 + 4f_8) \\ &\leq 4 + 5(4) = 24 \end{aligned}$$

Hence, $e \leq 12$ and $v = \frac{e+2}{2} \leq 7$. By Lemma 4.5.3, G has at least 4 vertices. \square

Lemma 5.2.4. *Let G be an irreducible (2,2)-tight \mathbb{T} -graph with $f_4 = 2$. Then G has at least 6 vertices and at most 8 vertices.*

Proof. Clearly G is cellular. By a similar argument to that one in the proof of Theorem 5.2.1, we have that $f_5 + 2f_6 + 3f_7 + 4f_8 = 4$ and $f_i = 0$ for all $i \in \{1, 2, 3, 9, 10, \dots\}$. So

$$\begin{aligned} 2e &= 4f_4 + 5f_5 + 6f_6 + 7f_7 + 8f_8 \\ &\leq 8 + 5(f_5 + 2f_6 + 3f_7 + 4f_8) \\ &\leq 8 + 5(4) = 28 \end{aligned}$$

Hence, $e \leq 14$ and $v = \frac{e+2}{2} \leq 8$. Now, consider Lemma 4.7.10. We have three cases.

1. Each of L_1 and L_3 is a single vertex, so $v \geq 6$.
2. One of L_i is a single vertex and the other is a nonseparating cycle of length two. Hence, $v \geq 7$.
3. For $i = 1, 2$, each of L_1 and L_3 is a nonseparating cycle of length two. Thus, $v = 8$.

\square

5.2.3 Computations by hand

Here we describe the first approach that we adopted to find all irreducible (2,2)-tight \mathbb{T} -graphs. In this approach, we used a mixture of brute force methods and theoretical insight into the structure of such torus graphs.

Structuring the irreducible (2,2)-tight torus graphs

In the following we sketch our plan of organising all nonisomorphic irreducible (2,2)-tight \mathbb{T} -graphs and also describe the way that we used to denote each irreducible (2,2)-tight \mathbb{T} -graph. Such a strategy of organising the irreducible (2,2)-tight \mathbb{T} -graphs contributes in checking that we find all nonisomorphic irreducible (2,2)-tight \mathbb{T} -graphs.

We use the number of 2-cycles of the underlying graphs of the irreducible (2,2)-tight \mathbb{T} -graphs to organise these irreducible (2,2)-tight \mathbb{T} -graphs with n vertices. Notice that by Theorem 4.7.12, n is at most 8.

We structure the irreducible (2,2)-tight \mathbb{T} -graphs firstly according to their order. We have an exception to this rule here as we combine irreducible (2,2)-tight \mathbb{T} -graphs of order 1, 2 and 3 in one group. Secondly, we categorise irreducible (2,2)-tight \mathbb{T} -graphs with order n according to the minimum degree of such \mathbb{T} -graphs. Apart from noncellular (2,2)-tight \mathbb{T} -graph with one vertex, we consider two groups of irreducible (2,2)-tight \mathbb{T} -graphs; one with minimum degree 3 and the other one with minimum degree 2. For each of the previous two groups, we categorise irreducible (2,2)-tight \mathbb{T} -graphs according to the number of 2-cycles in their underlying graphs. See Figure 5.13.

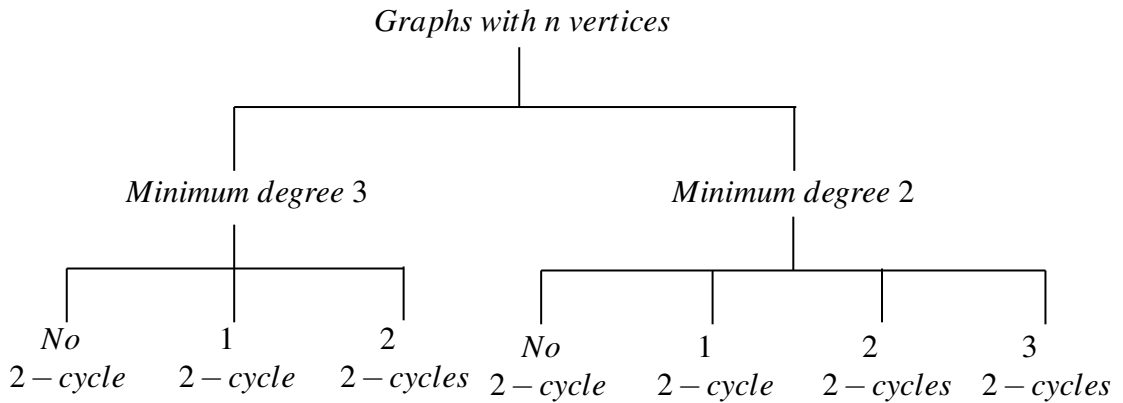


Figure 5.13: The structure of organising the irreducible (2,2)-tight \mathbb{T} -graphs.

Now we describe how the irreducible (2,2)-tight \mathbb{T} -graphs are denoted according to their orders and an indexing that we choose to distinguish nonisomorphic irreducible (2,2)-tight \mathbb{T} -graphs of the same orders from each other.

Notation 5.2.5. We denote each irreducible (2,2)-tight \mathbb{T} -graph as G_j^i where i refers to

the number of vertices of G and j is an index which is used to distinguish between the nonisomorphic irreducible (2,2)-tight \mathbb{T} -graphs with i vertices.

See the examples in Figure 5.14 of organising and notating two irreducible (2,2)-tight \mathbb{T} -graphs.

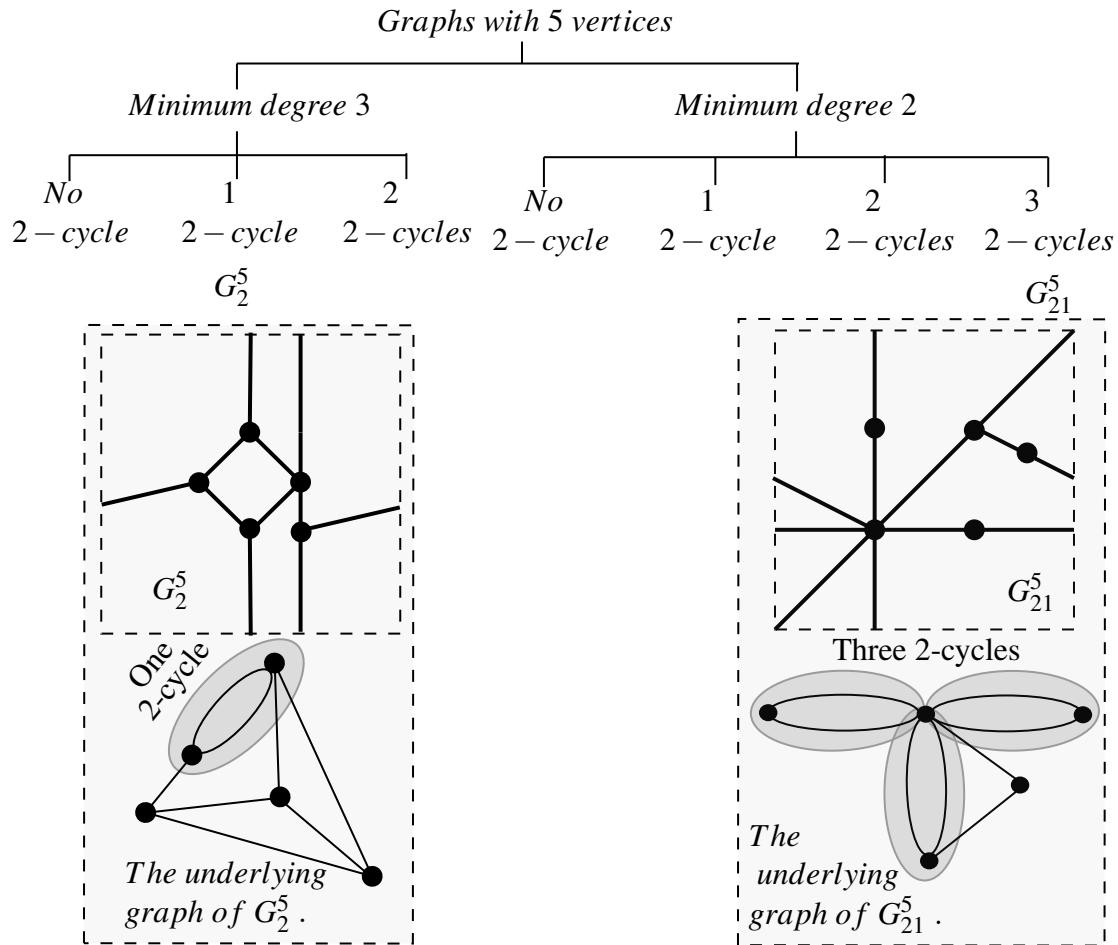


Figure 5.14: The \mathbb{T} -graph G_2^5 respectively G_{21}^5 is an irreducible (2,2)-tight \mathbb{T} -graph with five vertices such that its underlying graph has one 2-cycle respectively three 2-cycles.

5.2.4 Computer search approach

The second approach that we used to find all the irreducible (2,2)-tight \mathbb{T} -graphs with less than eight vertices is a computer assisted search. We used the SageMath computer algebra

5.2. SEARCHING FOR ALL IRREDUCIBLE (2,2)-TIGHT TORUS GRAPHS

system to automate the search, [100], [50]. Here we outline the basic data structures and algorithms that we used for calculating the irreducible (2,2)-tight \mathbb{T} -graphs, [19].

Graphs: the MyGraph class

The standard graph data structures that ship with the SageMath system are not particularly well adapted for our purposes, so we have implemented the MyGraph class which subclasses the SageMath Graph class. This models a graph as a set of darts (half-edges) D , together with a pair of partitions of D , \mathcal{V} and \mathcal{E} . The parts of \mathcal{V} correspond to vertices of the graph and the parts of \mathcal{E} are all 2-sets that correspond to the edges of the graph. MyGraph has the following methods (this list is not exhaustive, we only mention the most important methods):

- `digon_split`: this returns a MyGraph object that is obtained by splitting a vertex of `self` into two vertices joined by a pair of parallel edges. We also must specify how the darts of the vertex are to be divided among the new vertices.
- `zero_extension`: returns a MyGraph object corresponding to a Henneberg type 0 extension of `self`.
- `one_extension`: returns a MyGraph object corresponding to a Henneberg type 1 extension of `self`.
- `edge_deletion`: returns a MyGraphs object that is obtained by deleting an edge of `self`.
- `vertex_deletion`: returns a MyGraphs object that is obtained by deleting a vertex of `self`.

We also have some class methods (in the Python sense of that term). In particular:

- `isomorphism_class_reps`: this is a class method that takes a list of MyGraphs and filters out isomorphism. Here we have adapted SageMaths built in graph isomorphism checker to check for an isomorphism between two MyGraph objects.
- `extensions_of`: this returns a list of all possible digon splits, Henneberg type 0 extensions and Henneberg type 1 extensions of a given MyGraph instance.

The following lemma utilises constructing (2,2)-tight graphs up to 7 vertices inductively. However, let us recall some moves in Figure 5.15.

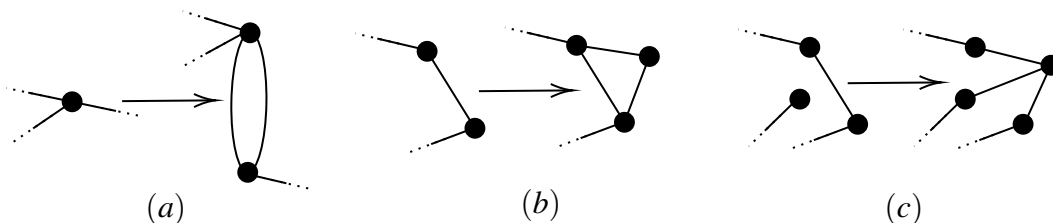


Figure 5.15: (a) A vertex-to-2-cycle which is the inverse of 2-cycle contraction move. (b) Henneberg 0-extension (Henneberg type 0 move). (c) Henneberg 1-extension (Henneberg type 1 move).

Lemma 5.2.6. *Every (2,2)-tight graph can be constructed from a vertex by a sequence of vertex-to-2-cycle, Henneberg 0-extension or Henneberg 1-extension.*

As a consequence of Lemma 5.2.6, using the class methods `digon_split`, `extensions_of` and `isomorphism_class_reps`, we can inductively construct lists of (2,2)-tight graphs with up to seven vertices.

5.2.5 Surface graphs: the `OrientedRotationSystem` class

Let S_n be the group of permutations of $\{1, \dots, n\}$. Recall that an oriented rotation system is a pair of permutations $\sigma, \tau \in S_{2e}$ where τ is a fixed point free involution.

We have also implemented a version of the pebble game algorithm of Lee and Streinu [62]. If Σ is an oriented surface and G is a cellular Σ -graph, then G gives rise to an oriented rotation system as follows. Label the darts of G by $1, \dots, 2|E|$. Now, let $\sigma(i)$ be the dart that is next to i with respect to the clockwise ordering of the darts around the vertex of i . Let $\tau(i)$ be the other dart in the edge of i . Oriented rotation systems are a convenient way to represent cellular surface graphs in a computer algebra system. We have implemented the class `OrientedRotationSystem` in Sagemath, along with the following methods for computing various invariants associated to the corresponding surface graph.

- `components`: returns a list of components of `self`. Note that components of an oriented rotation system correspond to orbits of group generated by σ and τ . Here

5.2. SEARCHING FOR ALL IRREDUCIBLE (2,2)-TIGHT TORUS GRAPHS

(and elsewhere) we make use of SageMath's built in permutation group functionality (which is based on an interface to the GAP computer algebra system).

- `vertices`: this returns the partition of $\{1, \dots, 2|E|\}$ induced by the cycles of σ .
- `edges`: this returns the partition of $\{1, \dots, 2|E|\}$ induced by the cycles of τ .
- `faces`: this returns the partition of $\{1, \dots, 2|E|\}$ induced by the cycles of $\sigma\tau$.
- `genus`: computes the genus of the underlying surface using Euler's formula $2 - 2g = f - e + v$.
- `edge_contraction` and `edge_deletion`: these return `OrientedRotationSystem` objects corresponding to the contraction and deletion operations defined for surface graphs, see Definitions 3.4.1, 3.4.2.
- `edge_insertion`: this inserts an edge in a face. We must specify where the corresponding darts are to be inserted into the appropriate vertex cycles.
- `based_isomorphism`: this checks for an isomorphism between two rotation systems for which the image of one of the darts is specified. This is quite fast to check and proceeds by extending the mapping one dart at a time using the vertex and edge permutations of the rotation systems. If the mapping can be extended over the whole dart set, then the rotation systems are isomorphic.

We have also implemented a standalone function `is_irreducible` which takes an `OrientedRotationSystem` whose graph is known to be (2,2)-tight and checks if the corresponding surface graph is irreducible. We summarise the algorithm for this as follows.

1. Check for any digon faces or triangle faces. If they exist return `False`.
2. Now find all quadrilateral faces using the `faces` method
 - if there is a degenerate quadrilateral, then return `False`.
 - check all possible contractions of the quadrilateral faces to see if any of these have a (2,2)-sparse graph. Here we use our implementation of the Pebble Game to check sparsity. If we find a sparse contraction Return `False`

3. Return True

See [20] for the SageMath code together with data files describing the rotation systems corresponding to each of cellular irreducible torus graphs and corresponding diagrams.

5.2.6 A sample interactive session

In the following we give a sample computation using our code to demonstrate the basic functionality.

```
In [1]: from sparsity import MyGraph
```

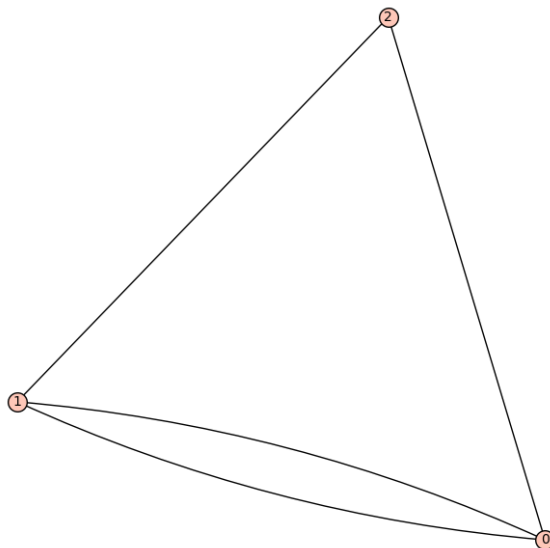
```
In [2]: vertex_parts = [[1,2,7],[3,4,8],[5,6]]
edge_parts = [[1,3],[2,5],[4,6],[7,8]]
g = MyGraph(dart_partitions=[vertex_parts,edge_parts])
```

```
In [3]: g.edges()
```

```
Out[3]: [(0, 1, 0), (0, 1, 3), (0, 2, 1), (1, 2, 2)]
```

```
In [4]: g.plot()
```

```
Out[4]:
```



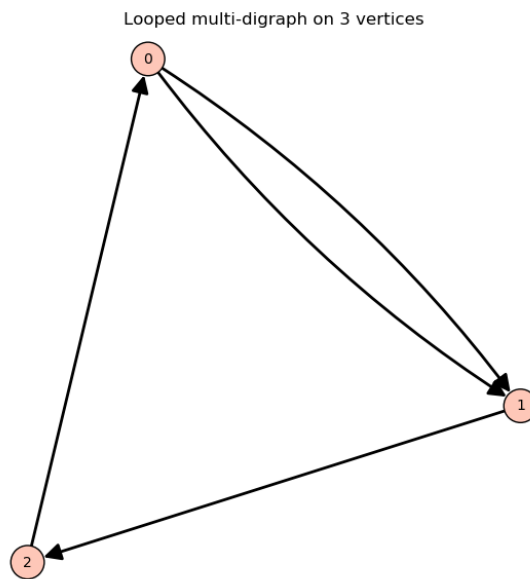
5.2. SEARCHING FOR ALL IRREDUCIBLE (2,2)-TIGHT TORUS GRAPHS

```
In [5]: from sparsity import PebbleGame
```

```
In [6]: p = PebbleGame(g.vertices(),2,2)
```

```
In [7]: p.run(g)
```

```
Out[7]:
```



```
In [8]: from rotation import OrientedRotationSystem
```

```
In [9]: l = OrientedRotationSystem.from_mygraph(g)
```

```
In [10]: l
```

```
Out[10]: [<rotation.OrientedRotationSystem object at 0x7f265720db50>]
```

```
In [11]: ors = l[0]
```

```
In [12]: ors.faces()
```

```
Out[12]: [[1, 5, 4, 7, 3, 6, 2, 8]]
```

```
In [ ]: # so this ors has a single face of degree 8
```


5.3 Irreducible $(2,2)$ -tight torus graphs with less than three vertices

In this section we list the irreducible $(2,2)$ -tight \mathbb{T} -graphs with less than four vertices. By Theorem 4.4.14, up to isomorphism, the only irreducible $(2,2)$ -tight \mathbb{T} -graph with one respectively two vertices is given in Figure 4.28 (a) respectively (b). We denote the irreducible $(2,2)$ -tight \mathbb{T} -graphs in Figure 4.28 (a) and Figure 4.28(b) by G_1^1 and G_1^2 , respectively.

Now, we consider the possible embeddings of the graphs Ω_1 and Ω_2 , see Figure 5.16, as irreducible $(2,2)$ -tight \mathbb{T} -graphs. In fact, we shall show that there are exactly two nonisomorphic irreducible $(2,2)$ -tight \mathbb{T} -graphs with three vertices. Notice that the graphs Ω_1 and Ω_2 in Figure 5.16 are the only two nonisomorphic $(2,2)$ -tight graphs with three vertices.

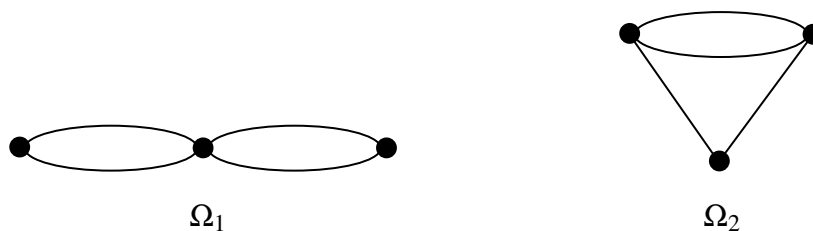


Figure 5.16: The graphs Ω_1 and Ω_2 are $(2,2)$ -tight graphs with three vertices.

Lemma 5.3.1. *Up to isomorphism, there is a unique embedding of Ω_1 as an irreducible $(2,2)$ -tight \mathbb{T} -graph.*

Proof. By Lemma 5.1.5, each of the 2-cycles of Ω_1 is a nonseparating cycle. To embed the two 2-cycles as nonseparating cycles there are only two ways to do that. Either they are homotopic to each other or they are not. The former embedding leads to a reducible $(2,2)$ -tight torus graph, see Figure 5.17(a), while the latter embedding yields an irreducible $(2,2)$ -tight torus graph, see Figure 5.17(b). \square

We denote the irreducible embedding of Ω_1 in the torus which is given in Lemma 5.3.1 by G_1^3 .

5.3. IRREDUCIBLE (2,2)-TIGHT TORUS GRAPHS WITH LESS THAN THREE VERTICES

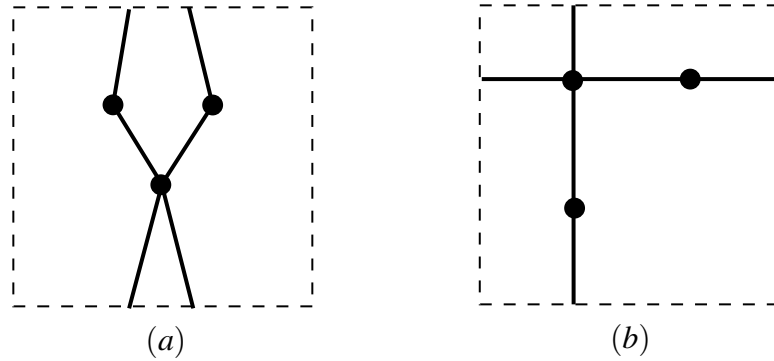


Figure 5.17: (a) The two 2-cycles of Ω_1 are embedded homotopic to each other. It is clear that the quadrilateral face is contractible. (b) The two 2-cycles of Ω_1 are not homotopic to each other.

Lemma 5.3.2. *Up to isomorphism, there is a unique embedding of Ω_2 as an irreducible (2,2)-tight \mathbb{T} -graph.*

Proof. Consider the 2 respectively 3-cycle in Ω_2 . By Lemma 5.1.5, respectively, Lemma 5.1.6, each of these two cycles forms a nonseparating cycle in \mathbb{T} . To embed the two cycles as nonseparating cycles, there are only two ways to do that. Either they are homotopic to each other or they are not. The former embedding leads to a reducible (2,2)-tight torus graph, see Figure 5.18(a), while the latter embedding yields an irreducible (2,2)-tight torus graph, see Figure 5.18(b). \square

We denote the irreducible embedding of Ω_2 which is given in Lemma 5.3.2 by G_2^3 . Hence, we have the following theorem.

Theorem 5.3.3. *There are exactly two irreducible (2,2)-tight \mathbb{T} -graphs with three vertices.*

Lemma 5.3.4. *Let K be a \mathbb{T} -subgraph of an irreducible (2,2)-tight \mathbb{T} -graph G whose underlying graph is Ω_1 respectively Ω_2 . Then K is isomorphic to G_1^3 respectively G_2^3 .*

Proof. This follows immediately from Lemmas 5.3.1, 5.3.2 and Theorem 5.1.1. \square

In Figure 5.19(b) respectively 5.19(d), we present the polygon representation corresponding to the irreducible (2,2)-tight \mathbb{T} -graph G_1^3 respectively G_2^3 .

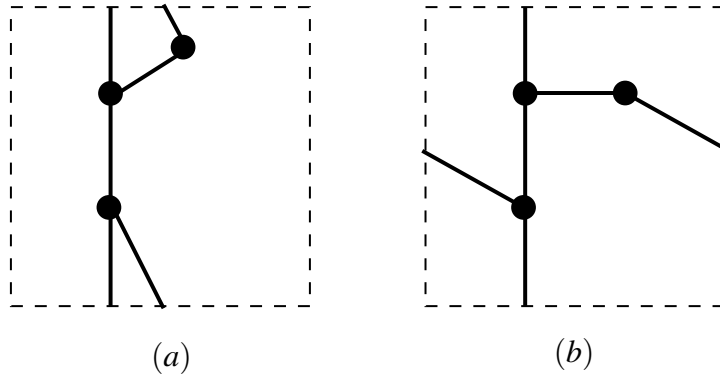


Figure 5.18: (a) The embedding of the 2 and 3-cycle of Ω_2 are homotopic to each other. (b) The embedding of the 2 and 3-cycle of Ω_2 are not homotopic to each other.

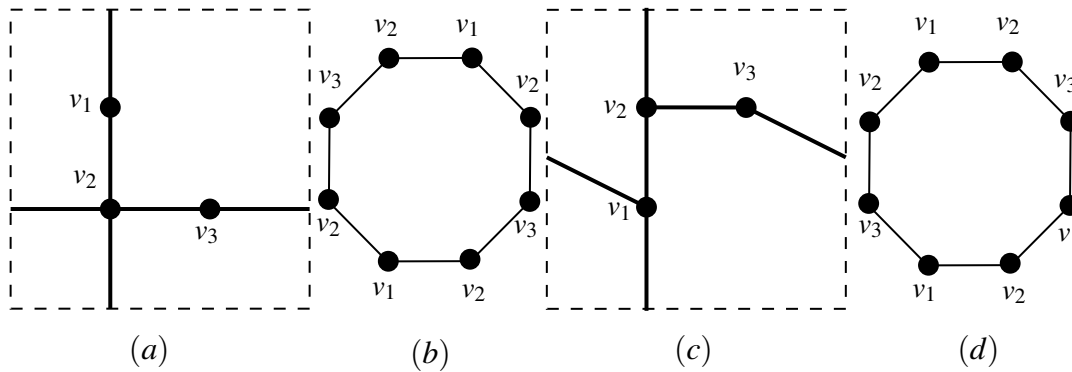


Figure 5.19: (a) A labelling of G_1^3 . (b) The polygon representation of G_1^3 in (a). (c) A labelling of G_2^3 . (d) The polygon representation of G_2^3 in (c).

The following lemma is another tool that we used to utilise the search for irreducible (2,2)-tight \mathbb{T} -graphs with vertices greater than 3. Consider the 2-cycle graph, O_1 , which is given in Figure 5.1.

Lemma 5.3.5. *Let Γ be a (2,2)-tight graph that contains a subgraph Π that is isomorphic to either Ω_1 or Ω_2 and a subgraph Θ that is isomorphic to O_1 . If Π and Θ are disjoint, then Γ cannot be embedded as an irreducible (2,2)-tight \mathbb{T} -graph.*

Proof. It is clear that Θ must be embedded as a separating 2-cycle contained in a face of G_1^3 (or G_2^3). By Lemma 5.3.1, this means that there is some digon in the embedding so it is not irreducible. \square

5.4. IRREDUCIBLE (2,2)-TIGHT TORUS GRAPHS WITH FOUR VERTICES

Figure 5.20 summarise Lemma 5.3.5. We use the polygon representation of G_1^3 to visualise the embedding of Θ .

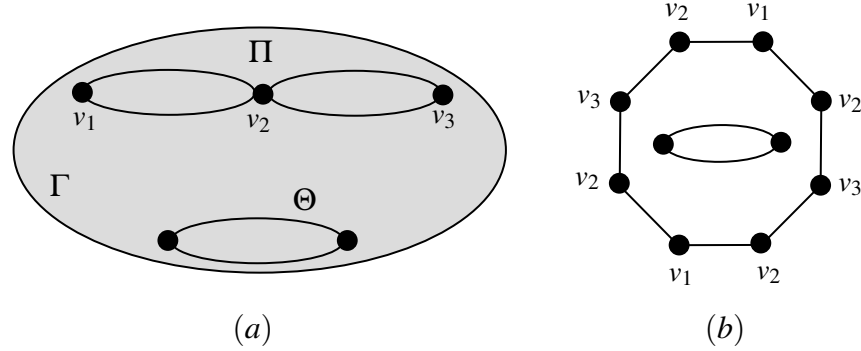


Figure 5.20: (a) A (2,2)-tight graph Γ that contains Π and Θ as subgraphs. (b) The polygon representation of G_1^3 and a digon in its interior.

5.4 Irreducible (2,2)-tight torus graphs with four vertices

In this section we present all the irreducible (2,2)-tight \mathbb{T} -graphs with four vertices. Consequently, we prove the following theorem.

Theorem 5.4.1. *There are 9 nonisomorphic irreducible (2,2)-tight \mathbb{T} -graphs with four vertices.*

Notice that there are 9 nonisomorphic (2,2)-tight graphs with four vertices. These graphs are displayed in Figure 5.21. Table 5.1 contains the notations that we choose to notate the (2,2)-tight graphs with four vertices. Table 5.2, contains the notations of the nine irreducible (2,2)-tight \mathbb{T} -graphs with four vertices.

| Gr. | Ref. | Gr. | Ref. | Gr. | Ref. |
|------------|-----------------------|------------|-----------------------|------------|-----------------------|
| Θ_1 | Fig. 5.21, Lem. 5.4.2 | Θ_4 | Fig. 5.21, Lem. 5.4.5 | Θ_7 | Fig. 5.21, Lem. 5.4.5 |
| Θ_2 | Fig. 5.21, Lem. 5.4.2 | Θ_5 | Fig. 5.21, Lem. 5.4.5 | Θ_8 | Fig. 5.21, Lem. 5.4.5 |
| Θ_3 | Fig. 5.21, Lem. 5.4.5 | Θ_6 | Fig. 5.21, Lem. 5.4.5 | Θ_9 | Fig. 5.21, Lem. 5.4.6 |

Table 5.1: The notations for all nonisomorphic (2,2)-tight graphs with four vertices. Abbreviations: Gr.=Graph, Ref.=Reference(s).

| Gr. | Ref. | Gr. | Ref. | Gr. | Ref. |
|---------|-----------------------|---------|-----------------------|---------|-----------------------|
| G_1^4 | Lem. 5.4.2 | G_4^4 | Lem. 5.4.5, Fig. 5.27 | G_7^4 | Lem. 5.4.5, Fig. 5.27 |
| G_2^4 | Lem. 5.4.4 | G_5^4 | Lem. 5.4.5, Fig. 5.27 | G_8^4 | Lem. 5.4.5, Fig. 5.26 |
| G_3^4 | Lem. 5.4.5, Fig. 5.27 | G_6^4 | Lem.5.4.5, Fig. 5.26 | G_9^4 | Lem. 5.4.5, Fig. 5.26 |

Table 5.2: The notations for all nonisomorphic irreducible (2,2)-tight \mathbb{T} -graphs with four vertices. Abbreviations: Gr.= \mathbb{T} -Graph, Ref.=Reference(s).

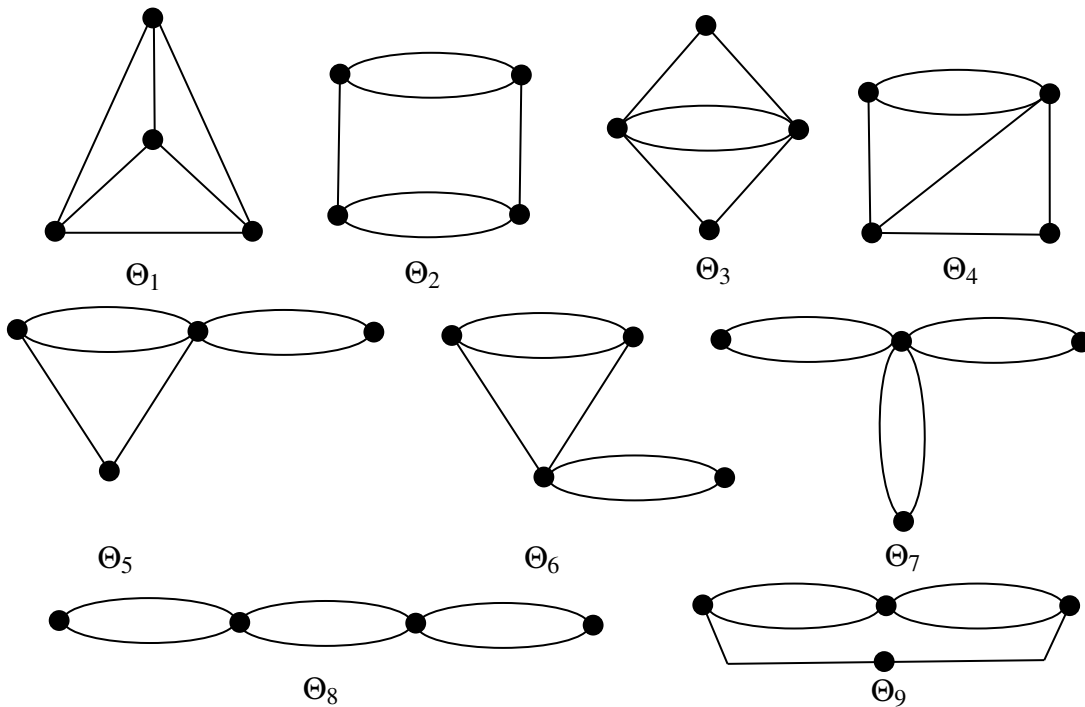


Figure 5.21: All nonisomorphic (2,2)-tight graphs with four vertices.

5.4.1 Embedding Θ_1

In the following we show that Θ_1 , see Figure 5.21, can be embedded in the torus as an irreducible (2,2)-tight \mathbb{T} -graph.

Lemma 5.4.2. *Let G be an irreducible (2,2)-tight \mathbb{T} -graph with $f_4 = 1$ and its underlying graph is Θ_1 . Then G is isomorphic to the \mathbb{T} -graph shown in Figure 5.22.*

Proof. The proof follows from Lemma 4.5.3. □

5.4. IRREDUCIBLE (2,2)-TIGHT TORUS GRAPHS WITH FOUR VERTICES

Consider the irreducible embedding of Θ_1 in Lemma 5.4.2. We denote this embedding by G_1^4 .

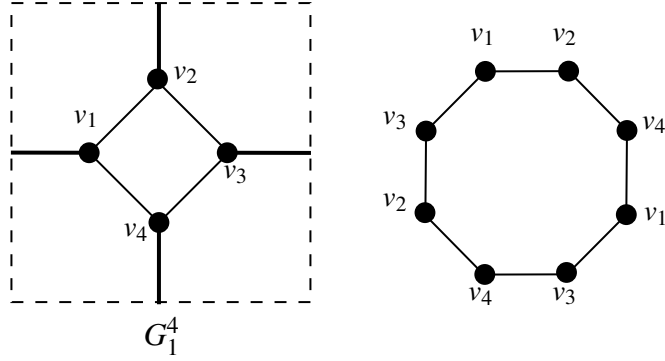


Figure 5.22: The embedding of Θ_1 as an irreducible (2,2)-tight \mathbb{T} -graph (G_1^4).

Lemma 5.4.3. Θ_1 cannot be embedded as an irreducible (2,2)-tight \mathbb{T} -graph with $f_4 = 0$.

Proof. Assume that Θ_1 can be embedded as an irreducible (2,2)-tight \mathbb{T} -graph with $f_4 = 0$. Let us label Θ_1 as in Figure 5.23(a). By Lemma 5.1.4, any 4-cycle in Θ_1 has to be embedded as nonseparating cycle in \mathbb{T} . Let us consider the subgraph $\Theta_1 - j$. So the embedding of its nondegenerate 4-cycle has to be embedded as a nonseparating cycle as in Figure 5.23(b). We embed the edge in the noncellular face as it is depicted in Figure 5.23(b) which represents the embedding of $\Theta_1 - j$. It follows that the cellular embedding of $\Theta_1 - j$ gives rise to a polygon representation which is depicted in Figure 5.23(c). We can see that it is impossible to add the edge j in the 10-gon without creating a triangle or a quadrilateral face in the interior of this polygon. \square

5.4.2 Embedding Θ_2

In the following we consider the embedding of Θ_2 , see Figure 5.21, as an irreducible (2,2)-tight \mathbb{T} -graph. Notice that this graph has O_4 , see Figure 5.1, as a subgraph.

Lemma 5.4.4. Θ_2 can be embedded as an irreducible (2,2)-tight \mathbb{T} -graph. This embedding is unique up to isomorphism.

Proof. Consider the labelled Θ_2 in Figure 5.24(a). By Lemma 5.1.7, the two 2-cycles together forms two disjoint nonseparating cycles, see Figure 5.24(b). The two edges e and f have to be embedded as in Figure 5.24(b). \square

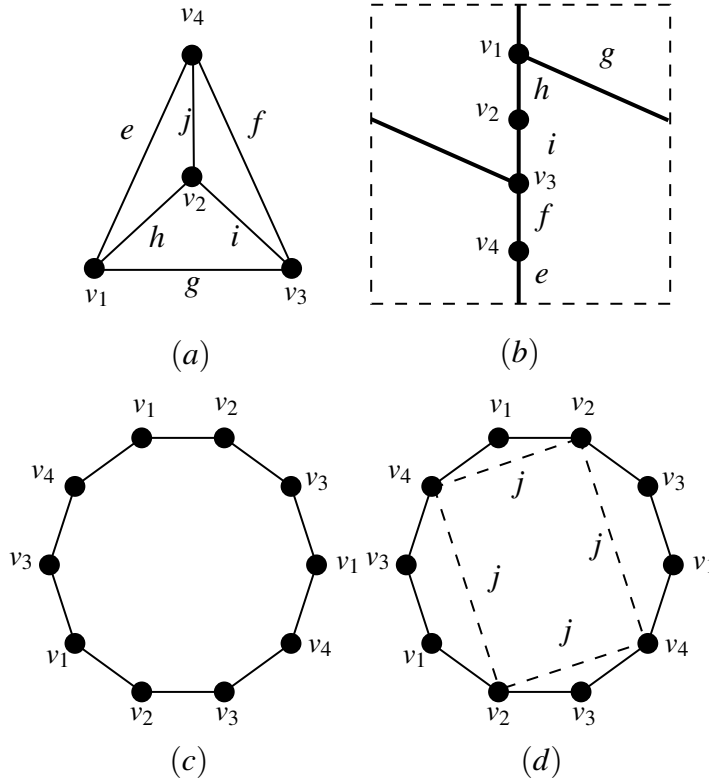


Figure 5.23: Embedding Θ_1 with $f_4 = 0$: (a) A labelling of Θ_1 . (b) The embedding of the subgraph $\Theta - j$ in the torus. (c) The polygon representation of the embedding in (b). (d) All possible cases of inserting the edge j inside the polygon representation of the \mathbb{T} -graph in (b).

We denote the embedding given in Lemma 5.4.2 by G_2^4 . Consider the labelling of G_2^4 in Figure 5.24(b). The polygon representation of G_2^4 is depicted in Figure 5.24(c).

5.4.3 Irreducible (2,2)-tight \mathbb{T} -graphs that are derived from either G_1^3 or G_2^3

In the following we show that there are exactly 7 nonisomorphic (2,2)-tight \mathbb{T} -graphs where either G_1^3 , see Figure 5.17(b), or G_2^3 , see Figure 5.18(b), is a \mathbb{T} -subgraph of each of them. We use polygon representations of G_1^3 and G_2^3 to find such irreducible (2,2)-tight \mathbb{T} -graphs.

Consider the (2,2)-tight graphs with four vertices such that either Ω_1 , see Figure 5.16, or Ω_2 , see Figure 5.16, is a subgraph of each them. In Figure 5.25, we categorise

5.4. IRREDUCIBLE (2,2)-TIGHT TORUS GRAPHS WITH FOUR VERTICES

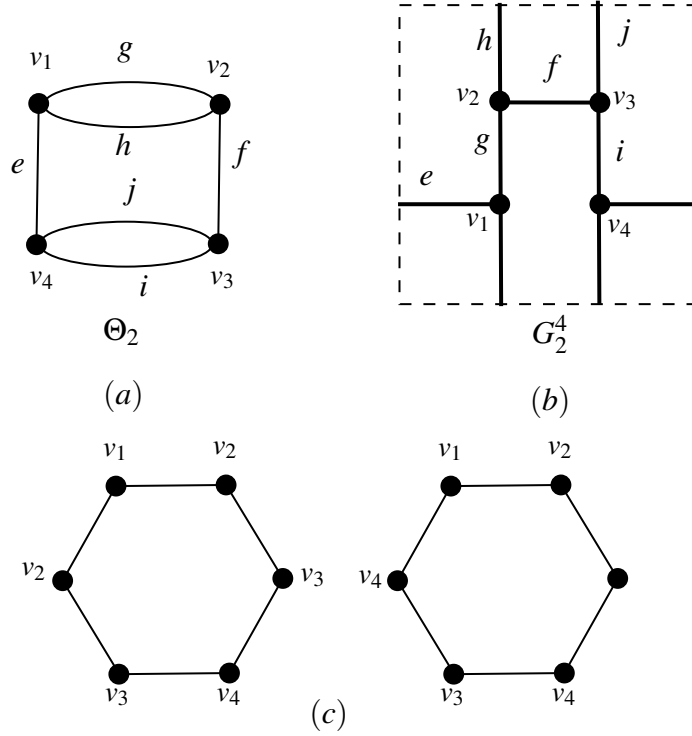


Figure 5.24: (a) A labelling of Θ_2 . (b) The embedding of Θ_1 as an irreducible (2,2)-tight \mathbb{T} -graph, i.e. G_2^4 . (c) The polygon representation of G_2^4

such graphs into three groups. We use this categorisation to find irreducible (2,2)-tight \mathbb{T} -graphs such that their underlying graphs are from these three groups.

Lemma 5.4.5. *There are 7 nonisomorphic irreducible (2,2)-tight \mathbb{T} -graphs with four vertices in which either G_1^3 or G_2^3 is a \mathbb{T} -subgraph of each of them.*

Proof. Consider the seven (2,2)-tight graphs in Figure 5.25. We use the polygon representation of G_1^3 to decide if the graphs Θ_6, Θ_7 and Θ_8 can be embedded as an irreducible (2,2)-tight \mathbb{T} -graphs. We use the method that we described in Subsection 5.1.3. See also Appendix B, which contains all possible polygon representations that can be generated from the polygon representation of G_1^3 . Of course many of them are equivalent. We found up to isomorphism that for each of Θ_6 respectively, Θ_7 and Θ_8 , see Figure 5.21, there is a unique embedding as an irreducible (2,2)-tight \mathbb{T} -graph G_6^4 respectively G_8^4 and G_9^4 , see Figure 5.26.

Now, for the graphs Θ_3, Θ_4 and Θ_5 , we find from the polygon representation of G_2^3

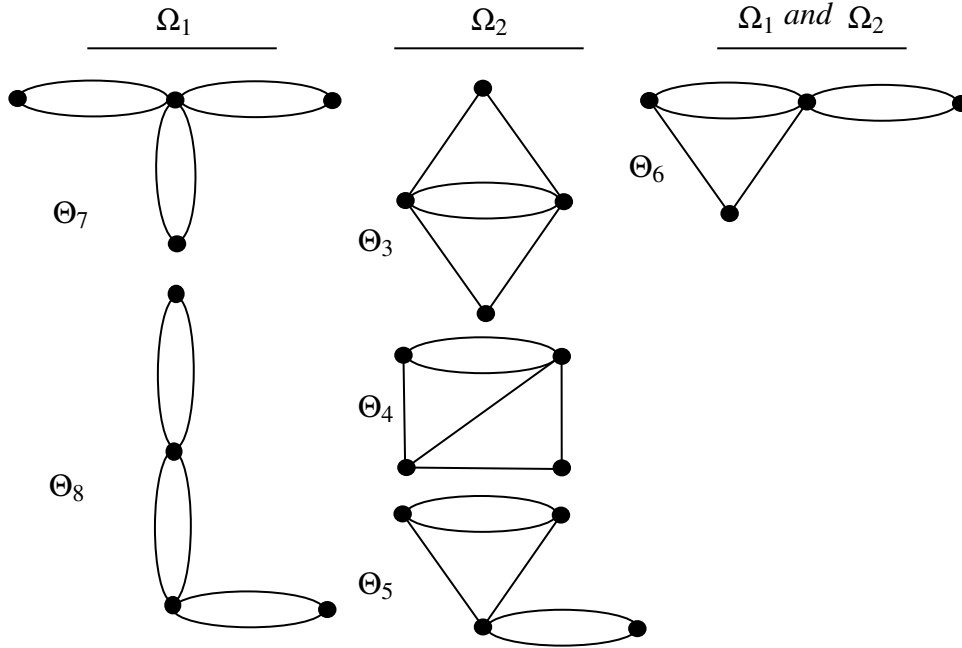


Figure 5.25: The six nonisomorphic $(2,2)$ -tight graphs of order 4 that contain either Ω_1 , see Figure 5.16, or Ω_2 , see Figure 5.16, as a subgraph. We group them in three groups.

the following. The graph Θ_3 is the underlying graph of two nonisomorphic irreducible $(2,2)$ -tight \mathbb{T} -graphs, G_3^4 and G_4^4 , see Figure 5.27. Moreover, up to isomorphism, for Θ_4 respectively, Θ_5 there is a unique embedding as an irreducible $(2,2)$ -tight \mathbb{T} -graph, which is denoted by G_5^4 respectively G_7^4 , see Figure 5.27. \square

5.4. IRREDUCIBLE (2,2)-TIGHT TORUS GRAPHS WITH FOUR VERTICES

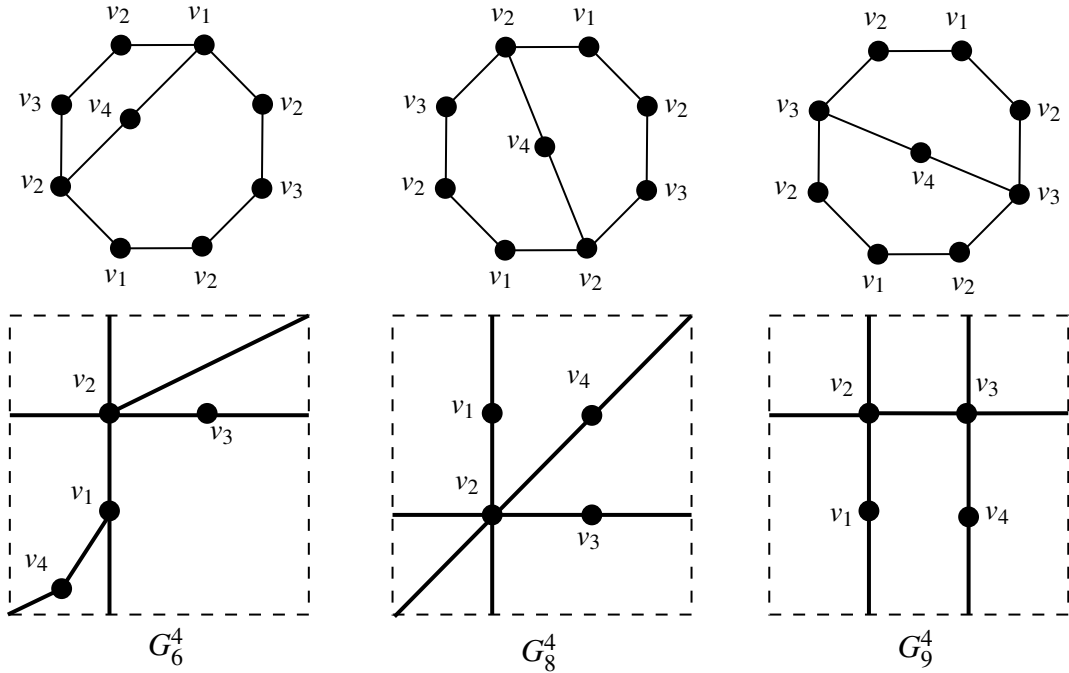


Figure 5.26: The irreducible (2,2)-tight \mathbb{T} -graphs G_6^4, G_8^4 and G_9^4 .

5.4.4 The smallest (2,2)-tight graph with no irreducible embedding

Consider the last (2,2)-tight graph in Figure 5.21, Θ_9 . Although Ω_1 is a subgraph of Θ_9 , we see in the following that Θ_9 cannot be embedded as an irreducible (2,2)-tight \mathbb{T} -graph.

Lemma 5.4.6. Θ_9 cannot be embedded as an irreducible (2,2)-tight \mathbb{T} -graph.

Proof. Notice that Ω_1 is a subgraph of Θ_9 . So let us consider the polygon representation of G_1^3 and the labelled Θ_9 in Figure 5.28(a). Now, we have to embed the vertex v_4 and its two adjacent edges in the interior of the plane polygon in Figure 5.28(b). It is clear that there is no way to do so without creating a quadrilateral. Thus, the conclusion follows. \square

Lemma 5.4.7. Let Γ be a (2,2)-tight graph. If Θ_9 is a subgraph of Γ , then Γ cannot be embedded as an irreducible (2,2)-tight \mathbb{T} -graph.

Proof. The conclusion follows from Theorem 5.1.1. \square

Consequently, we notice that Θ_9 is the smallest (2,2)-tight graph which cannot be embedded in the torus as an irreducible (2,2)-tight \mathbb{T} -graph.

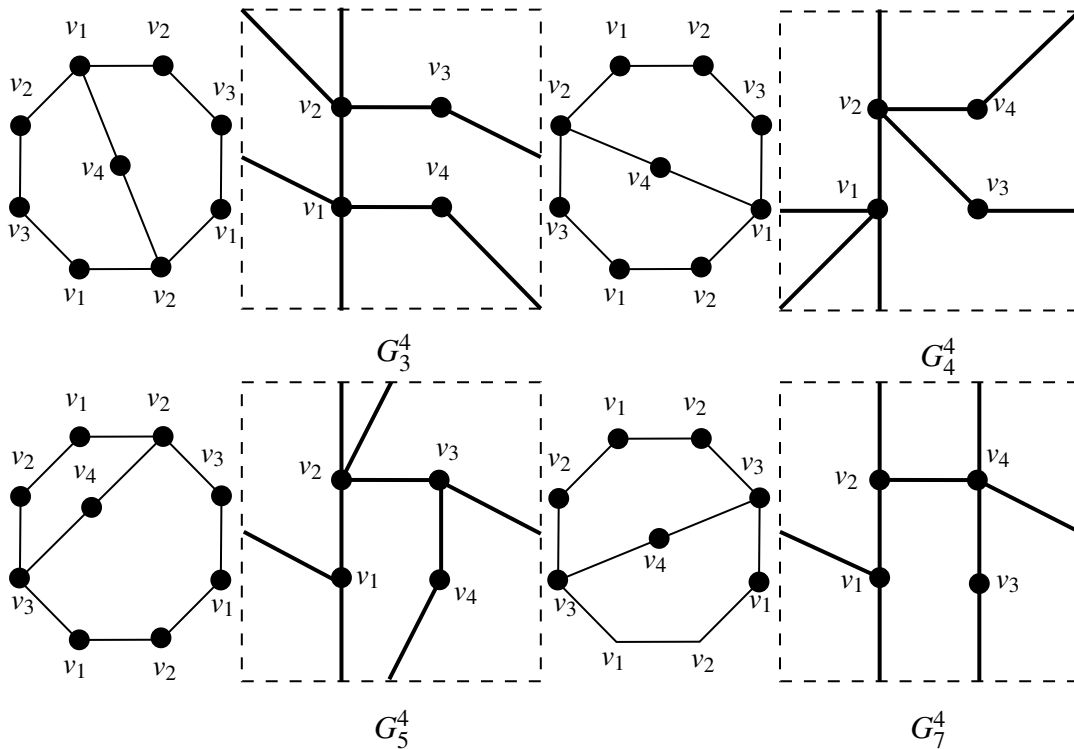


Figure 5.27: The irreducible (2,2)-tight \mathbb{T} -graphs G_3^4, G_4^4, G_5^4 and G_7^4 .

Hence, we proved Theorem 5.4.1. We present the notations for all irreducible (2,2)-tight \mathbb{T} -graphs with four vertices in Figure 5.29. In Appendix E (E.2), we present the irreducible (2,2)-tight \mathbb{T} -graphs with four vertices in one group. Figure 5.29 shows how the notations of all irreducible (2,2)-tight \mathbb{T} -graphs with four vertices are categorised.

5.5 Irreducible (2,2)-tight torus graphs with five vertices

In this section we present all the irreducible (2,2)-tight \mathbb{T} -graphs with five vertices. We prove the following theorem.

Theorem 5.5.1. *There are 23 nonisomorphic irreducible (2,2)-tight \mathbb{T} -graphs with five vertices.*

Table 5.3 contains all the notations of the irreducible (2,2)-tight \mathbb{T} -graphs with five vertices.

5.5. IRREDUCIBLE (2,2)-TIGHT TORUS GRAPHS WITH FIVE VERTICES

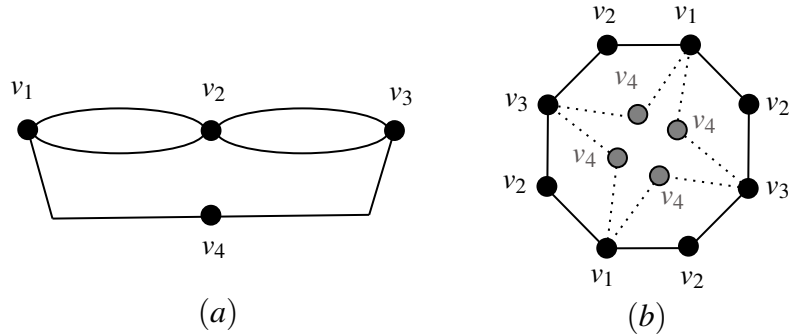


Figure 5.28: (a) A labelling of Θ_9 . (b) The polygon representation of G_1^3 which is used to show that Θ_9 cannot be embedded as an irreducible (2,2)-tight \mathbb{T} -graph.

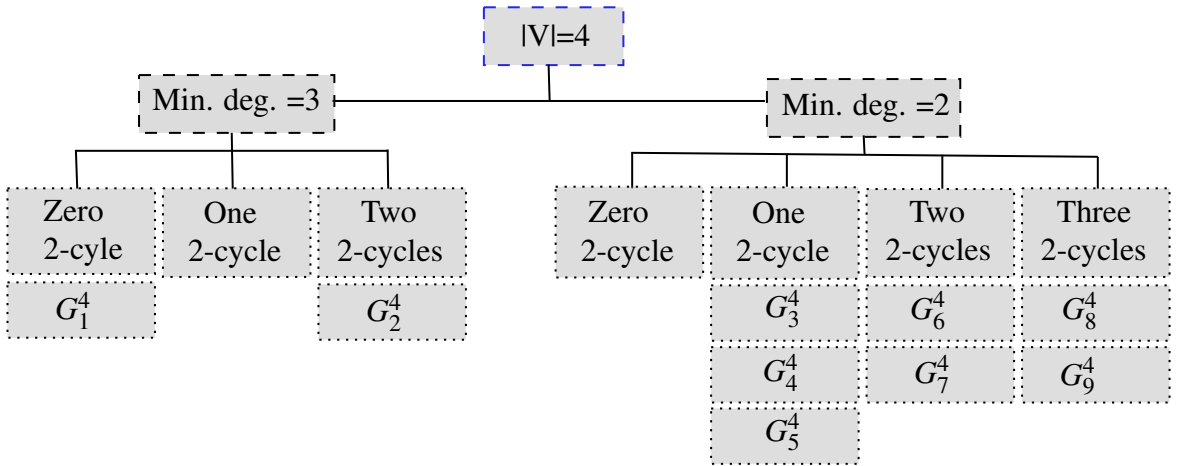


Figure 5.29: Notations of all nonisomorphic irreducible (2,2)-tight \mathbb{T} -graphs with four vertices.

We observe that there are only two simple (2,2)-tight graphs with five vertices, [80]. These graphs are Δ_1 and Δ_2 , see Figure 5.30. Also, we observe that the graph Δ_3 , Figure 5.30, is the only nonsimple underlying graph with minimum degree three among all the other underlying (2,2)-tight graphs of irreducible (2,2)-tight \mathbb{T} -graphs with five vertices.

5.5.1 Embedding Δ_1

In the following we investigate the embedding Δ_1 , see Figure 5.30, as an irreducible (2,2)-tight \mathbb{T} -graph.

| Gr. | Ref. | Gr. | Ref. | Gr. | Ref. |
|---------|--------------|------------|--------------|------------|-----------|
| G_1^5 | Fig. 5.31(d) | G_9^5 | Fig. 5.42 | G_{17}^5 | Fig. 5.43 |
| G_2^5 | Fig. 5.34(b) | G_{10}^5 | Fig. 5.42 | G_{18}^5 | Fig. 5.43 |
| G_3^5 | Fig. 5.32(b) | G_{11}^5 | Fig. 5.35(c) | G_{19}^5 | Fig. 5.36 |
| G_4^5 | Fig. 5.32(c) | G_{12}^5 | Fig. 5.40 | G_{20}^5 | Fig. 5.36 |
| G_5^5 | Fig. 5.40 | G_{13}^5 | Fig. 5.41 | G_{21}^5 | Fig. 5.38 |
| G_6^5 | Fig. 5.42 | G_{14}^5 | Fig. 5.37 | G_{22}^5 | Fig. 5.39 |
| G_7^5 | Fig. 5.42 | G_{15}^5 | Fig. 5.37 | G_{23}^5 | Fig. 5.39 |
| G_8^5 | Fig. 5.42 | G_{16}^5 | Fig. 5.37 | | |

Table 5.3: The notations of all nonisomorphic irreducible (2,2)-tight \mathbb{T} -graphs with five vertices. Abbreviations: Gr.= \mathbb{T} -Graph, Ref.=Reference(s).

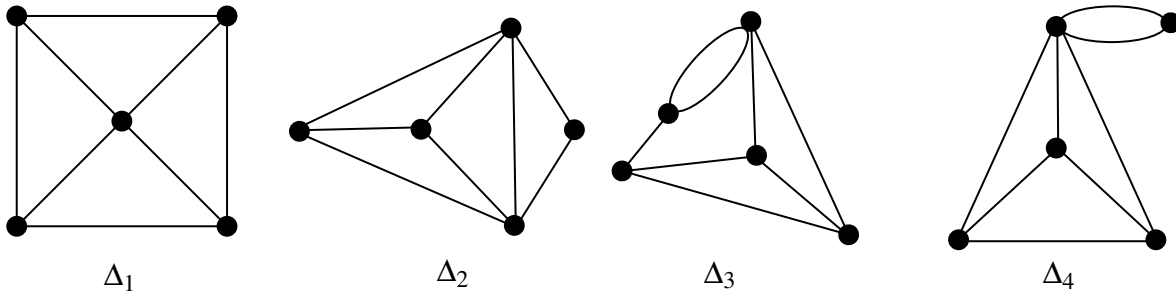


Figure 5.30: Some (2,2)-tight graphs with five vertices.

Lemma 5.5.2. *Up to isomorphism, there is a unique embedding for the graph Δ_1 as an irreducible (2,2)-tight \mathbb{T} -graph.*

Proof. Let us label the graph Δ_1 as in Figure 5.31(a). Let K be the subgraph K_4 minus one edge with the vertices v_1, v_2, v_4, v_5 . By a similar argument to the one in the proof of Lemma 5.4.3, we embed K as in Figure 5.31(b).

Now, consider the polygon representation of the embedding of K . We need to embed the vertex v_3 together with its adjacent three edges g, k and l . We do that on the polygon representation of the embedding of K . Let us first insert the edge g . As v_2 appears on the boundary of the polygon representation of the embedding of K twice, we have an arbitrary choice to pick between these two. Let us fix one of these vertices, see Figure 5.31(c). Now, let us consider inserting the edge l in the polygon representation. We can see that the vertex v_4 appears on the boundary of the polygon twice. Notice that we can choose the one which is distanced from v_2 by two. But this choice creates a triangle. So

5.5. IRREDUCIBLE (2,2)-TIGHT TORUS GRAPHS WITH FIVE VERTICES

we choose the other one. Finally, the edge k is enforced to be inserted as depicted in the Figure 5.31(c). Consequently, we get a polygon representation for a graph with five vertices such that the embedding corresponding to such polygon representation satisfies the 5-tuple $(f_4, f_5, f_6, f_7, f_8) = (0, 2, 1, 0, 0)$. This embedding which is depicted in Figure 5.31(d) is an irreducible embedding for the graph Δ_1 . \square

We denote the embedding of Δ_1 given in the previous lemma by G_1^5 .

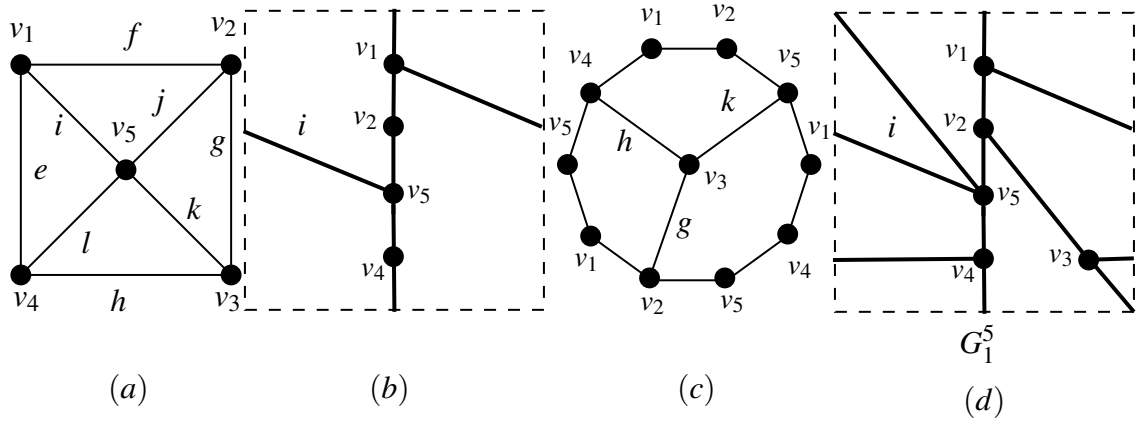


Figure 5.31: (a) A labelling of Δ_1 . (b) The embedding of K_4 minus one edge with vertices v_1, v_2, v_3 and v_4 which is a subgraph of Δ_1 . (c) The polygon representation of the \mathbb{T} -graph, G_1^5 . (d) Embedding Δ_1 as an irreducible (2,2)-tight \mathbb{T} -graph, G_1^5 .

5.5.2 Embedding Δ_2

In the following we consider the embedding of the graph Δ_2 , see Figure 5.30, in the torus.

Lemma 5.5.3. Δ_2 has two nonisomorphic embeddings in \mathbb{T} as an irreducible (2,2)-tight \mathbb{T} -graphs.

Proof. Consider the labelled Δ_2 in Figure 5.32(a). Notice that Δ_2 contains Θ_1 , as a subgraph. So Δ_2 cannot be embedded as an irreducible (2,2)-tight \mathbb{T} -graph with $f_4 = 0$. Now, let us consider the polygon representation of G_1^4 . From the labelling 5.32(a), we have to insert the vertex v_5 and its two adjacent edges in the polygon representation of G_1^4 . It is clear that there are only two possible non-equivalent polygon representations we can get. These polygon presentations are depicted in Figure 5.32(b) and (c). Consequently, their

corresponding \mathbb{T} -graphs are nonisomorphic irreducible (2,2)-tight torus graphs with five vertices, Figure 5.32(b) and (c). \square

We denote the irreducible (2,2)-tight \mathbb{T} -graph in Figure 5.32(b) respectively 5.32(c) by G_3^5 respectively G_4^5 .

Notice that Δ_2 cannot be embedded as an irreducible (2,2)-tight torus graph with $f_4 = 0$.

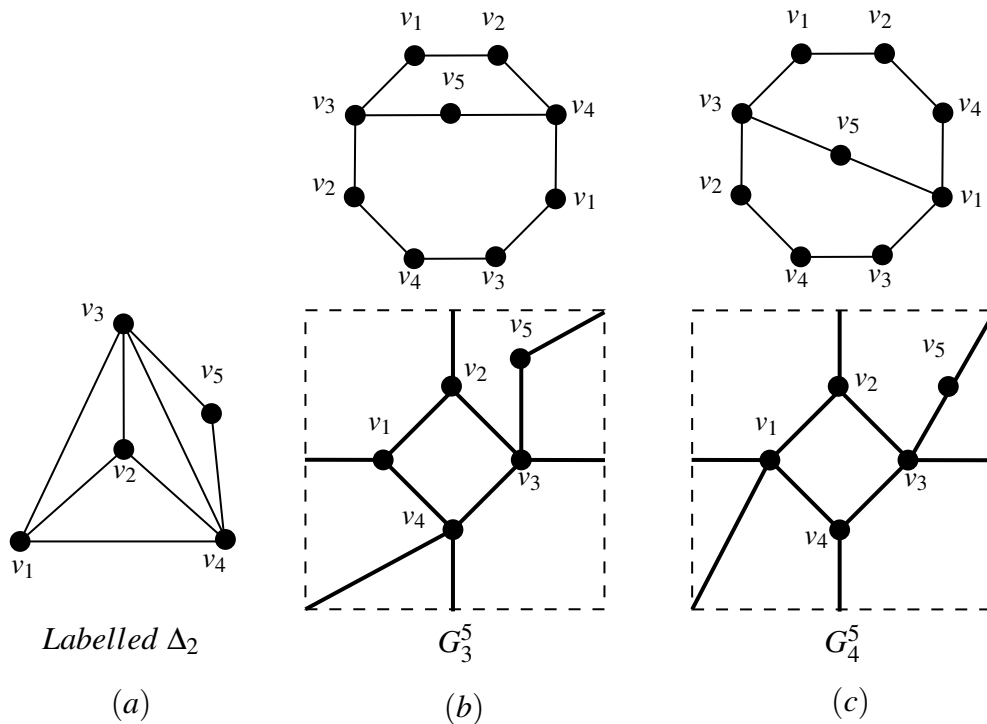


Figure 5.32: (a) A labelling of Δ_2 . (b) G_3^5 and its polygon representation. (c) G_4^5 and its polygon representation.

5.5.3 Embedding Δ_3

Consider the graph Δ_3 in Figure 5.30. In the following, we investigate the embedding of this graph.

Lemma 5.5.4. *Suppose $f_4 = 0$. Then the graph Δ_3 cannot be embedded as an irreducible (2,2)-tight \mathbb{T} -graph.*

5.5. IRREDUCIBLE (2,2)-TIGHT TORUS GRAPHS WITH FIVE VERTICES

Proof. Consider the subgraph K_4 minus one edge of Δ_3 with vertices v_1, v_2, v_3 and v_4 , see Figure 5.33(a). The embedding of this graph is depicted in Figure 5.33(b). Consider the polygon representation of this embedding in Figure 5.33(c). Notice that v_5 is adjacent to v_2 with two edges. Therefore, we add these two edges and v_5 inside the polygon representation. We can notice that there is no way to add the edge e inside the polygon representation without creating a contractible quadrilateral, see Figure 5.33(c). \square

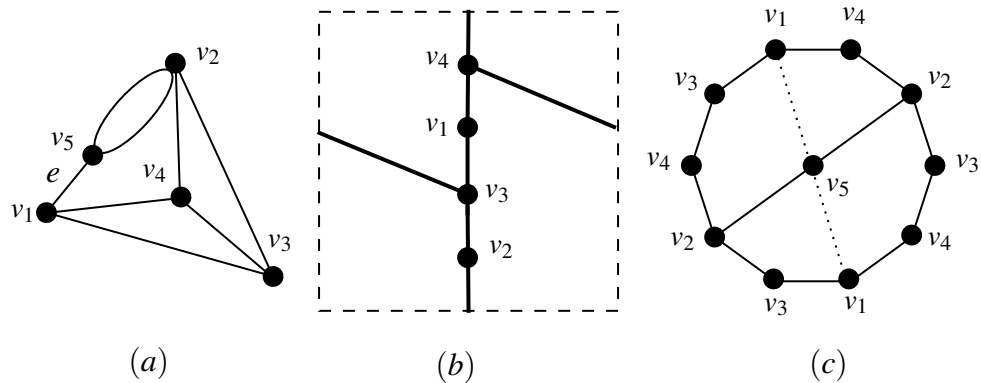


Figure 5.33: (a) A labelling of Δ_3 . (b) The embedding of K_4 minus one edge with vertices v_1, v_2, v_3 and v_4 which is a subgraph of Δ_3 (the graph in (a)). (c) The polygon representation of the embedding in (b). Notice that in both cases of trying to insert the edge e , quadrilateral faces will be created.

Lemma 5.5.5. *Suppose that $f_4 = 1$, up to isomorphism, Δ_3 has a unique embedding as an irreducible (2,2)-tight \mathbb{T} -graph.*

Proof. Consider the subgraph K_4 minus one edge with vertices v_1, v_2, v_3 and v_4 . This graph can be embedded in the torus as an irreducible as shown in Figure 5.34(b). Now, we build an essential blocker for the quadrilateral face. We first add v_5 in the noncellular face. Notice that the 2-cycle with vertices v_2 and v_5 has to be embedded as a nonseparating loop, Lemma 5.1.5. Finally, the edge e should be embedded as it is shown in Figure 5.34(b). \square

We denote the embedding of Δ_3 by G_2^5 .

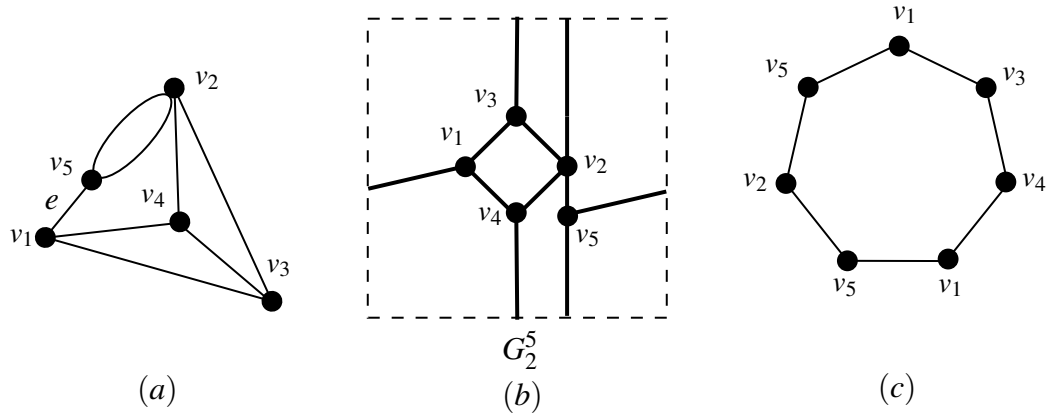


Figure 5.34: (a) A labelling of Δ_3 . (b) The irreducible embedding of Δ with one quadrilateral face. (c) The polygon representation of the embedding in (b).

5.5.4 Embedding Δ_4

In the following we investigate the embedding of the graph Δ_4 , see Figure 5.30, in the torus as an irreducible (2,2)-tight \mathbb{T} -graph. Notice that since Θ_1 , see Figure 5.21, is a subgraph of Δ_4 , Δ_4 cannot be embedded as an irreducible (2,2)-tight \mathbb{T} -graph with $f_4 = 0$, Lemma 5.4.3. So let us examine embedding this graph with $f_4 = 1$ in the following lemma.

Lemma 5.5.6. *Up to isomorphism, Δ_4 has a unique embedding as a \mathbb{T} -graph.*

Proof. The proof follows from the polygon representation of G_1^4 , see Figure 5.35. □

We denote the embedding shown in Figure 5.35(c) by G_{11}^5 .

5.5. IRREDUCIBLE (2,2)-TIGHT TORUS GRAPHS WITH FIVE VERTICES

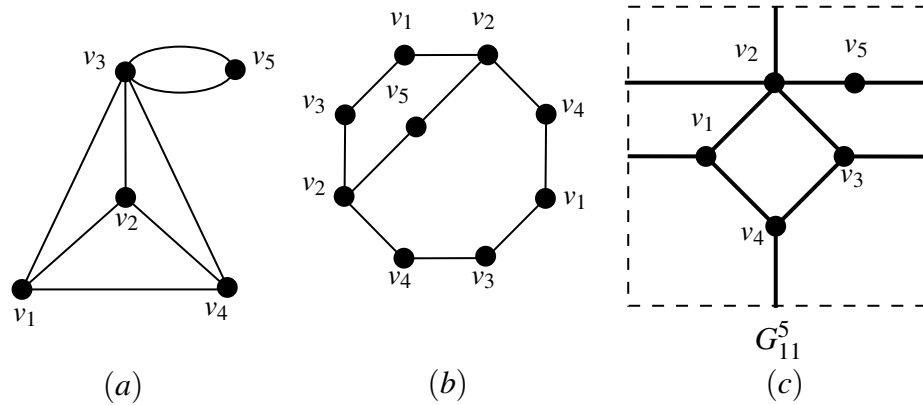


Figure 5.35: (a) A labelling of Δ_4 . (b) The polygon representation of the embedding of Δ_4 in (c). (c) The embedding of Δ_4 as an irreducible (2,2)-tight \mathbb{T} -graph, i.e. G_{11}^5 .

5.5.5 Irreducible (2,2)-tight torus graphs in which G_2^4 is a torus subgraph of each of them

In the following we find all nonisomorphic irreducible (2,2)-tight \mathbb{T} -graph with five vertices such that G_2^4 , see Figure 5.24(b), is a \mathbb{T} -subgraph of each of them.

Lemma 5.5.7. *There are 2 nonisomorphic irreducible (2,2)-tight \mathbb{T} -graphs such that each of such \mathbb{T} -graphs contains G_2^4 as a \mathbb{T} -subgraph.*

Proof. The conclusion follows from the polygon representation of G_2^4 , see Figure 5.36. □

We denote the two irreducible (2,2)-tight \mathbb{T} -graphs by G_{19}^5 and G_{20}^5 , see Figure 5.36.

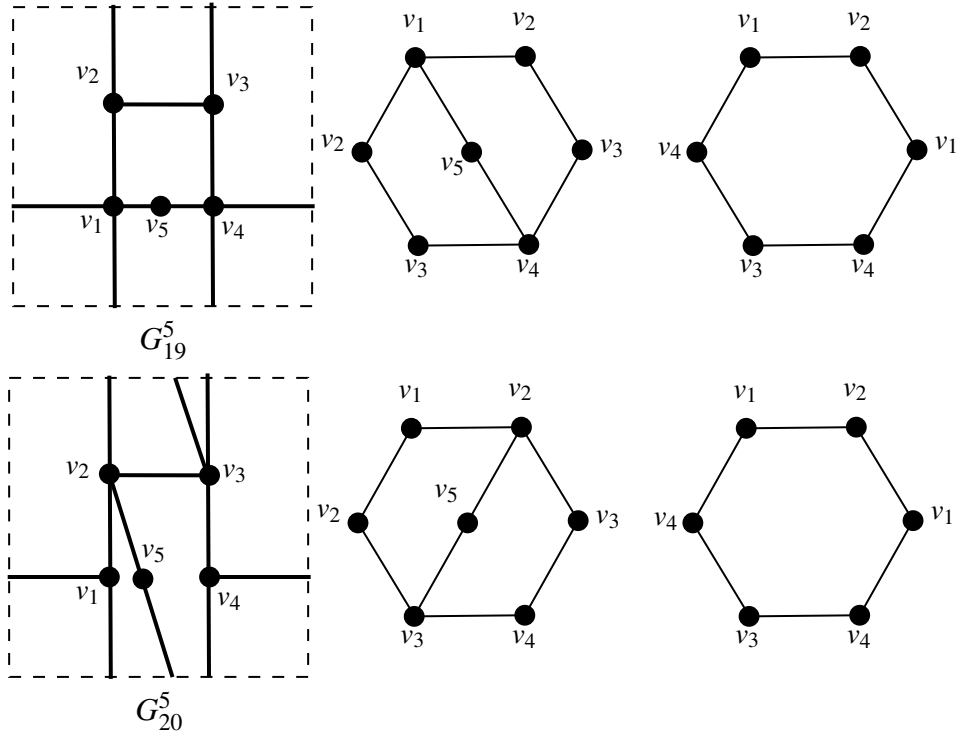


Figure 5.36: G_{19}^5 and G_{20}^5 their polygon representations.

5.5.6 Irreducible (2,2)-tight torus graphs which are derived from G_1^3 or G_2^3

In the following, we find all nonisomorphic irreducible (2,2)-tight \mathbb{T} -graphs that are derived from G_1^3 , see Figure 5.17(b), or G_2^3 , see Figure 5.18(b).

See also Figure 5.44 which presents an organisation of the notations of all such \mathbb{T} -graphs.

We check all possible polygon representations that can be generated from the polygon representations of G_1^3 and G_2^3 . From these polygon representations, we find all non-equivalent ones, and then we find the corresponding nonisomorphic irreducible (2,2)-tight \mathbb{T} -graphs. In the following we list these irreducible (2,2)-tight \mathbb{T} -graphs by declaring their ancestors paths (Subsection 5.1.3).

Via $G_1^3 - G_6^4$

The irreducible (2,2)-tight \mathbb{T} -graphs in Figure 5.37 are derived from G_6^4 , (Figure 5.26).

5.5. IRREDUCIBLE (2,2)-TIGHT TORUS GRAPHS WITH FIVE VERTICES

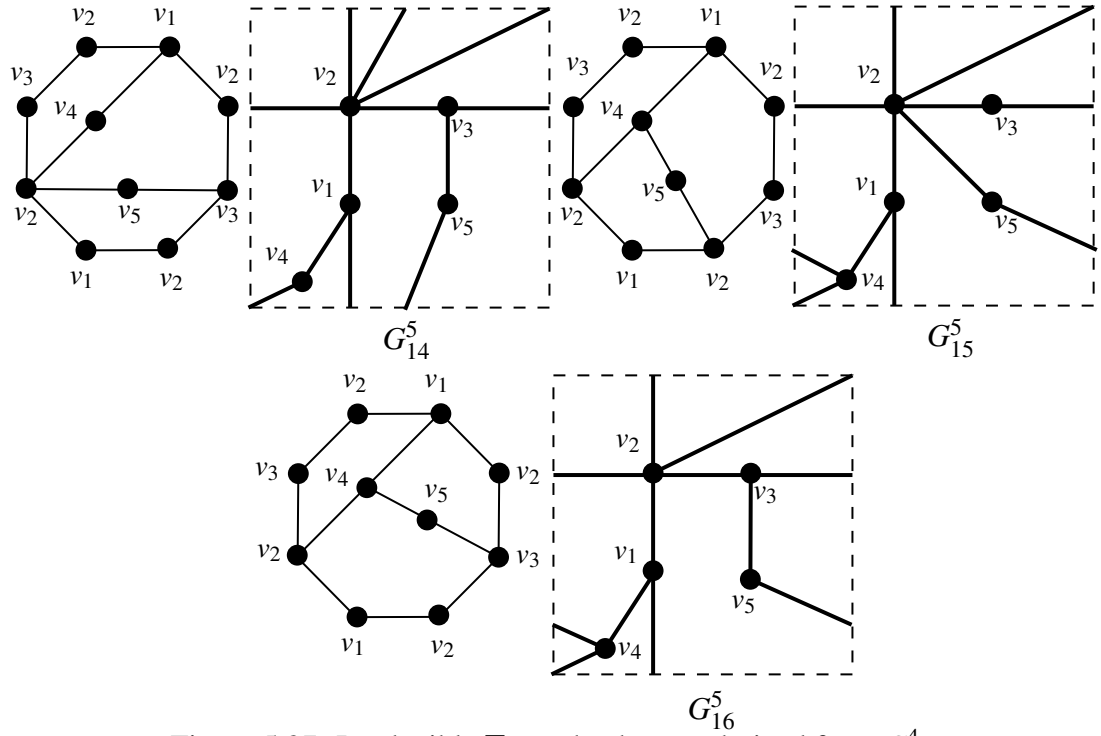


Figure 5.37: Irreducible \mathbb{T} -graphs that are derived from G_6^4 .

Via $G_1^3 - G_8^4$

The irreducible (2,2)-tight \mathbb{T} -graph in Figure 5.38 is derived from G_8^4 (Figure 5.26).

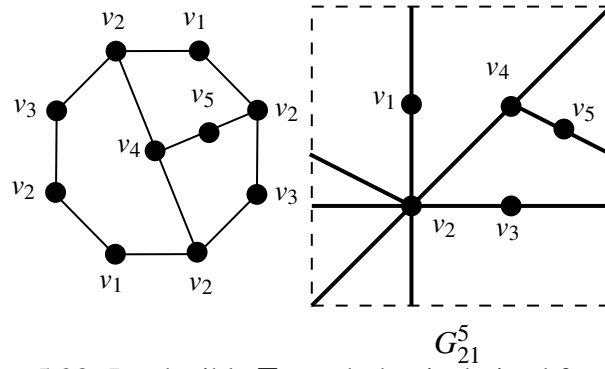


Figure 5.38: Irreducible \mathbb{T} -graph that is derived from G_8^4 .

Via $G_1^3 - G_9^4$

The irreducible (2,2)-tight \mathbb{T} -graphs in Figure 5.39 are derived from G_9^4 (Figure 5.26).

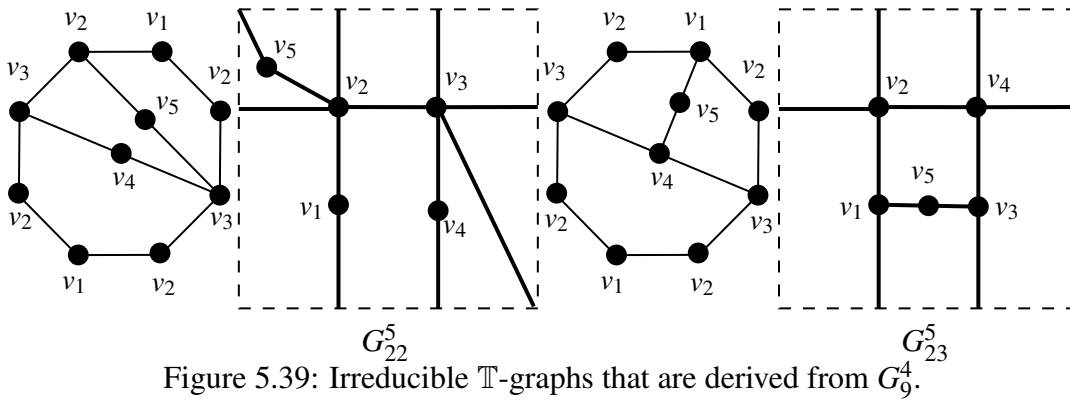


Figure 5.39: Irreducible \mathbb{T} -graphs that are derived from G_9^4 .

Via $G_2^3 - G_3^4$

The irreducible (2,2)-tight \mathbb{T} -graphs in Figure 5.40 are derived from G_3^4 (see Figure 5.27).

Via $G_2^3 - G_4^4$

The irreducible (2,2)-tight \mathbb{T} -graph in Figure 5.41 is derived from G_4^4 (see Figure 5.27).

5.5. IRREDUCIBLE (2,2)-TIGHT TORUS GRAPHS WITH FIVE VERTICES

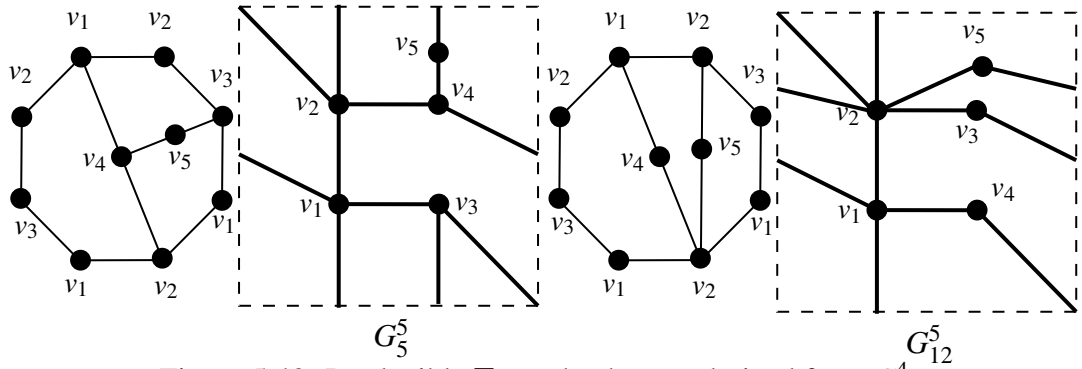


Figure 5.40: Irreducible \mathbb{T} -graphs that are derived from G_3^4 .

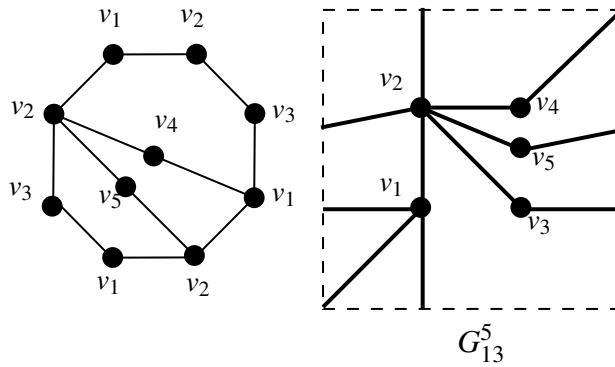


Figure 5.41: Irreducible \mathbb{T} -graph that is derived from G_4^4 .

Via $G_2^3 - G_5^4$

The irreducible (2,2)-tight \mathbb{T} -graphs in Figure 5.42 are derived from G_5^4 (see Figure 5.27).

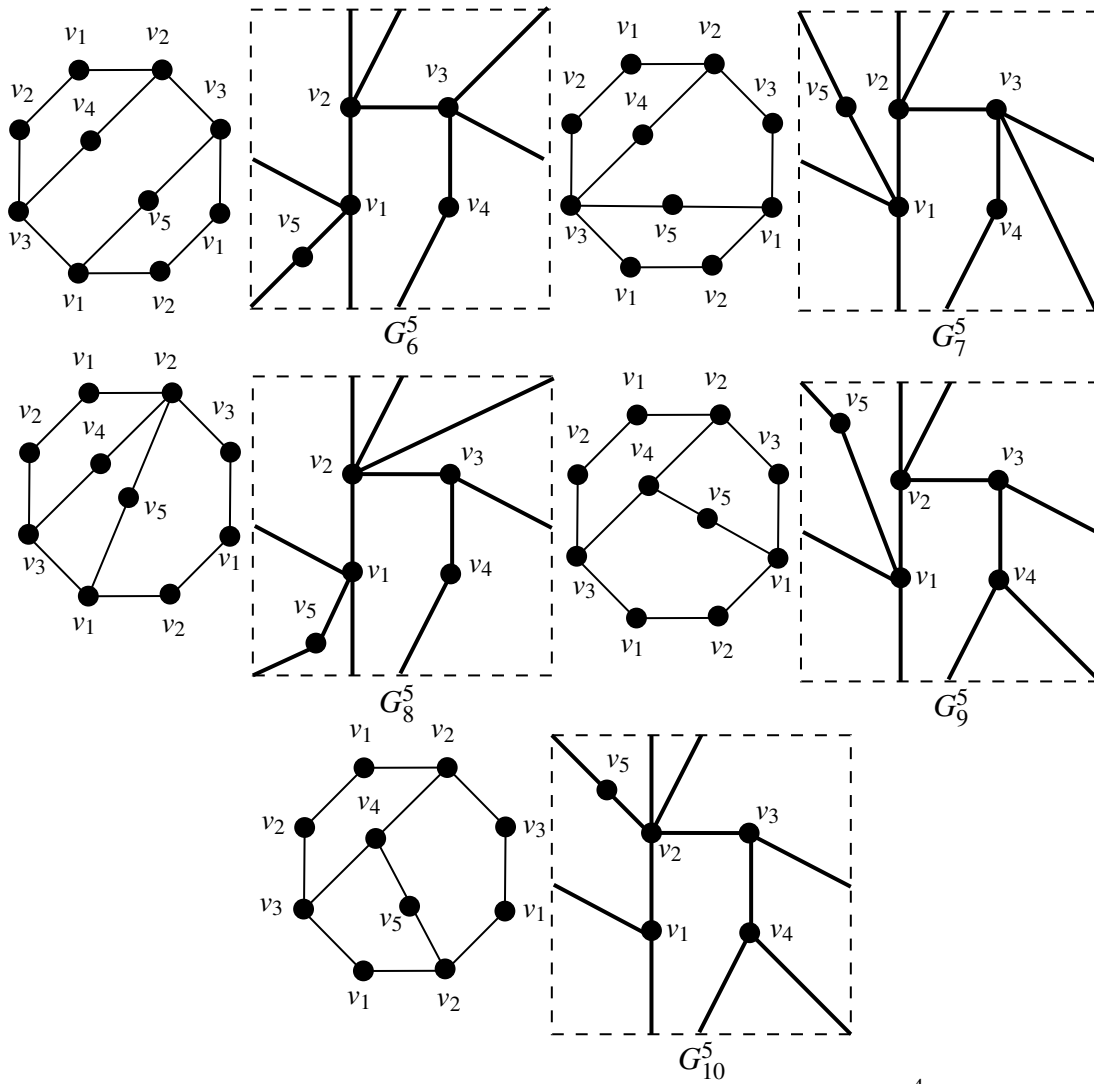


Figure 5.42: Irreducible \mathbb{T} -graphs that are derived from G_5^4 .

5.5. IRREDUCIBLE (2,2)-TIGHT TORUS GRAPHS WITH FIVE VERTICES

Via $G_2^3 - G_7^4$

The irreducible (2,2)-tight \mathbb{T} -graphs in Figure 5.43 are derived from G_7^4 (see Figure 5.27).

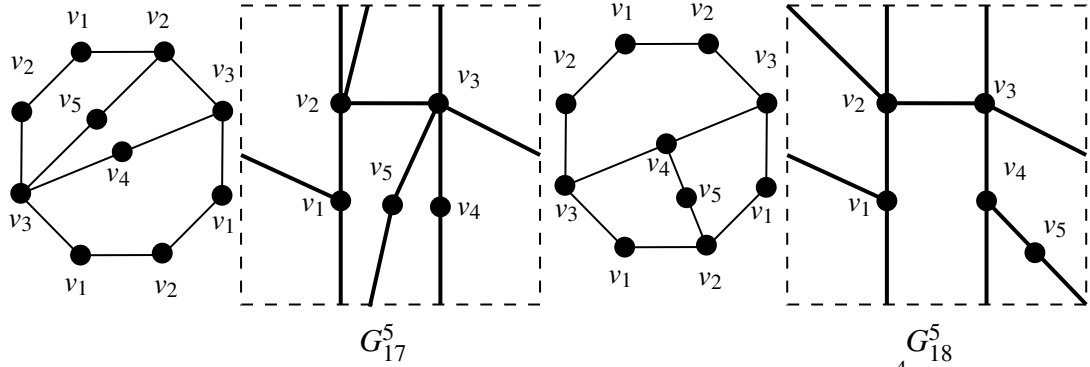


Figure 5.43: Irreducible \mathbb{T} -graph that are derived from G_7^4 .

The diagram in Figure 5.44 includes a summary of the ancestor paths that we previously discussed.

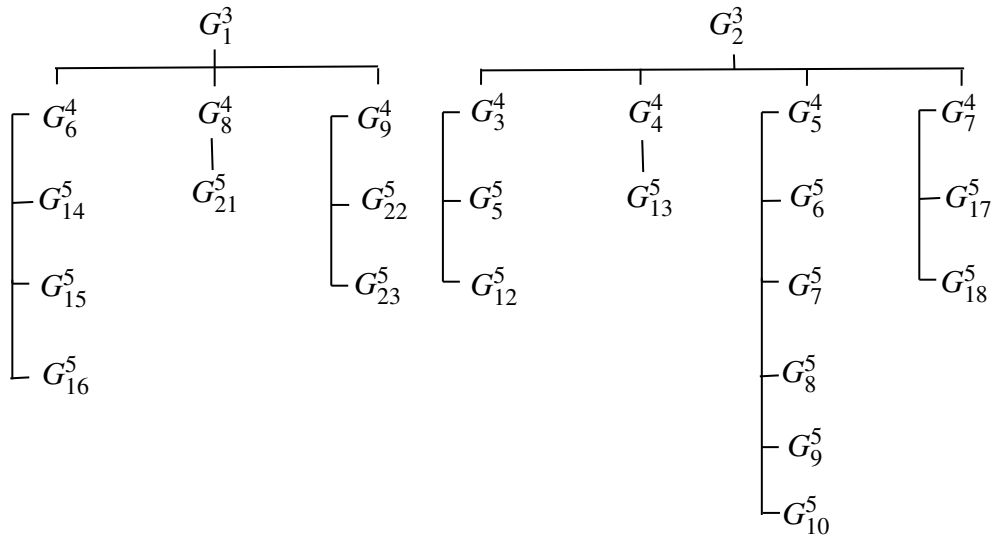


Figure 5.44: Irreducible (2,2)-tight \mathbb{T} -graphs that are derived from G_1^3 or G_2^3 .

At this stage, we finished proving Theorem 5.5.1. We present the notations of all the irreducible (2,2)-tight \mathbb{T} -graphs with five vertices in Figure 5.45. In Appendix E(E.3, E.4 and E.5), we present the irreducible (2,2)-tight \mathbb{T} -graphs with five vertices.

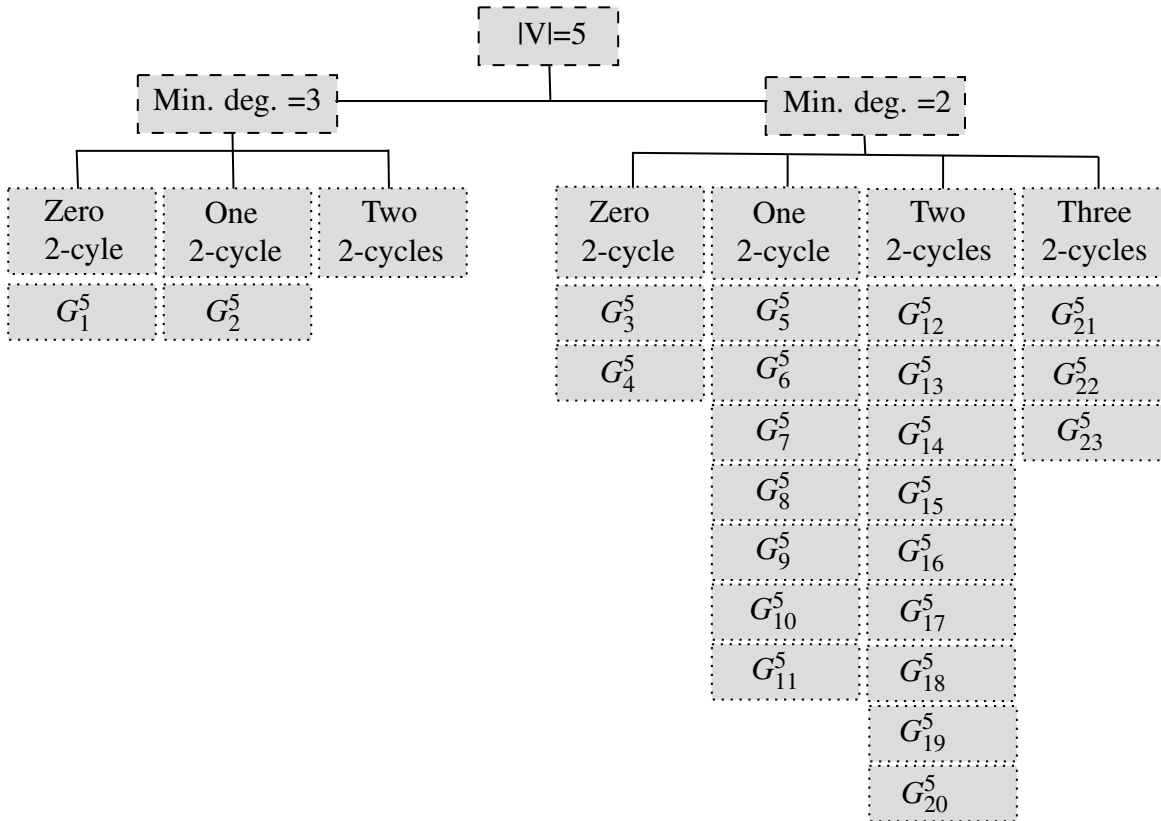


Figure 5.45: All nonisomorphic irreducible (2,2)-tight \mathbb{T} -graphs with five vertices.

5.6 Irreducible (2,2) -tight torus graphs with six and seven vertices

In this part of this chapter, we explain how we found all nonisomorphic irreducible (2,2)-tight (2,2)-tight \mathbb{T} -graphs with six and seven vertices. These irreducible (2,2)-tight \mathbb{T} -graphs were found by using the SageMath code which is described in Subsection 5.2.4. We found 47 irreducible (2,2)-tight \mathbb{T} -graphs with 6 vertices and 27 irreducible (2,2)-tight \mathbb{T} -graphs with 7 vertices. These are shown in Appendix E (E.6, E.7,E.8,E.9,E.10

5.6. IRREDUCIBLE (2,2) -TIGHT TORUS GRAPHS WITH SIX AND SEVEN VERTICES

and E.11) and Appendix E (E.12, E.13 and E.14) respectively. We have also verified these lists independently by hand - we omit the details of these calculations here. We found that both hand calculations and computer assisted searches yield the same list of irreducible (2,2)-tight \mathbb{T} -graphs.

In the following, we give an idea of how we compared the results of both approaches. Consider the irreducible (2,2)-tight \mathbb{T} -graph in Figure 5.46 that we found by hand computing. We label all the half edges in an anti-clockwise order. Then we record the rotation system of this \mathbb{T} -graph as follows.

$$\sigma = [[1, 2, 3], [4, 5, 6, 7], [8, 9, 10, 11, 12], [13, 14, 15, 16], \\ [17, 18, 19, 20], [21, 22], [23, 24]]$$

$$\tau = [[1, 10], [2, 7], [6, 8], [12, 14], [3, 13], [4, 24], [19, 23], \\ [18, 21], [16, 22], [5, 15], [9, 20], [11, 17]]$$

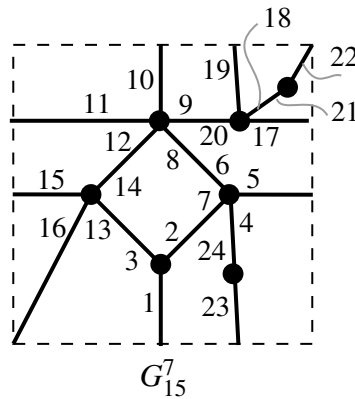


Figure 5.46: One irreducible (2,2)-tight \mathbb{T} -graph with seven vertices. All half edges are labelled with specific numbers.

Figure 5.47 presents a SageMath session to test the irreducibility of the \mathbb{T} -graph in Figure 5.46.

We present the notations for all irreducible (2,2)-tight \mathbb{T} -graphs with six respectively seven vertices in Appendix C Figure C.1 respectively Figure C.2.

```
sage: load('rotation.py')
sage: o=OrientedRotationSystem([[1,2,3],[4,5,6,7],[8,9,10,11,12],[13,14,15,16],[
....: 17,18,19,20],[21,22],[23,24]],[[1,10],[2,7],[6,8],[12,14],[3,13],[4,24],[1
....: 9,23],[18,21],[16,22],[5,15],[9,20],[11,17]])
sage: is_irreducible(o)
True
sage: o.faces()
[[1, 7, 24, 19, 9],
 [10, 17, 21, 16, 3],
 [2, 13, 12, 6],
 [8, 20, 11, 14, 5],
 [4, 15, 22, 18, 23]]
sage:
```

Figure 5.47: The output of the OrientedRotationSystem class shows that the (2,2)-tight \mathbb{T} -graph in Figure 5.46 is irreducible.

5.7 Irreducible (2,2)-tight torus graphs with eight vertices

This section is devoted to present all the irreducible (2,2)-tight \mathbb{T} -graphs with eight vertices. We prove the following theorem.

Theorem 5.7.1. *There are exactly 6 nonisomorphic irreducible (2,2)-tight \mathbb{T} -graphs with eight vertices.*

We use the hand computations to reach our goal of proving Theorem 5.7.1. We start by presenting two simple lemmas.

Lemma 5.7.2. *Let G be an irreducible (2,2)-tight \mathbb{T} -graph with eight vertices. Then there are exactly two quadrilateral faces in G .*

Proof. It is clear that G is cellular and $e = 14$. By a similar argument to the one in the proof of Theorem 5.2.1, we have that $f_5 + 2f_6 + 3f_7 + 4f_8 = 4$ and $f_i = 0$ for all $i \in \{1, 2, 3, 9, 10, \dots\}$. So

$$\begin{aligned} 2e &= 4f_4 + 5f_5 + 6f_6 + 7f_7 + 8f_8 \\ &\leq 4f_4 + 5(f_5 + 2f_6 + 3f_7 + 4f_8) \\ &\leq 4f_4 + 5(4) \end{aligned}$$

Thus, $f_4 \geq \frac{28-20}{4} = 2$. However $f_4 \leq 2$, Theorem 4.7.11. Thus, $f_4 = 2$. □

5.7. IRREDUCIBLE (2,2)-TIGHT TORUS GRAPHS WITH EIGHT VERTICES

Lemma 5.7.3. *Let G be an irreducible (2,2)-tight \mathbb{T} -graph with eight vertices. Then the faces of G , other than the two quadrilateral faces, are pentagons and there are exactly four of them.*

Proof. By a similar argument to the one of the proof of Lemma 5.7.2, $28 = 4f_4 + 5f_5 + 6f_6 + 7f_7 + 8f_8$. But $f_4 = 2$, thus $f_5 = 4$. \square

Now we prove Theorem 5.7.1.

Proof. Let G be an irreducible (2,2)-tight \mathbb{T} -graph with 8 vertices. By Lemma 5.7.2, G has two quadrilateral faces, say Q and R . Now, by Lemma 4.7.10, for $i = 1, 3$, L_i is either a single vertex or a nonseparating cycle of length two. So we have three cases here.

Case 1: Each of L_1 and L_3 is a single vertex, see Figure 5.48(a). So we consider the polygon representation, see Figure 5.48(b), of the \mathbb{T} -graph in 5.48(a). There are three nonisomorphic irreducible (2,2)-tight \mathbb{T} -graphs shown in Figure 5.49 and Figure 5.50 which can be derived from the \mathbb{T} -graph that is depicted in Figure 5.48(a).

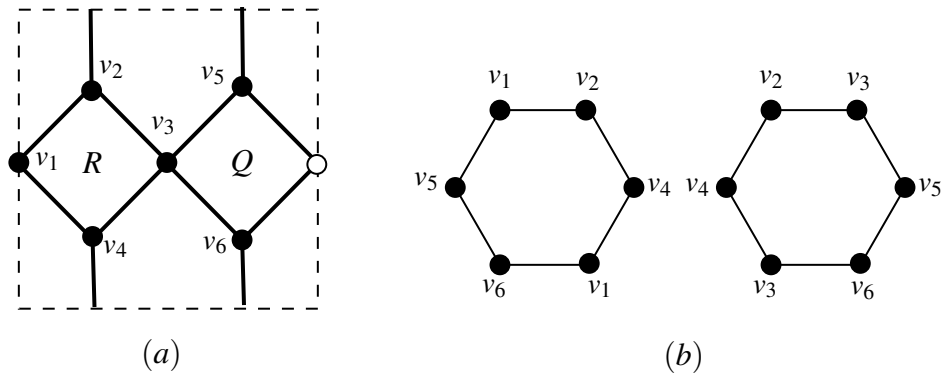


Figure 5.48: An irreducible (2,2)-tight torus graph with two quadrilateral faces such that both of L_1 and L_3 are vertices.

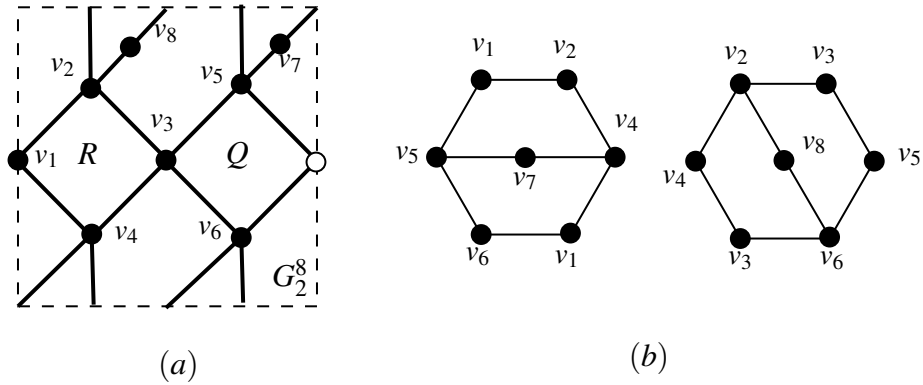


Figure 5.49: An irreducible (2,2)-tight \mathbb{T} -graph that is derived from the irreducible \mathbb{T} -graph in Figure 5.48(a).

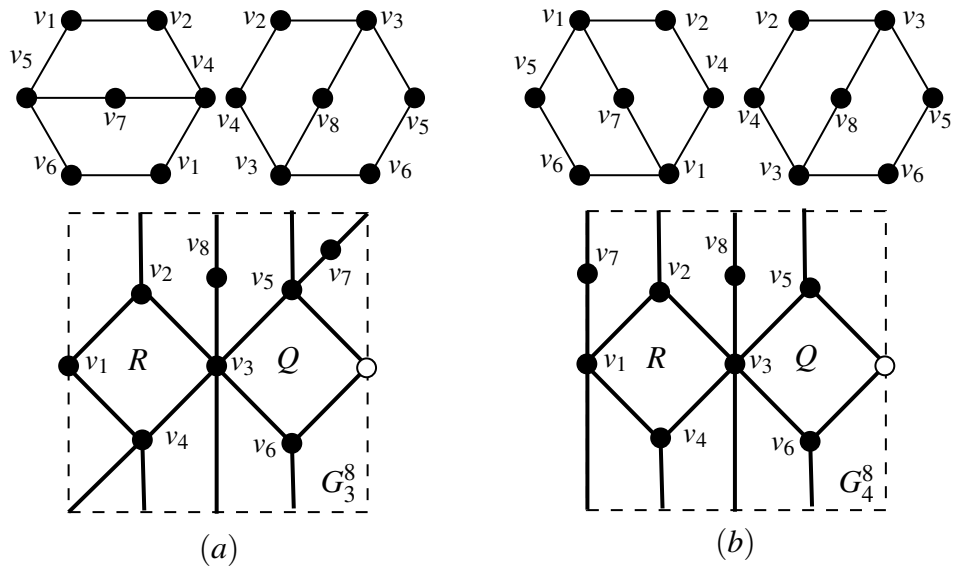


Figure 5.50: The two irreducible (2,2)-tight \mathbb{T} -graph in (a) and (b) are derived from the irreducible \mathbb{T} -graph in Figure 5.48(a).

Case 2: L_1 is a single vertex and L_3 is a nonseparating cycle of length two. Therefore, we have the embedding which is depicted in Figure 5.51(a). It follows from the polygon representation in Figure 5.51(b) that there are two nonisomorphic irreducible (2,2)-tight \mathbb{T} -graphs, see Figure 5.52(a) and (b), such that the \mathbb{T} -graph in Figure 5.51(a) is a \mathbb{T} -subgraph of each of them.

5.7. IRREDUCIBLE (2,2)-TIGHT TORUS GRAPHS WITH EIGHT VERTICES

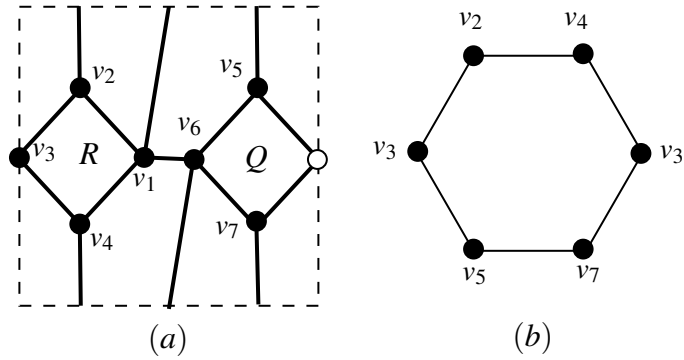


Figure 5.51: A \mathbb{T} -graph with two quadrilaterals such that L_1 is a vertex and L_3 is a non-separating cycle of length two. Notice that this is an irreducible (2,2)-tight \mathbb{T} -graph with 7 vertices.

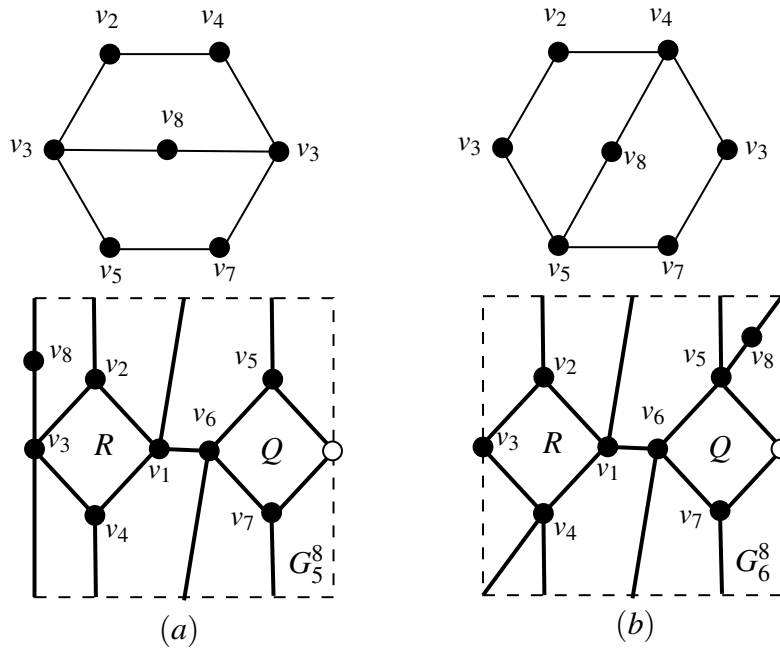


Figure 5.52: The two irreducible (2,2)-tight \mathbb{T} -graph in (a) and (b) are derived from the irreducible \mathbb{T} -graph in Figure 5.51(a).

Case 3: Each of L_1 and L_2 is a nonseparating cycle of length two. So we have the embedding which is depicted in Figure 5.53.

□

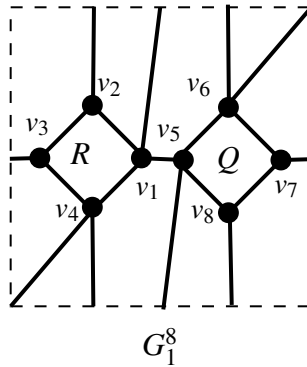


Figure 5.53: L_1 and L_3 are nonseparating cycles of length two.

We present the notations for all irreducible (2,2)-tight \mathbb{T} -graphs with eight vertices in Figure 5.54. In Appendix E (E.15), we present the irreducible (2,2)-tight \mathbb{T} -graphs with eight vertices in one group.

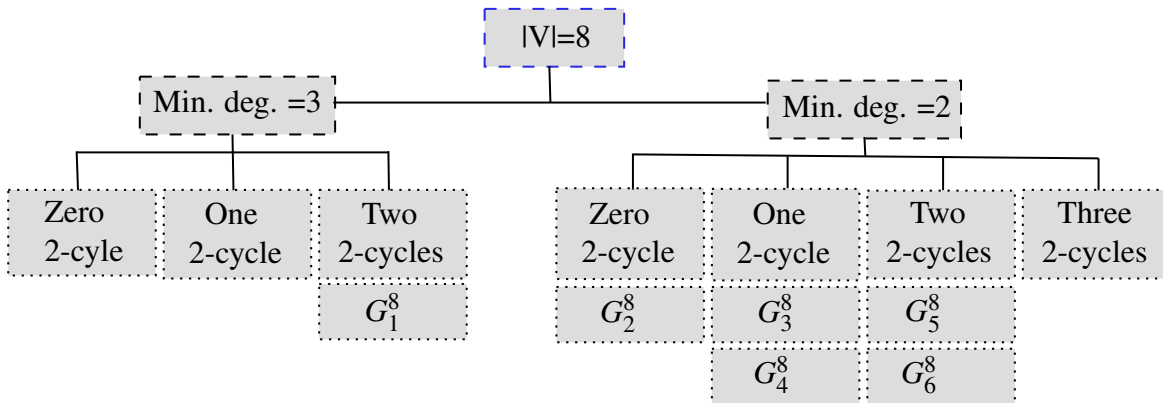


Figure 5.54: All nonisomorphic irreducible (2,2)-tight \mathbb{T} -graphs with eight vertices.

5.7. IRREDUCIBLE (2,2)-TIGHT TORUS GRAPHS WITH EIGHT VERTICES

We end this chapter by summarising the counting of the irreducible (2,2)-tight \mathbb{T} -graphs according to their order in Table 5.4.

| n | No. of irreducible (2,2)-tight \mathbb{T} -graphs | Section |
|---|---|---------|
| 1 | 1 | 5.3 |
| 2 | 1 | 5.3 |
| 3 | 2 | 5.3 |
| 4 | 9 | 5.4 |
| 5 | 23 | 5.5 |
| 6 | 47 | 5.6 |
| 7 | 27 | 5.6 |
| 8 | 6 | 5.7 |

Table 5.4: Irreducible (2,2)-tight \mathbb{T} -graphs with n vertices.

Now we present the following theorem.

Theorem 5.7.4. *Every (2,2)-tight torus graph can be constructed from one of the 116 irreducible (2,2)-tight torus graphs by a sequence of digon, triangle or quadrilateral splitting move.*

Chapter 6

Contacts of Circular Arcs Representation

One of the fundamental topics in geometric graph theory is the topic of geometric representations of graphs. In general, the topic of geometric representations of graphs investigates whether a given graph admits a certain kind of geometric representation. The algorithmic aspects of geometric representations are also considered in the topic of geometric representations.

Geometric representations of graphs are indeed related to the theory of intersection graphs. Specifically, geometric representations of graphs are related to those intersection graphs that arise from various collections of geometric contexts. For example, if a graph Γ is the intersection graph of a collection of curves, then Γ admits a curve intersections representation. In Section 6.1, we briefly survey the theory of intersection graphs. Special types of intersection graphs are contact graphs. In Section 6.2, we review some fundamental concepts of contact graphs.

The main goal of this chapter is to investigate the recognition problem for contact graphs. Specifically, this chapter is designed to find necessary and/or sufficient conditions for a surface graph to be the contact graph of a collection of curves. The main result of this chapter is the following theorem.

Theorem 6.0.1. *Every $(2,2)$ -tight torus graph is the contact graph of a collection of circular arcs in the flat torus.*

6.1 Intersection graphs

Intersection graph theory is a major topic in the discipline of graph theory. The studies of intersection graphs extensively focus on the geometric intersection graphs. The geometric intersection graphs are intersection graphs of geometric contexts such as curves, lines, discs defined in the plane. Several classes of geometric intersection graphs have been applied in many fields such as biology, statistics, psychology and computing [65]. More background of the intersection graph theory can be found in [39] and [77]. In this section, we briefly survey some fundamental concepts and results of the theory of intersection graphs.

6.1.1 Definition of intersection graphs

In the following we review the general definition of the intersection graph.

Definition 6.1.1. [51] Let \mathcal{F} be a family of sets. The intersection graph of \mathcal{F} is defined as a simple graph $\Gamma_{\mathcal{F}} = (V, E, s, t)$ such that its vertex set is \mathcal{F} and its edge set is the intersections between sets of \mathcal{F} which can be defined as follows. Given $S_i, S_j \in \mathcal{F}$, if $i \neq j$ and $S_i \cap S_j \neq \emptyset$, then define an edge e such that $s(e) = S_i$ and $t(e) = S_j$.

Definition 6.1.2. [51] A graph Γ is an intersection graph if there exists a family \mathcal{F} such that $\Gamma \cong \Gamma_{\mathcal{F}}$.

Example 6.1.3. Consider the family set $\mathcal{F} = \{S_1, S_2, S_3, S_4, S_5\}$ where $S_1 = \{1\}$, $S_2 = \{1, 2, 3\}$, $S_3 = \{3, 4\}$, $S_4 = \{1, 2, 3, 4, 5\}$ and $S_5 = \{5\}$. Then the intersection graph $\Gamma_{\mathcal{F}}$ is illustrated in Figure 6.1.

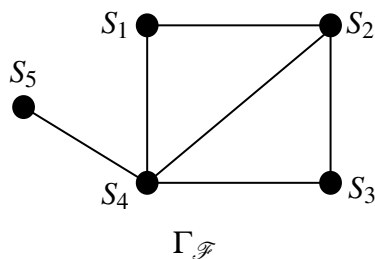


Figure 6.1: The intersection graph of the set family \mathcal{F} .

6.1. INTERSECTION GRAPHS

One of the important results of the intersection graph theory presented by Marczewski in 1945 is the following.

Theorem 6.1.4. [87] *Every graph is an intersection graph.*

6.1.2 Intersection graphs of some geometric contexts

Many kinds of geometric contexts have been used in the topic of geometric intersection graphs. For example, curves, polylines, triangles and so on. The intersection graph of a collection of specific geometric contexts admits that geometric contexts representation. For example, if a graph Γ is the intersection graph of a collection of curves, then Γ admits a curve intersections representation.

The surface where the geometric contexts live plays a role in the theory of intersection graphs. Most of the known results of geometric intersection graphs considered the flat plane. One of the main results of that vein is given in [26]: every planar graph is an intersection graph of curves in the plane, Figure 6.2.

Intersection graphs of line segments in the plane is another type of geometric intersection graphs. In [81], the author conjectured that all planar graphs can be represented as a collection of intersections of line segments in the plane. This conjecture was proven in [14], see Figure 6.2.

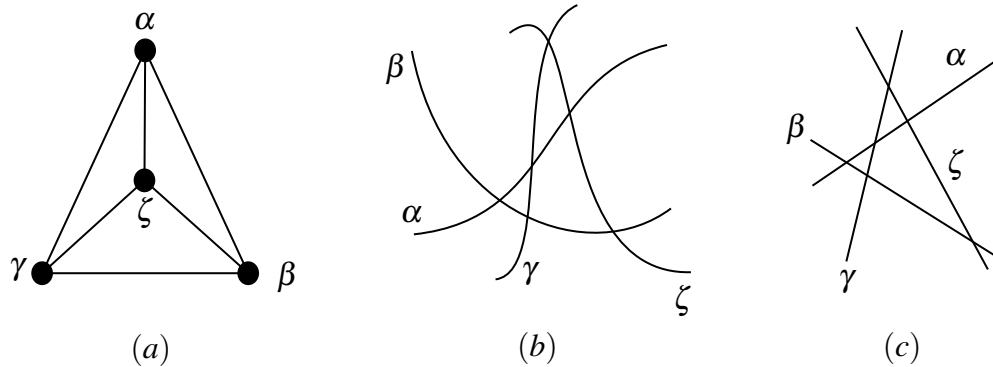


Figure 6.2: The graph in (a) is the intersection graph of the collection of curves respectively line segments in (b) respectively (c).

6.2 Contact graphs

Contact graphs of geometric contexts are special graphs of intersection graphs of geometric contexts. However, the geometric contexts under consideration are not allowed to cross but only to touch each other. In this section, we review some results of this topic.

6.2.1 Circle packing theorem

The foundational result in the area of contact graphs is the well known Koebe-Andreev-Thurston circle packing theorem which was proved independently by Koebe in [57], Andreev [5], [4] and Thurston in [91]. This theorem about representing planar graphs as contact graphs of circles in the plane, see Figure 6.3. In the following we restate the circle packing theorem.

Theorem 6.2.1. *Every planar simple graph can be realised as the contact graph of some arrangement of circles with nonoverlapping interiors in the Euclidean plane.*

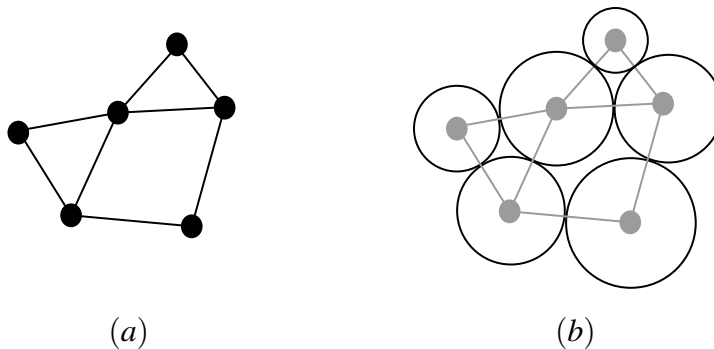


Figure 6.3: An example of a simple plane graph and its corresponding circle packing representation.

6.2.2 Some types of contact representations

After Theorem 6.2.1 was established, many researchers introduced and investigated various types of geometric representations in the plane. We only state a few of such representations. A triangle contact graph is one example of such contact graphs where the geometric contexts are triangles. De Fraysseix *et al.* [22] showed that any planar graph

6.3. CONTACT GRAPHS OF CURVES

can be represented as a triangle contact graph. Specifically, every planar graph has a contact representation which is realised by touching isosceles triangles with horizontal bases, Figure 6.4.

Every bipartite planar graph has a so-called grid intersection representation [47], [21], which is a contact representation of segments such that the partitions are represented by horizontal and vertical segments, respectively.

In the next section, we study the contacts of curves representation.

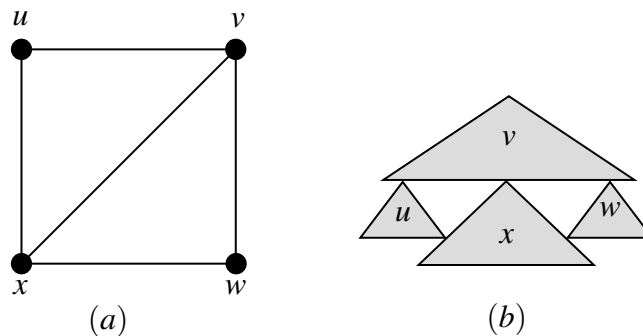


Figure 6.4: (a) A plane (2,3)-tight graph. (b) The contacts of triangles representation of the graph in (a).

6.3 Contact graphs of curves

This section is devoted to study in more details contact graphs of curves.

6.3.1 Contacts of curves in surfaces

In the following we carefully restate and introduce concepts which are concerned with curves on surfaces. We also define the contact graph of curves in a surface.

Definition 6.3.1. A curve $\alpha : [0, 1] \rightarrow \Sigma$ is a continuous map from the closed interval $[0, 1]$ into the surface Σ . $\alpha(0)$ and $\alpha(1)$ are called the endpoints of the curve α . For $x \in (0, 1)$, $\alpha(x)$ is called an interior point of α . The set of all interior points of α is called the relative interior of α .

Definition 6.3.2. Two curves $\alpha, \beta : [0, 1] \rightarrow \Sigma$ have disjoint relative interiors if there are no $x, y \in (0, 1)$ such that $\alpha(x) = \beta(y)$. α and β are in contact if at least one endpoint of

one of the curves lies in the relative interior of the other curve. An endpoint of one curve which lies in the relative interior of the other curve is called a touching point.

Figure 6.5 depicts two cases of disjoint relative interiors of two curves.

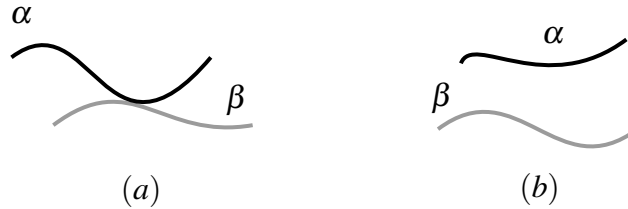


Figure 6.5: The curves α and β in (a) and (b) have disjoint relative interior.

Definition 6.3.3. Two curves $\alpha, \beta : [0, 1] \rightarrow \Sigma$ are nonoverlapping to each other if there are no $x, y \in (0, 1)$ such that $\alpha(x) = \beta(y)$.

Definition 6.3.4. A curve α is called non-self overlapping if there are no $x, y \in (0, 1)$ with $x \neq y$ such that $\alpha(x) = \alpha(y)$.

Remark 6.3.5. A non-self overlapping curve α is still non-self overlapping even if it satisfies:

- $\alpha(x) = \alpha(y)$ where $x \in \{0, 1\}$ and $y \in (0, 1)$.
- $\alpha(0) = \alpha(1)$.

Figure 6.6 includes two examples. One example depicts two curves that have a common endpoint and the other example presents two curves which they have a normal touching point.

Definition 6.3.6. A collection of curves is nonoverlapping if they are pairwise nonoverlapping and each curve is non-self overlapping and no single curve whose endpoints are coincided.

Definition 6.3.7. If α and β are nonoverlapping with $\alpha(0) = \beta(x)$ for some $x \in (0, 1)$, then we say that α touches β . Similarly, if $\alpha(1) = \beta(x)$, then we say that α touches β .

Figure 6.7 presents various cases of overlapping, self-overlapping, nonoverlapping curves.

6.3. CONTACT GRAPHS OF CURVES

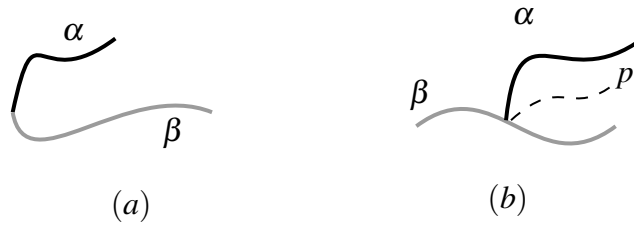


Figure 6.6: (a) The curves α and β have a common endpoint. (b) The curve α touches the curve β at the point p .

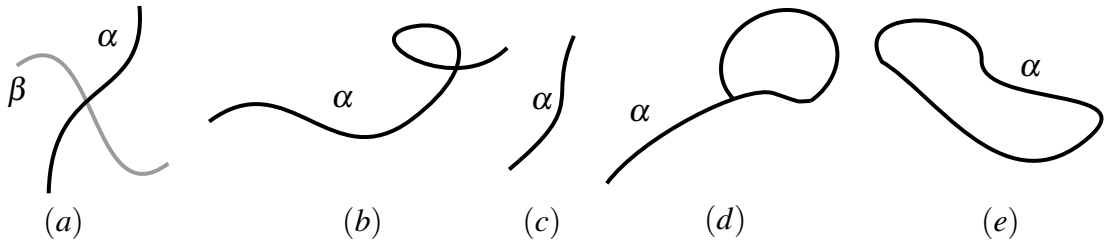


Figure 6.7: (a) The curves α and β are overlapping to each other. (b) The curve α is self-overlapping. The curve α in (c), (d) and (e) is non-self overlapping.

Definition 6.3.8. A collection of curves \mathcal{C} is called *nondegenerate* if no pair of curves have a common endpoint and no curve with endpoints coincide.

In case that there is degeneracy in a collection of curves, then it is possible to transform it into nondegeneracy by an arbitrary small perturbation for each pair that have degenerate contact, see Figure 6.8.



Figure 6.8: (a) The pair of curves α and β have a common endpoint. (b) The curve α is perturbed at the common endpoint with β .

The contacts of a geometric representation induces an orientation for the corresponding contact graph. In the following we recall the definition of orientation of a graph.

Definition 6.3.9. Consider the graph $\Gamma = (V, E, s, t)$. The number of targets associated to a vertex $v \in V$ is called the in-degree of v while the number of sources associated to v is called the out-degree of v . Γ is a 2-orientation if every vertex has an out-degree equal to 2. If every vertex has an out-degree at most 2, then Γ is a 2^- -orientation.

See Figure 6.9 which provides two examples of oriented graphs.

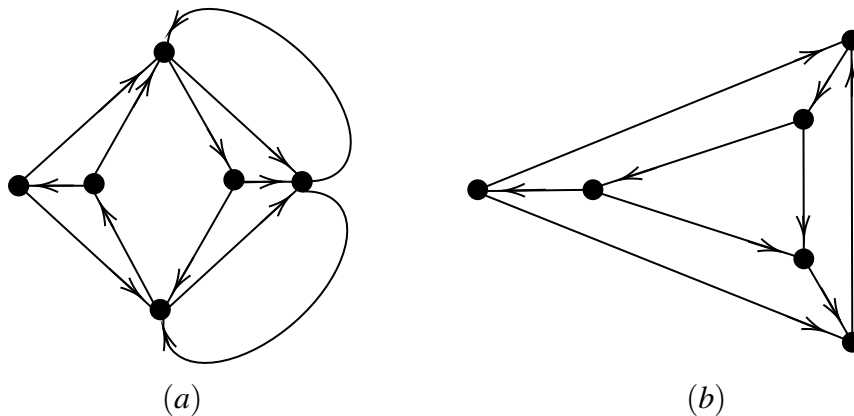


Figure 6.9: (a) A 2-orientation of the given graph. (b) A 2^- -orientation of the given graph.

Now we define the contact graph of a collection of curves in a surface.

Definition 6.3.10. Let \mathcal{C} be a collection of nonoverlapping curves in a surface Σ . The corresponding contact graph, denoted by $\Gamma_{\mathcal{C}}$, is the multigraph (V, E, s, t) such that its vertex set is \mathcal{C} and its edge set is the contacts between curves which can be defined as follows. Given a contact between $\alpha, \beta \in \mathcal{C}$ with $\alpha(0) = \beta(r)$, where $r \in (0, 1)$, define an edge e such that $s(e) = \alpha$ and $t(e) = \beta$ (this is also applied in the case $\alpha(1) = \beta(r)$).

6.3.2 Embedding a contact graph of curves in a surface

It is worthwhile to mention that almost all the studies of geometric representations used the plane to define the corresponding intersection graphs. However, in our case we are interested in finding whether a surface graph is a contact graph of curves. Thus, we need to define the embedding of contact graph in a surface. In the following we give a detailed definition of the embedding of contact graph $\Gamma_{\mathcal{C}}$ in a surface.

Definition 6.3.11. (The embedding of $\Gamma_{\mathcal{C}}$)

6.3. CONTACT GRAPHS OF CURVES

Let \mathcal{C} be a collection of nonoverlapping curves. For each $\alpha \in \mathcal{C}$ we choose a closed subinterval $J_\alpha \subset [0, 1]$ satisfying.

- $\alpha(J_\alpha)$ contains all points in the relative interior of α that are endpoints of some $\beta \in \mathcal{C}$.
- J_α contains 0 (respectively 1) if and only if $\alpha(0)$ (respectively $\alpha(1)$) is not in the relative interior of β for any $\beta \in \mathcal{C}$.

Consider the geometric realisation of $\Gamma_{\mathcal{C}}$, see Definition 2.2.7. Fix $\alpha \in \mathcal{C}$. Let $q : \Sigma \rightarrow \Sigma/\alpha(J_\alpha)$ be the quotient mapping. As a consequence of the Jordan-Schoenflies theorem ([13]), there is a homeomorphism $h : \Sigma/\alpha(J_\alpha) \rightarrow \Sigma$ such that $h \circ q$ and $q \circ h$ are homotopic to the identity mappings of Σ respectively $\Sigma/\alpha(J_\alpha)$.

Now, the subsets $\alpha(J_\alpha), \alpha \in \mathcal{C}$ are pairwise disjoint Jordan arcs in Σ . Let X be the space obtained by collapsing each $\alpha(J_\alpha)$ to a point p_α . Observe that for each pair of curves α, β such that α touches β , the restriction of α defines a path in X from p_α to p_β . Therefore, we have an embedding $|\Gamma_{\mathcal{C}}| \rightarrow X$. By applying the observations of the previous paragraph we see that there is a canonical (up to homotopy) homeomorphism $g : X \rightarrow \Sigma$. We identify Σ and X by means of this homeomorphism and thus we have constructed an embedding $g : |\Gamma_{\mathcal{C}}| \rightarrow \Sigma$. We denote the embedding of the contact graph $\Gamma_{\mathcal{C}}$ by $G_{\mathcal{C}} = (\Gamma_{\mathcal{C}}, g)$, Figure 6.10.

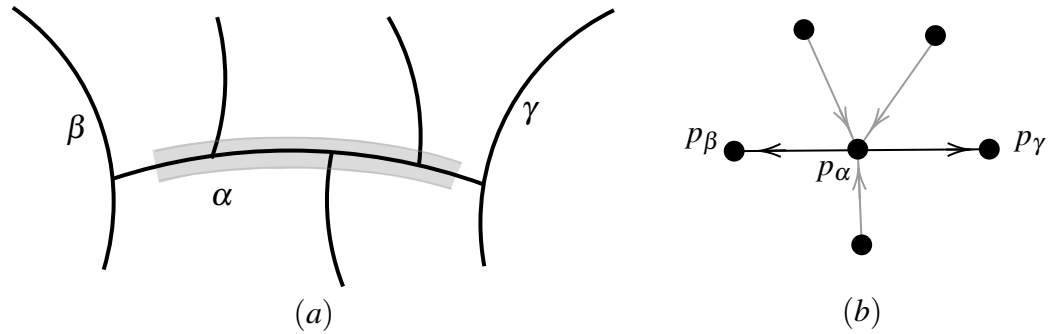


Figure 6.10: The construction of the contact graph associated with a collection of curves. In (a), we have a collection of curves. The shaded section of α represents $\alpha(J_\alpha)$. (b) The contact graph that is corresponding to the collection of curves in (a).

Definition 6.3.12. A curve contact representation of a Σ -graph, G , is a collection of curves \mathcal{C} in Σ such that $G \cong G_{\mathcal{C}}$.

Notice that the contacts of curves \mathcal{C} give rise to an orientation of the graph edges of the contact graph $\Gamma_{\mathcal{C}}$. Figure 6.11 presents a collection of curves and its contact graph and also the embedding of the contact graph. Figure 6.12 also presents an example of a contact representation of curves and the embedding of the corresponding contact graph to such representation.

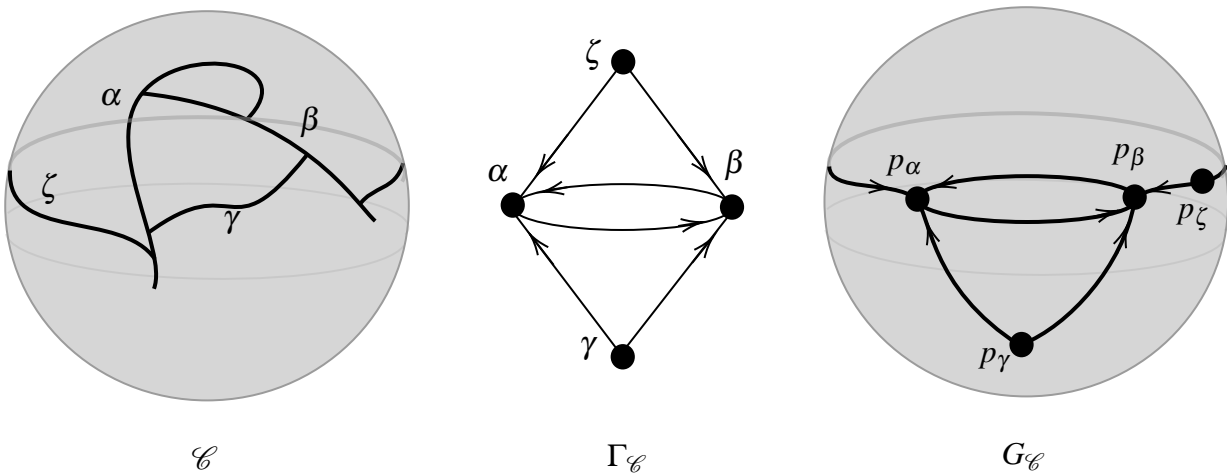


Figure 6.11: A collection of curves, \mathcal{C} , in the sphere. The corresponding contact graph, $\Gamma_{\mathcal{C}}$, of the collection of curves $\Gamma_{\mathcal{C}}$. $G_{\mathcal{C}}$ is the embedding of the contact graph $\Gamma_{\mathcal{C}}$.

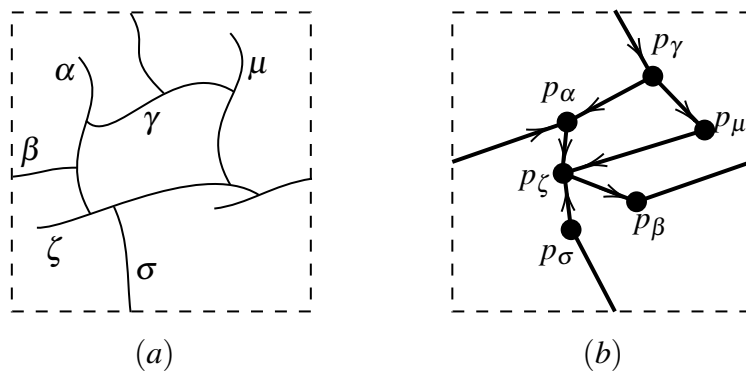


Figure 6.12: (a) A collection of curves, \mathcal{C} , on the flat torus. (b) The corresponding embedding of the contact graph of \mathcal{C} in the torus, i.e. $G_{\mathcal{C}}$.

6.3. CONTACT GRAPHS OF CURVES

Sparsity of graphs has been used in the investigation of geometric intersection graphs. For example, Thomassen in [90] showed that every plane $(2, 3)$ -sparse graph is the contact graph of a collection of line segments in the flat plane: see Figure 6.13.

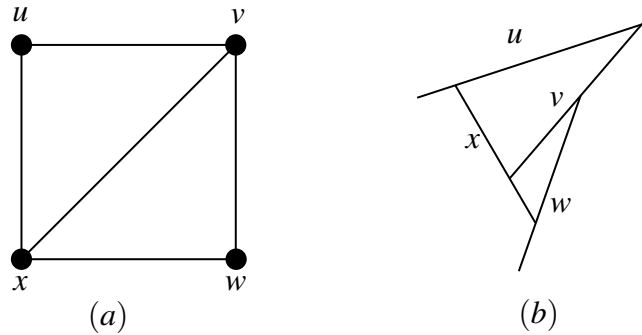


Figure 6.13: (a) A $(2, 3)$ -tight plane graph. (b) A contacts of line segments representation of the graph in (a).

In [51], Hliněný presented the following lemma.

Lemma 6.3.13. *A plane graph G admits a representation of contacts of curves if and only if G is $(2, 0)$ -sparse.*

Lemma 6.3.13 can be generalised to other surfaces as in the following lemma. See also Figure 6.15.

Lemma 6.3.14. *Let G be a Σ -graph. Then $G \cong G_{\mathcal{C}}$ for some nondegenerate collection of nonoverlapping curves \mathcal{C} if and only if G is $(2, 0)$ -sparse.*

Notice that if G is $(2, 0)$ -sparse, then it is 2^- -orientation. Thus, each vertex of G has an out-degree equal at most 2, see Figure 6.14. Consequently, the proof of Lemma 6.3.14 follows easily.

Here we highlight the difference between Definition 6.1.2 and Definition 6.3.11. In the literature, the contact graph is typically defined as the intersection graph of a collection of curves. This definition is equivalent to Definition 6.1.2. Notice that such a definition works well in the plane. However, for non simply connected surfaces it is more natural to consider multidigraphs and to define the contact graph as in Definition 6.3.11.

Now suppose that Σ is equipped with a metric of constant curvature. In this context, we can distinguish many interesting subclasses of non-self overlapping curves. For example,

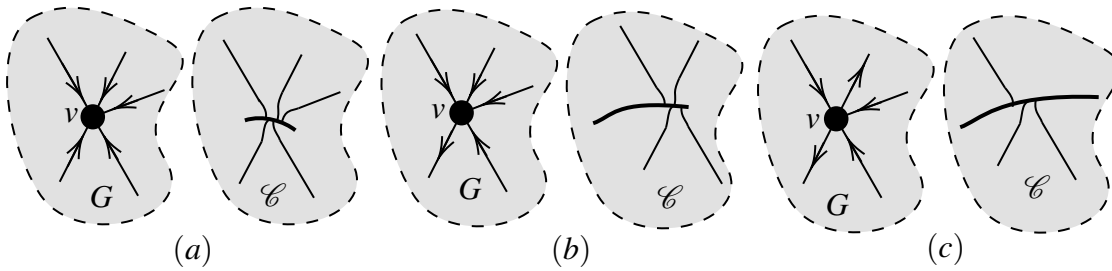


Figure 6.14: The out-degree of v in (a), (b) and (c) is 0, 1 and 2 respectively. The corresponding curve of v is bold. We perturb the curves that are corresponding to the edges for which their targets are v in (a), (b) and (c) respectively.

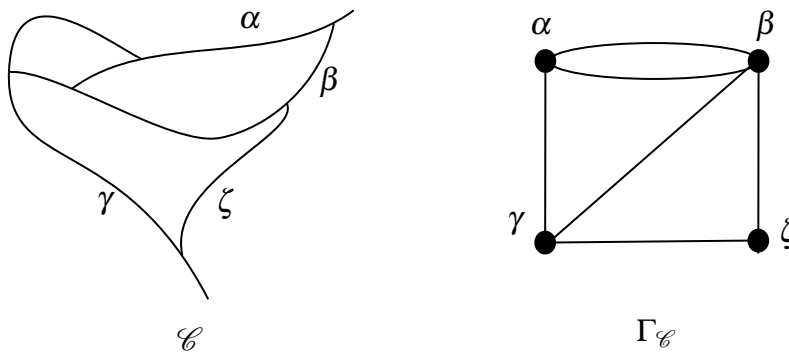


Figure 6.15: A family of curves in the plane, \mathcal{C} , and $\Gamma_{\mathcal{C}}$ the contact graph of \mathcal{C} . Notice that $\Gamma_{\mathcal{C}}$ is $(2,0)$ -sparse.

a circular arc is a curve of constant curvature and a line segment is a locally geodesic curve. For collections of such curves, the representability question can depend on the embedding of the graph and not on the graph itself (in contrast to Lemma 6.3.14), see the next example.

Example 6.3.15. Consider the graph in Figure 6.16(a). This graph cannot be represented as contacts of a collection of line segments in the flat plane. However, this graph can be embedded as a nonseparating cycle in the torus, Figure 6.16 (b). Then it is easy to construct a representation of the resulting surface graph as contacts of a collection of line segments in the flat torus, Figure 6.16(c).

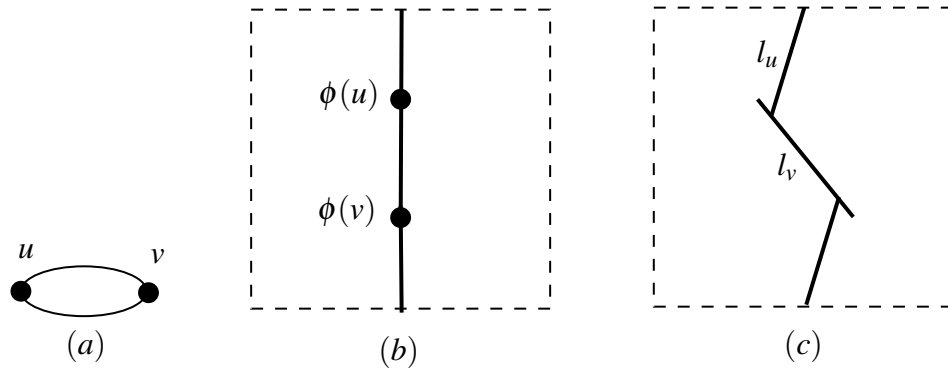


Figure 6.16: (a) A $(2,2)$ -tight graph with two vertices. (b) An embedding of the graph which is depicted in (a) in the torus. (c) A circular arc representation of the torus graph in (b).

6.4 Contacts of circular arcs representation

In this section, we investigate the contact of circular arcs representations for any surface graph. We show that digon, triangle and quadrilateral splitting moves are contacts of circular arcs representable in any surface. We also study representing $(2,2)$ -tight cylinder graphs as contacts of circular arcs in the flat cylinder. Moreover, in this section we briefly survey some results on the contacts of circular arcs representations of $(2,2)$ -tight plane graphs. We use the acronym CCA for contacts of circular arcs.

Definition 6.4.1. *Let G be a Σ -graph and let \mathcal{C} be a nondegenerate nonoverlapping collection of circular arcs \mathcal{C} such that $G \cong G_{\mathcal{C}}$. We say that \mathcal{C} is a contacts of circular arcs representation (CCA representation) of G .*

6.4.1 CCA representations of digon, triangle and quadrilateral splitting moves

As a part of the proof of Theorem 6.0.1, we need to show that certain topological moves have CCA representations in certain flat surfaces. Throughout this thesis we deal with three topological contraction moves; digon, triangle and quadrilateral contraction moves. Thus, we need to show that the inverse moves of these three contractions are CCA representable. In Subsection 3.4.5 we described such moves as digon/triangle/quadrilateral splits.

We appeal to the work in [3] which shows that digon and triangle splitting moves are CCA representable in three flat surfaces, plane, flat cylinder and flat torus, see Figures 6.17 and 6.18. For the quadrilateral splitting move, we appeal to Figure 6.19 which shows that quadrilateral splitting move is CCA representable by considering three cases.

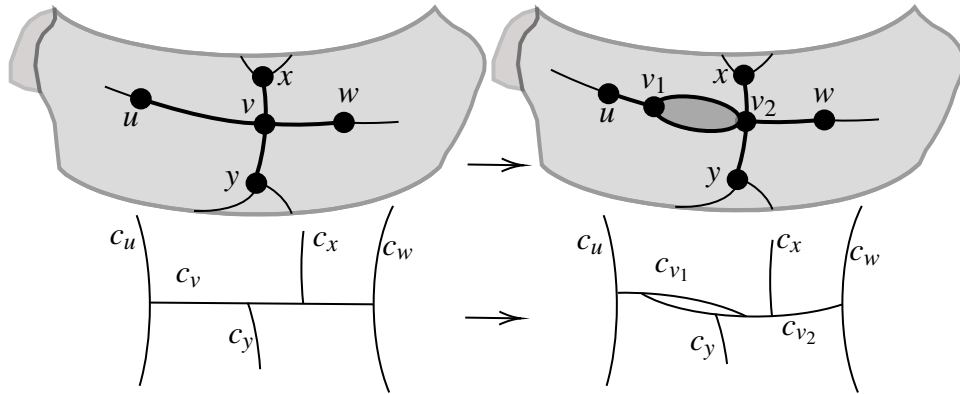


Figure 6.17: The first row of figures are snapshots of performing a digon splitting move on a surface graph. The second row of figures represents the CCA representations of the bold surface subgraphs of the surface graphs in the first row.

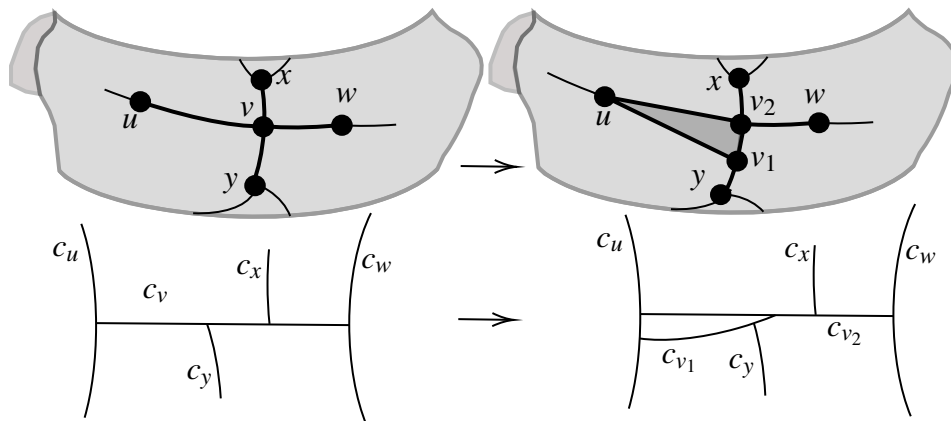


Figure 6.18: The first row of figures are snapshots of performing a triangle splitting move on a surface graph. The second row of figures represents the CCA representations of the bold surface subgraphs of the surface graphs in the first row.

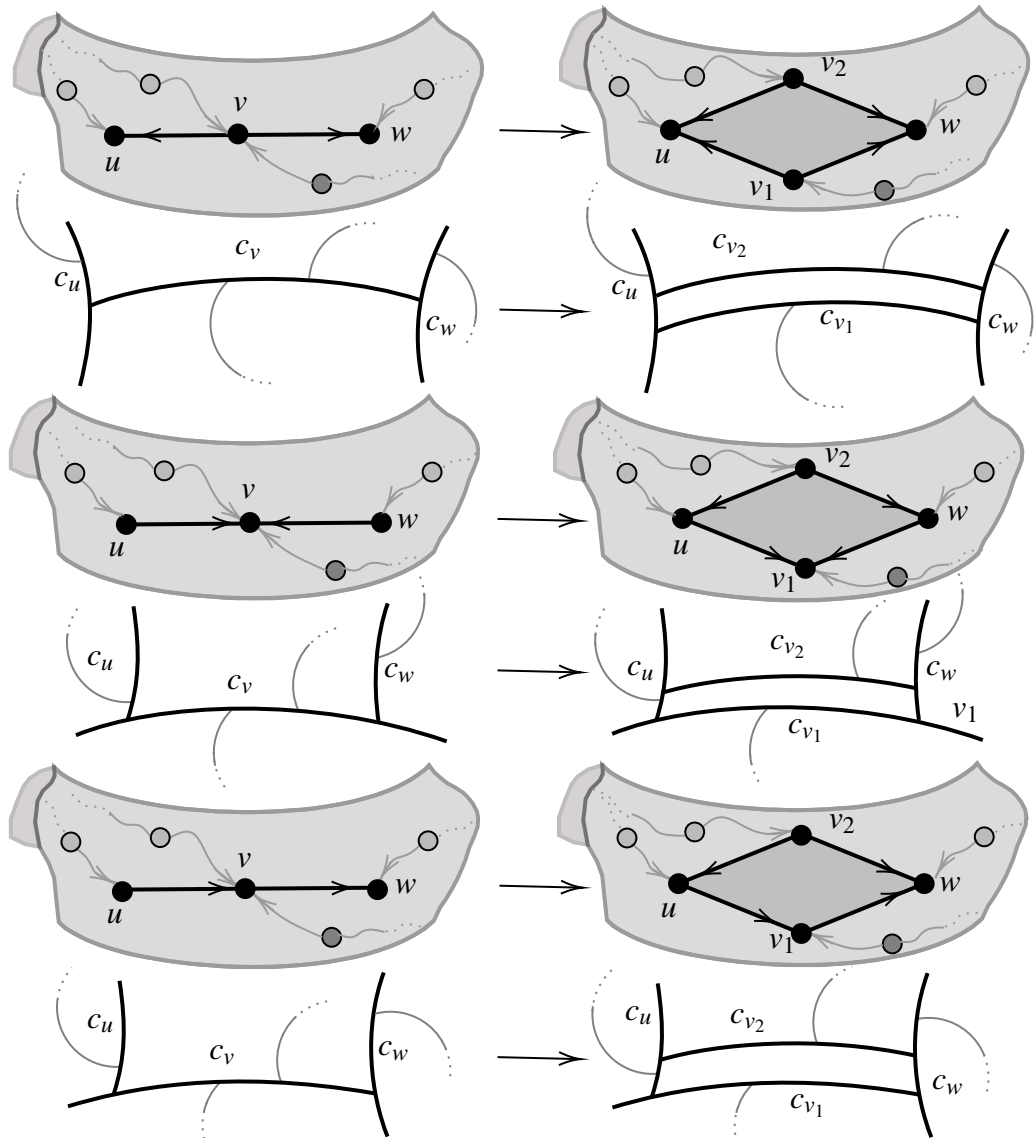


Figure 6.19: CCA representations of quadrilateral splitting move. We consider all cases of in-degree and out-degree of the vertex v .

Thus, we proved the following lemma.

Lemma 6.4.2. *The digon, triangle and quadrilateral splitting moves are CCA representable on the flat plane, cylinder and torus.*

6.4.2 CCA representation of $(2, 2)$ -tight cylindrical graphs

In the following we show that every $(2, 2)$ -tight cylinder graph admits a CCA representation in the flat cylinder. Consider the two irreducible $(2, 2)$ -tight cylinder graphs given in Figure 4.33. In Figure 6.20, we present CCA representations of these two irreducible $(2, 2)$ -tight cylinder graphs. Now, let us state and prove the following theorem.

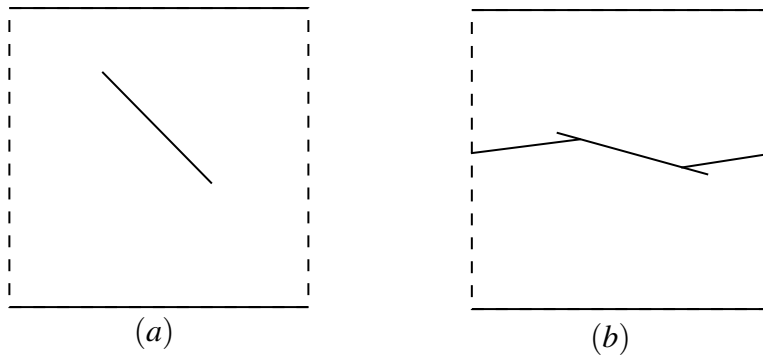


Figure 6.20: (a) respectively (b) is a CCA representation of the irreducible $(2, 2)$ -tight cylinder graph given in Figure 4.33(a) respectively Figure 4.33(b) in the flat cylinder-.

Theorem 6.4.3. *Every $(2, 2)$ -tight cylinder graph admits a CCA representation in the flat cylinder.*

Proof. By Lemma 6.4.2, digon, triangle and quadrilateral splitting moves are CCA representable in the flat cylinder. Also, the two irreducible $(2, 2)$ -tight cylinder graphs admit CCA representations in the flat cylinder. Thus, the result follows from Theorem 4.6.1. \square

In the following, we survey some results on representing some classes of plane graphs as contacts of circular arcs in the flat plane. Let us first consider the following definition.

Definition 6.4.4. *A plane circular arc is a simple curve $\alpha : [0, 1] \rightarrow \mathbb{R}^2$ such that there is some circle C for which $im(\alpha) \subset C$.*

Figure 6.21 presents contacts of circular arcs in the plane. Notice that a line segment can be considered as a circular arc by considering that $im(\alpha) \subset C$ where C is a circle with infinite diameter. In [3], CCA representations of $(2, 2)$ -tight plane graphs have been investigated. The authors presented the following theorem.

6.4. CONTACTS OF CIRCULAR ARCS REPRESENTATION

Theorem 6.4.5. *Every plane $(2,2)$ -sparse graph has a CCA representation in the flat plane.*

In Figure 6.22, we present two $(2,2)$ -tight plane graphs and their corresponding CCA representations.

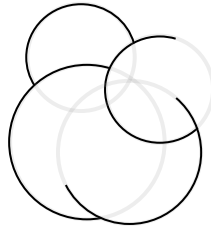


Figure 6.21: A collection of circular arcs in the plane.

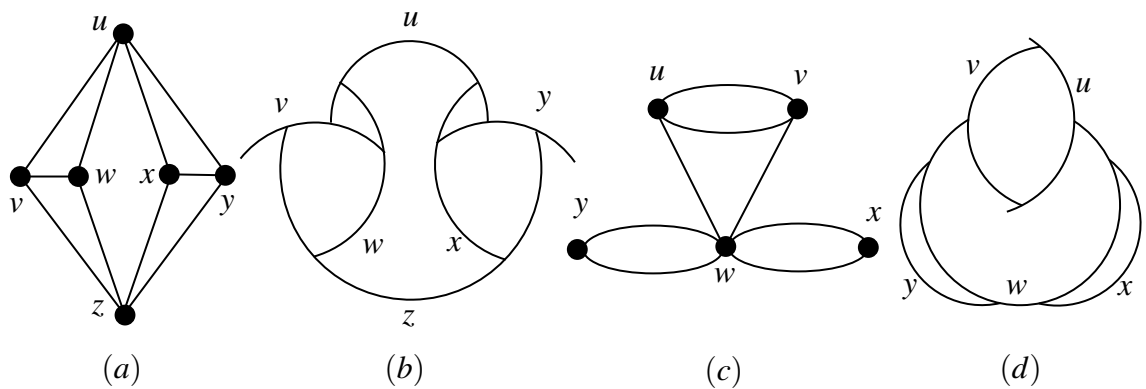


Figure 6.22: The $(2,2)$ -tight plane graph in (a) respectively (c) has a contacts of circular arcs representation in (b) respectively (d) in the flat plane.

Also, in [3], it has been shown that every plane graph with maximum degree four has a CCA representation in the plane.

6.5 CCA representations of $(2, 2)$ -tight torus graphs

In this section we prove that every $(2, 2)$ -tight \mathbb{T} -graph admits a CCA representation on the flat torus.

In Figure 6.23, we can see a circular arc in flat torus.

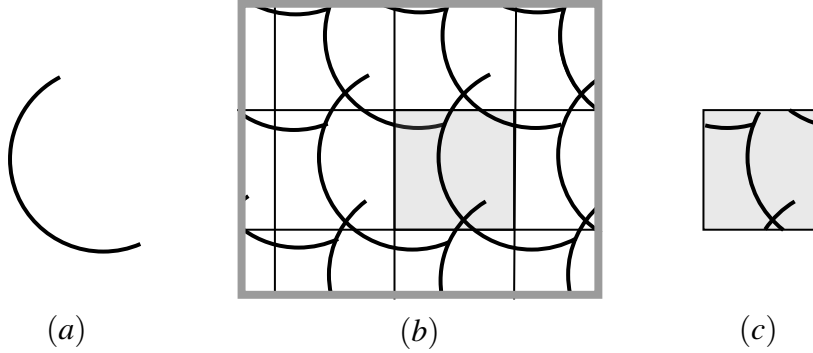


Figure 6.23: (a) A circular arc in the plane. (b) Lifting the circular arcs in (a) into the universal covering of the torus. (c) Fundamental domain of the torus.

6.5.1 Contacts of circular arcs representations of irreducible $(2, 2)$ -tight torus graphs

Here we show that each irreducible $(2, 2)$ -tight torus graph admits a CCA representation in the flat torus. We state and prove the following theorem.

Theorem 6.5.1. *Each irreducible $(2, 2)$ -tight \mathbb{T} -graph admits a CCA representation in the flat torus.*

Proof. By Theorem 5.0.1, there are 116 irreducible $(2, 2)$ -tight \mathbb{T} -graphs. Among these irreducible $(2, 2)$ -tight torus graphs, we found that there are exactly 12 of them are bases, see Subsection 5.1.3. The set B contains the notations of such base irreducible $(2, 2)$ -tight torus graphs.

$$B = \{G_1^1, G_1^4, G_2^4, G_1^5, G_2^5, G_1^6, G_2^6, G_3^6, G_4^6, G_5^6, G_1^7, G_1^8\}$$

In Figure 6.26, we present for each element in B a CCA representation in the flat torus. We observe that each of the 116 irreducible $(2, 2)$ -tight \mathbb{T} -graphs which are described in the previous chapter, can be constructed by a sequence of topological Henneberg type 0

6.5. CCA REPRESENTATIONS OF $(2, 2)$ -TIGHT TORUS GRAPHS

moves from some elements in B . Appendix D provides diagrams which describe the inclusion relationships between all the 116 irreducible $(2, 2)$ -tight torus graphs. Notice that such diagrams are not unique as some irreducible $(2, 2)$ -tight \mathbb{T} -graphs can be obtained from more than one irreducible $(2, 2)$ -tight graph by topological Henneberg type 0 moves. Also, we observe that at most five topological Henneberg type 0 moves are required to construct all the 116 irreducible $(2, 2)$ -tight \mathbb{T} -graphs from the set B .

It remains to show that the required topological Henneberg type 0 moves are CCA representable, Figure 6.24. For this, it is readily verified that given from the CCA representations in Figure 6.26, it is possible to represent all the necessary topological Henneberg type 0 moves that are required to construct CCA representations of the full set of the 116 irreducible $(2, 2)$ -tight torus graphs. \square

Notice that, in general, topological Henneberg type 0 moves can fail to be CCA representable given a fixed CCA representation of the initial surface graph, see Figure 6.25.

In Figure 6.26, we present for each element in B , (see also Appendix A), a CCA representation in the flat torus. In Appendix F, we present a comprehensive table which depicts the base irreducible $(2, 2)$ -tight torus graphs, their CCA representations and the equations that realise such representations in the flat torus.

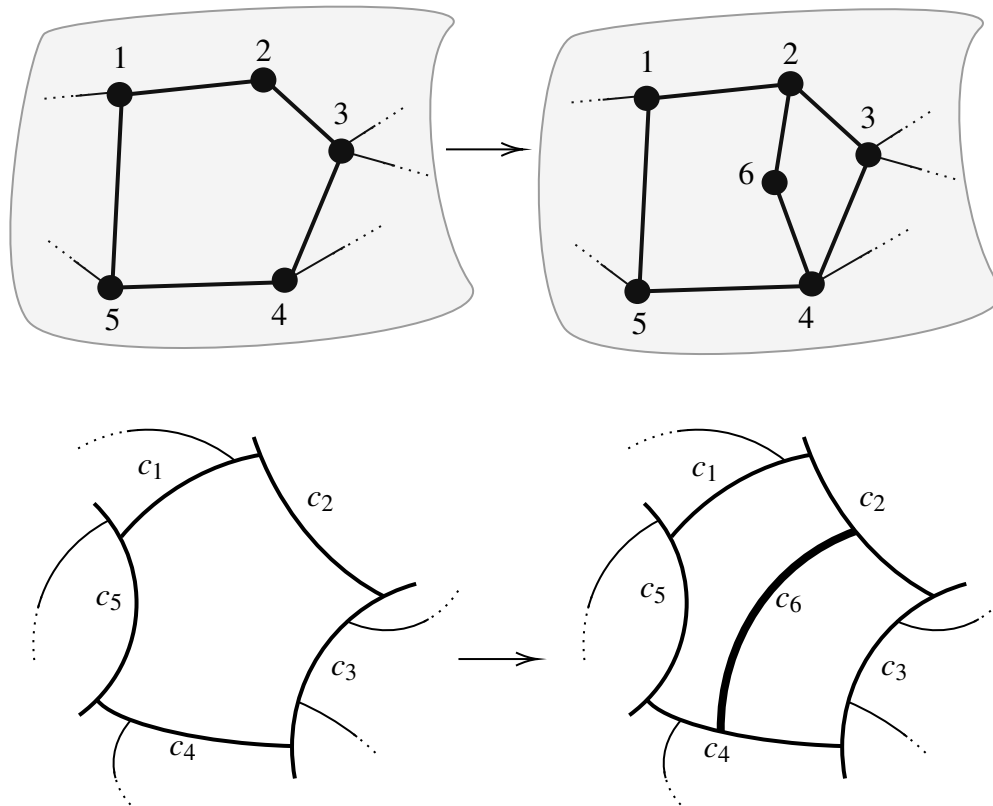


Figure 6.24: A CCA representation of a topological Henneberg type 0 move. The bold arc on the right represents the new vertex, that touches two of the initial arcs.

6.5.2 The outline of the main theorem

Now we present the outline of the proof of Theorem 6.0.1

Proof. The proof can be achieved in two steps:

Step 1: By Theorem 6.5.1, we showed that each of the 116 irreducible $(2,2)$ -tight torus graphs admits a CCA representation.

Step 2: By Lemma 6.4.2, if $G \rightarrow G'$ is a diagonal (respectively triangle or quadrilateral) splitting operation, then G' has a CCA representation.

Therefore, by Theorem 5.7.4 we get that every $(2,2)$ -tight torus graph admits a CCA representation in the flat torus.

□

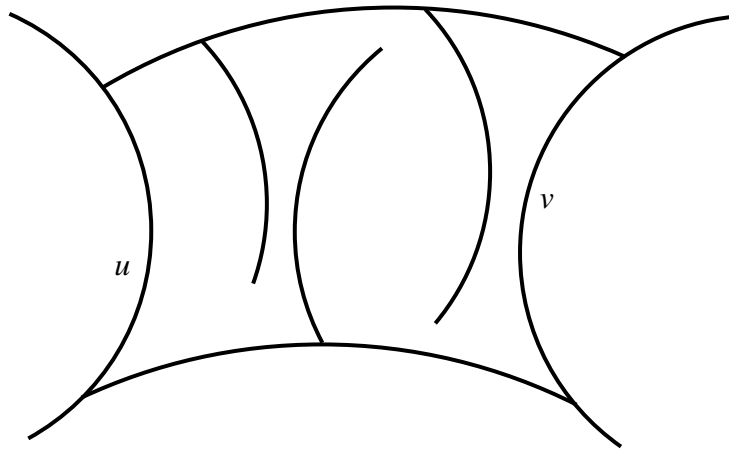


Figure 6.25: It is impossible to insert a circular arc that touches both u and v . This illustrates a topological Henneberg type 0 move that cannot be represented by contacts of circular arcs given this representation of the initial graph.

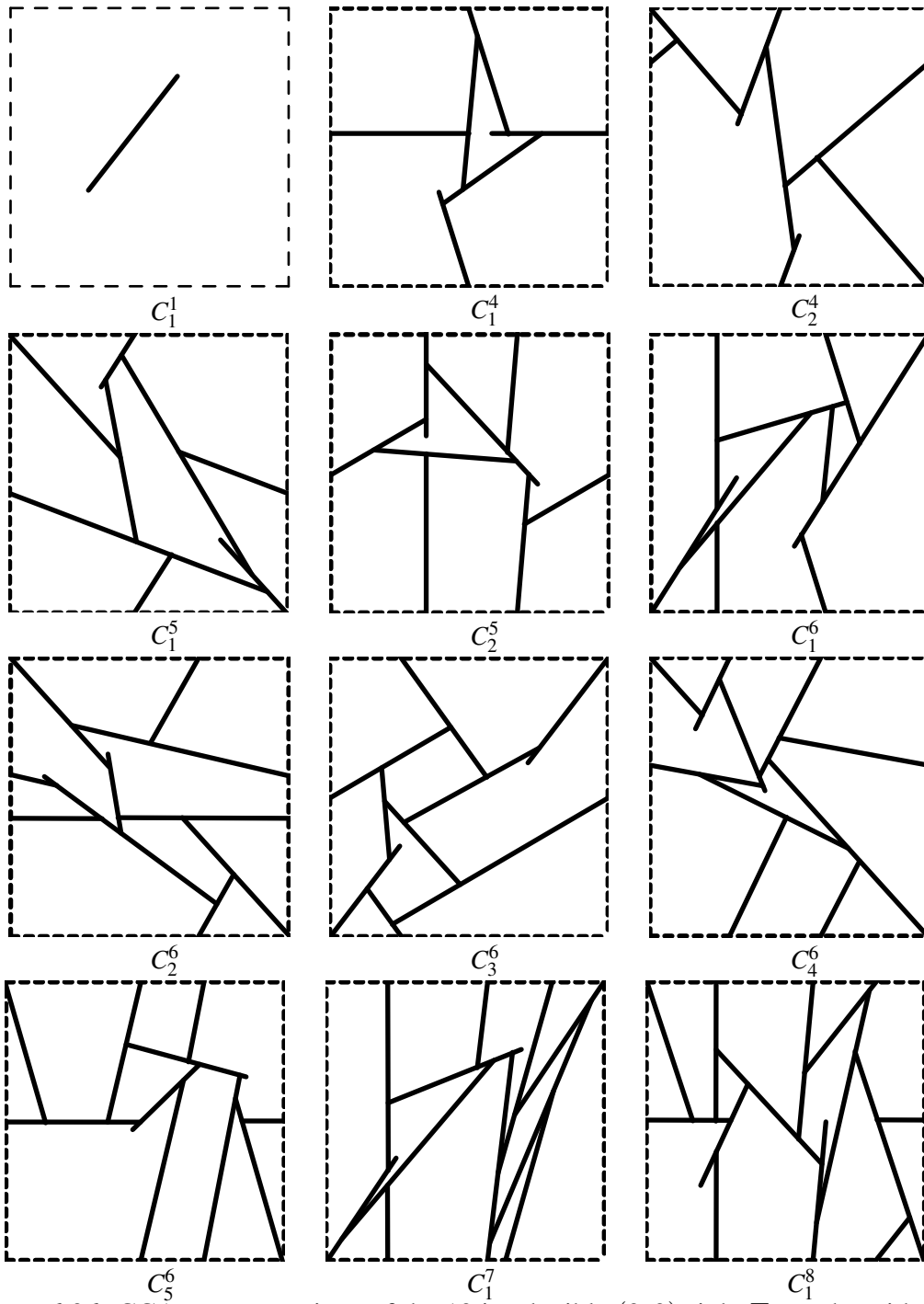


Figure 6.26: CCA representations of the 12 irreducible $(2, 2)$ -tight \mathbb{T} -graphs with no vertices of degree two: C_j^i is a CCA representation of G_j^i .

Bibliography

- [1] N. Aerts and S. Felsner. Vertex contact graphs of paths on a grid. In *Graph-theoretic concepts in computer science*, volume 8747 of *Lecture Notes in Comput. Sci.*, pages 56–68. Springer, Cham, 2014.
- [2] M. Aigner and G. M. Ziegler. *Proofs from The Book*. Springer, Berlin, sixth edition, 2018.
- [3] M. J. Alam, D. Eppstein, M. Kaufmann, S. G. Kobourov, S. Pupyrev, A. Schulz, and T. Ueckerdt. Contact graphs of circular arcs. In *Algorithms and data structures*, volume 9214 of *Lecture Notes in Comput. Sci.*, pages 1–13. Springer, Cham, 2015.
- [4] E. Andreev. On convex polyhedra of finite volume in lobachevskii space. 83. *Mat. Sb. (N.S.)*.
- [5] E. Andreev. Onconvex polyhedra in lobachevskii spaces. 81. *Mat. Sb. (N.S.)*.
- [6] D. Archdeacon. Topological graph theory: a survey. volume 115, pages 5–54. 1996. *Surveys in graph theory* (San Francisco, CA, 1995).
- [7] D. Barnette. Generating the triangulations of the projective plane. *J. Combin. Theory Ser. B*, 33(3):222–230, 1982.
- [8] D. W. Barnette and A. Edelson. All orientable 2-manifolds have finitely many minimal triangulations. *Israel J. Math.*, 62(1):90–98, 1988.
- [9] L. W. Beineke and R. J. Wilson, editors. *Topics in topological graph theory*, volume 128 of *Encyclopedia of Mathematics and its Applications*. Cambridge University Press, Cambridge, 2009.

BIBLIOGRAPHY

- [10] M. Berger. *A panoramic view of Riemannian geometry*. Springer-Verlag, Berlin, 2003.
- [11] J. A. Bondy and U. S. R. Murty. *Graph theory*, volume 244 of *Graduate Texts in Mathematics*. Springer, New York, 2008.
- [12] A. Boulch, E. Colin de Verdière, and A. Nakamoto. Irreducible triangulations of surfaces with boundary. *Graphs Combin.*, 29(6):1675–1688, 2013.
- [13] S. S. Cairns. An elementary proof of the Jordan-Schoenflies theorem. *Proc. Amer. Math. Soc.*, 2:860–867, 1951.
- [14] J. Chalopin and D. Gonçalves. Every planar graph is the intersection graph of segments in the plane. *Proceedings of the 41st Annual ACM Symposium on Theory of Computing*, 2009.
- [15] E. W. Chambers, E. Colin de Verdière, J. Erickson, F. Lazarus, and K. Whittlesey. Splitting (complicated) surfaces is hard. *Comput. Geom.*, 41(1-2):94–110, 2008.
- [16] R. Connelly, T. Jordán, and W. Whiteley. Generic global rigidity of body-bar frameworks. *J. Combin. Theory Ser. B*, 103(6):689–705, 2013.
- [17] J. Cruickshank, D. Kitson, and S. C. Power. The generic rigidity of triangulated spheres with blocks and holes. *J. Combin. Theory Ser. B*, 122:550–577, 2017.
- [18] J. Cruickshank, D. Kitson, and S. C. Power. The rigidity of a partially triangulated torus. 118:1277–1304, 2019.
- [19] J. Cruickshank, D. Kitson, S. C. Power, and Q. Shakir. Topological constructions for tight surface graphs. *arXiv:1909.06545*, 2019.
- [20] J. Cruickshank and Q. Shakir. Software for computing irreducible $(2, 2)$ -tight torus graphs. DOI 10.5281/zenodo.3379823, available at <https://doi.org/10.5281/zenodo.3379823>, 2019.
- [21] H. de Fraysseix, P. O. de Mendez, and J. Pach. Representation of planar graphs by segments. In *Intuitive geometry (Szeged, 1991)*, volume 63 of *Colloq. Math. Soc. János Bolyai*, pages 109–117. North-Holland, Amsterdam, 1994.

BIBLIOGRAPHY

- [22] H. de Fraysseix, P. Ossona de Mendez, and P. Rosenstiehl. On triangle contact graphs [MR1288442 (95j:05078)]. In *Combinatorics, geometry and probability (Cambridge, 1993)*, pages 165–178. Cambridge Univ. Press, Cambridge, 1997.
- [23] R. Diestel. *Graph theory*, volume 173 of *Graduate Texts in Mathematics*. Springer, Berlin, fifth edition, 2018.
- [24] F. J. E. Dillen and L. C. A. Verstraelen, editors. *Handbook of differential geometry. Vol. I*. North-Holland, Amsterdam, 2000.
- [25] J. Edmonds. combinatorial representation for polyhedral surfaces. *Notices Amer. Math. Soc.*, 7, 1960.
- [26] G. Ehrlich, S. Even, and R. E. Tarjan. Intersection graphs of curves in the plane. *J. Combinatorial Theory Ser. B*, 21(1):8–20, 1976.
- [27] B. Farb and D. Margalit. *A primer on mapping class groups*, volume 49 of *Princeton Mathematical Series*. Princeton University Press, Princeton, NJ, 2012.
- [28] Z. Fekete, T. Jordán, and W. Whiteley. An inductive construction for plane Laman graphs via vertex splitting. In *Algorithms—ESA 2004*, volume 3221 of *Lecture Notes in Comput. Sci.*, pages 299–310. Springer, Berlin, 2004.
- [29] Z. Fekete and L. Szegő. A note on $[k, l]$ -sparse graphs. In *Graph theory in Paris*, Trends Math., pages 169–177. Birkhäuser, Basel, 2007.
- [30] W. Finbow, E. Ross, and W. Whiteley. The rigidity of spherical frameworks: swapping blocks and holes. *SIAM J. Discrete Math.*, 26(1):280–304, 2012.
- [31] W. Finbow-Singh and W. Whiteley. Isostatic block and hole frameworks. *SIAM J. Discrete Math.*, 27(2):991–1020, 2013.
- [32] P. A. Firby and C. F. Gardiner. *Surface topology*. Ellis Horwood Series: Mathematics and its Applications. Ellis Horwood, New York; distributed by Prentice Hall, Inc., Englewood Cliffs, NJ, second edition, 1991.
- [33] A. Frank and L. Szegő. Constructive characterizations for packing and covering with trees. volume 131, pages 347–371. 2003. Submodularity.

BIBLIOGRAPHY

- [34] J. C. M. F.R.S. Xlv. on reciprocal figures and diagrams of forces. *The London, Edinburgh, and Dublin Philosophical Magazine and Journal of Science*, 27(182):250–261, 1864.
- [35] R. Gelca. *Theta functions and knots*. World Scientific Publishing Co. Pte. Ltd., Hackensack, NJ, 2014.
- [36] P. Giblin. *Graphs, surfaces and homology*. Cambridge University Press, Cambridge, third edition, 2010.
- [37] N. D. Gilbert and T. Porter. *Knots and surfaces*. Oxford Science Publications. The Clarendon Press, Oxford University Press, New York, 1994.
- [38] H. Gluck. Almost all simply connected closed surfaces are rigid. In *Geometric topology (Proc. Conf., Park City, Utah, 1974)*, pages 225–239. Lecture Notes in Math., Vol. 438, 1975.
- [39] M. C. Golumbic. *Algorithmic graph theory and perfect graphs*, volume 57 of *Annals of Discrete Mathematics*. Elsevier Science B.V., Amsterdam, second edition, 2004. With a foreword by Claude Berge.
- [40] J. E. Goodman, J. O’Rourke, and C. D. Tóth, editors. *Handbook of discrete and computational geometry*. Discrete Mathematics and its Applications (Boca Raton). CRC Press, Boca Raton, FL, 2018.
- [41] J. Graver, B. Servatius, and H. Servatius. *Combinatorial rigidity*, volume 2 of *Graduate Studies in Mathematics*. American Mathematical Society, Providence, RI, 1993.
- [42] J. E. Graver. *Counting on frameworks*, volume 25 of *The Dolciani Mathematical Expositions*. Mathematical Association of America, Washington, DC, 2001. Mathematics to aid the design of rigid structures.
- [43] J. L. Gross and T. W. Tucker. *Topological graph theory*. Dover Publications, Inc., Mineola, NY, 2001.

BIBLIOGRAPHY

- [44] B. Grünbaum. *Convex polytopes*, volume 221 of *Graduate Texts in Mathematics*. Springer-Verlag, New York, second edition, 2003. Prepared and with a preface by Volker Kaibel, Victor Klee and Günter M. Ziegler.
- [45] R. Haas, A. Lee, I. Streinu, and L. Theran. Characterizing sparse graphs by map decompositions. *J. Combin. Math. Combin. Comput.*, 62:3–11, 2007.
- [46] R. Haas, D. Orden, G. Rote, F. Santos, B. Servatius, H. Servatius, D. Souvaine, I. Streinu, and W. Whiteley. Planar minimally rigid graphs and pseudo-triangulations. *Comput. Geom.*, 31(1-2):31–61, 2005.
- [47] I. B.-A. Hartman, I. Newman, and R. Ziv. On grid intersection graphs. *Discrete Math.*, 87(1):41–52, 1991.
- [48] L. Heffter. Ueber das Problem der Nachbargebiete. *Math. Ann.*, 38(4):477–508, 1891.
- [49] L. Henneberg. Die graphische statik der starren systeme. *Leipzig*, 1911.
- [50] C. Heuberger, D. Krenn, and S. Kropf. Automata in SageMath—combinatorics meets theoretical computer science. *Discrete Math. Theor. Comput. Sci.*, 18(3):Paper No. 9, 21, 2016.
- [51] P. Hliněný. Classes and recognition of curve contact graphs. *J. Combin. Theory Ser. B*, 74(1):87–103, 1998.
- [52] R. Joan-Arinyo, M. Tarrés-Puertas, and S. Vila-Marta. Decomposition of geometric constraint graphs based on computing fundamental circuits. Correctness and complexity. *Comput.-Aided Des.*, 52:1–16, 2014.
- [53] G. A. Jones and D. Singerman. Theory of maps on orientable surfaces. *Proc. London Math. Soc. (3)*, 37(2):273–307, 1978.
- [54] T. Jordán. Combinatorial rigidity: graphs and matroids in the theory of rigid frameworks. In *Discrete geometric analysis*, volume 34 of *MSJ Mem.*, pages 33–112. Math. Soc. Japan, Tokyo, 2016.

BIBLIOGRAPHY

- [55] K.-i. Kawarabayashi, A. Nakamoto, and K. Ota. Subgraphs of graphs on surfaces with high representativity. *J. Combin. Theory Ser. B*, 89(2):207–229, 2003.
- [56] L. C. Kinsey. *Topology of surfaces*. Undergraduate Texts in Mathematics. Springer-Verlag, New York, 1993.
- [57] P. Koebe. Kontaktprobleme der konformen abbildung. pages 141–164, 1936. Ber. Verh. Saeachs. Akad.
- [58] C. Kosniowski. *A first course in algebraic topology*. Cambridge University Press, Cambridge-New York, 1980.
- [59] G. Laman. On graphs and rigidity of plane skeletal structures. *J. Engrg. Math.*, 4:331–340, 1970.
- [60] S. K. Lando and A. K. Zvonkin. *Graphs on surfaces and their applications*, volume 141 of *Encyclopaedia of Mathematical Sciences*. Springer-Verlag, Berlin, 2004. With an appendix by Don B. Zagier, Low-Dimensional Topology, II.
- [61] S. A. Lavrenchenko. Irreducible triangulations of a torus. *Ukrain. Geom. Sb.*, (30):52–62, ii, 1987.
- [62] A. Lee and I. Streinu. Pebble game algorithms and sparse graphs. *Discrete Math.*, 308(8):1425–1437, 2008.
- [63] Y. Liu. *Introductory Map Theory*. Multimedia Larga, 2010.
- [64] W. S. Massey. *A basic course in algebraic topology*, volume 127 of *Graduate Texts in Mathematics*. Springer-Verlag, New York, 1991.
- [65] T. A. McKee and F. R. McMorris. *Topics in intersection graph theory*. SIAM Monographs on Discrete Mathematics and Applications. Society for Industrial and Applied Mathematics (SIAM), Philadelphia, PA, 1999.
- [66] B. Mohar and C. Thomassen. *Graphs on surfaces*. Johns Hopkins Studies in the Mathematical Sciences. Johns Hopkins University Press, Baltimore, MD, 2001.
- [67] A. Nakamoto. Irreducible quadrangulations of the Klein bottle. *Yokohama Math. J.*, 43(2):125–139, 1995.

BIBLIOGRAPHY

- [68] A. Nakamoto. Irreducible quadrangulations of the torus. *J. Combin. Theory Ser. B*, 67(2):183–201, 1996.
- [69] A. Nakamoto and K. Ota. Note on irreducible triangulations of surfaces. *J. Graph Theory*, 20(2):227–233, 1995.
- [70] C. S. J. A. Nash-Williams. Edge-disjoint spanning trees of finite graphs. *J. London Math. Soc.*, 36:445–450, 1961.
- [71] C. S. J. A. Nash-Williams. Decomposition of finite graphs into forests. *J. London Math. Soc.*, 39:12, 1964.
- [72] S. Negami. *Iso kikagakuteki gurafu riron nyūmon*. Yokohama Publishers, Yokohama, 2001.
- [73] A. Nixon and J. C. Owen. An inductive construction of $(2, 1)$ -tight graphs. *Contrib. Discrete Math.*, 9(2):1–16, 2014.
- [74] A. Nixon, J. C. Owen, and S. C. Power. Rigidity of frameworks supported on surfaces. *SIAM J. Discrete Math.*, 26(4):1733–1757, 2012.
- [75] A. Nixon and E. Ross. One brick at a time: a survey of inductive constructions in rigidity theory. In *Rigidity and symmetry*, volume 70 of *Fields Inst. Commun.*, pages 303–324. Springer, New York, 2014.
- [76] A. Nixon and B. Schulze. Symmetry-forced rigidity of frameworks on surfaces. *Geom. Dedicata*, 182:163–201, 2016.
- [77] J. Pach. Geometric intersection patterns and the theory of topological graphs. In *Proceedings of the International Congress of Mathematicians—Seoul 2014. Vol. IV*, pages 455–474. Kyung Moon Sa, Seoul, 2014.
- [78] H. Pollaczek-Geiringer. Über die gliederung ebener fachwerke. *Zeitschrift für Angewandte Mathematik und Mechanik*, 7:58–72, 1927.
- [79] H. Pollaczek-Geiringer. Über die gliederung ebener fachwerke. *Zeitschrift für Angewandte Mathematik und Mechanik*, 12(6):369–376, 1932.

BIBLIOGRAPHY

- [80] R. C. Read and R. J. Wilson. *An atlas of graphs*. Oxford Science Publications. The Clarendon Press, Oxford University Press, New York, 1998.
- [81] E. R. Scheinerman. *Intersection classes and multiple intersection parameters of graphs*. ProQuest LLC, Ann Arbor, MI, 1984. Thesis (Ph.D.)—Princeton University.
- [82] M. Sitharam, A. St. John, and J. Sidman, editors. *Handbook of geometric constraint systems principles*. Discrete Mathematics and its Applications (Boca Raton). CRC Press, Boca Raton, FL, 2019.
- [83] E. Steinitz and H. Rademacher. *Vorlesungen über die Theorie der Polyeder unter Einschluss der Elemente der Topologie*. Springer-Verlag, Berlin-New York, 1976. Reprint der 1934 Auflage, Grundlehren der Mathematischen Wissenschaften, No. 41.
- [84] I. Streinu and L. Theran. Sparsity-certifying graph decompositions. *Graphs Combin.*, 25(2):219–238, 2009.
- [85] T. Sulanke. Note on the irreducible triangulations of the Klein bottle. *J. Combin. Theory Ser. B*, 96(6):964–972, 2006.
- [86] L. Szegő. On constructive characterizations of (k, l) -sparse graphs. *European J. Combin.*, 27(7):1211–1223, 2006.
- [87] E. Szpilrajn-Marczewski. Sur deux propriétés des classes d’ensembles. *Fund. Math.*, 33:303–307, 1945.
- [88] T.-S. Tay. Review: rigidity problems in bar-and-joint frameworks and linkages of rigid bodies. *Structural Topology*, (8):33–36, 1983. With a French translation.
- [89] C. Thomassen. The Jordan-Schönflies theorem and the classification of surfaces. *Amer. Math. Monthly*, 99(2):116–130, 1992.
- [90] C. Thomassen. *Presentation at Graph Drawing '93, Paris*. 1993.
- [91] W. Thurston. *The geometry and topology of three-manifolds*. 1980. Princeton lecture notes.

BIBLIOGRAPHY

- [92] T. tom Dieck. *Algebraic topology*. EMS Textbooks in Mathematics. European Mathematical Society (EMS), Zürich, 2008.
- [93] W. T. Tutte. On the problem of decomposing a graph into n connected factors. *J. London Math. Soc.*, 36:221–230, 1961.
- [94] V. I. Voloshin. *Introduction to graph and hypergraph theory*. Nova Science Publishers, Inc., New York, 2009.
- [95] G. S. Walsh. *Mostly surfaces*. *Amer. Math. Monthly*, 121(10):954–956, 2014.
- [96] A. T. White. *Graphs of groups on surfaces*, volume 188 of *North-Holland Mathematics Studies*. North-Holland Publishing Co., Amsterdam, 2001. Interactions and models.
- [97] W. Whiteley. Infinitesimally rigid polyhedra. II. Modified spherical frameworks. *Trans. Amer. Math. Soc.*, 306(1):115–139, 1988.
- [98] D. Zeps and P. Kikusts. How to draw combinatorial map? From graphs and edges to corner rotations and permutations. working paper or preprint, July 2012.
- [99] G. M. Ziegler. *Lectures on polytopes*, volume 152 of *Graduate Texts in Mathematics*. Springer-Verlag, New York, 1995.
- [100] P. Zimmermann, A. Casamayou, N. Cohen, G. Connan, T. Dumont, L. Fousse, F. Maltey, M. Meulien, M. Mezzarobba, C. Pernet, N. M. Thiéry, E. Bray, J. Cremona, M. Forets, A. Ghitza, and H. Thomas. *Computational mathematics with SageMath*. Society for Industrial and Applied Mathematics (SIAM), Philadelphia, PA, 2018.

BIBLIOGRAPHY

Appendix A

Base irreducible (2,2)-tight torus graphs

This appendix presents all base irreducible (2,2)-tight \mathbb{T} -graphs, i.e. irreducible (2,2)-tight torus graphs with no vertices of degree 2.

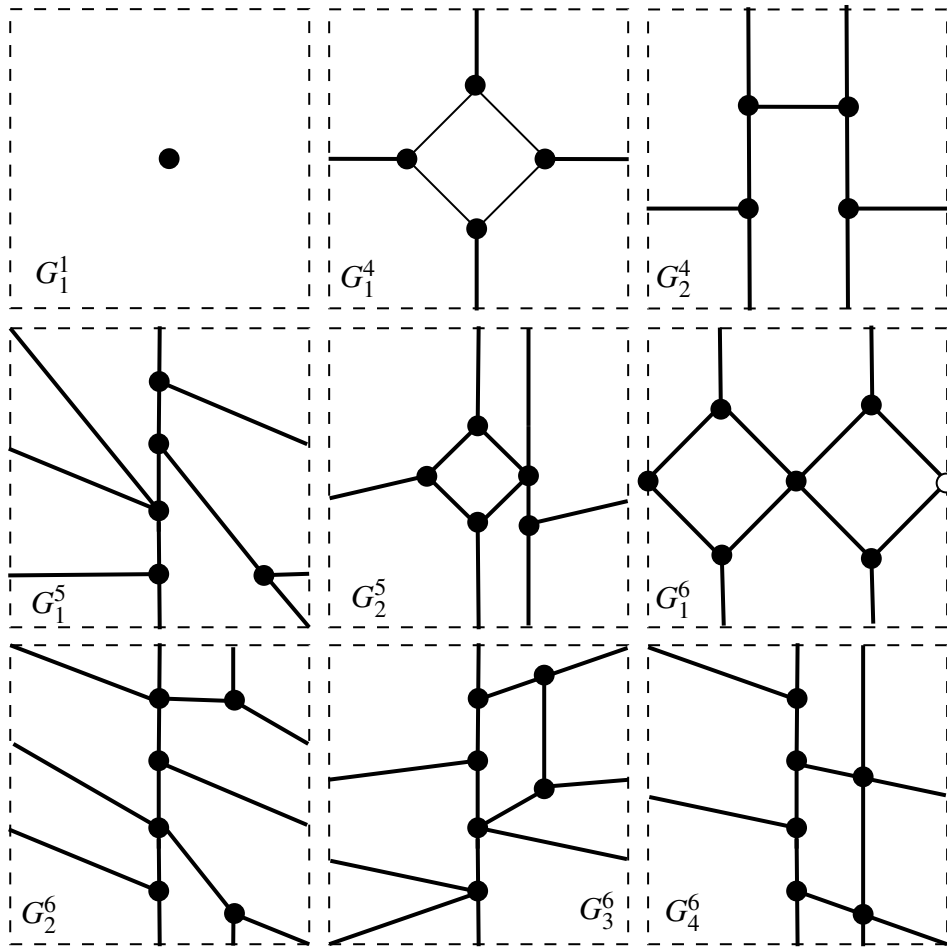


Figure A.1: All the irreducible (2,2)-tight \mathbb{T} -graphs with no vertices of degree 2: part 1.

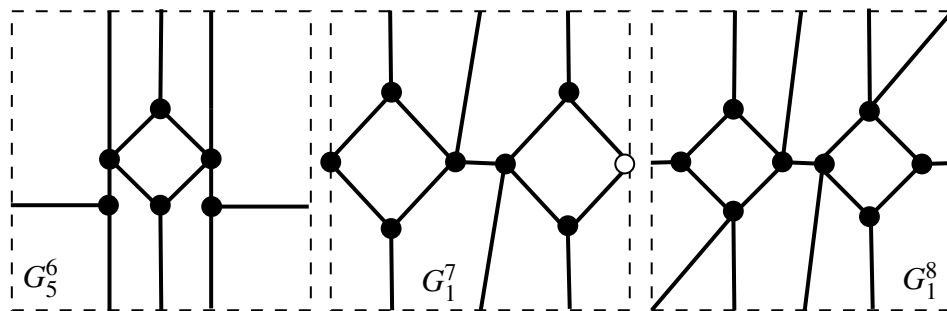


Figure A.2: All the irreducible (2,2)-tight \mathbb{T} -graphs with no vertices of degree 2: part 2.

Appendix B

Polygon representations derived from G_1^3 and G_2^3

In this appendix we present all possible cases of adding a new vertex of degree two to the polygon representations of G_1^3 and G_2^3 .

APPENDIX B. POLYGON REPRESENTATIONS DERIVED FROM G_1^3 AND G_2^3

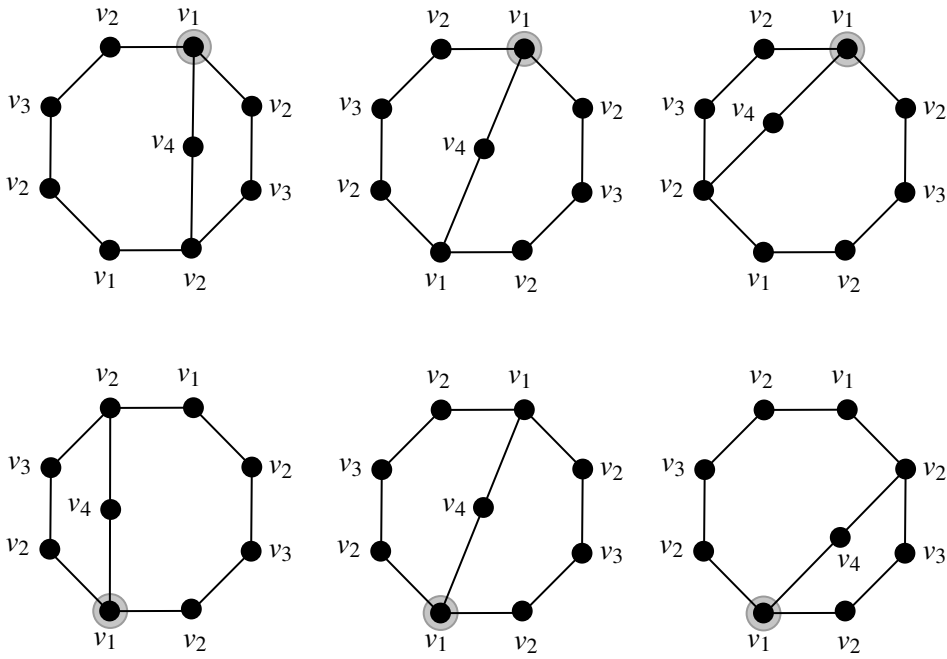


Figure B.1: Polygon representations that are derived from the polygon representation of G_1^3 . The vertex v_1 is fixed.

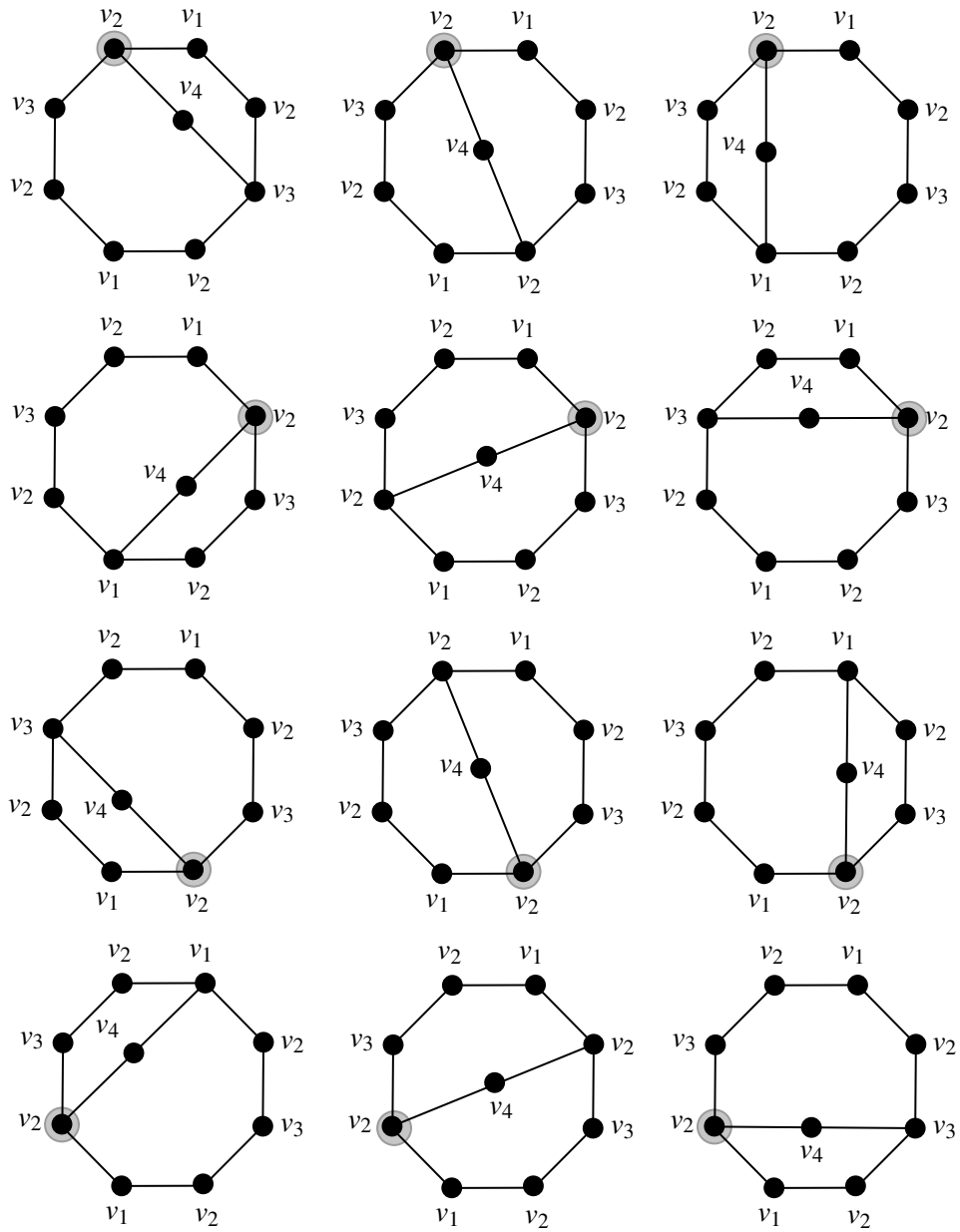


Figure B.2: Polygon representations that are derived from the polygon representation of G_1^3 . The vertex v_2 is fixed.

APPENDIX B. POLYGON REPRESENTATIONS DERIVED FROM G_1^3 AND G_2^3

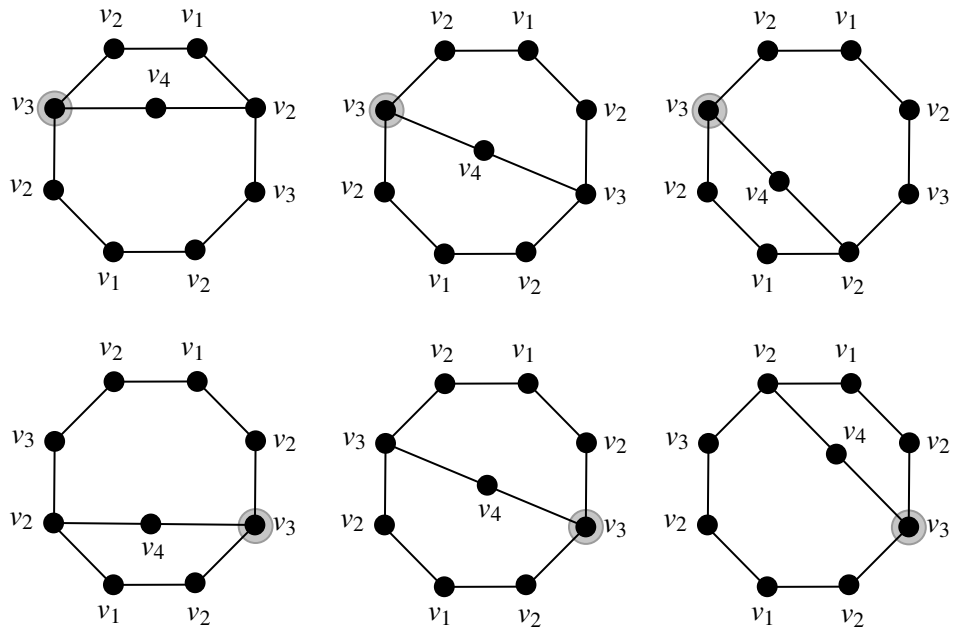


Figure B.3: Polygon representations that are derived from the polygon representation of G_1^3 . The vertex v_3 is fixed.

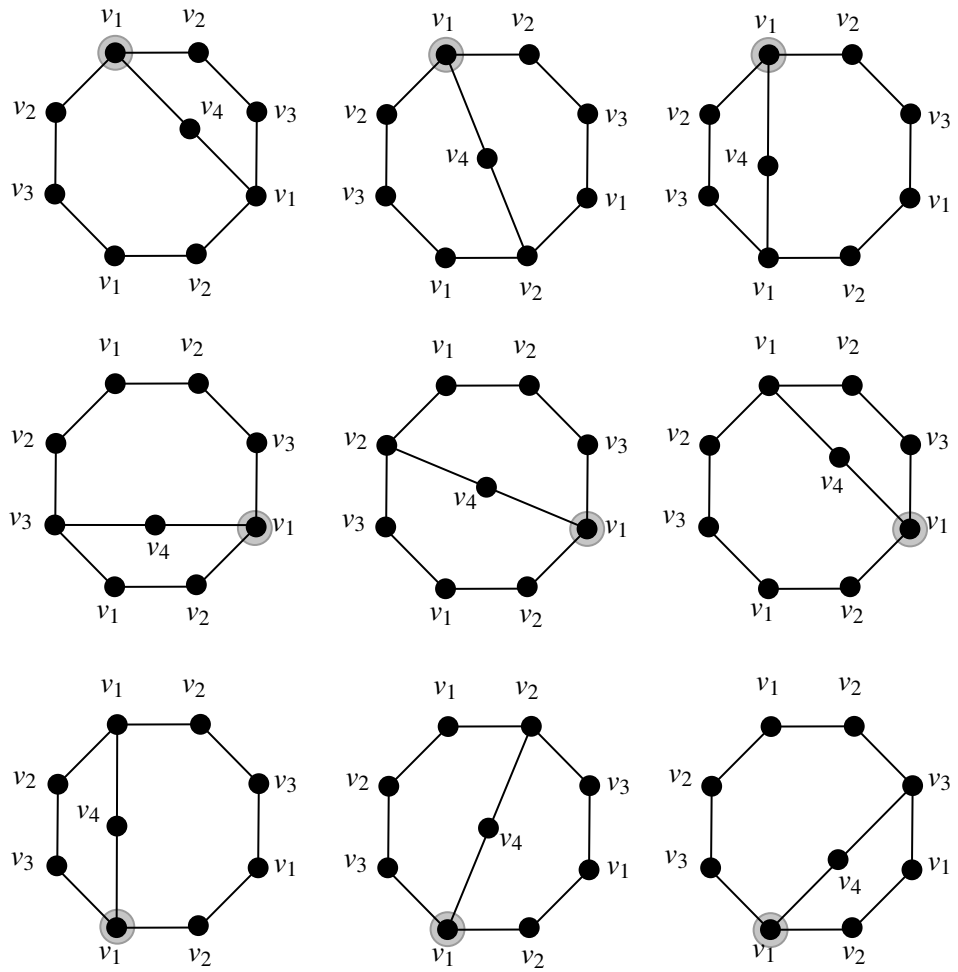


Figure B.4: Polygon representations that are derived from the polygon representation of G_2^3 . The vertex v_1 is fixed.

APPENDIX B. POLYGON REPRESENTATIONS DERIVED FROM G_1^3 AND G_2^3

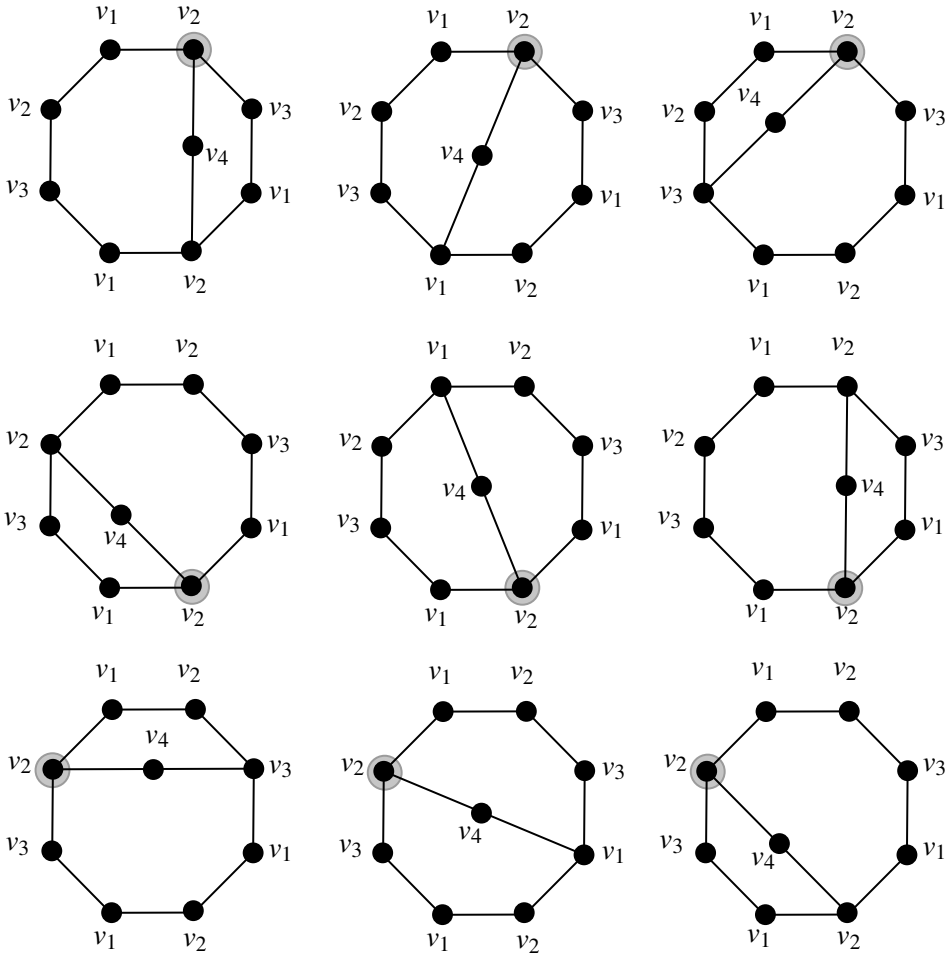


Figure B.5: Polygon representations that are derived from the polygon representation of G_2^3 . The vertex v_2 is fixed.

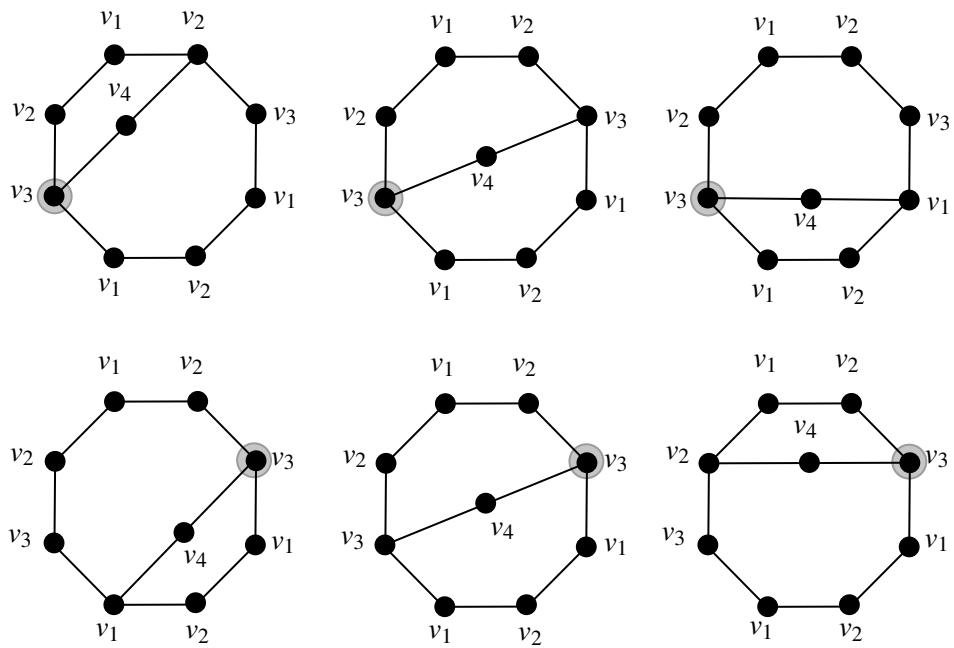


Figure B.6: Polygon representations that are derived from the polygon representation of G_2^3 . The vertex v_3 is fixed.

APPENDIX B. POLYGON REPRESENTATIONS DERIVED FROM G_1^3 AND
 G_2^3

Appendix C

Notations for all irreducible (2,2)-tight torus graphs with 6 and 7 vertices.

In this appendix we present the notations of all irreducible (2,2)-tight torus graphs with 6 and 7 vertices.

APPENDIX C. NOTATIONS FOR ALL IRREDUCIBLE (2,2)-TIGHT TORUS GRAPHS WITH 6 AND 7 VERTICES.

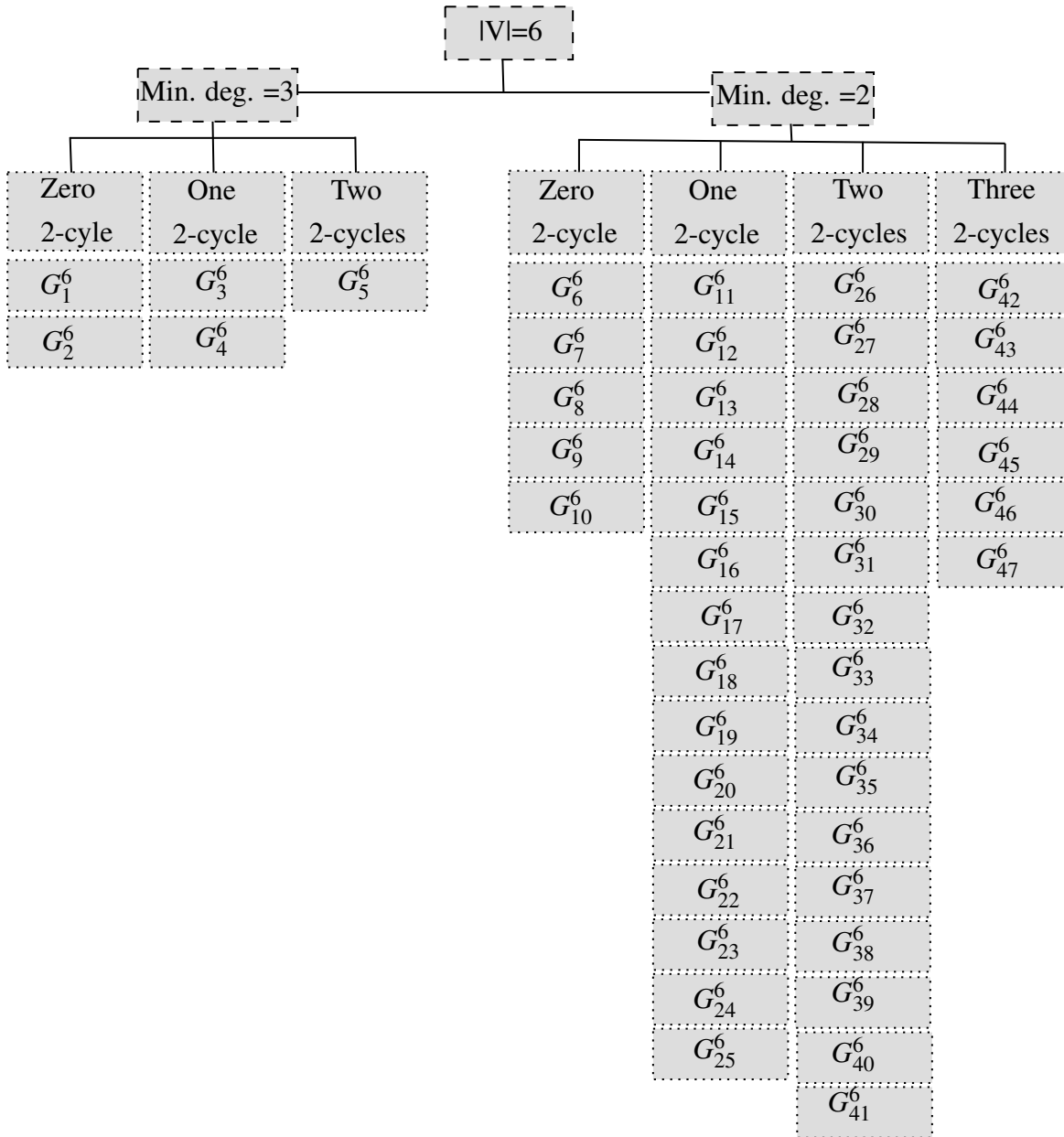


Figure C.1: Notations for irreducible (2,2)-tight torus graphs with 6 vertices.

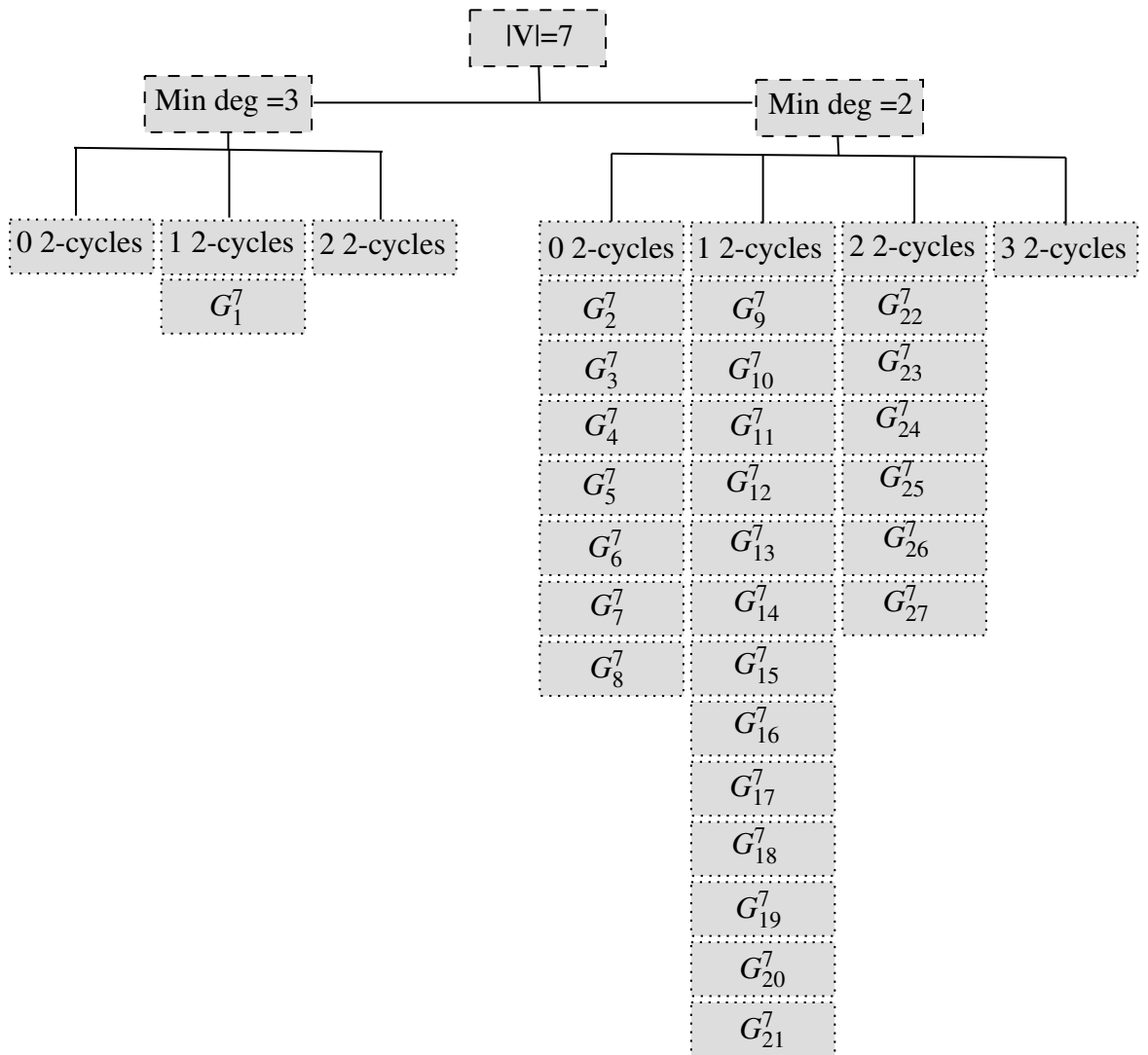


Figure C.2: Notations for irreducible (2,2)-tight torus graphs with 7 vertices.

APPENDIX C. NOTATIONS FOR ALL IRREDUCIBLE (2,2)-TIGHT TORUS
GRAPHS WITH 6 AND 7 VERTICES.

Appendix D

Ancestor trees for all 116 irreducible (2,2)-tight torus graphs.

In this appendix we present ancestor trees for the list of all irreducible $(2,2)$ -tight torus graphs.

APPENDIX D. ANCESTOR TREES FOR ALL 116 IRREDUCIBLE
(2,2)-TIGHT TORUS GRAPHS.

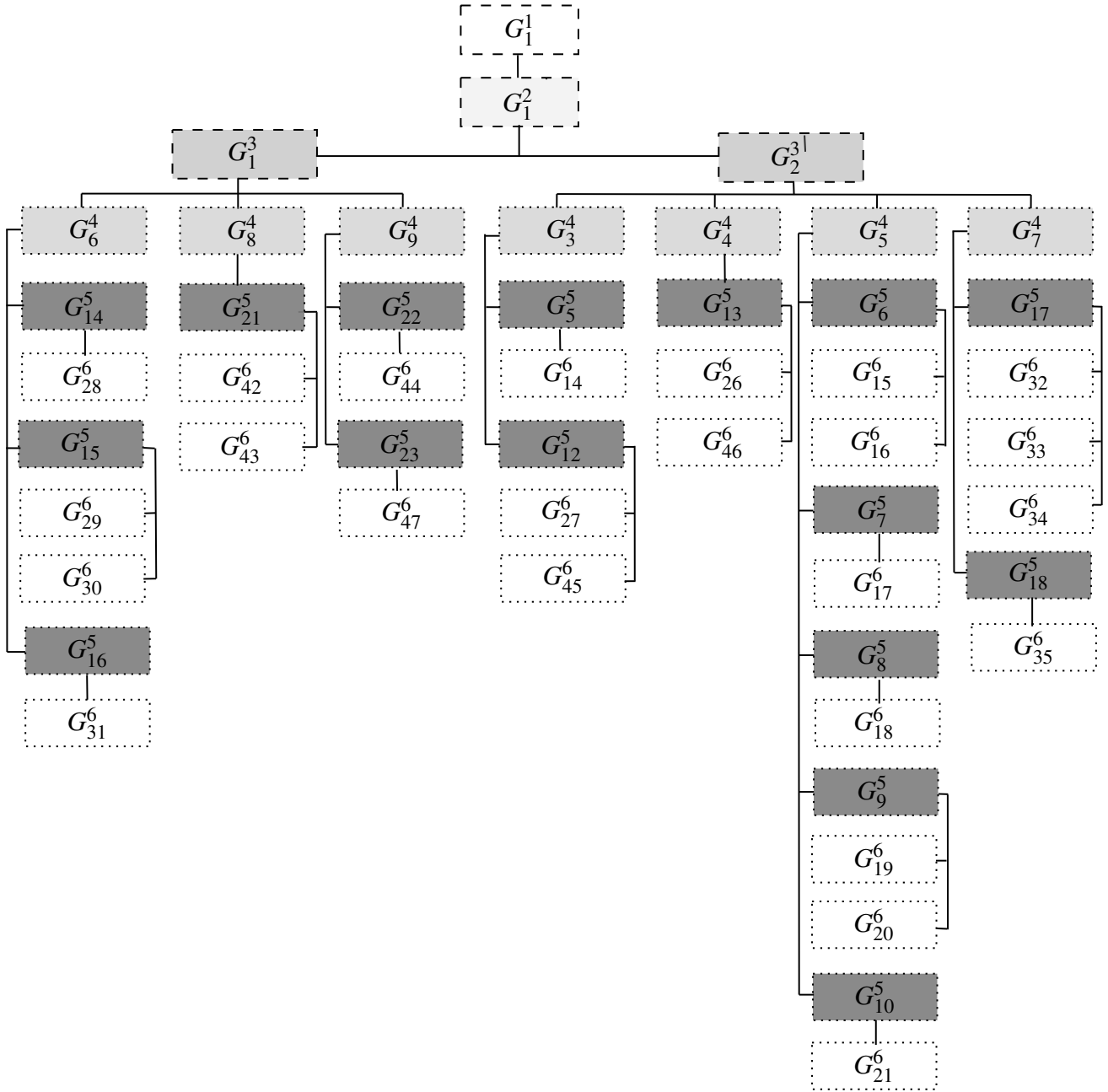


Figure D.1: All non-isomorphic (2,2)-tight \mathbb{T} -graphs that are derived from G_1^1 .

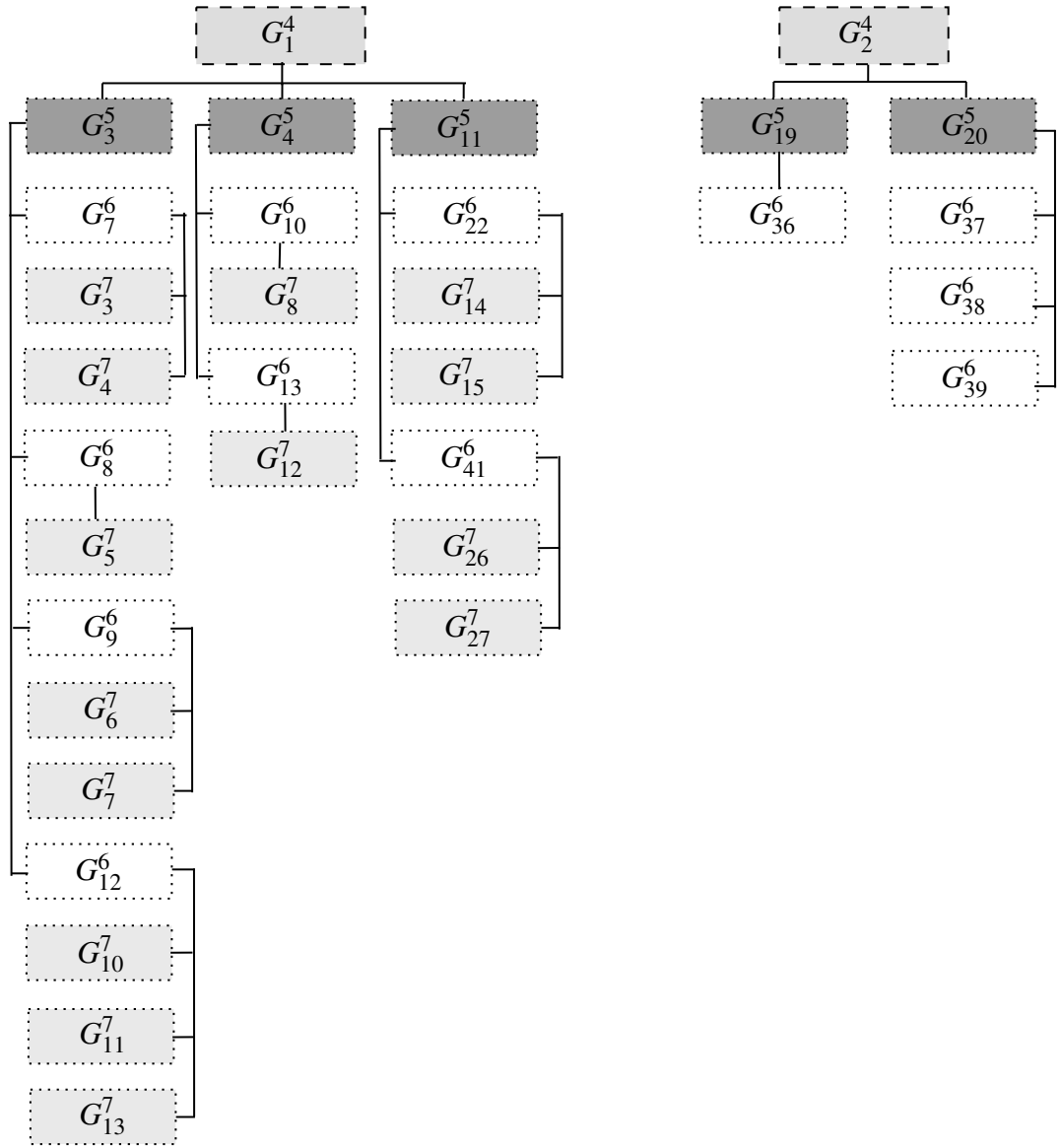


Figure D.2: All the notations of the irreducible (2,2)-tight \mathbb{T} -graphs that are derived from G_1^4 and G_2^4 .

APPENDIX D. ANCESTOR TREES FOR ALL 116 IRREDUCIBLE
(2,2)-TIGHT TORUS GRAPHS.

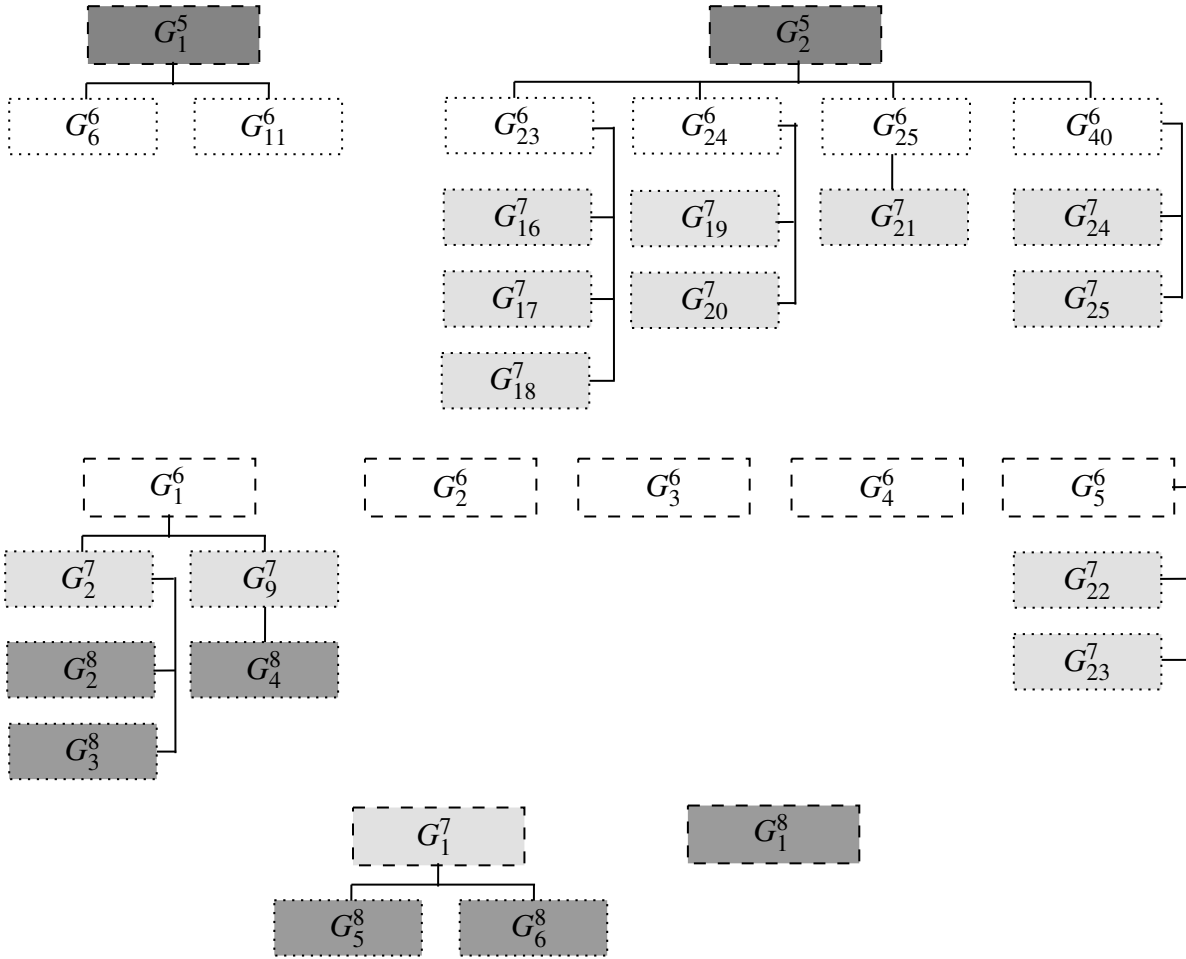


Figure D.3: All the notations of the irreducible (2,2)-tight \mathbb{T} -graphs that are derived from G_1^5 , G_2^5 , G_1^6 , G_2^6 , G_3^6 , G_4^6 , G_5^6 , G_1^7 and G_1^8 .

Appendix E

Irreducible (2,2)-tight torus graphs

This appendix contains all irreducible (2,2)-tight torus graphs. They are 116 torus graphs.

E.1 Irreducible (2,2)-tight torus graphs with less than 4 vertices.

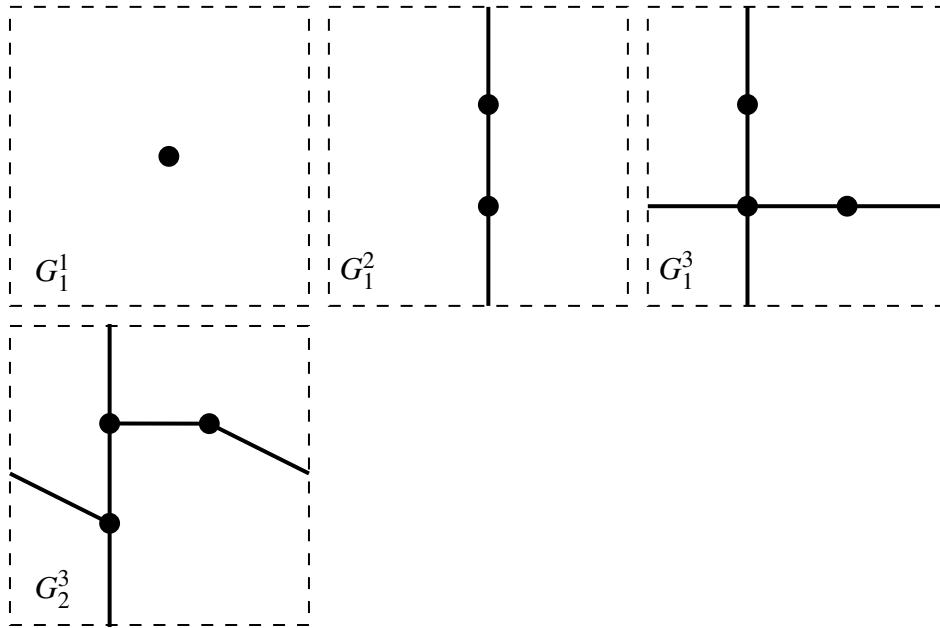


Figure E.1: G_1^1, G_1^2, G_1^3 and G_2^3 .

E.2 Irreducible (2,2)-tight torus graphs with 4 vertices.

Figures present all non-isomorphic irreducible (2,2)-tight \mathbb{T} -graphs with 4 vertices.

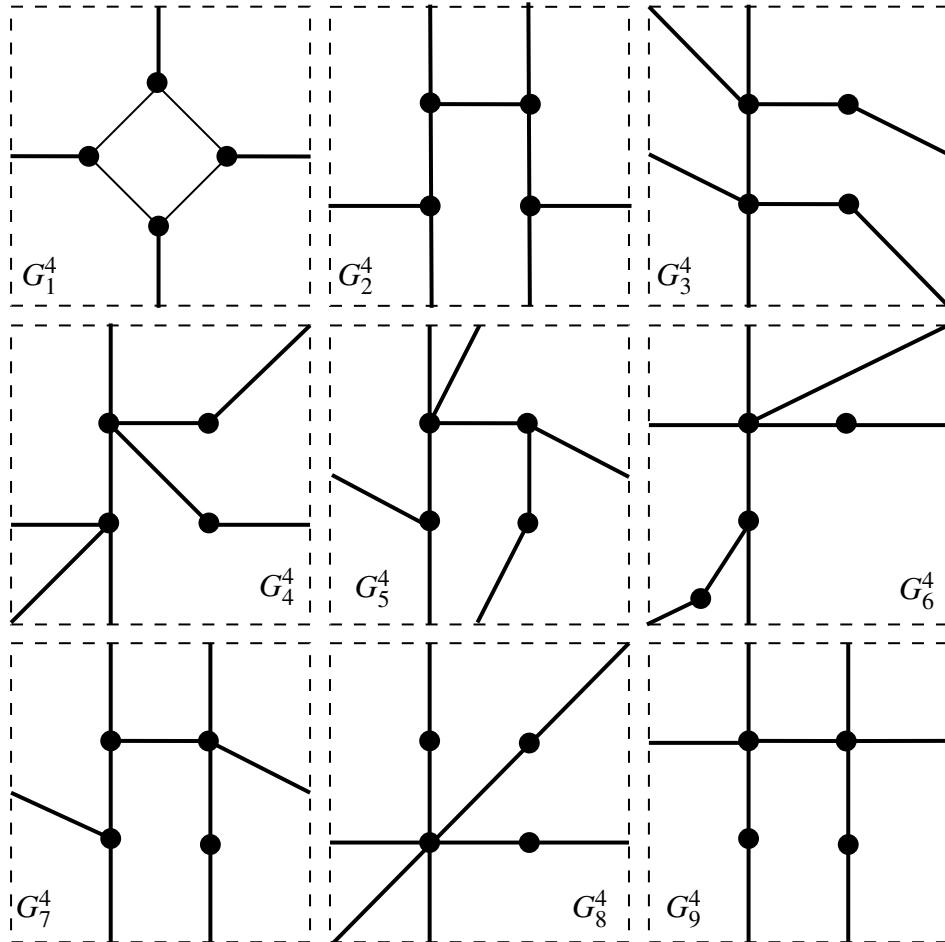


Figure E.2: From G_1^4 to G_9^4 .

E.3 Irreducible (2,2)-tight torus graphs with 5 vertices.

Figures present all non-isomorphic irreducible (2,2)-tight \mathbb{T} -graphs with 5 vertices.

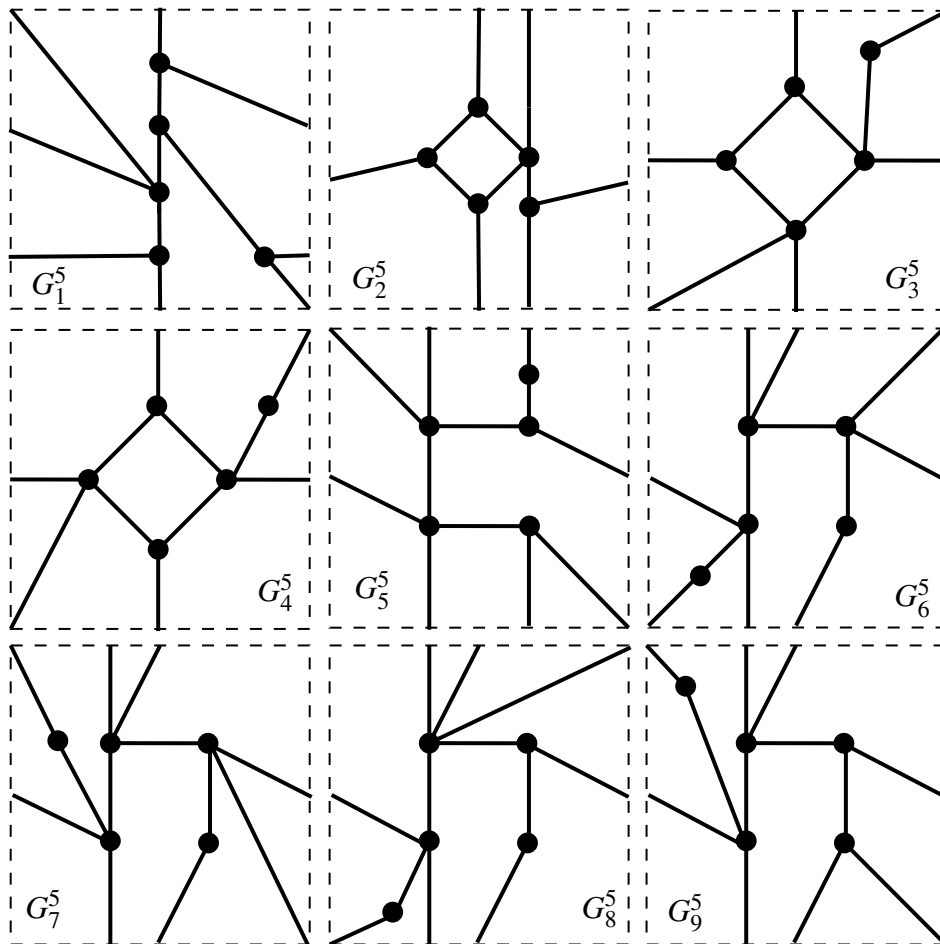


Figure E.3: From G_1^5 to G_9^5 .

E.3. IRREDUCIBLE (2,2)-TIGHT TORUS GRAPHS WITH 5 VERTICES.

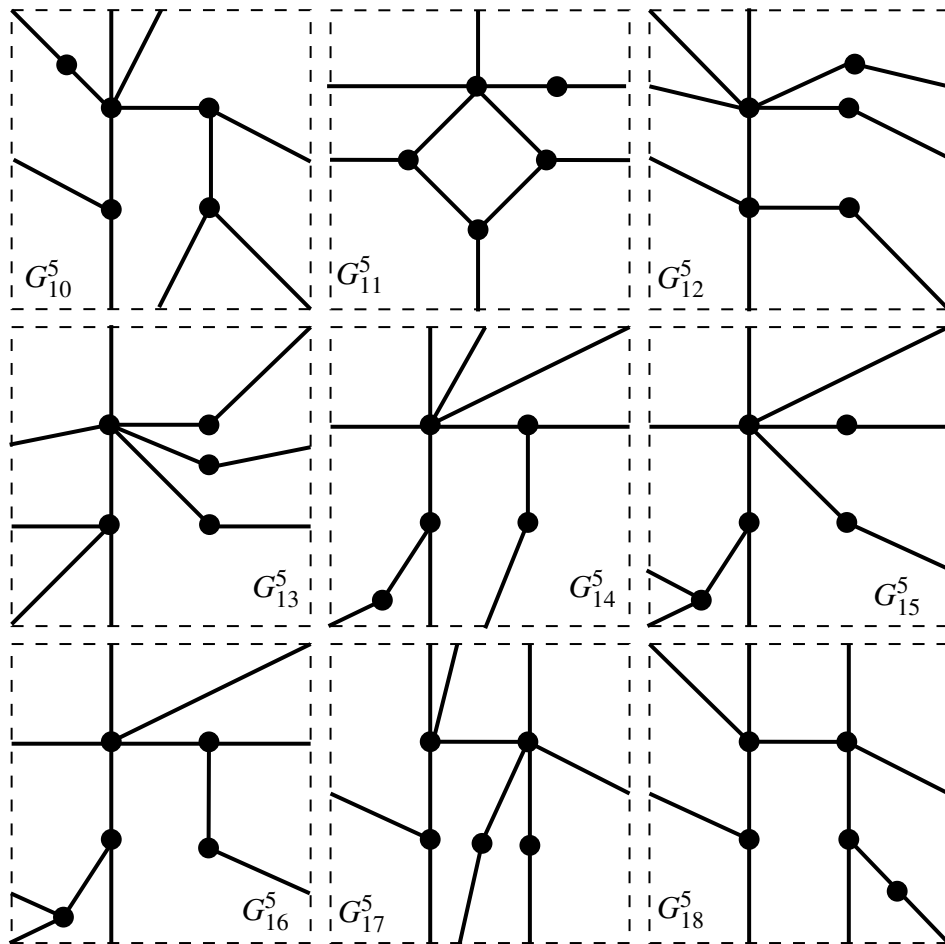


Figure E.4: From G^5_{10} to G^5_{18} .

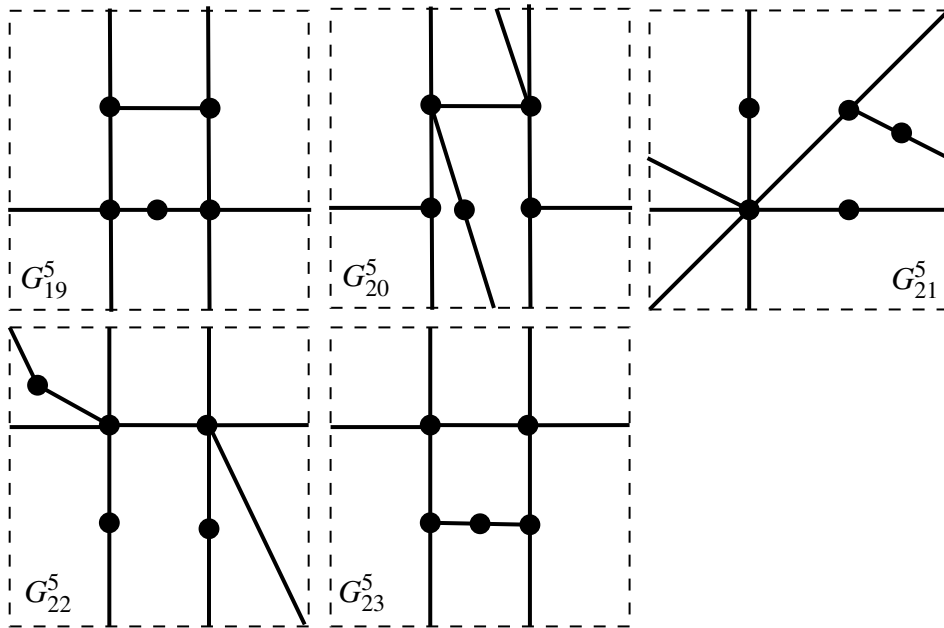


Figure E.5: From G_{19}^5 to G_{23}^5 .

E.4 Irreducible (2,2)-tight torus graphs with 6 vertices.

Figures present all non-isomorphic irreducible (2,2)-tight \mathbb{T} -graphs with 6 vertices.

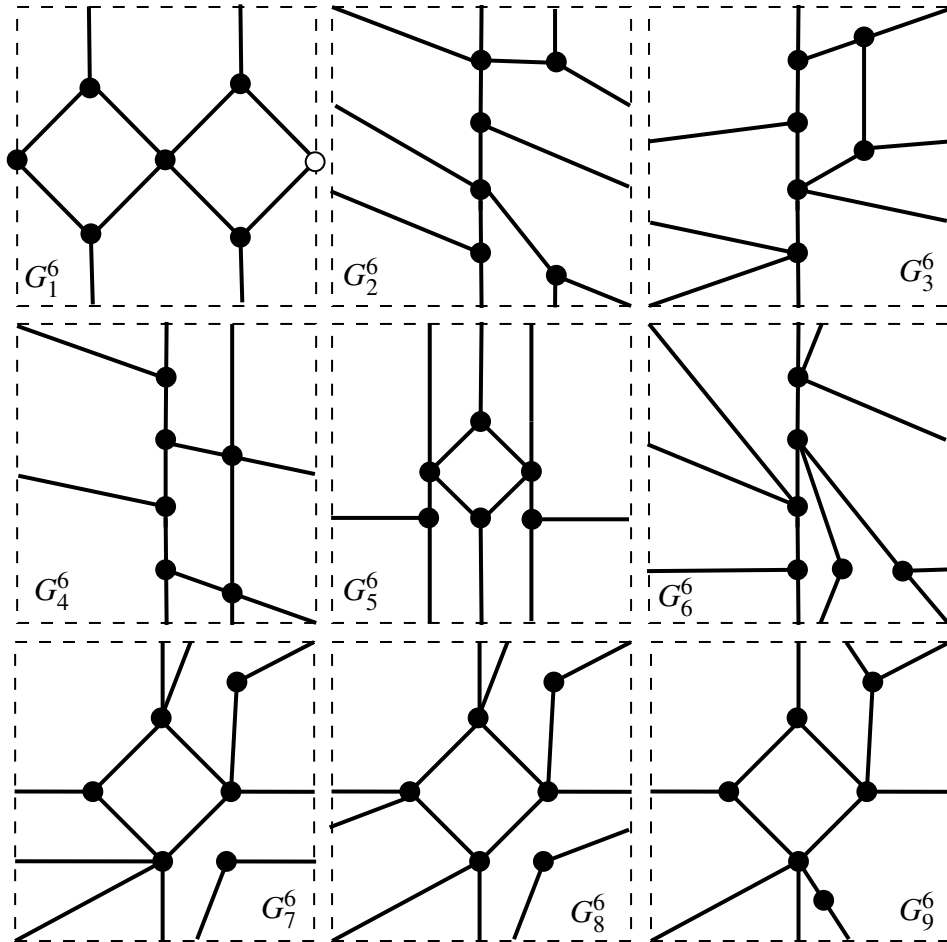


Figure E.6: From G_1^6 to G_9^6 .

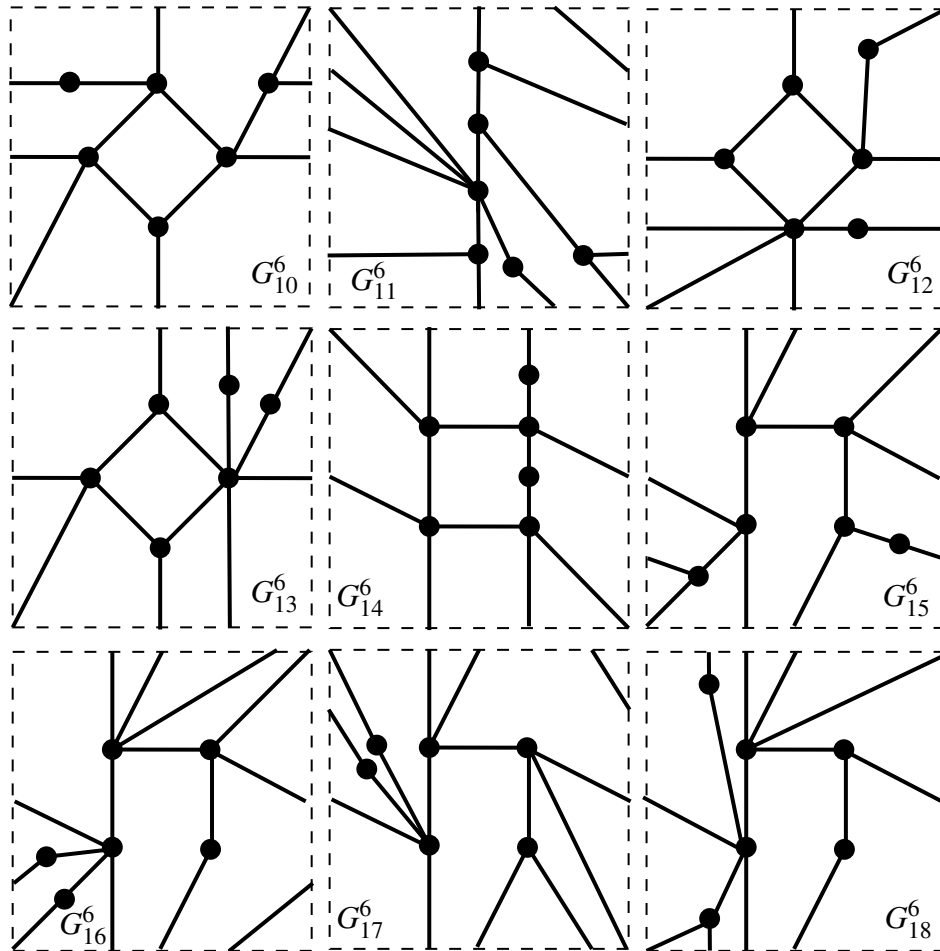


Figure E.7: From G_{10}^6 to G_{18}^6 .

E.4. IRREDUCIBLE (2,2)-TIGHT TORUS GRAPHS WITH 6 VERTICES.

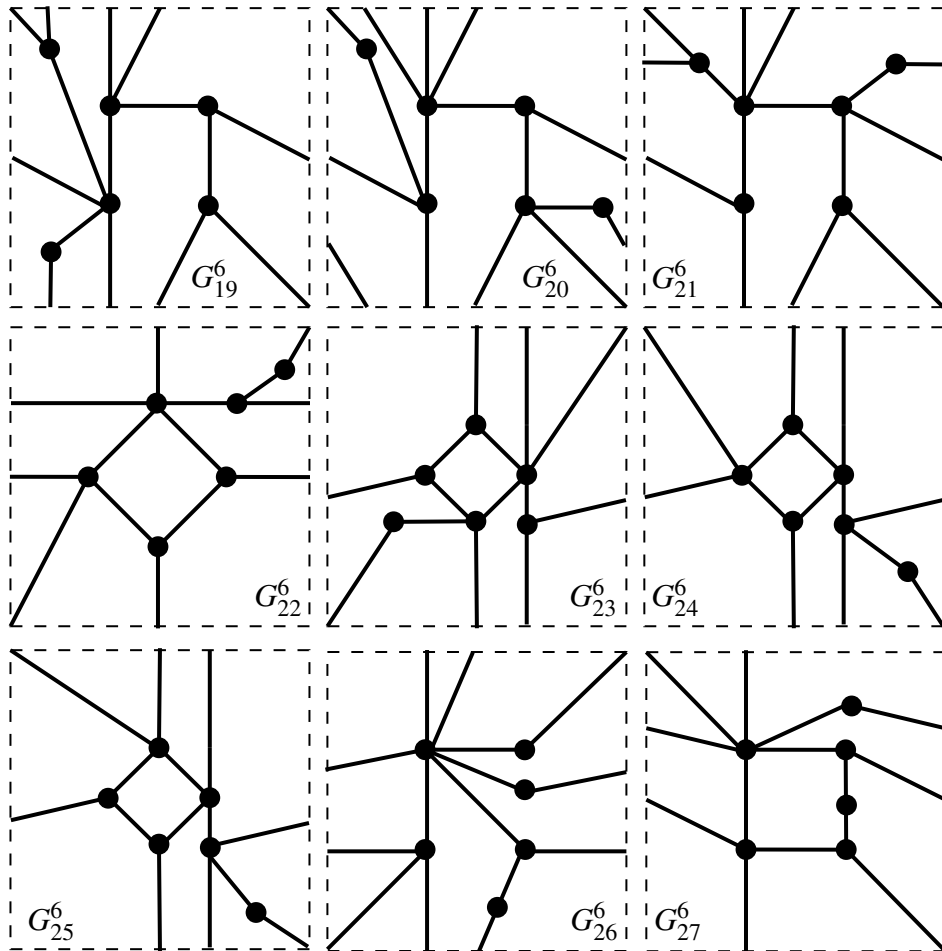


Figure E.8: From G_{19}^6 to G_{27}^6 .

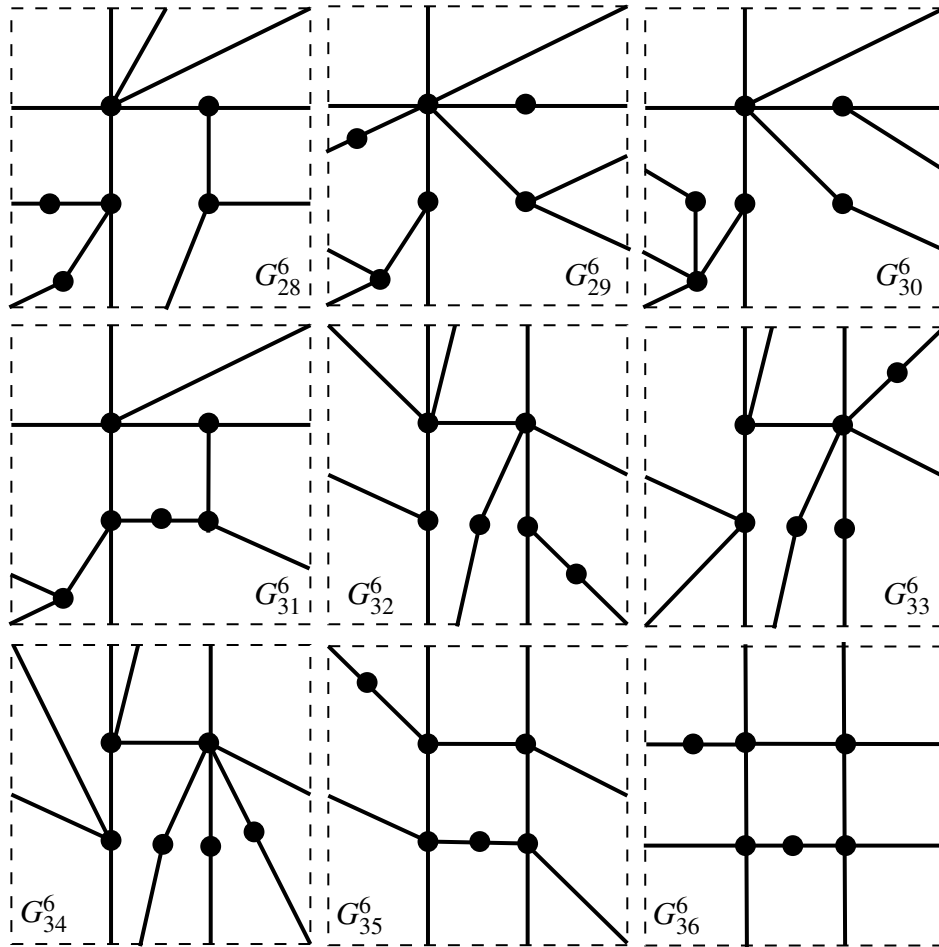


Figure E.9: From G_{28}^6 to G_{36}^6 .

E.4. IRREDUCIBLE (2,2)-TIGHT TORUS GRAPHS WITH 6 VERTICES.

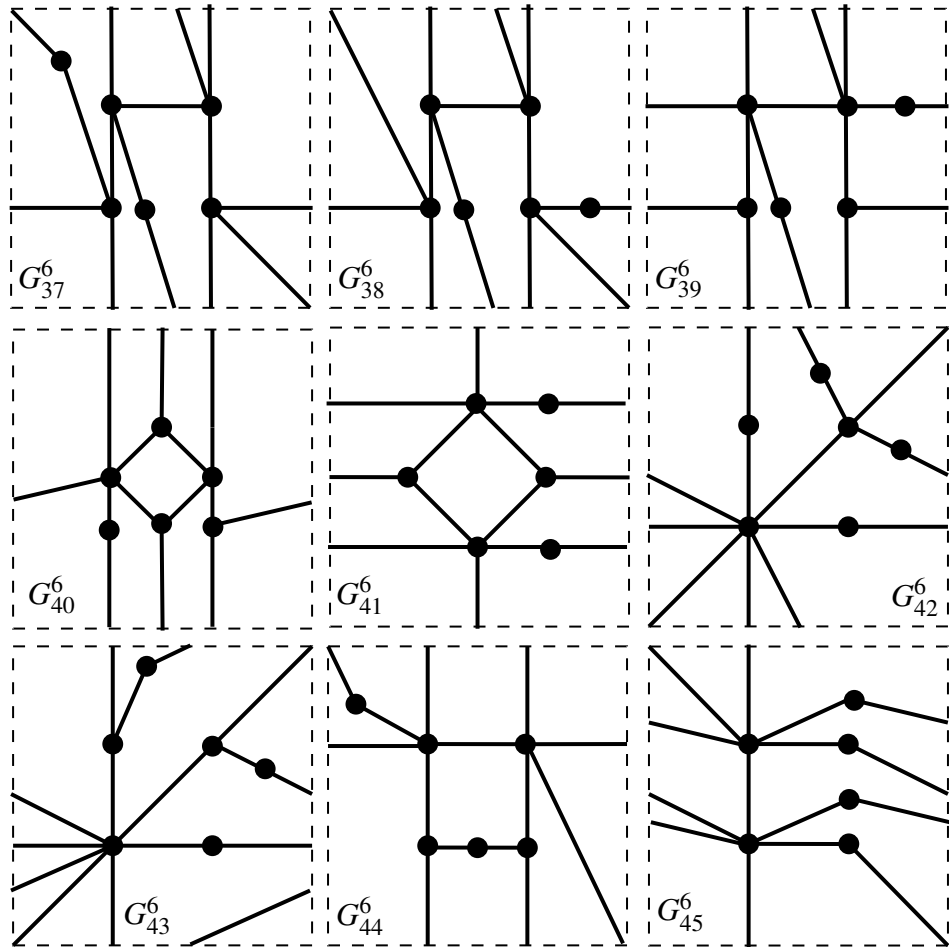


Figure E.10: From G_{37}^6 to G_{45}^6 .

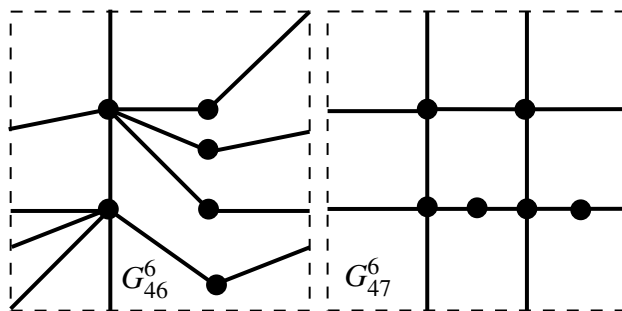


Figure E.11: G_{46}^6 and G_{47}^6 .

E.5 Irreducible (2,2)-tight torus graphs with 7 vertices.

Figures present all non-isomorphic irreducible (2,2)-tight \mathbb{T} -graphs with 7 vertices.

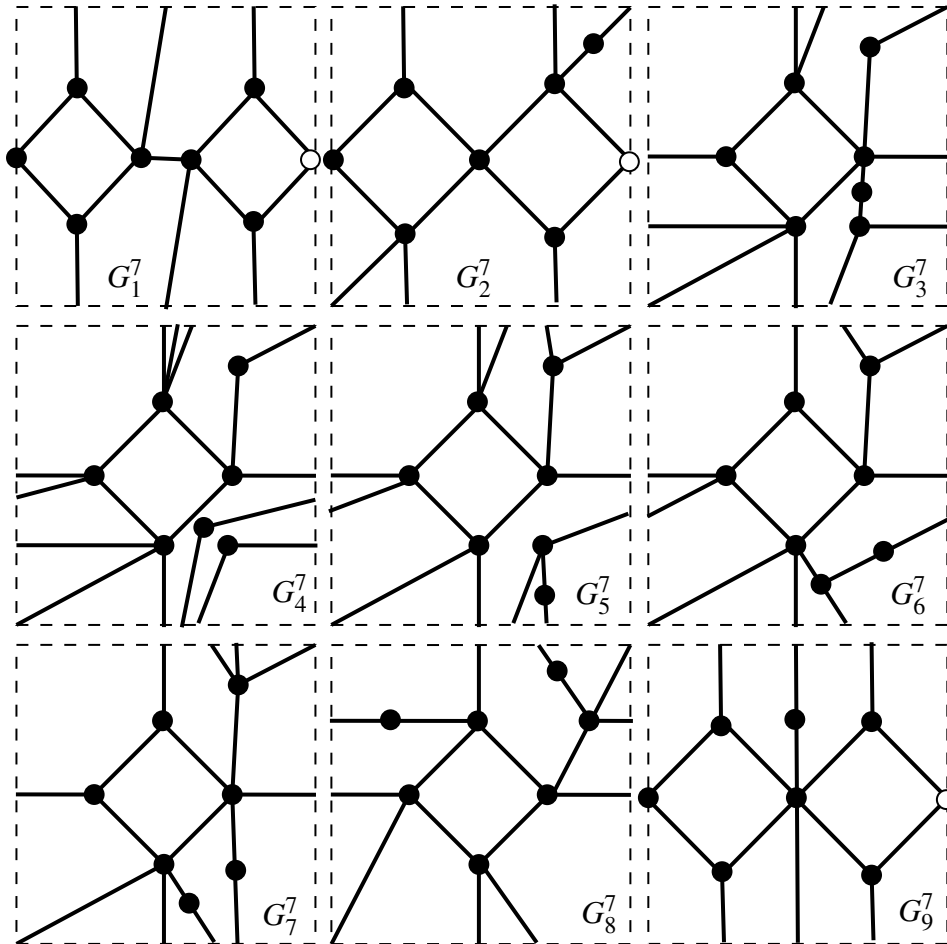


Figure E.12: From G_1^7 and G_9^7 .

E.5. IRREDUCIBLE (2,2)-TIGHT TORUS GRAPHS WITH 7 VERTICES.

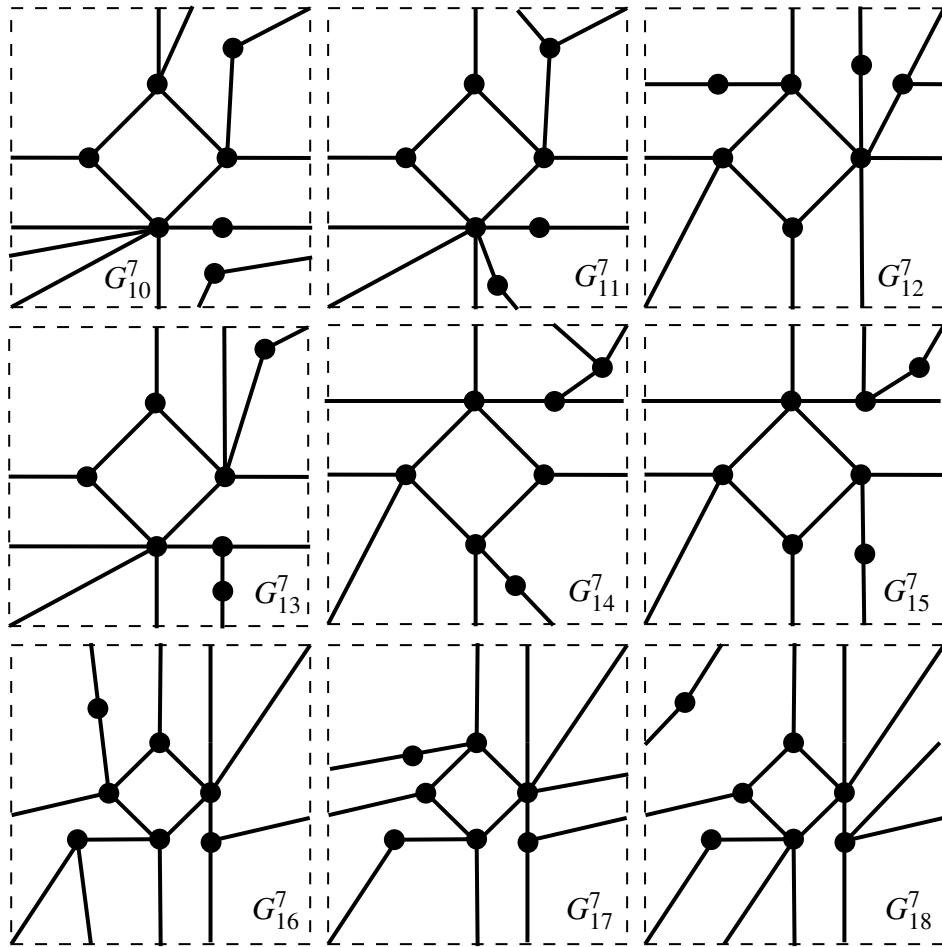


Figure E.13: From G^7_{10} and G^7_{18} .

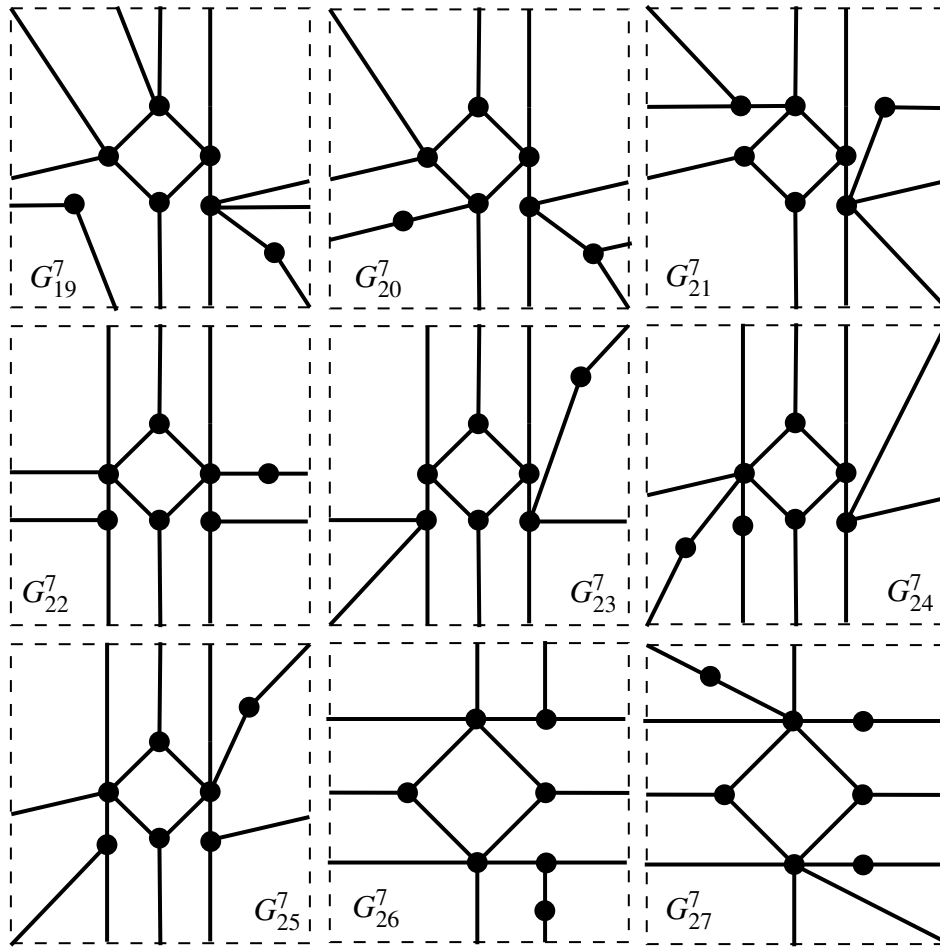


Figure E.14: From G_{19}^7 and G_{27}^7 .

E.6 Irreducible (2,2)-tight torus graphs with 8 vertices.

Figures present all non-isomorphic irreducible (2,2)-tight \mathbb{T} -graphs with 8 vertices.

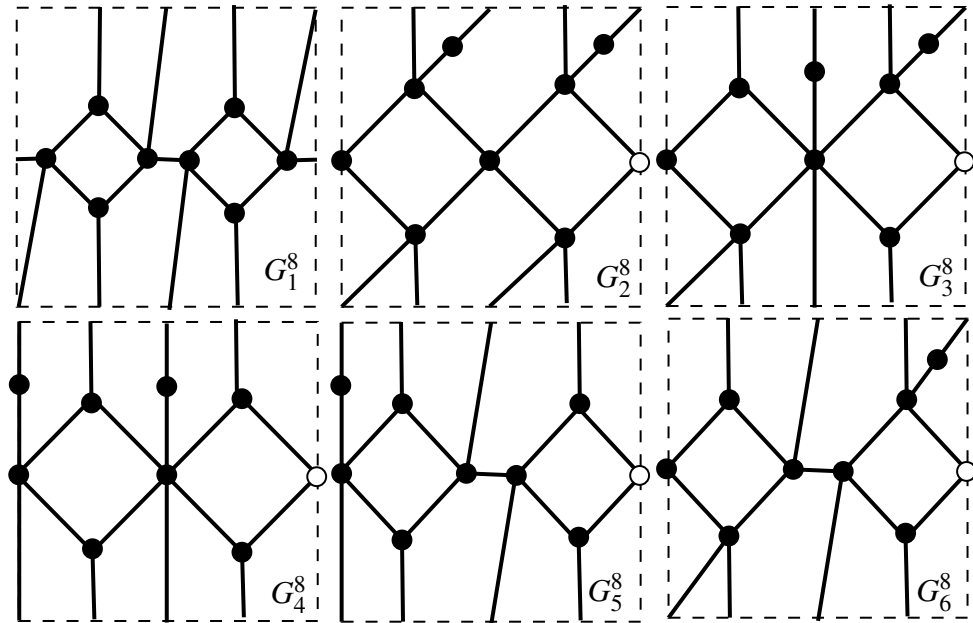


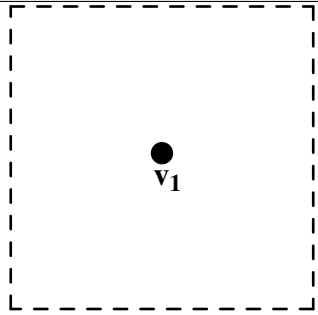
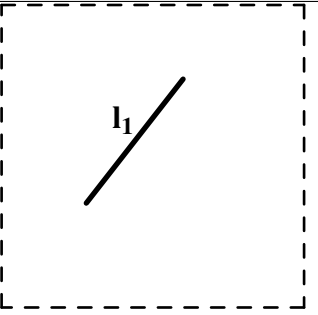
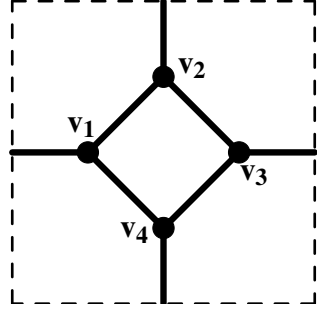
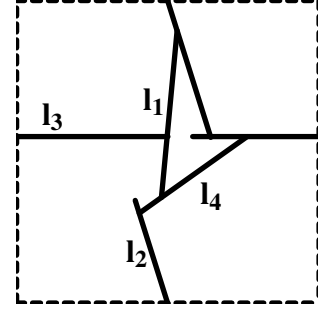
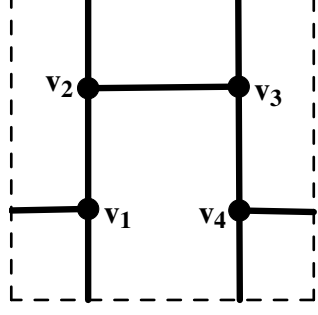
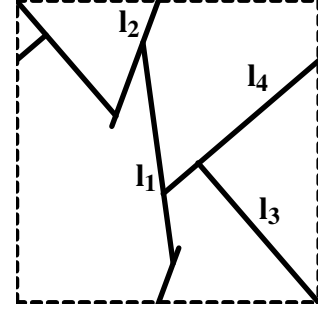
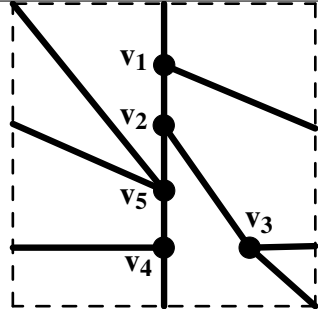
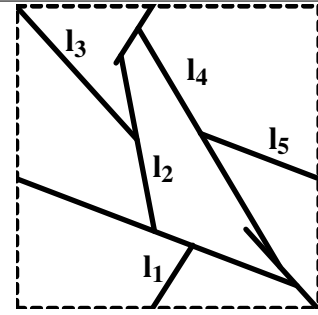
Figure E.15: From G_1^8 and G_6^8 .

Appendix F

CCA representations of the base irreducible (2,2)-tight torus graphs

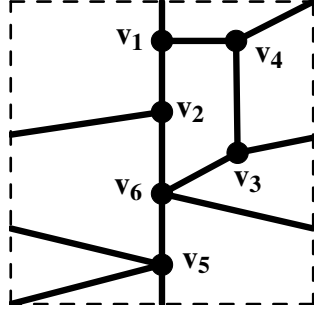
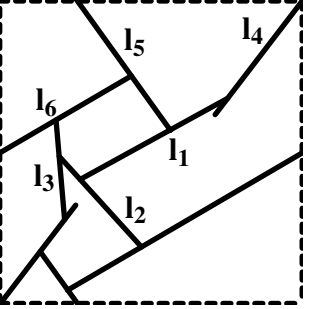
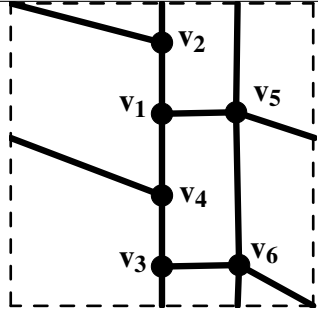
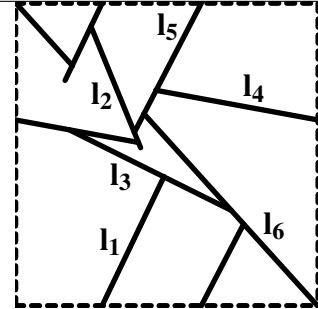
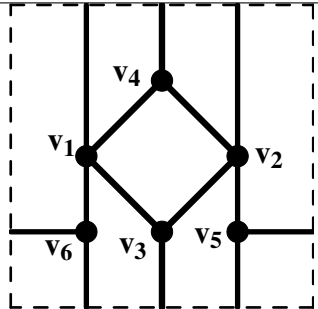
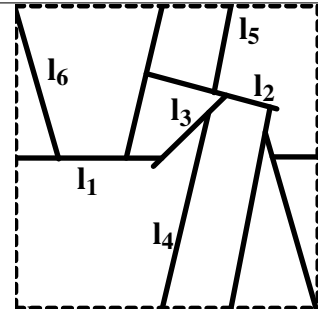
In this appendix we include again the CCA representations of the 12 irreducible (2,2)-tight \mathbb{T} -graphs with no vertices of degree two. In the following table we include the notation of each of such CCA representations as C_j^i which is a CCA representation of G_j^i . We label each of such C_j^i according to the labelling of the corresponding irreducible \mathbb{T} -graph G_j^i . Also, we give the equations of each of C_j^i .

APPENDIX F. CCA REPRESENTATIONS OF THE BASE IRREDUCIBLE
(2,2)-TIGHT TORUS GRAPHS

| Name | Labelled Torus Graph | Labelled Straight Rep. | Equations |
|---------|---|---|--|
| G_1^1 |  |  | |
| G_1^4 |  |  | $l_1 : y = 10.64x - 18.99$ $l_2 : y = 3.17x + 10.33$ $y = 3.17x + 6.33$ $l_4 : y = 0.71x + 0.04$ $l_3 : y = 2.2$ $(1, 0, 0, 0, 1)$ |
| G_2^4 |  |  | $l_1 : y = 7.3x + 15.64$ $l_2 : y = 2.7x - 1.07$ $y = 2.7x - 5.07$ $l_3 : y = 1.16x + 3.99$ $y = 1.16x + 4.63$ $l_4 : y = 0.86x - 0.22$ $y = 0.86x + 3.21$ $(0, 0, 2, 0, 0)$ |
| G_1^5 |  |  | $l_1 : y = 1.5x + 1.18$ $y = 1.5x + 2.82$ $l_2 : y = 5.23 + 10.57$ $l_3 : y = 1.1x + 3.99$ $y = 1.1x + 4.4$ $l_4 : y = 1.68x + 6.41$ $l_5 : y = 0.38x + 3.24$ $y = 0.38x + 1.72$ $(0, 2, 1, 0, 0)$ |
| | | 228 | |

| Name | Labelled Torus Graph | Labelled Straight Rep. | equations |
|---------|----------------------|------------------------|--|
| G_2^5 | | | $l_1 : y = 0.58x + 1.98$ $y = 0.58x - 0.35$ $l_2 : x = 1.37$ $l_3 : y = 1.08x + 5.05$ $y = 1.1x + 4.4$ $l_4 : y = 0.08x + 2.39$ $l_5 : y = 11.91x - 31.94$ $y = 11.91x - 27.94$ $(1, 1, 0, 1, 0)$ |
| G_1^6 | | | $l_1 : y = 1.58x - 2.31$ $y = 1.58x - 0.01$ $l_2 : x = 0.95$ $l_3 : y = 0.29x + 2.19$ $l_4 : y = 1.18x + 0.15$ $l_5 : y = 3.18x + 7.99$ $y = 3.18x + 11.99$ $l_6 : y = 9.54 - 21.95$ $(2, 0, 2, 0, 0)$ |
| G_2^6 | | | $l_1 : y = 1.1x + 4$ $y = 1.1x + 4.44$ $l_2 : y = 6.03x + 11.075$ $l_3 : y = 0.74x + 2.66$ $l_4 : y = 1.71$ $l_5 : y = 1.76x - 4.76$ $y = 1.76x - 0.76$ $l_6 : y = 0.23x + 3.24$ $y = 0.23x + 2.33$ $(0, 4, 0, 0, 0)$ |

APPENDIX F. CCA REPRESENTATIONS OF THE BASE IRREDUCIBLE
(2,2)-TIGHT TORUS GRAPHS

| Name | Labelled Torus Graph | Labelled Straight Rep. | Equations |
|---------|---|---|---|
| G_3^6 |  |  | $l_1 : y = 0.55x + 1.05$ $l_2 : y = 1.1x + 2.81$ $l_3 : y = 11.62x + 11.08$ $l_4 : y = 1.31x - 1.22$ $y = 1.31x - 0.01$ $l_5 : y = 1.39x + 5.43$ $y = 1.39x + 1.43$ $l_6 : y = 0.59x + 1.99$ $y = 0.59x - 0.35$ $(0, 4, 0, 0, 0)$ |
| G_4^6 |  |  | $l_1 : y = 2.09x - 2.39$ $y = 2.09x + 1.61$ $l_2 : y = 2.44x + 6.13$ $l_3 : y = 0.5x + 2.68$ $l_4 : y = 0.18x + 3.19$ $0.18x + 2.46$ $l_5 : y = 1.93x - 0.74$ $y = 2.09x - 2.39$ $l_6 : y = 1.11x + 4.41$ $y = 1.11x + 4$ $(0, 4, 0, 0, 0)$ |
| G_5^6 |  |  | $l_1 : y = 1.99$ $l_2 : y = 0.27x + 3.57$ $l_3 : y = 0.97x + 0.1$ $l_4 : y = 4.22x - 8.19$ $y = 4.22x - 4.19$ $l_5 : y = 5.14x - 10.63$ $y = 5.14x - 14.63$ $l_6 : y = 3.46x + 3.95$ $y = 3.46x + 13.74$ $(1, 2, 1, 0, 0)$ |

| Name | Labelled Torus Graph | Labelled Straight Rep. | Equations |
|---------|----------------------|------------------------|--|
| G_1^7 | | | $l_1 : y = 0.4x + 1.91$ $l_2 : y = 328.75x + 294.95$ $l_3 : y = 1.49x - 0.03$ $y = 1.49x - 1.94$ $l_4 : y = 1.17x + 0.04$ $l_5 : y = 3.53x - 7.47$ $y = 3.53x - 9.1$ $l_6 : y = 8.33x - 15.35$ $y = 8.33x - 19.35$ $l_7 : y = 2.38x - .36$ $(2, 2, 1, 0, 0)$ |
| G_1^8 | | | $l_1 : y = 2.02$ $l_2 : y = 612.74x - 610.74$ $l_3 : y = 1.08x + 4.11$ $l_4 : y = 2.15x - 0.6$ $l_5 : y = 10.79x - 21.86$ $y = 10.79x - 25.86$ $l_6 : y = 1.26x - 4.18$ $y = 1.26x - 0.18$ $l_8 : y = 3.03x + 4.03$ $y = 3.03x + 12.08$ $(2, 4, 0, 0, 0)$ |

Index

- contact graph, 166–170
- curve contact representation, 168
- nonseparating loop, 76
- separating loop, 77

- associated loop, 78, 79

- bar-joint framework, 21, 27, 28
- blocker (for a 3-cycle), 39, 40
- blocker of type 1 (for 4-cycle), 43–45
- blocker of type 2 (for 4-cycle), 43–45
- boundary walk, 17, 18

- contact graph, 168

- digon contraction, 46–48, 55

- edge deletion, 32
- edge-disjoint, 26, 27
- essential, 75, 84
- essential blocker, 85, 87, 88, 101, 102

- face, 13

- generic, 28
- genus, 10, 11, 13, 19, 20
- geometric intersection number, 76, 82
- geometric realisation, 13, 77
- graph decomposition, 21, 27
- graph decomposition , 26, 27

- half edge, 8, 9, 16, 19

- inessential, 84
- inessential blocker, 92, 93, 96, 108, 110
- involution, 15
- irreducible, 77
- irreducible , 51

- Laman graph, 59
- loop, 10, 75, 76

- multigraph, 7

- nondegenerate boundary, 18
- nondegenerate digon, 46
- nondegenerate quadrilateral, 49
- nondegenerate triangle, 48
- nonseparating cycle, 78
- nonseparating loop, 11, 76–79, 83, 92–94, 96, 99, 100

- orientable surface, 10

- permutation, 15
- polygon representation, 111–114, 128–130, 132–134, 136, 138–145, 154, 155

- quadrilateral contraction, 50, 55

- rigid, 28
- rotation system, 15, 17, 52–56

INDEX

separating cycle, 78

separating loop, 77

sparse, 22

surface, 9

tight , 22

topological edge contraction, 45, 46

topological edge deletion, 45, 46

topological Henneberg type 0 move, 176

torus, 10

triangle contraction, 48, 55

walk, 8

INDEX
